Cardiff University

Functional role of Epithelial Protein Lost in Neoplasm (EPLIN) in prostate cancer metastasis

By

Ross Collins

Cardiff China Medical Research Collaborative (CCMRC), School of Medicine, Cardiff University, Cardiff

PhD Thesis

Submitted: June 2017

Thesis submitted to Cardiff University for the degree of Doctor of Philosophy

Acknowledgements

I would like to thank Professor Wen Jiang for providing me with the opportunity to pursue my PhD and conduct my research at Cardiff University. I would also like to thank Cancer Research Wales for proving the funding for me to carry out my studies.

I would like to thank the CCMRC group for all the help throughout my PhD; you've made my time an extremely enjoyable experience. I would especially like to thank Andrew Sanders for being such a supportive, patient and generous supervisor. I appreciate how no matter what you were doing, you'd always take the time to listen to my (many) questions, whatever the issue. You particularly have made my PhD both informative and enjoyable; you've not just been a fantastic supervisor, but also a great friend throughout. I would also like to acknowledge Liam Morgan for the help with various questions, Fiona Ruge for your approachable nature and help with my tissue work, Emily Telford for the help with formatting and the CCMRC group for help with general laboratory work including use of buffers and reagents.

I would also like to thank my mother and father who have always encouraged and supported me, both in my academic career and throughout my whole life. You have always been there for me and I have both of you to thank for everything I am today.

Finally, I would like to dedicate this work to my partner Kate, and thank you for being with me and encouraging me throughout. Your support has been amazing, you gave me the motivation and determination to overcome the difficulties and frustrations and I couldn't have done it without you. I am eternally grateful for your patience and encouragement, and I look forward to spending the rest of my life with you.

Publications

Full papers published:

COLLINS RJ, JIANG WG, HARGEST R, MASON MD, SANDERS AJ. EPLIN: a fundamental actin regulator in cancer metastasis? *Cancer Metastasis Rev.*2015 Dec;34(4):753-64. doi: 10.1007/s10555-015-9595-8.

Papers in preparation:

COLLINS RJ, MORGAN LD, OWEN S, RUGE F, JIANG WG, SANDERS AJ. *Mechanistic action of EPLIN in prostate cancer progression.*

COLLINS RJ, MORGAN LD, OWEN S, RUGE F, JIANG WG, SANDERS AJ. *Implications of Epithelial Protein Lost in Neoplasm in prostate cancer establishment at the bone environment*

Abstracts and conference presentations

Poster presentations:

ROSS J. COLLINS, ANDREW J. SANDERS, RACHEL HARGEST, JIAFU JI, CHUNYI HAO, KE JI, MALCOLM D. MASON, WEN G. Jiang. *Clinical implications of EPLIN in pancreatic cancer.* China-UK Cancer conference (CUKC) 17th – 18th July 2015, City Hall, Cardiff, UK.

ROSS J. COLLINS, ANDREW J. SANDERS, RACHEL HARGEST, MALCOLM D. MASON, WEN G. JIANG. *A potential role of Epithelial Protein Lost in Neoplasm (EPLIN) in prostate cancer metastasis* Cancer Research Wales (CRW) symposium 1st March 2016, SWALEC stadium, Sofia Gardens, Cardiff, UK.

Oral presentations:

ROSS J. COLLINS, ANDREW J. SANDERS, WEN G. JIANG. *Aberrant expression of Epithelial Protein Lost in Neoplasm (EPLIN) in the progression of pancreatic cancer.* Capital Cancer Conference, 17th October 2015, Beijing, China.

ROSS J. COLLINS, ANDREW J. SANDERS, WEN G. JIANG. *A putative role for EPLIN in prostate cancer metastasis.* Division of Cancer and Genetics, 9th February 2016, Cardiff University, Cardiff, UK.

Summary

Prostate cancer is the second most common cancer in the UK and incidence is gradually rising. Prostate cancer has a specific tendency to establish bone metastases, and this process significantly affects patient mortality and morbidity. This PhD evaluates the importance of EPLIN in the development and progression of prostate cancer, aims to explore any relevance of EPLIN in the establishment of bone metastases and to clarify the functional and mechanistic implications governing EPLIN biology in prostate cancer.

EPLIN expression was established in clinical prostate cancer tissue and prostate cancer cell lines and revealed a downregulation or loss of EPLIN in more aggressive cancer phenotypes. Importantly, EPLIN was abolished in clinical cancer sections including hyperplasia and adenocarcinoma, in addition to being markedly lost in aggressive cell lines PC-3, LNCaP and VCaP. Subsequently, EPLINα, the main isoform linked to cancer progression, was overexpressed in PC-3 and LNCaP cells lines to explore the functional significance of EPLINα at a cellular level. *In vitro* functional analyses revealed EPLINα is able to influence several tumour cell characteristics. EPLINα overexpression reduced cell proliferation, migration and invasion, and was able to increase cellular adhesion, when compared to control cell lines. EPLINα expression was also explored in an *in vitro* bone environment via culturing cells with Bone Matrix Extract solution, and also using a co-culture method with human osteoblasts.

To establish the mechanism of action of EPLINα in prostate cancer progression, the EPLIN interactome was evaluated, identifying several key molecular associations.

EPLINα expression influenced transcript, protein and phosphoprotein expression of signalling molecules paxillin and FAK in PC-3 and LNCaP cell lines. Lastly, a protein microarray was performed and identified several potential signalling pathways for EPLINα's mechanism in prostate cancer. Namely, molecular associations between EPLINα and ITGB1, ERK1/2 and Src were identified for validation and verified by Western Blotting, proposing a role for EPLINα's ability to regulate the aggressive characteristics of prostate cancer cells.

Collectively, this thesis explores the functional role of EPLIN in prostate cancer progression and provides insights into the mechanism of action of EPLIN in prostate cancer pathophysiology.

Contents

Table of Figures

Table of Tables

Abbreviations

AJ: Adherens Junction

ALCAM: activated leukocyte cell adhesion molecule

AP-1: Activator protein 1

APS: Ammonium Persulfate

AR: Androgen Receptor

ARCaPM: Androgen Refractory Cancer of the Prostate

AREs: Androgen Response Elements

Arp2/3: Actin related protein 2/3 complex

ARPC1A: Actin related protein 2/3 complex, subunit 1A

Arv1: ACAT-related protein required for viability 1

ATP6V1B1: ATPase, H+ transporting, lysosomal 56-58kDa, V1 subunit B1

BAP: Bone-specific alkaline phosphatase

bFGF: basic fibroblast proliferation factor

BME: Bone matrix extract

BMP6: Bone-morphogenetic protein-6

BSA: Bovine Serum Albumin

Cav-1: Caveolin-1

ccRCC: clear-cell renal cell carcinoma

cdc42: cell division cycle 42

CDH1: Cadherin 1

CDS: Coding DNA sequence

CFC: Change From Control

C-src – Cellular proto-oncogene tyrosine-protein kinase src

CTNNA1: Catenin-α1

CTNNB1: Catenin-β1

CTNND1: Catenin-δ1

DAB: Diaminobenzidine

DEPC: Diethyl pyrocarbonate

DHT: Testosterone and Dihydrotestosterone

DMEM: Dulbecco's Modified Eagle's Medium

DRE: Digital Rectal Exam

ECM: Extracellular Matrix

EDTA: Ethylene Diaminetetraacetic Acid

EGF: Epidermal proliferation factor

EMT: Epithelial-mesenchymal transition

EPLIN: Epithelial Protein Lost in Neoplasm

ERK: Extracellular signal–regulated kinase

ETK: Epithelial and endothelial tyrosine kinase

FAK: Focal Adhesion Kinase

FAT: Focal adhesion targeting

FCS: Foetal Calf Serum

FERM: N-terminal ezrin-radixin-moesin

GAPDH: Glyceraldehyde 3-phosphate dehydrogenase

GEO: Gene Expression Omnibus

GRAF: GTPase Regulator Associated with Focal adhesion Kinase (

Grb2: Proliferation Factor Receptor Bound Protein

GTP: Guanosine triphosphate

HIFU: High intensity focused ultrasound

HPV: Human Papilloma Virus

IGF1: Insulin-like proliferation factor 1

IHC: Immunohistochemistry

IL-6: Interleukin 6

ILK: Integrin Linked Kinase

ITGB1: Integrin beta 1

KIF14: Kinesin Family Member 14

LB: Luria Bertani

LIMA1: LIM domain and actin binding 1

MAPK: Mitogen Activated Protein Kinase

MIP-1α: Macrophage inflammatory protein 1 alpha

MPGN: Membranoproliferative glomerulonephritis

NF-kB: Nuclear factor kappa-light-chain-enhancer of activated B cells

NHS: National Health Service

NICE: National Institute for Health and Care Excellence

N-WASP: Neural Wiskott - Aldrich syndrome Protein

OPG: Osteoprotegerin

p120 RASGAP: P120-Ras GTPase activating protein

P1NP: Procollagen type 1 amino-terminal propeptide

PAK1/2/3: Serine/threonine-protein kinase 1/2/3

PBS: Phosphate buffered saline

PCa: Prostate cancer

PCR: Polymerase Chain Reaction

PDGF: Platelet derived proliferation factor

PINCH-1: Particularly interesting new cysteine-histidine-rich protein-1

PLCγ: phospholipase Cγ

PSA: prostate specific antigen

PTEN: Phosphate and tensin homology

PTHrP: Parathyroid hormone related peptide

PTPLAD1: Protein tyrosine phosphatase-like a domain containing 1

PVDF: Polyvinylidene fluoride

Q-PCR: Quantitative Polymerase Chain Reaction

Rac1: Ras-related C3 botulinum toxin substrate 1

RANK: Receptor Activator of Nuclear factor kappa-B

RANKL: Receptor Activator of Nuclear factor kappa-B ligand

RTPCR: Reverse Transcription Polymerase Chain Reaction

SATB2: Special AT-rich sequence-binding protein 2

SDS-PAGE: .Sodium dodecyl sulfate polyacrylamide gel electrophoresis

SFM: Serum Free Medium

SH2: Src homology 2

SH3: Src homology 3

SOCS: suppressor of cytokine signalling

Src: Proto-oncogene tyrosine-protein kinase src

SVIL: Supervillin

TBE: Tris-Boric-Acid-EDTA

TBS: Tris Buffered Saline

TEMED: Tetramethylethylenediamine

TGF: Transforming proliferation factor

TMA: Tissue Microarrays

TNF: Tumour necrosis factor

TNM: Tumour Node Metastases

TRI: Total RNA Isolation

TRUS: Transrectal ultrasound-guided biopsy

TURP: Transurethral resection of the prostate.

UBC: Ubiquitin C

VEGF: Vascular endothelial proliferation factor

VEGFR1: Vascular endothelial proliferation factor receptor 1

WHO: World Health Organisation

YWHAH: Tyrosine 3-monooxygenase/tryptophan 5-monooxygenase activation protein

Chapter I: Introduction

1.1 Cancer

Cancer categorises over 200 types of disease and is a growing problem worldwide. Cancer originates following transformation of healthy cells to cancerous cells, a process involving abnormal cell proliferation and potential invasion of surrounding tissue. Cancer cells have various characteristics and traits which make them difficult to treat and manage and these include extensive cell proliferation, cellular invasion, increased motility and proliferation, evasion of cell death and the ability to ignore physiological extracellular signals like hormones and proliferation signals. These characteristics allow an abundant proliferation of cells, which divide continuously, leading to possible tumour formation. If a tumour is formed, it can potentially move to various sites in the body and this process is called metastasis (Hanahan and Weinberg, 2011). Cancer metastasis is a complex and sophisticated process which creates various complications for patients diagnosed with cancer. According to the World Health Organisation (WHO), 8.2 million people died from cancer in 2012 worldwide (WorldHealthOrganisation, 2016a). This clearly illustrates that better treatment, diagnosis and management of the disease is required. Although different cancers share characteristics in cancer progression, each cancer type can be unique in its mechanism of action, its pathophysiology and morphology, along with methods for diagnosis and treatment. This PhD will focus on prostate cancer metastasis and how the molecule Epithelial Protein Lost in Neoplasm (EPLIN) is associated with prostate cancer development and progression.

1.1.1 The prostate gland: structure, function and development

The prostate gland is an exocrine gland below the bladder whose main role is in the secretion of prostatic fluid which contributes to the production of semen in men

(CancerResearchUK, 2016h). The prostate is described as being the size of a walnut and can range in weight from 7-16 grams, consisting of various anatomical components including fibrous, elastic, vascular, lymphatic and muscular tissue (Leissner and Tisell, 1979, Wilson, 2014). The tissue morphology of the prostate gland consists predominantly of basal cells, luminal cells and neuroendocrine cells (ProstateCancerUK, 2016d) (Figure 1.1). These compact epithelial cells line the prostate and it is here where cancer can originate (ProstateCancerUK, 2016d).

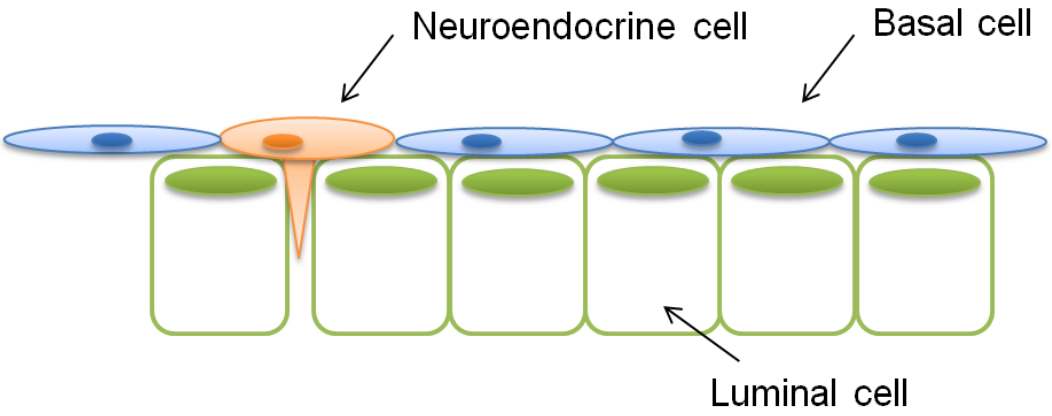

Figure 1.1 Schematic representation of the cellular morphology in the prostate gland.

Adapted from (ProstateCancerUK, 2016d).

For appropriate prostate gland function, regulation of the molecules and mechanisms involved in prostate organogenesis is crucial. The prostate generates from an area at the bottom of the bladder called the urogenital sinus and this happens at around the 9th week of embryonic development in males (Thomson, 2008). The prostate is an accessory sex gland with branched epithelia and is responsible for secreting various proteins and sugars into seminal plasma and thus contributing to a high proportion of the seminal fluid (Murashima et al., 2015). Key molecules in prostate gland development are groups of hormones called androgens. Androgen function relies on signalling mechanisms via the androgen receptor (AR), which is a member of the nuclear receptor superfamily (Escriva et al., 2000).

1.1.2 Prostate cancer: statistics

Cancer of the prostate occurs when healthy cells located in the prostate gland are transformed, begin to divide abnormally and ignore physiological body cell signals. What causes this is unknown, but there are various factors which can increase the likelihood of onset of prostate cancer. Approximately 1.11 million men were diagnosed with prostate cancer in 2012 worldwide (CancerResearchUK, 2017). In the UK, prostate cancer is the most common male cancer with 47,300 men diagnosed annually in 2013 (CancerResearchUK, 2017). In 2014, approximately 307,000 men died from prostate cancer across the world, including 11,287 men from the UK, making prostate cancer the second most common male cancer killer in the UK following lung cancer (CancerResearchUK, 2017). The incidence of prostate cancer has steadily increased over the last 40 years (Figure 1.2), with biggest increases in disease incidence occurring in the early 1990's and early 2000's (CancerResearchUK, 2017). This increase is not limited to men in the UK, with the

number of intermediate and high risk prostate cancers also on the rise in the United States; recent data suggests the number of men with higher-risk prostate cancer has increased sequentially by 3% each year from 2011-2013 (Hall et al., 2015). The reason for this steady increase in the rate of prostate cancer is generally unknown; however it is likely that better modern day detection and screening methods are contributors in addition to increased public awareness of cancer.

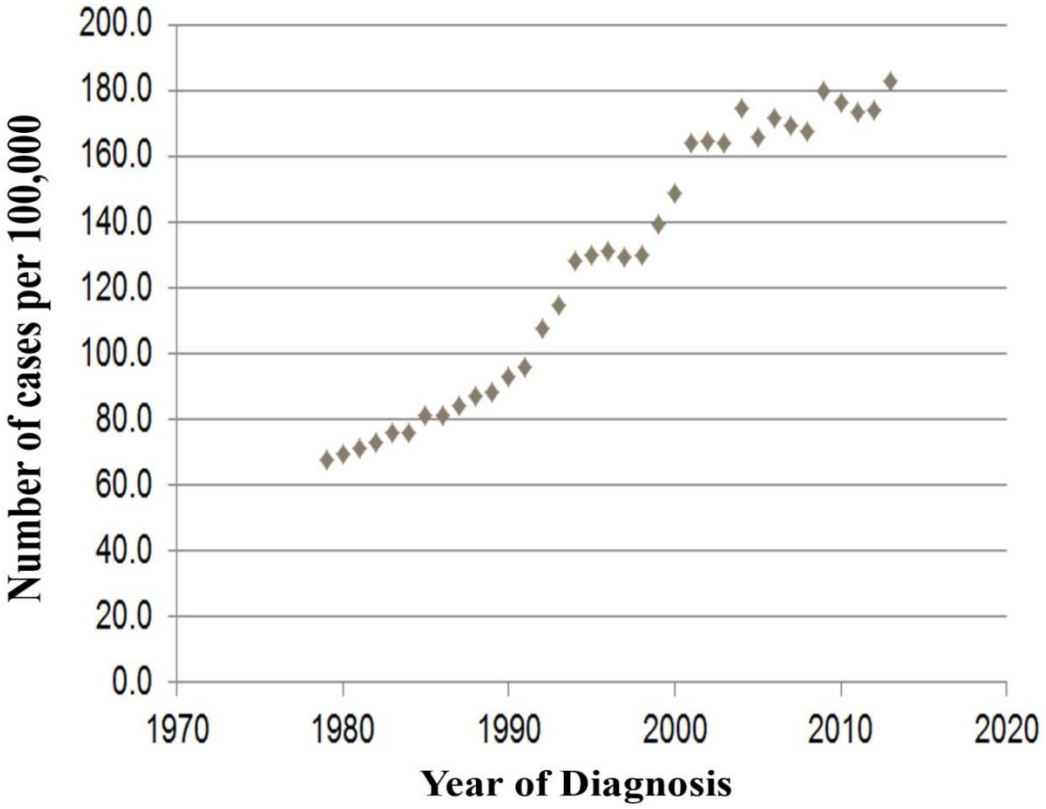

Figure 1.2 The incidence of prostate cancer in the UK between 1970 and 2013.

Adapted from (CancerResearchUK, 2017).

1.1.3 Prostate cancer: Detection

Early diagnosis and detection of prostate cancer is critical to successfully manage and treat the disease. Prostate cancer presents various signs and symptoms and doctors regularly check for these to ensure the right diagnostic test is used if required. In 2015, the National Institute for Health and Care Excellence (NICE) published guidelines for doctors to aid diagnosis (NationalInstituteforHealthandCareExcellence(NICE), 2016), and the symptoms include:

- Increased need to urinate
- Difficultly urinating
- Weak or interrupted flow of urine
- Blood in urine or semen
- Painful or burning urination
- Erectile dysfunction
- Painful ejaculation

If someone experiences some of these symptoms, it is recommended they visit their GP in order to be examined for presence of prostate cancer (ProstateCancerFoundation, 2016).

1.1.3.1 Prostate Specific Antigen (PSA) testing

PSA was discovered three decades ago and named as the prostate specific antigen in 1970 by Richard J Ablin (Ablin et al., 1970, Ablin, 1985). It is a glycoproteinenzyme encoded in humans by the KLK3 gene, and also known as gamma-seminoprotein or

kallikrein-3 (KLK3)(Lundwall and Lilja, 1987) and initially purified from prostate tissues (Wang et al., 1979) and blood (Papsidero et al., 1980). PSA is secreted by the prostate epithelial cells, with a main function in liquidifying semen and allowing sperm to freely swim (Ablin et al., 1970, Ablin, 1993, Wang et al., 1981, Ablin, 1985).

The PSA test involves a blood test which determines the level of PSA in a patient's blood. PSA is a protein produced by the prostate gland present in both normal and cancer cells, however the amount of PSA in normal cells increase with age and higher levels of PSA may be an indication of altered prostate function (ProstateCancerUK, 2017). Prostate cancer can cause the amount of PSA production to be upregulated, so a PSA test is used to evaluate levels in the blood to give indication of prostate cancer presence. The main drawback of PSA testing is its specificity; PSA testing will not give a definitive answer for prostate cancer, it is only a predictive test and some men with prostate cancer may not have raised PSA (NHS, 2016a, Ablin, 2000, Haythorn and Ablin, 2011). In addition, some men with high PSA level may not have cancer but can be attributed to conditions like prostatitis or benign prostatic hyperplasia (BPH) (Sarwar and Adil, 2017). The lack of specificity with PSA testing creates a fundamental problem for doctors and patients in diagnosis of the disease and illustrates the critical demand for a specific molecular test in determining cancer initiation and establishment.

1.1.3.2 Digital Rectal Exam (DRE)

Once PSA levels have been established, the next confirmatory measure would be a DRE, carried out by a GP. A DRE is a physical exam where a doctor puts a

lubricated, gloved finger into the rectum of the patient with another hand on the lower back. This is done to evaluate proliferation or enlargement of the prostate, including if the gland is hard or bumpy which could indicate presence of a tumour (WebMD, 2016a).

1.1.3.3 Biopsy

Following on from a PSA test and a DRE, a GP may refer the patient to a specialist or consultant at a hospital to discuss further diagnostic testing. The most common procedure after the initial tests is a transrectal ultrasound-guided biopsy (TRUS) (NHS, 2016a). This involves a probe which is inserted into the rectum and produces harmless high-frequency sound waves which can be used to generate an image of the prostate gland (WebMD, 2016b). These images are then used to estimate the size of the prostate and provide indication of any unusual proliferations (WebMD, 2016b). Once the images are taken, a doctor can then visualise where a biopsy needs to be taken and a needle is passed through the rectum wall and tissue is extracted from the prostate (NHS, 2016a). Once the sample is taken, the biopsy can be analysed in a laboratory and if any cancer cells are found they can be studied further to decide their metastatic capacity. The next step in prostate cancer detection is to evaluate the stage and grade of a cancer.

1.1.4 Prostate cancer: Staging and grading

Staging and grading of a cancer describes how far along a cancer may have progressed and is useful for deciding the type of treatment which is necessary. For prostate cancer detection, the TNM system is used (Table 1.1), standing for Tumour (T), Node (N) and Metastases (M) (ProstateCancerUK, 2016e). The early stages (T

stages) represent the initial developments which occur when a tumour is formed in the prostate gland (Figure 1.3). Node stages demonstrate tumour stages with nodal involvement, and Metastases stages illustrate advanced stages of tumour development where metastases are present. Table 1.1 illustrates the differences in staging and how each stage is identified.

Table 1.1 Prostate cancer TNM staging.

Adapted from (CancerResearchUK, 2016f).

Stage	Description
T1	Localised prostate cancer, small tumours, too small to be seen/felt during prostate examination, possible to be identified by needle biopsy or seen under microscope
T2	Localised prostate cancer, cancer is big enough to be seen on scans but is contained inside the prostate gland. Stage T2 can be divided into 3 sub-stages; T2a, T2b and T2c.
T2a	Localised prostate cancer, the tumour is in only half of one of the lobes of the prostate gland
T2b	Localised prostate cancer, the tumour is in more than half of one of the lobes of the prostate gland
T2c	Localised prostate cancer, the tumour is in both of the lobes of the prostate gland
T3	Locally advanced prostate cancer, the cancer starts to break away through the capsule of the prostate; this can be felt/seen on a scan. The cancer is yet to spread to additional organs. Stage T3 can be divided into 2 sub-stages; T3a and T3b.
T3a	Locally advanced prostate cancer, the cancer has broken through the capsule of the prostate but is yet to spread to the seminal vesicles.
T3b	Locally advanced prostate cancer, the cancer has broken through the capsule of the prostate and has spread to the seminal vesicles.
T4	Locally advanced prostate cancer, the cancer has penetrated the capsule of the prostate and began to infiltrate organs of the body in the immediate area, such as the bladder and the rectum.
NX	Locally advanced prostate cancer. Stage NX is when the lymph nodes cannot be measured.
N0	Locally advanced prostate cancer. Stage N0 is when the lymph nodes can be measured and reveals there are no cancer cells in lymph nodes surrounding the prostate.
N1	Locally advanced or metastatic advanced prostate cancer. Stage N1 is when the lymph nodes surrounding the prostate are measured and contain cancer cells.
MX	Locally advanced or advanced metastatic prostate cancer. Stage MX may indicate results were unclear as to whether metastases were present or not.
M0	Locally advanced or advanced metastatic prostate cancer. Stage M0 means the cancer hasn't progressed outside of the pelvic region.
M1	Locally advanced or advanced metastatic prostate cancer. Stage M1 means the cancer has progressed outside of the pelvic region.
M1a	Advanced metastatic prostate cancer. Stage M1a indicates there are cancer cells in lymph nodes outside of the pelvic region.
M1b	Advanced metastatic prostate cancer. Stage M1b indicates there are cancer cells present in the bone.
M1c	Advanced metastatic prostate cancer. Stages M1c indicates there are cancer cells in other organs such as the liver, brain or lungs.

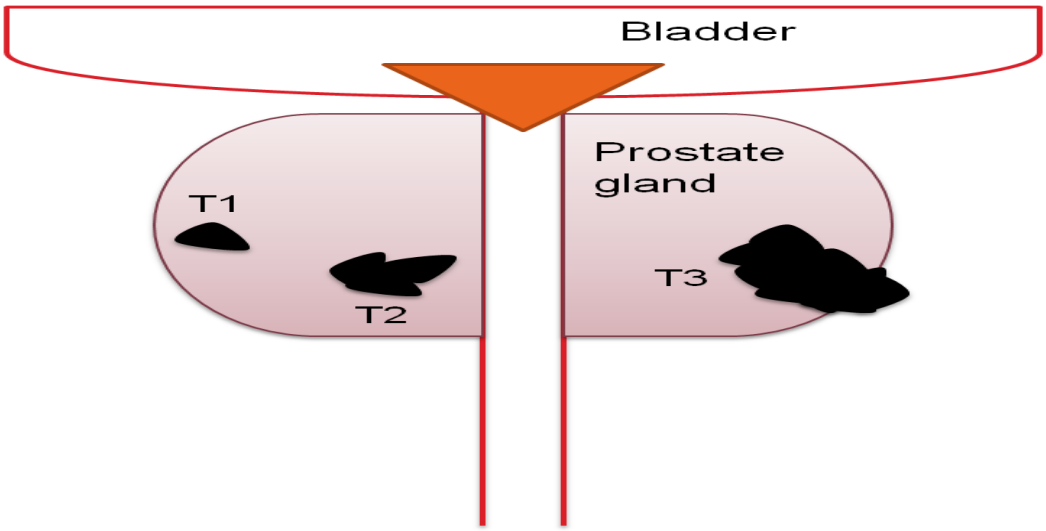

Figure 1.3 Schematic representation illustrating early stages of prostate cancer development.

The prostate gland is situated below the bladder. The proximity to the bladder and urinary organs can lead to bladder related issues when cancer is present. T1 prostate cancer is the first stage of prostate cancer where the cancer is difficult to observe during a prostate examination. The next stage, T2, is when the cancer has grown slightly larger and can now be clearly identified on prostate scans. Stage T3 is where the cancer first starts to penetrate the lining of the prostate. This stage can be both felt during a prostate examination and seen on a prostate scan. During T3 the cancer has yet to reach other organs of the body but may have reached the seminal vesicles near the prostate.

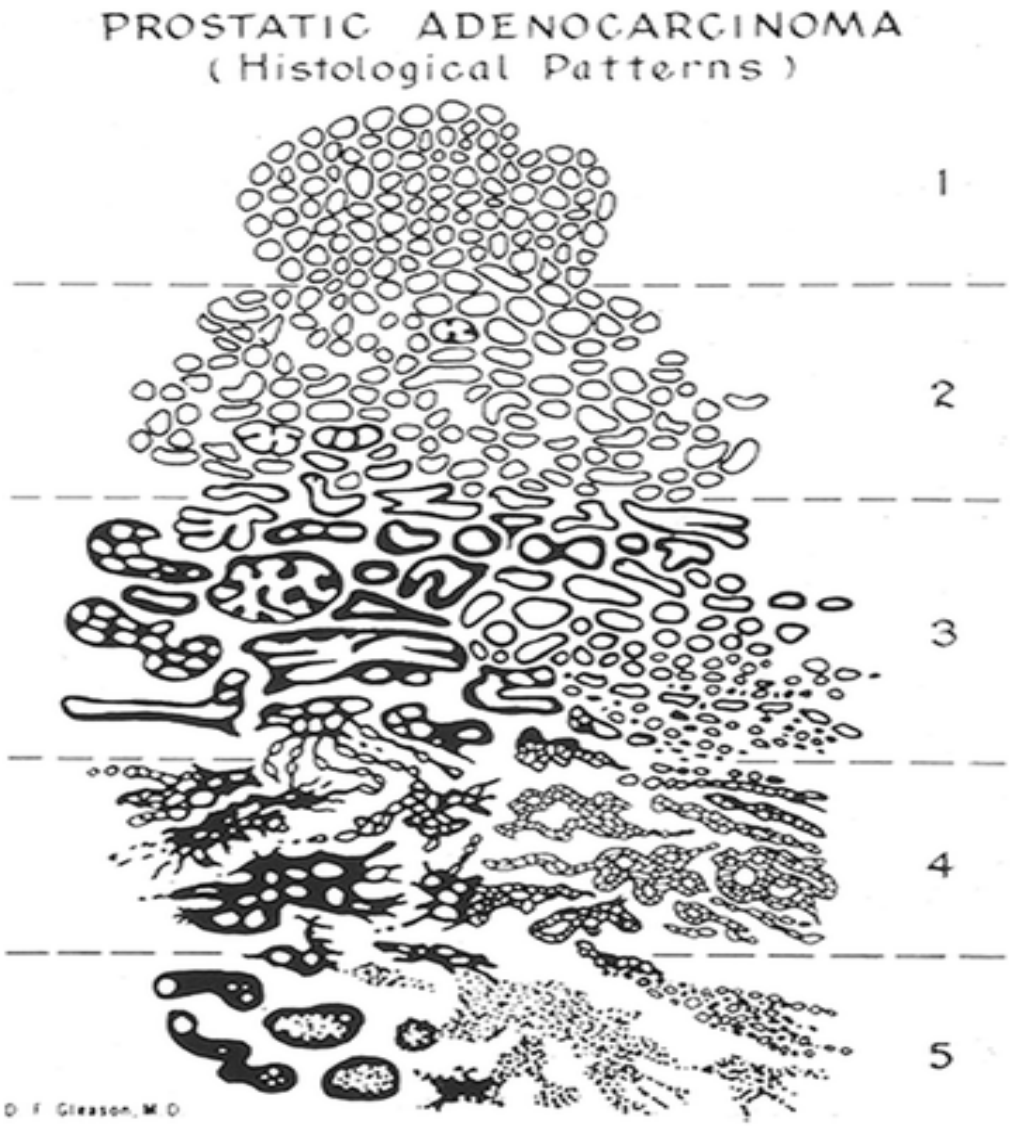

Figure 1.4 Illustration of Gleason Grading System, a microscopic based grading method for prostate cancer (Gleason et al 1974).

The total Gleason score is generated from the sum of two key scoring: The appearance of the most common cell morphology and the appearance of the second most common cell morphology are each assigned to grade 1-5. Using this system the most well-differentiated tumours have a Gleason score/grade of 2, and the least-differentiated tumours a score of 10. Grade 2-4 being well-differentiated neoplasm, Grade 5-6 intermediate-grade neoplasm, Grade 7 moderately - poorly differentiated grade neoplasm, Grade 8-10 high-grade neoplasm.

The prostate cancer staging system is used to describe how far the cancer has spread, starting with primary localised prostate cancer and finalising with advanced metastatic cancer. Additionally, a method to determine how aggressive the cancer will be is calculated using the Gleason score and Gleason grade, named after David Gleason who initiated the scoring method (Gleason and Mellinger, 1974) and modified in the following decades (Brimo et al., 2013) (Figure 1.4). Once the tissue biopsy has been evaluated under a microscope in the laboratory, a Gleason score is determined using a total of Gleason grades, and this illustrates the level of differentiation to the cells. The morphology or pattern of the tumour is given a Gleason grade by numbering from 1-5, depending on the extent of abnormality to the cells, with 1 being the lowest and 5 the highest, then varying Gleason grades are added together to give an overall Gleason score (ProstateCancerUK, 2016c). The two most common morphologies of tissue are graded, then added together to give the Gleason score. The higher the Gleason score, the more aggressive the tumour is and more likely it is to spread to distinct areas of the body (TackleProstateCancer, 2016). The tests described above provide significant clues on whether the cancer will metastasise and become more aggressive, infiltrating other areas of the body, in addition to providing aspects on patient morbidity and mortality. However, the main disadvantage for the tests in use for prostate cancer diagnosis and prognosis is the specificity of the test; currently, there is no single diagnostic assay which can give a definitive result for presence of prostate cancer and whether a cancer will metastasise or not. For this to be achieved, a specific, molecular target which correlates with prostate cancer progression is therefore required. A crucial part of this PhD will be to evaluate EPLIN for its role in prostate cancer and to establish whether EPLIN can be

successfully utilised as a suitable prognostic marker or therapeutic strategy for prostate cancer development and progression.

1.1.5 Prostate cancer: Risk factors

The cause of prostate cancer is unknown but there are various risk factors which can increase the likelihood of developing prostate cancer. Age and ethnicity are prominent factors determining prostate cancer risk. Men in their 20's have been reported to have a 1-2% chance of developing histological prostate cancer, whereas men aged 90+ have a 59-72% risk of developing the disease (Leal et al., 2014). Similar reports have been made highlighted age as a critical risk factor of prostate cancer development with men younger than 39 having a 0.005% risk of developing the disease, with the risk increasing to 13.7% for men aged 60-79 (AmericanCancerSociety, 2007). Men most at risk are aged 65-75 and this age group contributed ~62% of all new prostate cancer cases in the UK between 2009 and 2011 (Figure 1.5) (CancerResearchUK, 2017). Estimations on ethnic associations with prostate cancer have also highlighted areas of risk for males; white men, for example, have been reported to be at significantly higher risk than Chinese/Japanese men (Leal et al., 2014). Additionally, black men are the most susceptible in developing prostate cancer, and it has been estimated that 1 in 4 British black men will acquire prostate cancer during their lifetime (ProstateCancerUK, 2016b). Recent estimations in England reveal that black men are twice as likely as white men to develop, and die from, prostate cancer (Lloyd et al., 2015).

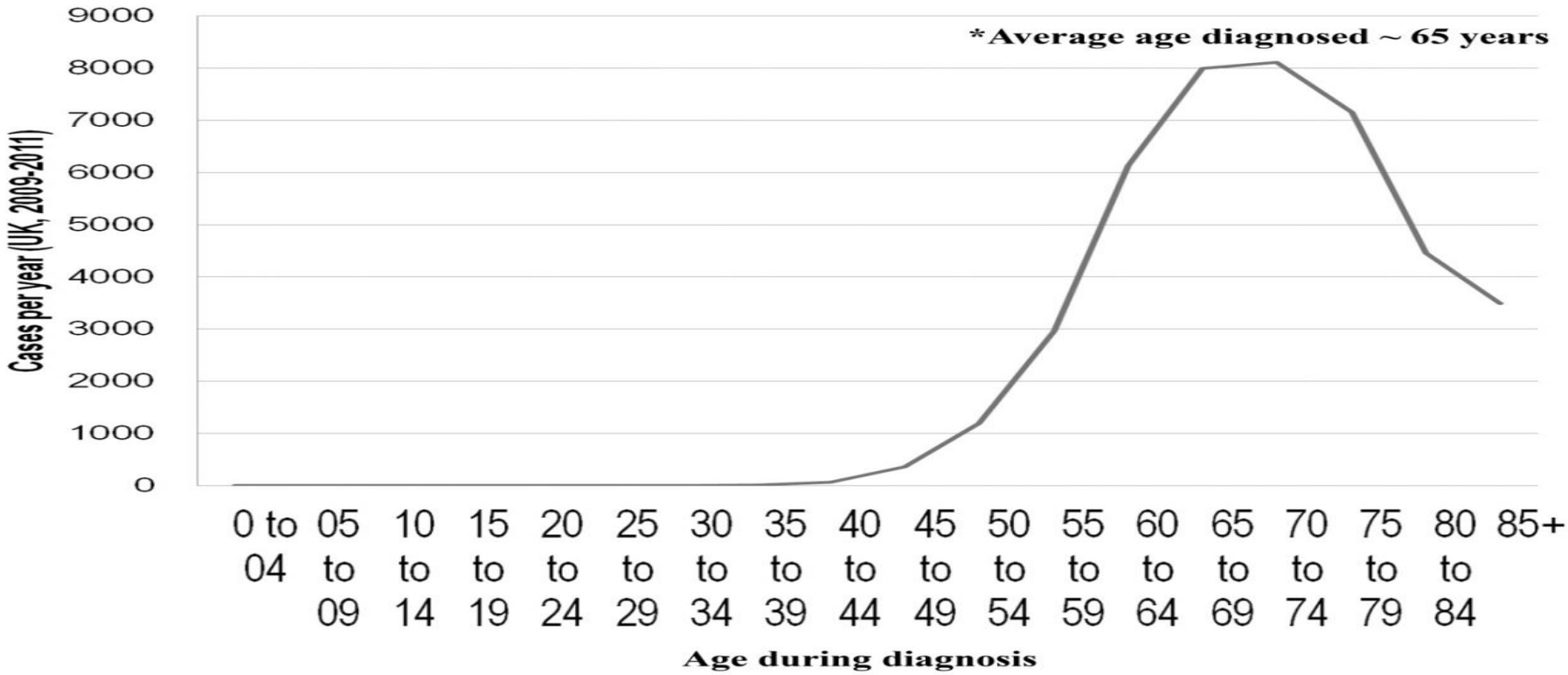

Figure 1.5 Average number of male new prostate cancer cases per year based on age of individual, UK, 2009-2011.

Adapted from (CancerResearchUK, 2017).

1.1.5.1 Risk factors: Diet and lifestyle

There is also growing evidence that prostate cancer may be circumvented by modifications to diet and lifestyle, with certain lifestyle choices having a reduced risk of disease onset. For example, diets that are high in naturally occurring phytochemicals like lycopene, curcumin and resveratrol may induce cancer protective effects (Bommareddy et al., 2013). The cancer protective effects of these dietary compounds have been analysed recently in prostate cancer cell lines PC-3, DU-145 and immortalised normal prostate cell line PNT-2 where addition of lycopene influenced cell adhesion and migration of cancer cells (Elgass et al., 2014). The use of curcumin, resveratrol and lycopene also has potential as anti-cancer foods via their ability to target tumour angiogenesis. These compounds have been shown to exert anti-angiogenic effects, with stronger anti-angiogenic efficacies than certain cancer drugs like Tamoxifen (Li, 2010) suggesting a combination of medical treatment and dietary treatment may be optimal for treating cancer proliferation and progression. Other dietary measures which could be implemented to protect from cancer include a plant based lifestyle void of animal products. There is growing evidence to suggesting eliminating animal products from a person's diet can lead to a reduced risk of not only cancer, but other chronic ailments like heart disease and diabetes, in addition to increasing longevity (Dinu et al., 2016, Gilsing et al., 2016, van Nielen et al., 2014). A recent comprehensive meta-analysis illustrated a significant protective effect from total cancer (-8%) and ischemic heart disease (-25%) of those who adopted a vegetarian diet vs. those who chose to eat meat (Dinu et al., 2016). In prostate cancer, a recent report demonstrated how a vegan lifestyle

can reduce the risk of developing prostate cancer by up to 35% (Tantamango-Bartley et al., 2016). This compliments previous work in prostate cancer and lifestyle intervention where LNCaP cells were incubated with serum of someone eating standard American diet vs. those eating a plant based diet (Ornish et al., 2005). The study revealed that treatment of LNCaP cells with blood of those eating a plant based diet had an eight fold inhibitory action on LNCaP proliferation compared to cells treated with serum of participants consuming a standard American diet, and further illustrates the potential of a plant based/vegan lifestyle in the prevention of prostate cancer in this model (Ornish et al., 2005). These data compliments recent announcements from the World Health Organisation that processed meat is carcinogenic and red meat is a likely carcinogen (WorldHealthOrganisation, 2016b). Various other animal products like calcium containing dairy products may also contribute to cancer progression (Raimondi et al., 2010). Calcium levels in milk greater than 2000mg/d have been associated with advanced stage and high grade prostate cancer (Wilson et al., 2015). Other dietary issues include a low dietary fibre intake which can increase the likelihood of prostate cancer and may act via influencing sex hormone levels (Sawada et al., 2015). Other elements influencing prostate cancer may be higher levels of cadmium and folate where high levels are associated with increased prostate cancer risk (CancerResearchUK). Lastly, in addition to dietary measures, there is growing evidence to suggest increased exercise and physical activity, opposed to a sedentary lifestyle may have a protective effect in prostate cancer (Peisch et al., 2016). Accompanying dietary measures and exercise, smoking may have a detrimental effect on prostate cancer development with smokers potentially being at an increased risk of prostate cancer incidence and mortality (Islami et al., 2014, Huncharek et al., 2010).

1.1.5.2 Risk factors: Family history and genetics

Prostate cancer susceptibility can also be related to family history. Men who have a father or brother with prostate cancer are significantly more likely to develop the disease (CancerResearchUK, 2016c, ProstateCancerUK, 2016a) Research suggests known cancer genes *BRCA1* and *BRCA2* may be involved in prostate cancer development (CancerResearchUK, 2016c, ProstateCancerUK, 2016a). The *BRCA1* gene has been implicated in prostate cancer in a number of publications (Fiorentino et al., 2010, Mitra et al., 2011, Leongamornlert et al., 2012). For example, a nonsynonymous A>G substitution at c.1067 of chromosome 17q21, resulting in a Glu-Arg amino acid change at position 356, has been associated with prostate cancer susceptibility (Douglas et al., 2007). Further genetic and molecular changes have also been implicated in the pathogenesis of prostate cancer. The tumour suppressor gene, Phosphate and tensin homology (*PTEN*), is down-regulated or deleted in a number of cancer types and frequently is so in prostate cancer (Li et al., 1997). Additional genetic changes in prostate cancer can include modifications to the AR. During physiological processes, Testosterone and Dihydrotestosterone (DHT) bind to the androgen receptor (AR) in the cytoplasm; this causes the AR to translocate to the nucleus and bind to Androgen Response Elements (AREs) in target genes to engender cellular processes like cell proliferation and apoptosis (Figure 1.6) (Heinlein and Chang, 2004). However, when this process goes awry due to genetic changes to the AR, for example, variability in the polymorphic CAG repeat sequence which regulates transcriptional activity, an increased risk of prostate cancer is frequently associated (Giovannucci et al., 1997). Due to the complexity of cancer cell biology, the molecular pathology of prostate cancer remains largely elusive.

Different genes exert various downstream cellular effects and may be subject to deleterious mutation, potentially initiating a cascade of complications ultimately leading to cancer.

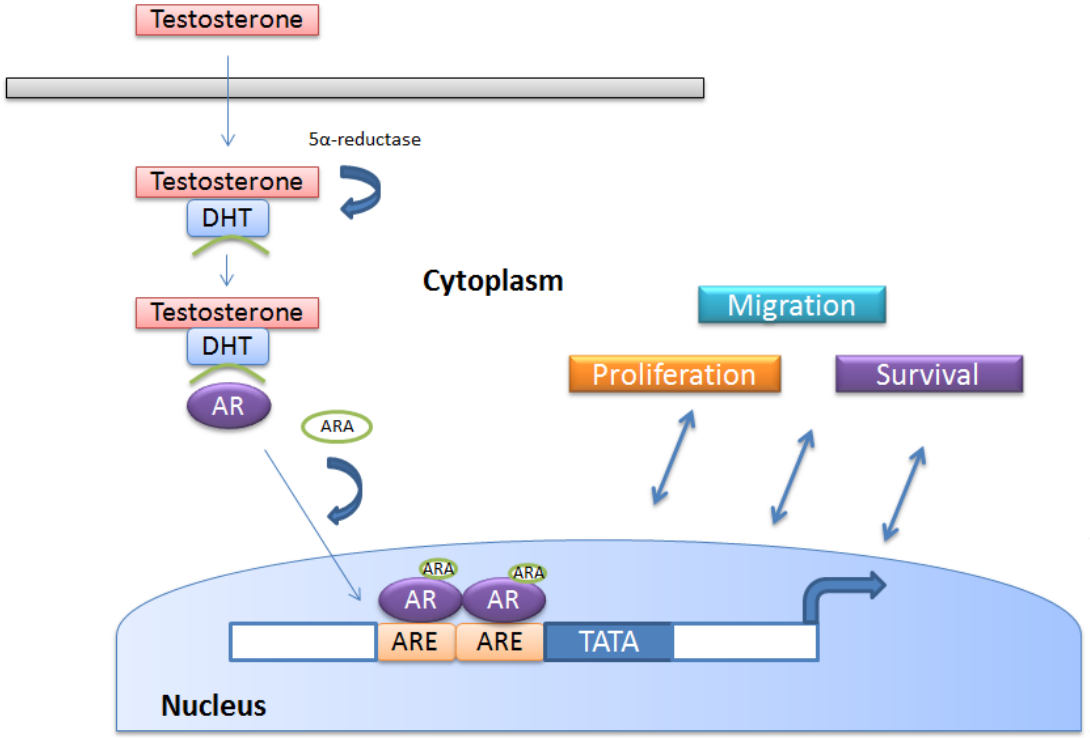

Figure 1.6 Action of Androgen receptor in prostate gland.

Binding of Testosterone and DHT to the androgen receptor causes association with androgen receptor coregulators (ARAs) and translocation of the AR to the nucleus. At the nucleus the AR binds to AREs in the promoter region of target genes and causes downstream cellular processes. Adapted from (Lattouf et al., 2006).

1.1.6 Prostate cancer: Treatment

Currently, there are a number of different treatment options for people with prostate cancer. These typically include surgery (removal of the prostate gland), radiotherapy (use of high energy rays) and hormone therapy (targeting testosterone in the body) (CancerResearchUK, 2016g). Current treatment options, however, have a number of associated problems such as the harshness of certain treatments, cost and unavoidable side effects. For example, hormone therapy can lead to erectile problems (impotence), fatigue, long term weight gain, long term memory problems, depression and osteoporosis (CancerResearchUK, 2016e). As a way of avoiding side effects associated with prostate cancer treatment, some patients may opt for the monitoring of slow growing prostate cancer by long term tracking of the cancer, known as Watchful Waiting or Active Surveillance (ProstateCancerUK, 2016f). In addition to surgery, radiotherapy and hormone therapy, there are other treatments which could be utilised for suppressing or treating prostate cancer development, listed in Table 1.2.

Table 1.2 Prostate Cancer Treatment

Adapted from (ProstateCancerUK, 2016f) and (NHS, 2016b).

Treatment	Description
Radical Prostectomy (surgery)	Surgical removal of the prostate gland. This treatment can be used when a cancer has not metastasised and is localised to the prostate. Possible to remove cancer cells, however if not all cells are removed, the cancer may return. Side effects and risks include: erectile dysfunction, infertility and lack of ejaculate, urinary incontinence and in some very rare cases, death.
Radiotherapy	Radiation uses high energy beams and radiation to damage, prevent proliferation and kill cancer cells. Can be utilised to treat local cancer or slow down advanced cancer. The treatment is pain free but has side effects including: anal discomfort, tiredness and fatigue, loss of pubic hair, cystitis, erectile dysfunction, urinary incontinence and back passage issues.
Hormone therapy	Hormone therapy works by targeting testosterone and stopping it from reaching cancer cells and thus preventing cell proliferation. Hormone therapy is often used in conjunction with radiotherapy as a means of slowing down the cancer prior to radiation treatment. Side effects of hormone use include: erectile dysfunction, weight gain and loss of libido.
Temporal brachytherapy	Temporal brachytherapy is a treatment method utilising high dose radiation that is inserted into the prostate gland at varying intervals as a means of damaging or destroying the prostate cancer cells. Advantages of this treatment option include: quick and easy (1/2 day treatment) and that nearby healthy cells are less likely to be damaged due to receiving a smaller dose of radiation. Disadvantages of the treatment include: bowel, urinary and erectile issues, and lack of certainty as to whether the treatment has been successful. Side effects with the treatment include: tiredness and fatigue, urinary incontinence, erectile dysfunction and bowel issues.
Permanent seed brachytherapy	This treatment option is similar to temporal brachytherapy but uses low doses of radiation in the form of seed implants being inserted into the prostate gland. The treatment has similar advantages to temporal brachytherapy including lack of damage to surrounding tissue and length of treatment time. The disadvantages of the treatment include lack of certainty as to whether the treatment has worked, use of a general anaesthetic, and bowel, erectile and urinary issues. Side effects of the procedure include: semen discolouration and blood in urine, testicle bruising and pain, pelvic pain, urinary discomfort, frequent urination, erectile dysfunction, tiredness and fatigue, and urinary incontinence.
Transurethral resection of the prostate (TURP).	TURP is a procedure where a looped metal wire is inserted into the urethra to relieve pressure from the urethra. TURP doesn't prevent cancer but can aid some of the symptoms involved with other prostate cancer treatments.

High intensity focused ultrasound (HIFU) for prostate cancer	HIFU is a relatively low risk procedure used to kill cancer cells by heating them to high temperatures using high frequency sound waves that are inserted into the rectum using an ultrasound probe. Risks of HIFU can include urinary incontinence, erectile dysfunction and back passage issues. HIFU is usually a technique used for men who have localised prostate cancer rather than advanced cancer.
Cryotherapy	Cryotherapy is the use of extremely cold temperatures to destroy cancer cells. There are two types of this procedure known as Whole Prostate Cryotherapy where the whole prostate is frozen, or Focal Cryotherapy which targets the area where the cancer is in the prostate. Side effects of cryotherapy include urinary incontinence and erectile dysfunction.
Chemotherapy	Chemotherapy is the use of drugs to target and destroy cancer cells, usually utilised for advanced metastatic cancer. Chemotherapy isn't curative but aims to slow down cancer cell progression and development. The main drawback of chemotherapy is the lack of specificity, meaning healthy cells will also be damaged in addition to cancer cells. Side effects of chemotherapy include tiredness and fatigue, hair loss, vomiting and nausea and infections due to immunocompromisation.
Steroids	Steroids, like hydrocortisone and dexamethasone, are used to treat cancer cells by preventing cell proliferation and shrinking the tumour.
Bisphosphonates	Bisphosphonates are drugs specifically used to treat cancer that has spread to the bones. If a cancer has spread to bone sites, they can cause bone breakdown and osteolysis. Bisphosphonates aim to reduce this effect by promoting bone generation. Prostate cancer can cause both osteolytic lesion and osteoblastic lesions (more common in prostate cancer). Importantly, Bisphosphonates act to inhibit bone destruction by osteoclasts. As prostate cancer generally forms osteoblastic lesions when it moves to bone, it makes Bisphosphonates less effective for use in metastatic prostate cancer, compared to cancer which form osteolytic lesions (for example breast cancer). Bisphosphonates can also be used to alter calcium levels in the blood, as high blood calcium is common in patients with metastatic bone cancer. Side effects of Bisphosphonates include nausea and vomiting, flu-like symptoms, kidney issues and loss of appetite.
Abiraterone and Enzalutamide	Abiraterone and Enzalutamide are two new types of hormone therapy which can be utilised for men with advanced metastatic prostate cancer, specifically if other hormone therapies have previously failed. Abiraterone (also known as Zytiga® or abiraterone acetate) works via targeting the enzyme cytochrome P17 and, through this enzyme, prevents testosterone production thus causing shrinkage of the tumour. Enzalutamide (also known as Xtandi) is a drug which works via the androgen receptor which blocks male signalling hormones controlling cancer cells proliferation. As with abiraterone this will cause the tumour to shrink. Side effects of Enzalutamide include tiredness and fatigue, loss of fertility, muscle spasms and weakness and hot flushes. Side effects of Abiraterone include tiredness and fatigue, diarrhoea, high blood pressure, low potassium levels, bladder infections and heart problems.

As illustrated in the above table, there are various ways in which prostate cancer can be managed depending on how far the cancer has progressed and the type of cancer. A significant issue with almost all of the treatments however is the often debilitating risks and side effects of each individual treatment. The majority of prostate cancer patients undergo chemotherapy, hormone therapy and radiotherapy, all of which present unpleasant effects. This epitomises the global need for better treatment utilising a specific molecular target in prostate cancer.

1.1.7 The metastatic cascade

When cancer cells break away from the primary tumour and begin to move around the body, the process is known as metastasis. Metastasis and oncogenic progression is difficult to decipher and elucidating molecules involved in metastasis and their mechanism of action is extremely important in cancer biology. The transition of localised cancer to advanced, metastatic cancer involves various biochemical and morphological cellular changes. The process for how cells become cancerous was first evaluated in 1889 by a surgeon called Stephen Paget, where he postulated on how otherwise healthy cells became unhealthy and dysfunctional. This reasoning led to a milestone publication of his hypothesis which became known as the ‘seed and soil’ hypothesis of cancer (Paget, 1989b). Although little was known at the time of biochemical interactions and cell signalling mechanisms, the idea proposed that the process of cancer spread depends on interaction or cross-talk between various cancer cells (the ‘seeds’) and the surrounding microenvironment (the ‘soil’) (Fidler, 2003, Paget, 1989a). This discovery was ground-breaking and served as a basis for future discoveries and developments in the field of cancer biology and medicine.

Metastatic cancer arises when cancer cells escape the primary site where the tumour originated (for example, the prostate gland) and travel to a distinct, secondary site (for example, bone). This is a multi-step process involving cancer cell proliferation, migration, proliferation, invasion, survival, adhesion and colonisation. The cancer cells travel to other parts of the body via the circulatory system, where cancer cells enter the bloodstream, or the lymphatic system, where cancer cells enter the lymph vessels and lymph nodes (Figure 1.7). This complex metastatic cascade remains poorly understood, and is one of the most important factors for patient prognosis. An initial trigger, for example a genetic mutation or a chemical carcinogen, can cause generation of multiple abnormal cells which divide continuously, forming an initial tumour localised to one area of the body. Upon expansion, these cancer cells will start to infiltrate the cell barrier and pass into the extra cellular matrix (ECM) and this process is referred to as Local Invasion (CancerResearchUK, 2016a). Cancer cells can penetrate blood vessels and lymph vessels, in a process known as intravasation, and this allows them to move to secondary sites forming secondary tumours. For successful metastatic spread of cancer cells, a development and expansion of a vascular network is crucial in order to supply cancer cells with oxygen and vital nutrients and to remove waste products (Nishida et al., 2006). Once this is achieved, metastatic cancer cells can then effectively rely on this network for sustenance and don't require pre-existing vessels. Tumour angiogenesis itself is a complex process and is regulated by a number of pro- and anti- angiogenic factors which influence metastasis proliferation (Russo et al., 2012). Various proteins have been implicated in activation of tumour angiogenesis; these include but are not limited to vascular endothelial proliferation factor (VEGF) (Moens et al., 2014), angiogenin (Adams and Subramanian, 1999), transforming proliferation factor

(TGF)-α (Schreiber et al., 1986), TGF-β (Ferrari et al., 2009), basic fibroblast proliferation factor (bFGF) (Rifkin and Moscatelli, 1989) and tumour necrosis factor (TNF) (Wajant, 2009). VEGF, a key player in tumour angiogenesis, is a potent angiogenic factor promoting angiogenesis during embryonic development, contributing to wound healing in healthy cells and also inducing angiogenesis in malignant tumours (Carmeliet, 2005). The VEGF family help orchestrate angiogenesis by triggering signalling cascades, binding to one or more specific receptors, VEGF receptor 1 (VEGFR1) for example, on the surface of target cells like endothelial cells (Ferrara et al., 2003). This ultimately can lead to downstream processes influencing angiogenic signalling pathways and hence tumour angiogenesis (Seguin et al., 2014). Once this is accomplished it provides tumours with sufficient resources to expand rapidly and also, due to abnormal structures, provides close links to the circulatory system for metastatic cancer cells to break away, further facilitating metastatic dissemination to secondary sites. Once cancer cells are able to migrate around the body, they may arrest at secondary locations, begin to leak out of blood vessels and into surrounding tissue, a process known as extravasation (Strell and Entschladen, 2008). Finally, this allows cancer cells to reach a secondary site and form secondary tumours (Figure 1.7). Cancer cells have various mechanisms enabling enhanced cell survival and thus allow them to evade the anoikis process or programmed cell death (Paoli et al., 2013). Collectively, this perpetuates cancer progression and ultimately contributes to a more aggressive form of cancer.

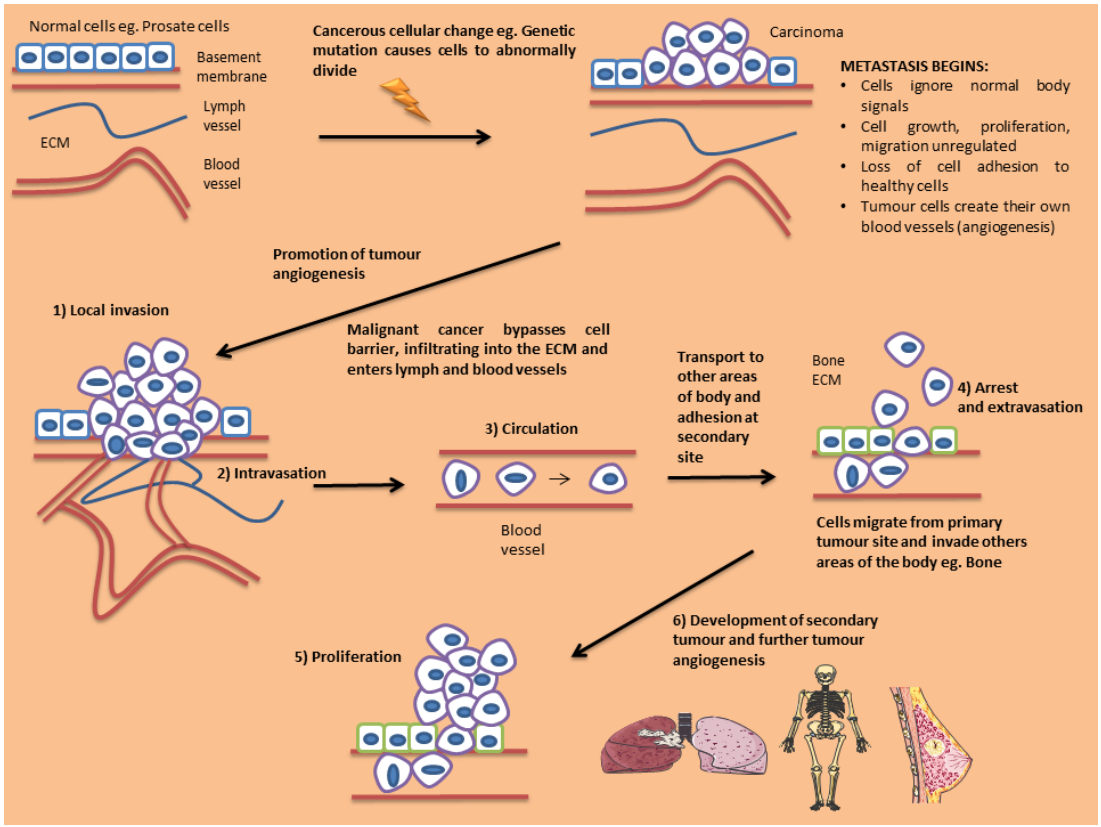

Figure 1.7 The metastatic cascade.

Schematic diagram describing steps involved in the transition from normal cells to cancerous metastatic cells and how they are distributed to distinct regions in the body. 1) Local Invasion: Cells invade nearby tissue and surrounding area. 2) Intravasation: Cancer cells bypass basement membrane and move through nearby blood vessels and lymph vessels. 3) Circulation: Cells travel to other parts of the body utilising the lymph or blood system. 4) Arrest and extravasation: Cancer cells reach secondary site of the body and infiltrate surrounding tissue. 5) Proliferation: Cancer cells proliferate at secondary site forming secondary tumours. 6) Development of secondary tumour and angiogenesis: Cancer cells stimulate the proliferation of new blood vessels creating their own blood supply, promoting further tumour proliferation. Adapted from (NationalCancerInstitute).

1.1.8 Prostate cancer metastasis: bone metastasis

As discussed above, at an early stage of cancer, cancer cells will be confined to the immediate areas of origin and in the case of prostate cancer, cancer cells are confined to the prostate gland. The main sites in which prostate cancer may spread to are the adrenal gland, bone, liver, and lung (NationalCancerInstitute) and a key area of interest for this study will be to evaluate any implications EPLIN has in the spread of prostate cancer to the bone.

Bone metastasis involves the infiltration, invasion and adhesion of migrating tumour cells to bone, which utilises various molecular mechanisms (Weidle et al., 2016). Bone cells are a frequent target for metastases from multiple cancers including prostate, breast and lung and can progress rapidly. Of all people with prostate cancer, bone is frequently the first target for metastasis and greater than 2 out of 3 prostate cancers that spread to secondary tumour sites will spread to bone (AmericanCancerSociety, 2016). The preference of prostate cancer spread to bone is likely due to the bone microenvironment and its favourable proliferation conditions and proliferation factor abundance, rich vasculature and cytokine enrichment for tumour cells (Bussard et al., 2008, Paget, 1989a). Bone metastasis is commonly associated with severe bone pain, osteolysis, increased bone fragility, increased fracture risk, bone deformity, hypercalcaemia and leukoerythroblastic anaemia (Mundy, 2002). Bone metastasis has a significant and detrimental effect on survival rates of people with prostate cancer. Mortality rates and outlook can depend on various factors including age and how far the cancer has spread, but metastatic bone cancer is significantly worse compared to primary prostate cancer with approximately 50% of patients surviving only 5 years following diagnosis

(CancerResearchUK, 2016d). A study established the five year survival rate of prostate cancer patients will drop from 56% to just 3% comparing those with or without bone metastasis (Norgaard et al., 2010). Treatment options for metastatic bone cancer can include hormone therapy, radiotherapy, chemotherapy and surgery, but can also include the use of drugs like bisphosphonates to alter and control blood calcium levels (Table 1.2). Bone metastasis therefore is an extremely important consideration for patients with prostate cancer, along with researchers investigating prostate cancer metastasis and cancer biology.

1.1.8.1 Bone microenvironment - Osteoblasts, osteoclasts and osteocytes

Bone is a specialised type of connective tissue which makes up the vertebral skeleton and has many vital functions including structural support, protection and in the regulation of calcium levels in the body (Marks, 2002). Bone is made up of various cellular constituents and these include osteoblasts and osteoclasts. Osteoblasts are derived from mesenchymal stem cells and make up a large proportion of bone cells which function in bone formation (Clarke, 2008). Osteoblasts are mononuclear cells which play a pivotal role in regulating and maintaining skeletal architecture and regulating osteoclast activation (Caetano-Lopes et al., 2007). Osteoclasts on the other hand are multinucleated cells responsible for breaking down bone cells and bone resorption. Osteoclasts function to repair, maintain and remodel bones of the skeleton but are also utilised by cancer cells for osteolytic bone destruction (Roodman, 2001). For appropriate bone turnover in the body, bone remodelling must continuously occur and osteoblasts and osteoclasts are pivotal for this process. Figure 1.8 illustrates a simplified overview of the process of osteogenesis in which osteoblasts are formed.

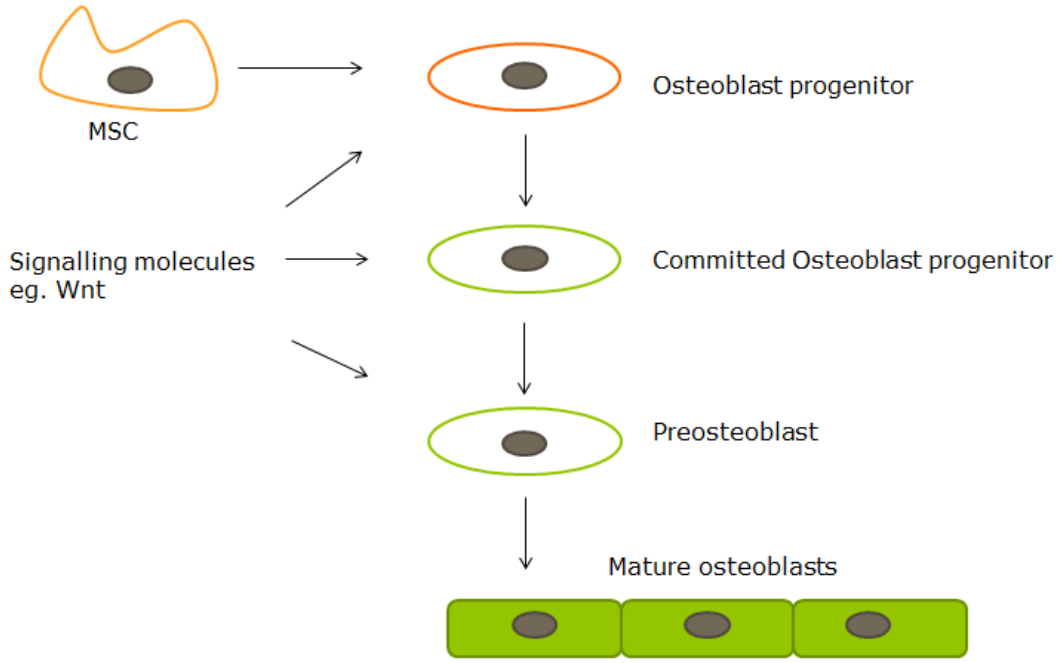

Figure 1.8 Schematic representation of osteogenesis and the bone formation process.

MSC, Mesenchymal stem cell. Adapted from (Bose et al., 2013).

1.1.8.2 Bone metastasis: pathophysiology and molecular genetics

1.1.8.2.1 Receptor Activator of Nuclear factor kappa-B ligand (RANKL)

There are various molecular factors established in the development and progression of metastatic bone cancer. These can include molecules involved in osteoblast and osteoclast signalling, cytokines and angiogenic molecules. For example, one of the factors involved in the formation of bone lesions is receptor activator of nuclear factor kappa-B ligand (RANKL) which is a protein involved in bone regeneration and remodelling and signals via the receptor activator of nuclear factor kapp B (RANK) / RANKL / osteoprotegerin (OPG) pathway. RANKL is positively associated with prostate cancer progression, with high levels in prostate cancer cell lines PC-3, LNCaP and DU-145 compared to normal prostate cell line RWPE2 (Li et al., 2014). In addition, increased RANKL is also seen in aggressive cancer samples and samples which have metastasised to bone, compared to non-aggressive samples (Li et al., 2014). It has been reported that RANKL can influence cancer cell invasiveness, with treatment of RANKL significantly increasing cellular invasion in prostate cancer, and knockdown of RANK suppressing this pro-metastatic effect (Li et al., 2014). Manipulation of RANKL expression has also revealed *in vivo* implications on cell proliferation. Mice which have been injected with MDA-MB-231 breast cancer cells with RANKL knock-down demonstrated an 80% reduction in osteolytic lesions compared to control mice (Zheng et al., 2014).

1.1.8.2.2 Receptor Activator of Nuclear factor kappa-B (RANK)

RANK is the signalling receptor for RANKL and both molecules are synergistic in their related function, and have key regulatory roles in bone remodelling and bone

physiology (Boyce and Xing, 2007). Similar to RANKL, RANK expression is frequently elevated in various cancers (Santini et al., 2011), can act as a predictive marker in cancer progression (Zhang et al., 2012), and can influence chemotherapy response and survival rates in osteosarcoma (Bago-Horvath et al., 2014). RANK/RANKL is also able to influence several cellular functions in cancer progression including cellular migration and invasion (Li et al., 2014, Song et al., 2014), in addition to having roles in the establishment of bone metastasis (Mori et al., 2007), suggesting a complex network of regulatory molecules co-ordinating this signalling cascade.

1.1.8.2.3 Osteoprotegerin (OPG)

An additional molecule in RANKL signalling and cancer progression is the cytokine receptor OPG. OPG acts as a decoy receptor to RANKL and like RANKL has implications in bone metastasis. It has been recently demonstrated that patients with clear-cell renal cell carcinoma (ccRCC) have an increased ratio of RANK/OPG and elevated RANK/OPG levels were associated with bone metastasis and reduced patient survival (Beuselinck et al., 2015). This increased ratio also has implications in non-small cell lung cancer patients where elevated RANK/OPG ratios were associated bone metastases and correlated with lymph node involvement, tumour stage and overall cancer aggressiveness and metastatic potential (Peng et al., 2013).

These findings indicate the RANK/RANKL/OPG pathway is a paramount signalling pathway involved in cancer progression and bone metastasis. Both RANKL and OPG display differential expression in cancer, demonstrate potential for manipulating cancer cell characteristics and have potential to control bone

metastases formation by targeting cellular invasion, osteolytic lesion proliferation and influencing overall cancer development.

1.1.8.2.4 Interleukin 6 (IL-6)

A further prominent molecule implicated in bone metastasis is interleukin 6 (IL-6). Interleukins are a group of cytokines involved in a myriad of biological functions and there is an abundance of evidence linking IL-6 to cancer development and progression. IL-6 has been shown to promote cell proliferation and proliferation in many tumour cells including prostate cancer via activation of various signalling pathways (Ogata et al., 1997, Smith et al., 2001). IL-6 also has roles in promoting osteolysis via RANKL/OPG signalling (Itoh et al., 2006), angiogenesis (Huang et al., 2004) and immunomodulation (Yu et al., 2007). The diversity of IL-6 on physiological functions and the abundance of evidence associating IL-6 as a pro-cancer molecule and in bone metastasis has led to IL-6 being utilised in various clinical trials via inhibitor models testing therapeutic potential (Ara and Declerck, 2010).

1.1.8.2.5 Parathyroid hormone related peptide (PTHrP)

Another relevant player in the establishment of bone metastases is the parathyroid hormone related peptide PTHrP. Physiologically, PTHrP functions in autocrine and paracrine signalling specifically in embryonic development and in the regulation of cell proliferation and proliferation in various cell types (Devys et al., 2001). PTHrP has been evaluated for its potential role in the regulation of bone cancer in several cancer systems and in bone metastasis. In lung cancer, it has been demonstrated that PTHrP facilitates bone metastasis in SBC-5 cells (Miki et al., 2004) and in breast

cancer, PTHrP is associated with the formation of bone metastases and poor patient outcome alongside TGF-β (Xu et al., 2015). In prostate cancer, increased expression of PTHrP has been found in bone metastases from prostate cancer (Iddon et al., 2000) and PTHrP has been shown to promote Epithelial to Mesenchymal Transition (EMT) (Ongkeko et al., 2014). PTHrP is therefore an important molecule in cancer progression and bone metastasis not only through its physiological cell function but also with its persuasive implications in bone metastasis pathophysiology.

1.1.8.2.6 Macrophage inflammatory protein 1 alpha (MIP-1α)

A further molecule associated specifically in the formation of osteolytic bone metastasis is the chemokine macrophage inflammatory protein 1 alpha (MIP-1α). MIP-1α functions as a pro inflammatory protein able to induce osteoclast formation and has been associated in cancer development (Kukita et al., 1997). MIP-1α has been evaluated as a stimulatory factor in multiple myeloma where it induces cell migration and causes activation of the Mitogen Activated Protein Kinase (MAPK) pathway accelerating proliferation and survival (Lentzsch et al., 2003). Additionally, elevated MIP-1α has also been associated with poor patient prognosis and formation of osteolytic bone lesions in multiple myeloma (Hashimoto et al., 2004). These data suggest an integral role for MIP-1α in multiple myeloma and thus may be a crucial regulator in the establishment of bone metastases.

1.1.8.2.7 Bone metastasis: The Vicious Cycle

The Vicious Cycle is a term used in cancer biology to describe how cancer cells hijack the characteristics of bone forming osteoblasts and bone absorbing osteoclasts to promote cancer cell proliferation, survival and proliferation (Figure 1.9). The

vicious cycle is a complex process involving many molecular factors including TGF-β, PTHrP, OPG, RANK and RANKL. These molecules play key roles in osteoblast/osteoclast activity in normal cells and in cancer and thus have a crucial impact on bone remodelling. Firstly, PTHrP is secreted by cancer cells which can cause osteoclastic bone resorption and bone destruction in metastatic breast cancer cells (Guise et al., 2002). TGFβ has also been implicated with the vicious cycle in association with PTHrP; TGFβ acts upstream increasing PTHrP to mediate osteolysis via the Smad and MAPK signalling pathway (Kakonen et al., 2002). The osteoclast activating increase in PTHrP seen in tumour cells also produces RANKL and downregulates OPG, further causing osteolysis (Mundy, 2002). Once RANKL is activated, RANK signalling can then further activate downstream transcription factors including nuclear factor kappa-light-chain-enhancer of activated B cells (NF-kB) and Activator protein 1 (AP-1) promoting osteoclast differentiation, encouraging bone resorption (Mundy, 2002). Osteolysis, mediated by osteoclasts formed in response to RANKL, PTHrP and TGFβ then causes the release of proliferation factors including insulin-like proliferation factor 1 (IGF1) and TGFβ, in addition to activating the Smad and MAPK signalling pathway, which stimulate tumour cell proliferation, thus continuing the cycle (Mundy, 2002). This process is not limited to these molecules but they play important roles to tightly regulate and promote the cycle. The vicious cycle is multifactorial involving various cell types and intricate regulation and is therefore a target for cancer therapy, utilising molecules like RANKL, PTHrP and TGFβ, for preventing bone metastases formation.

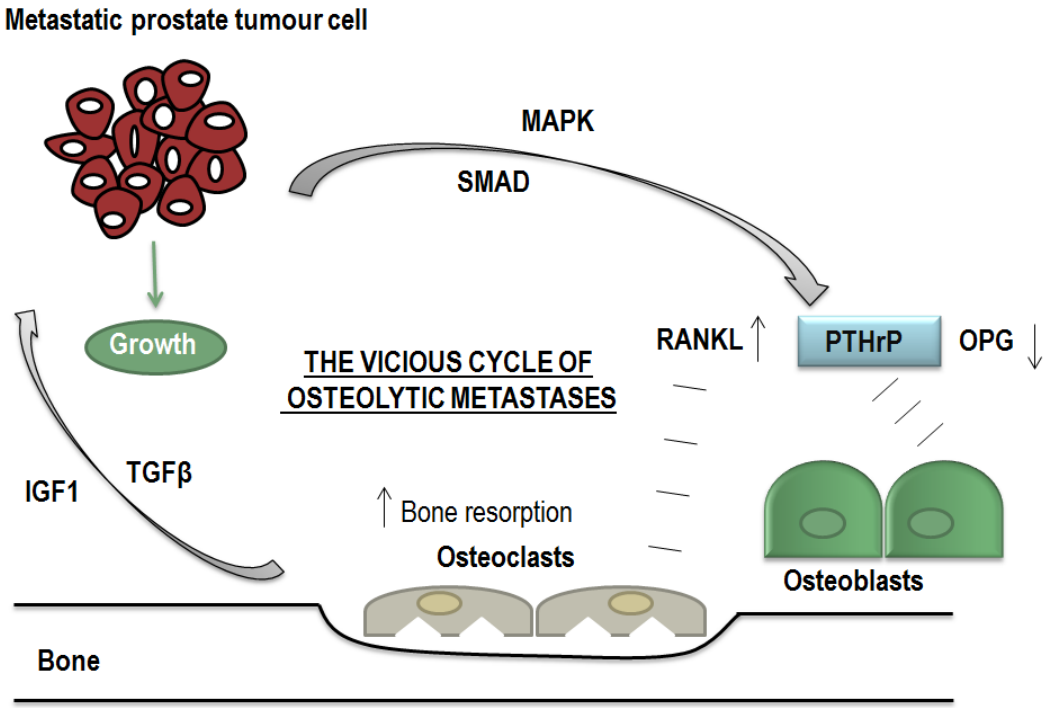

Figure 1.9 The Vicious Cycle.

The vicious cycle is a term used to describe the signalling mechanisms and molecules involved in bone remodelling in metastatic bone cancer. PTHrP, RANK, RANKL, OPG and TGFβ are all key components of the cycle. PTHrP is secreted by metastatic cancer cells and initiates osteoclastogenesis by binding osteoblasts. PTHrP causes an increase in the expression of RANKL, in addition to other molecular factors like IL-6 and TNF, and decreases expression of OPG. RANKL binds osteoclasts, induces osteoclast formation and drives bone resorption and osteolysis. This process generates proliferation factors like TGFβ and IGF1, which promote production of PTHrP by cancer cells, in addition to causing tumour expansion. With the generation of PTHrP, the cycle continues and bone is further destroyed accompanying further tumour proliferation. Adapted from (Gartrell and Saad, 2014).

The vicious cycle illustrates that the establishment of bone metastases is a crucial determinant for mortality rates and in the progression of cancer due to the sophisticated nature of signalling mechanisms in bone remodelling. Subsequent to this, biomarkers for detecting pre-bone metastases are vital. Currently, there is no validated biomarker to establish whether prostate cancer will metastasise to bone and bone metastasis itself is difficult to specifically identify. Prognostic indicators like the PSA test, Gleason score and clinical tumour stage exist but are limited and it is difficult to get definitive answers on metastatic potential (Briganti et al., 2014). Various suggested biomarkers including bone-morphogenetic protein-6 (BMP6) (Deligezer et al., 2010), bone-specific alkaline phosphatase (BAP) (Zhao et al., 2011) and procollagen type 1 amino-terminal propeptide (P1NP) (Klepzig et al., 2009) have provided recent prognostic clues in bone metastasis however there is yet an identified biomarker with sufficient prognostic clinical value for prostate cancer and bone metastasis. EPLIN has been established by our lab as a putative tumour suppressor and as an indicator of prognosis in multiple cancer phenotypes (Jiang et al., 2008, Liu et al., 2012a, Liu et al., 2012b, Sanders et al., 2011). Based on this previous research, and the current lack of a suitable molecular biomarker for bone metastasis, a key consideration of this PhD will be to elucidate if EPLIN can provide prognostic value in the metastatic cascade of prostate cancer to bone locations.

1.2 Epithelial Protein Lost in Neoplasm (EPLIN)

The primary focus of this PhD is on EPLIN; a cytoskeletal, actin-binding protein encoded by the *LIMA1* gene. EPLIN is expressed preferentially in epithelial cells, with high levels in the placenta, prostate, kidneys, ovary and heart but low levels can be detected ubiquitously around the body. EPLIN was initially identified in oral

cancers for its differential expression between normal oral epithelial cells and Human Papilloma Virus (HPV)-immortalised oral epithelial cells (Chang et al., 1998). EPLIN exists as 2 distinct isoforms, a 600 amino acid, 90kDa EPLINα isoform and a larger 759 amino acid, 110kDa EPLINβ isoform, and these isoforms are generated from an alternative pre-mRNA splicing event (Figure 1.10) (Maul and Chang, 1999). The EPLINα isoform has been implicated in the progression of various cancers and this was initially recognised in oral cancer, breast, prostate and xenograft tumours where EPLIN expression was either down regulated or completely abolished (Maul and Chang, 1999). The EPLIN genomic structure consists of 11 exons and 10 introns, with exons 1-3 only present in EPLINβ and EPLINα utilising exons 4-11 of *LIMA1* for transcription (Chen et al., 2000). EPLIN is present on chromosome 12 and the EPLIN gene has 2 separate promoter regions; the EPLINβ promoter is near the start of the gene in exon 1, whilst EPLINα initiates ~50Kb downstream near the end of intron 3, prior to exon 4 and at amino acid position 161 in the EPLINβ protein (Figure 1.10) (Chen et al., 2000).

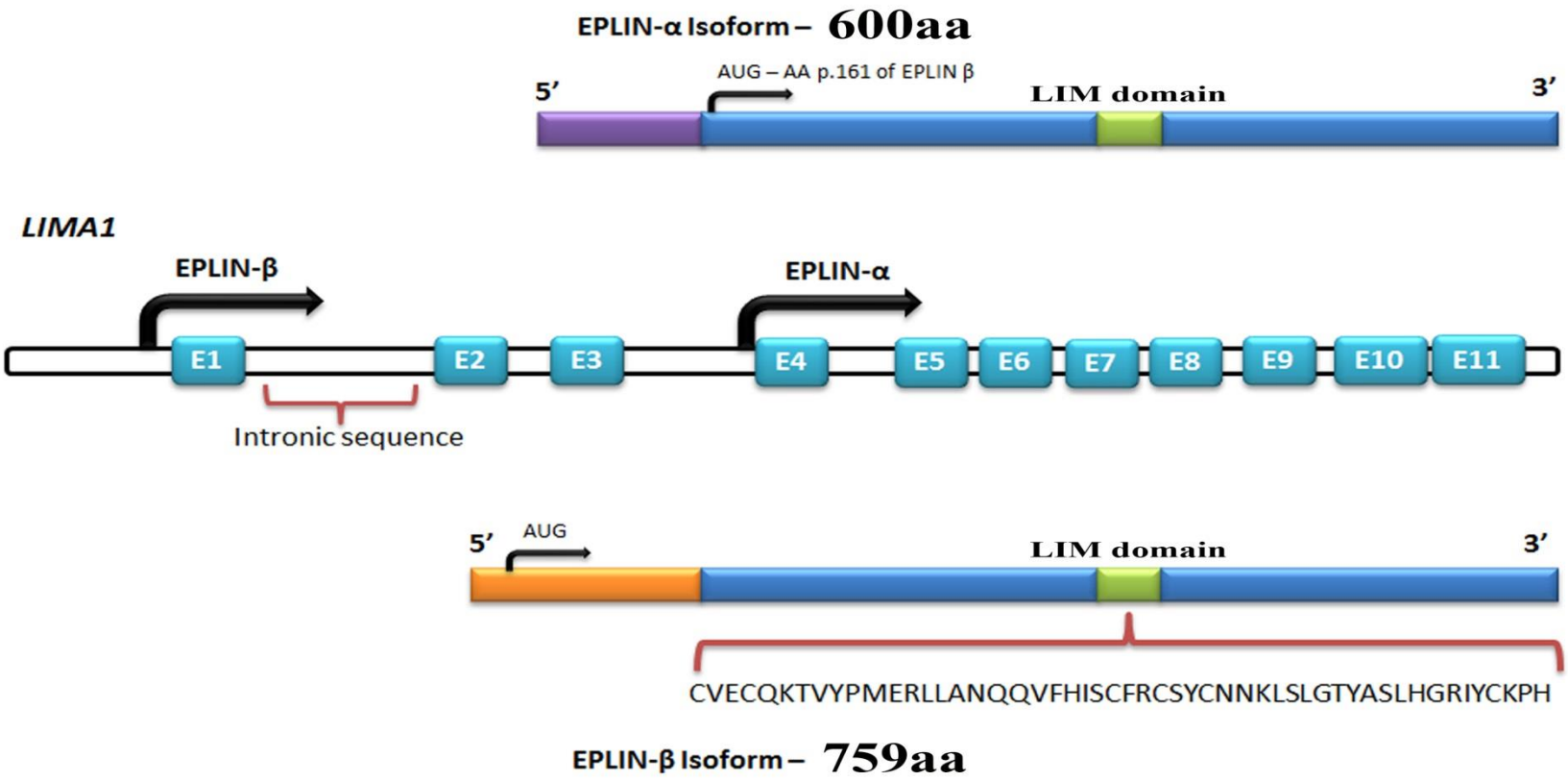

Figure 1.10 Schematic diagram of the *LIMA1* genomic structure and EPLIN structural isoforms.

The *LIMA1*gene consists of 11 exons and 10 introns. EPLINα differs from EPLINβ at the amino terminus where an additional 159 amino acids is present in EPLINβ. Shown below EPLINβ is the 52 amino acid centrally located LIM domain common to both EPLIN isoforms. Adapted from (Maul and Chang, 1999).

The amino acid sequence of EPLIN is characterised by a single centrally located LIM domain which supposedly aid structural self-dimerisation and contains subdomains for Zinc binding (Figure 1.11) (Maul and Chang, 1999, Chen et al., 2000). LIM-domain containing proteins are frequently present in molecules responsible for cytoskeletal organisation, such as the focal adhesion phosphoprotein, paxillin, and the LIM domain is generally responsible for sites of protein-protein interaction (Brown et al., 1996). LIM domain proteins are also associated with important cellular roles including cell cycle progression, are involved in developmental processes and are implicated in several cancers including leukaemia, breast cancer and neuroblastoma (Matthews et al., 2013). EPLIN is important in the regulation of actin dynamics and aids actin filament bundle assembly, and the amino terminal of the EPLIN protein structure is essential for this localisation to the actin cytoskeleton (Song et al., 2002).

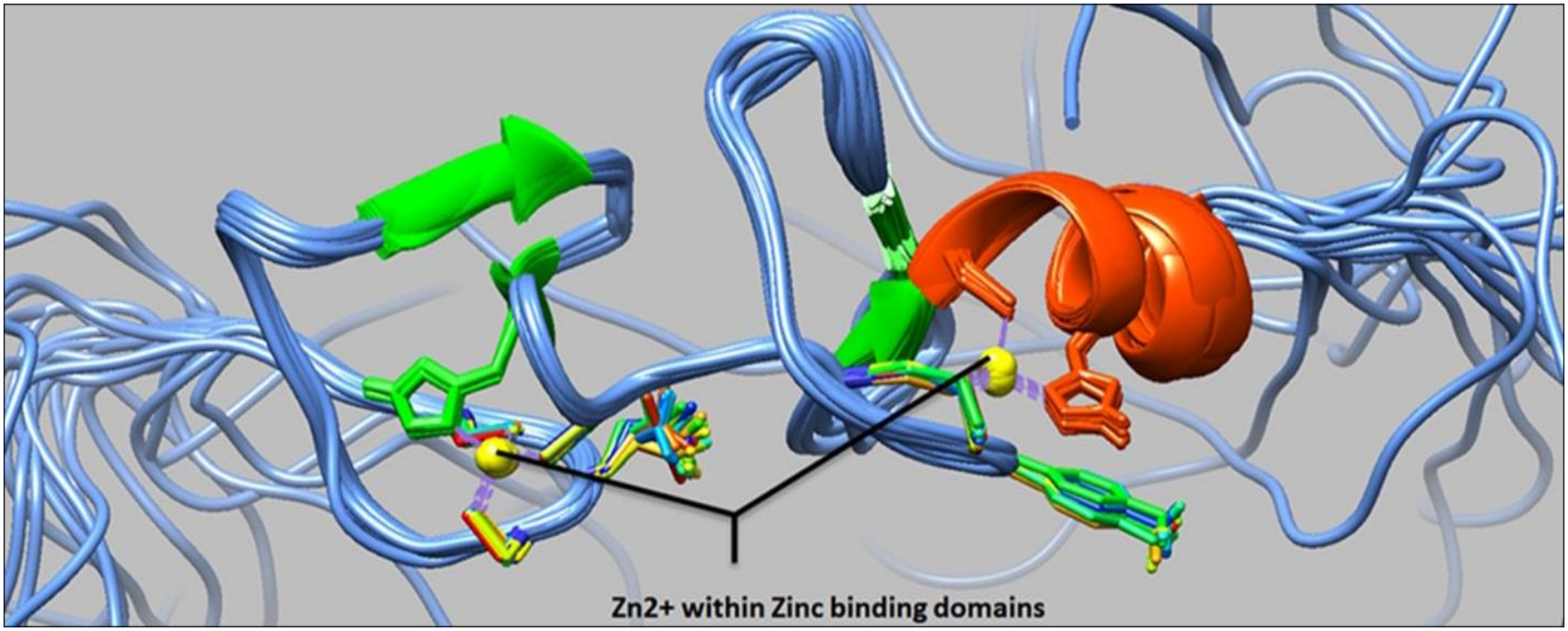

Figure 1.11 Protein structure of EPLIN LIM domain (PDB ID=2D8Y).

Protein structure of the EPLIN centrally located LIM domain. Zinc binding domains depicted. This domain may aid self-dimerisation. Image generated using UCSF Chimera software.

Sequence analysis has revealed EPLIN is conserved across species with EPLINα and EPLINβ isoforms present in mouse, displaying 77% and 75% identity similarity for human EPLINα and EPLINβ, respectively (Figure 1.12) (Maul et al., 2001). A role for EPLIN has also been suggested in muscle development in pigs, where EPLIN displayed a temporal expression pattern with only the EPLINα isoform present in developing skeletal muscle (Wang et al., 2007). Since the discovery of EPLIN, our lab has shown that aberrant EPLIN expression is associated with the progression of various cancer types including breast, oesophageal, pulmonary and prostate cancer. EPLIN levels decrease as the cancer progresses and become more advanced, giving EPLIN potential to provide prognostic value, and overexpression analysis suggests EPLINα is a putative tumour suppressor (Jiang et al., 2008, Liu et al., 2012a, Sanders et al., 2011, Sanders et al., 2010, Liu et al., 2012b). The described loss of EPLIN in cancer has functional implications on the actin cytoskeleton and may contribute to enhanced metastatic potential of cancer cells.

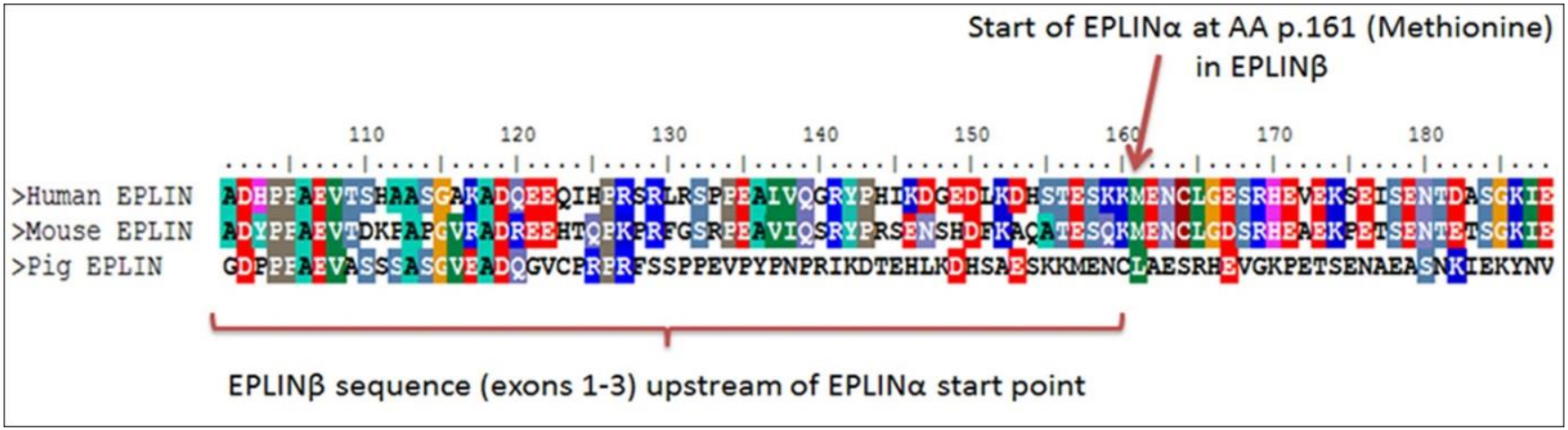

Figure 1.12 ClustalW protein alignment of Human, Mouse and Pig EPLINβ.

Areas of amino acids that are conserved across species are highlighted. The region shown is amino side of the EPLINβ protein, where EPLINα originates at amino acid (AA) p.161. ClustalW generated using BioEdit Biological Sequence Alignment software.

1.2.1 The EPLIN interactome: regulation in actin dynamics

EPLIN has a number of functional partners (Figure 1.13/Table 1.3) and the globular protein actin is central to the function of EPLIN. EPLIN has 2 functional actin binding sites which flank the central LIM domain and it is this binding capacity that engenders actin cross linking and actin filament bundle assembly (Maul et al., 2003). A fibrillar pattern is displayed by both isoforms and expression of EPLINα enhances the size and number of actin filament stress fibres and can also inhibit membrane ruffling via the signalling GTPase, Ras-related C3 botulinum toxin substrate 1 (Rac1) (Maul et al., 2003). EPLIN therefore directly interacts with actin which suggests a possible role for EPLIN in cell migration, adhesion and cell morphology. Actin is an abundant, multifunctional protein responsible for cell migration in eukaryotic cells. Actin is part of the cytoskeletal network which consists of microtubules, microfilaments and intermediate filaments which are vital for cellular functions. Actin exists as monomers (G-actin) and filamentous polymers (F-actin) and is important for physiological functions including cell locomotion, cytokinesis, maintenance of cell shape and muscle contraction (Stricker et al., 2010). Transcription of the *LIMA1* gene is suggested to be primarily controlled by monomeric G actin, with the actin-MAL-SRF signalling pathway regulating EPLIN production (Leitner et al., 2010). Maul *et al*., (Maul et al., 2003) illustrated that EPLINα has 3 significant features: EPLINα has binding sites for actin and can cross-link and bundle actin filaments, EPLINα stabilises actin filaments *in vitro* and EPLINα inhibits branching nucleation of actin filaments by the Actin related protein (Arp) 2/3 complex (Maul et al., 2003). Therefore, this suggests EPLIN may orchestrate actin filament dynamics by stabilising actin cytoskeletal networks (Maul

et al., 2003). Additionally, EPLIN has been shown to form part of an actin-remodelling complex comprising of EPLIN, β-actin, γ-actin and gelsolin which co-localises at the plasma membrane to the tumour suppressor, PTEN (Kim et al., 2011). PTEN is a well-established tumour suppressor molecule so this postulates whether the interaction of PTEN and the actin-remodelling complex is itself an element supressing the development of neoplastic tissue and whether any interruption of these complexes may promote cancer progression. Based on these findings, EPLIN accommodates actin to accomplish various actin-related cellular processes including cell motility and migration and cell junctional adhesion (Abe and Takeichi, 2008).

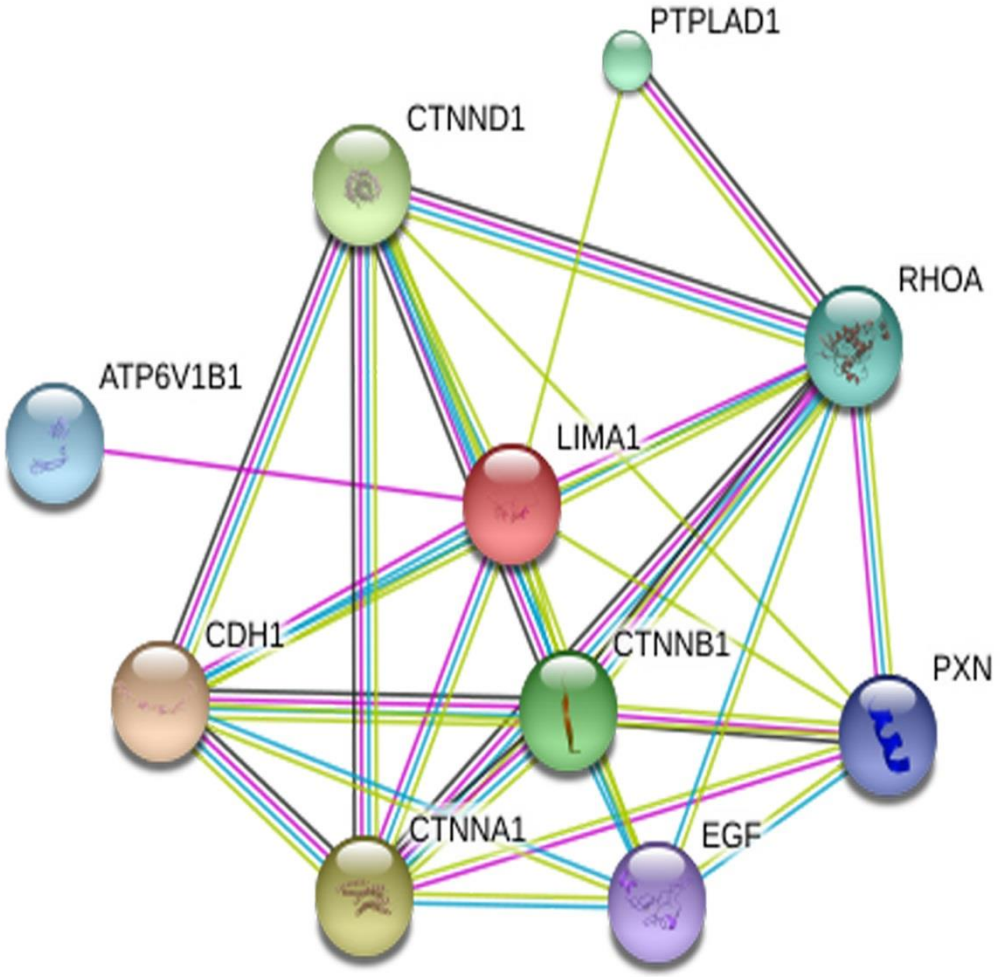

Figure 1.13 EPLIN predicted functional partners.

EPLIN (LIMA1) has various associations including Cadherin and Catenin molecules which contribute to cytoskeleton regulation. LIMA1: LIM domain and actin binding 1; CDH1: Cadherin 1; CTNNA1: Catenin-α1; CTNND1: Catenin-δ1; CTNNB1: Catenin-β1; EGF: Epidermal Growth Factor C; PTPLAD1: Protein tyrosine phosphatase-like A domain containing 1; ATP6V1B1: ATPase, H+ transporting, lysosomal 56-58kDa, V1 subunit B1; PXN: Paxillin; RHOA: Ras homolog gene family, member A. Image generated and extracted from online STRING database.

Table 1.3 EPLIN associated molecules.

EPLIN association	Biological significance	References
Actin	Actin is an abundant protein important for cell migration. EPLIN has 2 actin binding domains that flank the EPLIN LIM domain. Pull down assays revealed EPLIN binds actin monomers and these results in actin cross linking and actin filament bundle assembly.	(Maul et al., 2003)
Paxillin	May form a complex with EPLIN to co-ordinate actin dynamics. Immunohistochemical analysis of prostate cancer tissue/cells vs. normal revealed EPLIN overexpression influences paxillin expression and localisation. Co-localisation, co-precipitation and an *in situ* proximal ligation assay revealed direct association between the two molecules in cultured human mesangial cells.	(Sanders et al., 2010, Sanders et al., 2011, Tsurumi et al., 2014)
α-Catenin	Immunoprecipitation and GST pull down assays reveal EPLIN interacts with α-catenin, forming a cadherin-β-catenin-α-catenin-EPLIN complex.	(Abe and Takeichi, 2008)
Supervillin	*In vivo* co-localisation studies and *in vitro* GST pull down revealed EPLIN interacts with the peripheral membrane protein, supervillin.	(Smith et al., 2010)
PINCH-1 (Particularly interesting new cysteine-histidine-rich protein-1)	Pull down assays revealed endogenous EPLIN co-immunoprecipitates with endogenous PINCH-1 in keratinocytes.	(Karakose et al., 2015)
ERK Extracellular signal–regulated kinase	ERK phosphorylates EPLIN and decreases EPLINs affinity to F-actin promoting cell migration. Inhibition of ERK abolishes EPLIN expression and reduces tumour suppressive ability of EPLIN.	(Han et al., 2007, Jiang et al., 2008, Sanders et al., 2010)

DNp73 (TP73)	In melanoma cells, both EPLIN isoforms are inhibited by DNp73 and this drives a more invasive phenotype.	(Steder et al., 2013)
SATB2 (Special AT-rich sequence-binding protein 2)	EPLIN is differentially regulated by the DNA binding protein, SATB2. SATB2 regulates the actin cytoskeleton via EPLIN association. When SATB2 is knocked out, osteosarcoma cells show reduced migration and are less invasive and this is mediated by EPLIN.	(Seong et al., 2014)
Arv1 (ACAT-related protein required for viability 1)	EPLIN interacts with and recruits Arv1 to the cleavage furrow during cell division. Co-immunoprecipiation experiments reveal EPLIN interacts with Arv1 and show a stronger association with the EPLINβ isoform.	(Sundvold et al., 2016)
Cav-1(Caveolin-1)	EPLIN regulates the lipid raft tumour suppressive protein, Cav-1. Co-immunoprecipitation and mass spectroscopy analysis revealed that EPLIN and Cav-1 bind to each other in normal and RasV12 cells.	(Ohoka et al., 2015)

1.2.2 Paxillin and Focal Adhesion Kinase (FAK): potential links with EPLIN

There is increasing evidence to suggest EPLIN regulates actin structures in cooperation with the focal adhesion protein paxillin. Paxillin is a 68kDa phosphotyrosine containing protein involved in signal transduction and focal adhesion and associated in various signalling pathways. Similarly to EPLIN, paxillin contains LIM domains which mediate protein-protein interactions but also accommodates further structural domains including SH2 and SH3 domain binding sites and LD motifs which co-ordinate cytoskeletal dynamics via interaction with cytoskeletal proteins, GTP activating proteins and various kinases that form a complex with paxillin (Figure 1.14) (Schaller, 2001). Paxillin therefore functions as a regulatory docking molecule with diverse roles in cellular adhesion, movement and motility acting via various signalling mechanisms and thus has implications in cancer development. Due to the complex molecular architecture and diverse signalling mechanisms of paxillin, paxillin is strongly associated in cancer development and progression, with paxillin being linked with various invasive, aggressive tumours including lung, colorectal, breast and prostate (Bhattacharjee et al., 2001, Farmer et al., 2005, Mackinnon et al., 2011, Mestayer et al., 2003, Yang et al., 2010). Paxillin is widely expressed in normal tissue but displays differential expression in cancer and expression can be targeted to manipulate cancer cell characteristics; for example, overexpression of paxillin influences cell motility, migration, and inhibits filopodia formation in lung cancer (Salgia et al., 1999). In prostate cancer, paxillin knockdown can inhibit *in vivo* cancer cell proliferation in prostate cancer xenografts (Sen et al., 2012), and in breast cancer paxillin can influence cellular invasion, morphology and metastasis (Deakin and Turner, 2011).

In addition to potential use as a molecular therapeutic, paxillin is a promising agent for use as a prognostic marker in various cancers including breast (Madan et al., 2006), lung (Kanteti et al., 2009) and ovarian cancer (Kim et al., 2012).

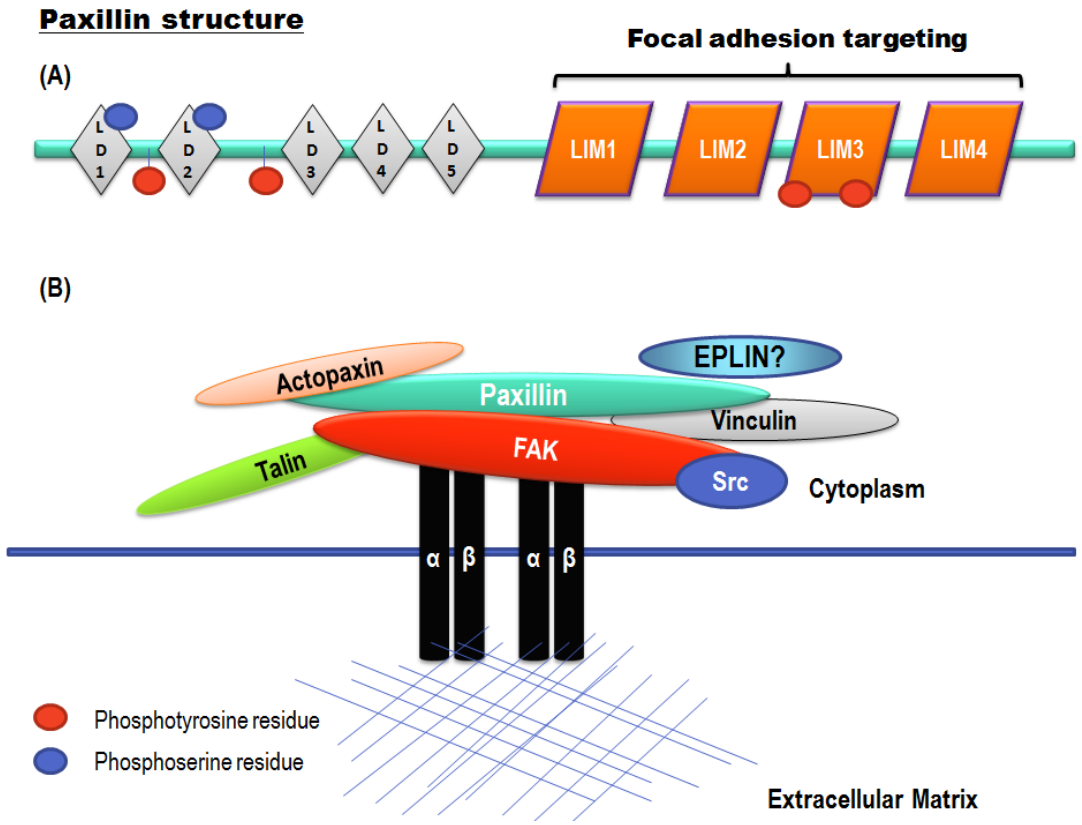

Figure 1.14 Paxillin domain structure and paxillin interactions in integrin signalling.

(A) Paxillin structure. *Paxillin* gene is located on chromosome 12 and has 4 isoforms. Paxillin contains 4 LIM domains which co-ordinate protein-protein interactions. Paxillin has multiple phosphorylation sites including phosphotyrosine and phosphoserine residues (indicated by red and blue circles respectively) and these aid cellular functions including cellular adhesion. Tyrosine phosphorylation creates docking sites for SH2 domain containing proteins encouraging downstream signalling. Serine phosphorylation contributes to paxillin conformation and thus influences interaction with paxillin binding partners. (B) Paxillin interactions in integrin signalling. Paxillin serves as a scaffolding protein to facilitate the functional organisation of various focal adhesion signalling molecules. These include but are not limited to FAK, Src, Vinculin, Talin and Actopaxin. The paxillin complex associates with integrin heterodimers and initiates integrin signalling which co-ordinates various cellular processes. The putative EPLIN associated to paxillin site is depicted. Adapted from (Brown and Turner, 2004) and (Deakin and Turner, 2008).

Paxillin has strong implications in cancer due to its diverse roles as a signalling molecule and in focal adhesion. Paxillin may be functionally linked to EPLIN as recent reports highlight a link between the two molecules. When EPLINα is overexpressed, paxillin exhibits an increased staining pattern for both HECV endothelial cells and PC-3 prostate cancer cells (Sanders et al., 2011, Sanders et al., 2010). This co-localisation pattern is also observed in cultured human mesangial cells at focal adhesion sites and co-immunoprecipitation results confirm an association between the two molecules (Tsurumi et al., 2014). EPLIN and paxillin may form a complex and potentially stabilise focal adhesions to co-ordinate actin dynamics in a complimentary manner. Given EPLINs role in actin dynamics it is strongly implicated in cellular processes including cell migration and invasion and thus down-regulation or loss of EPLIN in cancer may affect the metastatic potential of cancer cells, which could have downstream effects on paxillin signalling. Although there is an apparent association between these two molecules, exactly how they interact mechanistically remains elusive.

Focal Adhesion Kinase (FAK) is also a crucial cytoplasmic regulatory protein involved in tyrosine kinase signalling and actin dynamics. FAK is located on chromosome 8 and has structural domains consisting of an N-terminal FERM (ezrin-radixin-moesin) domain, a central catalytic domain, proline rich domains and a carboxy C-terminal domain for focal adhesion targeting (Figure 1.15) (Schaller, 2010). These domains are responsible for focal adhesion targeting (FAT domain) and for interactions of FAK with other signalling molecules (FERM domain) including epidermal proliferation factor (EGF) receptor (EGFR), platelet derived proliferation factor (PDGF) receptor (PDGFR), the epithelial and endothelial tyrosine kinase

(ETK) and ezrin (Mitra et al., 2005). A key role of FAK is to recruit additional signalling molecules (including paxillin) at focal contacts during cellular adhesion (Mitra et al., 2005). In additional to the role of FAK as a docking protein in cellular adhesion, FAK is a critical component of actin cellular dynamics. FAK is known to interact with various signalling molecules to co-ordinate actin-related cellular processes like cell movement and these include but are not limited to Neural Wiskott-Aldrich Syndrome Protein (N-WASP), Arp2/3, GTPase Regulator Associated with Focal adhesion Kinase (GRAF) and paxillin (Schaller, 2010), suggesting a complex network of molecules orchestrating cellular function. FAK has two crucial phosphorylation events; Tyr397 and Tyr925. These two phospho-tyrosine residues are critical to FAK function and for interaction with molecules including the tyrosine kinase Src and paxillin. Phosphorylation of FAK Tyr397 creates a SH2 binding site for Src and promotes the binding of Src to FAK leading to Src-FAK signalling and downstream FAK phosphorylation (Schlaepfer et al., 2004) whereas phosphorylation of FAK Tyr925 in the FAT region is responsible for Proliferation Factor Receptor Bound Protein (Grb)2 adaptor protein binding and induces integrin associated focal adhesion autophosphorylation (Cheng et al., 2014).

FAK and paxillin both play key roles in integrin signalling. Paxillin can act as a scaffolding protein for many integrin related signalling molecules, including FAK, and these proteins act cooperatively to engage integrin's at the extracellular matrix (Turner, 2000b). Upon docking of paxillin and FAK at integrin sites, FAK can phosphorylate paxillin to create additional binding sites for further downstream signalling molecules (Shen and Schaller, 1999). This interaction of FAK and paxillin leads to signal activation of the MAPK pathway and thus stimulates gene expression

of genes involved in critical cell functions, including cancer cell migration (Crowe and Ohannessian, 2004). Overexpression of either of FAK and/or paxillin can promote cancer cell migration and invasion, illustrating the importance of cellular regulation of these two molecules in MAPK signalling and cancer development (Crowe and Ohannessian, 2004). The notion linking FAK and paxillin to integrin signalling and MAPK signalling is well documented (Giancotti and Ruoslahti, 1999), however significantly less is available on the importance of EPLIN in integrin signalling. A recent article illustrated that EPLIN associates to integrin sites via interaction with the LIM-only domain protein, PINCH-1, and when depleted can exert an effect on keratinocyte spreading and migration (Karakose et al., 2015) suggesting EPLIN may have a crucial role on cell function via integrin signalling. It will be interesting to explore this potential role further via the interaction of EPLIN with paxillin and FAK.

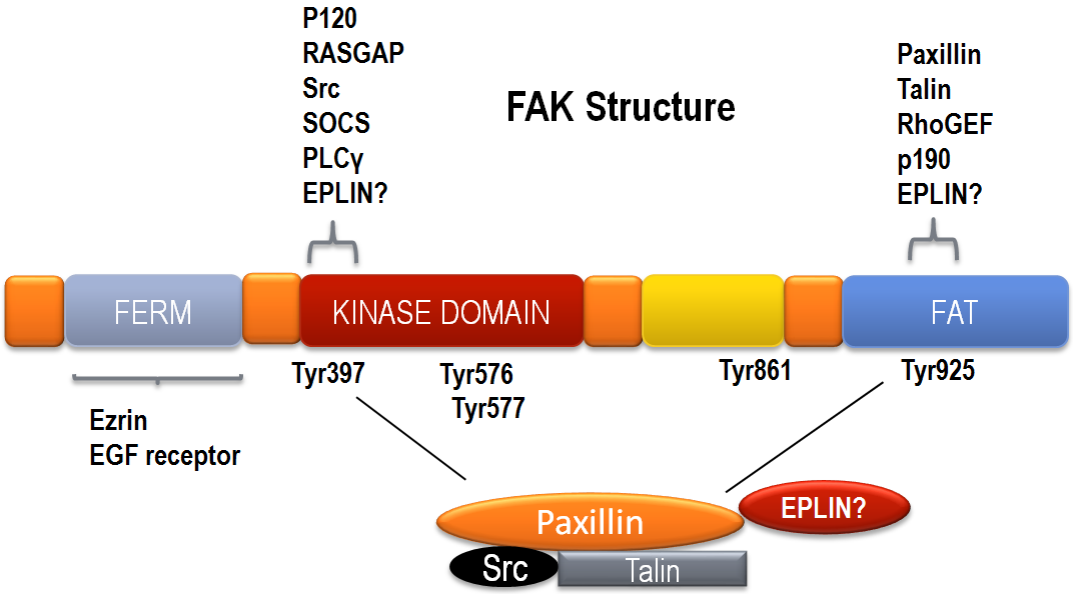

Figure 1.15 Schematic representation of FAK domain structure.

FAK has 3 major domains consisting of a FERM domain (ezrin, radixin and moesin homology) domain, a kinase domain and a focal adhesion targeting (FAT) domain. The FERM domain is responsible for interactions with molecules including ezrin and the epidermal proliferation factor (EGF) receptor. The FAT domain of FAK orchestrates focal adhesion activity of FAK via integrin signalling with molecules like talin and paxillin. FAK is subjected to various phosphorylation events primarily by tyrosine kinases and these include Tyr397, 576, 577, 861 and 925. FAK interacts with paxillin via Tyr925 phophorylation and also at Tyr397 with molecules including Src (via the SH2 binding domain), phospholipase Cγ (PLCγ), suppressor of cytokine signalling (SOCS) and p120 RASGAP. Phosphorylation of central tyrosine residues 576 and 577 is critical for catalytic response. The proposed sites for EPLIN interaction with FAK is illustrated in the figure. Adapted from (Mitra et al., 2005).

Due to FAK's primary role in cellular adhesion and movement, dysregulation of FAK has diverse implications in cancer which can act via various signalling pathways. FAK has been proposed to be activated and phosphorylated by integrin signalling to co-ordinate cell adhesion (Guan, 1997), in addition to having roles in cytokine receptor, proliferation factor and G-protein coupled receptor signalling (Yoon et al., 2015). These complex signalling mechanisms make FAK a key player in cancer development and progression. FAK has been shown to be upregulated in several cancers including pancreatic, colon and breast (Golubovskaya, 2014, Jiang and Hegde, 2016, Heffler et al., 2013a), with increased FAK levels correlating with poorer patient prognosis (Yom et al., 2011). This increased FAK expression has led to the development of inhibitor models for cancer therapy specifically targeting FAK, one of which is the small molecule inhibitor 1,2,4,5-Benzenetetraamine tetrahydrochloride (Y15). This inhibitor acts by blocking autophosphorylation of FAK at Y397 and has promising implications in colon cancer where it could influence cellular traits including cell attachment and apoptosis and effectively inhibited tumour proliferation in mouse models (Daily, 2010). This inhibitor for FAK has also been used successfully as a supplement to chemotherapy with enhanced efficacy of therapeutic potential observed in colon cancer (Heffler et al., 2013b). With the established use of FAK inhibitors in various cancer models, it will be interesting to see if FAK inhibition can be targeted in prostate cancer accompanying EPLIN expression manipulation. With FAK being overexpressed in cancer, and EPLIN being lost in cancer, and with the potential link between the two molecules it would be useful to see if they could be utilised to influence cancer cell characteristics and thus used to create a novel therapy for prostate cancer.

Although a putative link between EPLIN and paxillin has been previously demonstrated, less is known about interaction between EPLIN and FAK. It may be that interactions occur via tyrosine phosphorylation of FAK, possibly at Tyr397 or Tyr925, as there is already an established link between FAK and paxillin at the FAT domain of FAK (Hayashi et al., 2002) and between EPLIN and paxillin (Tsurumi et al., 2014, Sanders et al., 2011).

1.2.3 Role of EPLIN in the Adherens Junction (AJ)

The Adherens Junction (AJ) is a type of anchoring junction found predominantly in epithelial cells which functionally attach the actin cytoskeleton together in cells via linker molecules. EPLIN is an actin binding protein which functions to bundle actin filaments, suggesting the presence of EPLIN at AJ along with filamentous actin. The AJ contain various protein complexes along with EPLIN and these include cadherins, catenins and p120 catenins (Figure 1.16) (Meng and Takeichi, 2009). Within the AJ, cadherins and catenins associate together to form the cadherin-catenin complex and EPLIN provides a direct physical link for this complex to the actin cytoskeleton (Abe and Takeichi, 2008). The cadherin-catenin complex is comprised of E-cadherin, β-catenin and α-catenin, with E-cadherin positioned between adjacent cells and the catenins positioned in the cytoplasmic space of each cell (Mege et al., 2006). E-cadherin binds directly to β–catenin which sequentially binds α-catenin, generating the cadherin–catenin complex (Yonemura, 2011). α-Catenin is a crucial component at the AJ and was initially recognised as being responsible for providing the bridge between the cadherin-catenin complex and actin (Nelson, 2008, Meng and Takeichi, 2009). This principle however has come under scrutiny as direct *in vitro* binding between α-catenin and actin had never been detected (Drees et al., 2005,

Yamada et al., 2005). Cavey *et al.,* (Cavey et al., 2008) realised that α-catenin is not essential for E-cadherin stability, as complexes of β-catenin and E-cadherin were detected in RNAi α-catenin embryos (Cavey et al., 2008). Therefore, it's apparent that cadherin-actin interaction is regulated not only by α-catenin but by a number of actin-binding proteins that are associated with α-catenin, including EPLIN (Yonemura, 2011, Taguchi et al., 2011). Abe and Takeichi (Abe and Takeichi, 2008) demonstrated, using immunoprecipitation and GST pull down assays, that both EPLIN isoforms directly interact with the α-catenin VH3 plus C-terminal region to generate a cadherin-catenin-EPLIN-actin complex at cell junctions (Abe and Takeichi, 2008). When EPLIN is depleted, the bridge to F actin was unable to form due to loss of organisation of the apical actin belt, with punctate accumulation of E-cadherin at cell junctional points (Abe and Takeichi, 2008). This illustrates the importance of EPLIN in producing functional epithelial junctions.

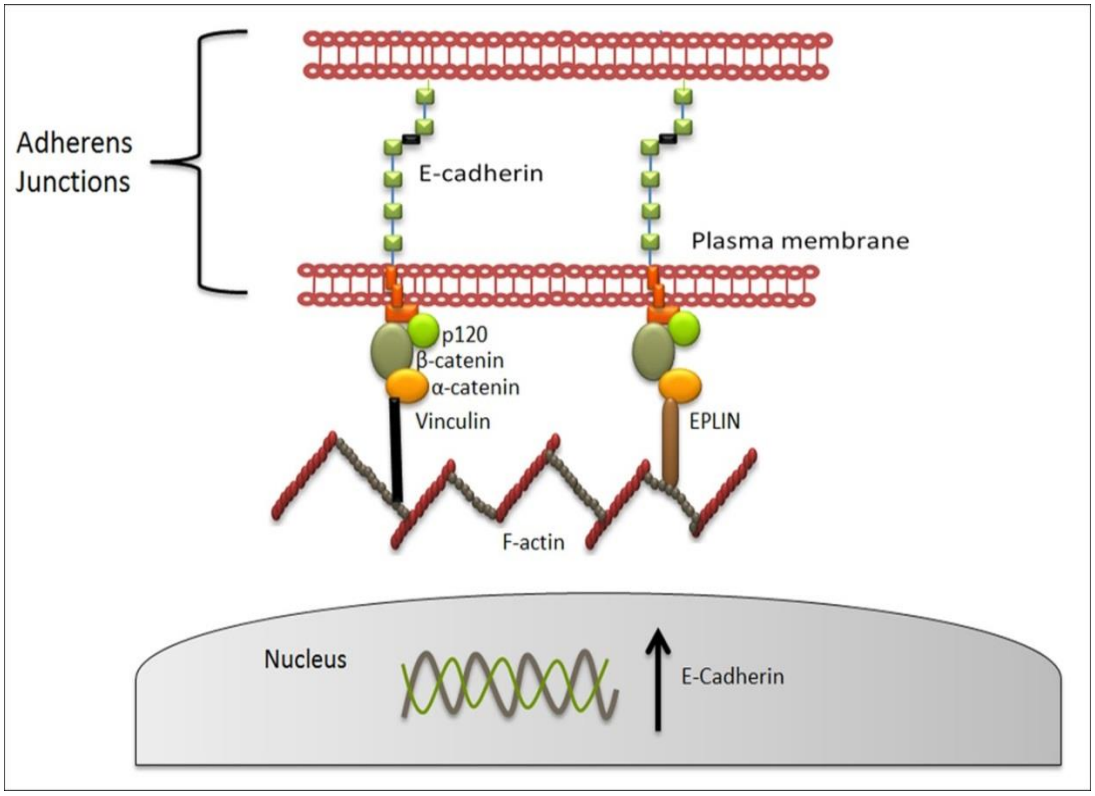

Figure 1.16 Schematic representation of Adherens Junctions.

The AJ between epithelial cells consists of various protein complexes to orchestrate actin cytoskeletal dynamics. The cadherin-catenin complex is associated with filamentous actin via EPLIN and/or vinculin which bind α-catenin in the cytoplasm. During functional AJ formation, E-Cadherin is expressed in the nucleus. During cancer progression and processes like EMT, proteins including E-Cadherin and EPLIN are downregulated or lost, enhancing cancer development. Adapted from (Ratheesh and Yap, 2012).

Additional molecules involved in regulating the AJ include the membrane-cytoskeletal protein, vinculin, and the actin filament-binding protein, afadin (Geiger et al., 1980, Sawyer et al., 2009). Recent work from Taguchi *et al*., (Taguchi et al., 2011) illustrated that EPLIN and vinculin may collaborate together in AJ formation via binding α-catenin either together or individually and cooperatively aid junctional adhesion (Taguchi et al., 2011). The cooperation of EPLIN and vinculin in cellular adhesion is also evident in endothelial cells. At the endothelial AJ, the endothelial E-cadherin homolog, VE-cadherin, interacts with β- and γ- catenins which sequentially bind α-catenin and EPLIN in an analogous fashion to epithelial cells (Chervin-Petinot et al., 2012). This allows the recruitment of vinculin and ultimately promotes strengthening of inter-endothelial junctions (Chervin-Petinot et al., 2012). The authors propose a role for EPLIN in tension dissemination at the endothelial AJ in a mechanosensory mechanism (Chervin-Petinot et al., 2012). The machinery from actomyosin exerts tension through EPLIN, which causes α-catenin to adopt a more accessible conformation, revealing a vinculin-binding site and allowing vinculin recruitment and actin association at endothelial cell-cell AJ (Gulino-Debrac, 2013). This mechanotransduction mechanism consisting of EPLIN and α-catenin suggests the endothelial AJ is regulated in a spatial and temporal pattern (Gulino-Debrac, 2013). Finally, EPLIN also appears to be important for attachment to F-actin in endothelial cells; when EPLIN expression is down-regulated the organisation of F-actin is considerably disrupted, leading to multiple holes in the actin cytoskeleton (Chervin-Petinot et al., 2012). Altogether this suggests that the AJ of epithelial and endothelial cells are orchestrated by various actin-binding, α-catenin-associated molecules and are dynamically regulated, with EPLIN having a critical role in cell adhesion, creating further implications of EPLIN loss in cancer

1.2.4 EPLIN– a key player in cell division?

Cell division is the splitting of one cell into two, where biological information is passed onto daughter cells. For this process to successfully occur, various proteins need to functionally regulate the division and these include molecules like Rho GTPases, cyclin dependant kinases, integrins, cell division control protein homolog 42 (cdc42), focal adhesion kinases, myosin and the globular protein actin (Heng and Koh, 2010). With this in mind, an actin-binding protein, such as EPLIN, may potentially have a regulatory role in cell division. This has been recently shown using HeLa cells where EPLIN depletion resulted in large numbers of multinucleated cells, signifying cytokinesis failure during cell division (Chircop et al., 2009). In successful mitotic division, actin and myosin II accumulate at the cleavage furrow during cytokinesis and EPLIN loss compromised each proteins ability to efficiently do this (Chircop et al., 2009). EPLIN appears to be important for the accumulation of other mitotic regulatory proteins including the GTPases RhoA and cdc42, where EPLIN depletion resulted in either a significantly reduced concentration of RhoA or a miss-placed location of cdc42 at the cleavage furrow (Chircop et al., 2009). EPLIN aids this successful cell division in conjunction with a number of regulatory proteins including supervilin and the oncogenic kinesin, Kinesin Family Member 14 (KIF14), suggesting a complex network of regulatory proteins at the cleavage furrow (Smith et al., 2010). More recently it has been suggested that EPLIN plays a role as a recruitment protein in cell division where EPLIN recruits the membrane lipid transporter protein, Arv1 (Sundvold et al., 2016). Liquid chromatography-tandem mass spectrometry and co-immunoprecipitation experiments demonstrated an interaction between the two molecules and suggested both co-localised to the

cleavage furrow during early telophase (Sundvold et al., 2016). Altogether, this suggests EPLIN may have an integral role in cytokinesis and loss may lead to aneuploidy and genomic instability of daughter cells (Chircop et al., 2009). Therefore, EPLIN likely acts at various stages of the cell cycle with crucial roles co-ordinating actin and myosin dynamics and functions as a recruitment protein for molecules involved in cytokinesis. This multifunctional role may have implications in cancer cells resulting in downstream effects on successful cytokinesis, increasing their tendency to form a cancer (Chircop et al., 2009).

1.2.5 Post translational modification of EPLIN

Post translational modification refers to changes made to proteins following transcription and translation and these can include changes like phosphorylation, glycosylation and ubiquitination. EPLIN has functional links to Extracellular Signal-Regulated Kinase (ERK) which is a member of the MAPK family and is important in the regulation of actin organisation by phosphorylating various proteins including paxillin, FAK and other protein kinases and nuclear transcription factors to co-ordinate cellular processes (Pribic and Brazill, 2012, Pearson et al., 2001). ERK is implicated in cellular events including cell migration and may facilitate this by phosphorylation of actin bundling proteins like EPLIN (Han et al., 2007). The protein structure of EPLIN has multiple putative phosphorylation sites (Figure 1.17) and it has been shown that ERK phosphorylates EPLIN at Ser360, Ser602, and Ser692 *in vitro* and *in vivo* (Han et al., 2007). Phosphorylation at the carboxy terminal of EPLIN decreases affinity to F-actin and thus provokes a reorganisation of the actin cytoskeleton, enhancing cell migration (Han et al., 2007). This implicates ERK in actin organisation and cell motility with EPLIN being a critical substrate for

phosphorylation (Han et al., 2007). ERK also plays a role in targeting EPLIN to focal adhesions and effects the interaction with paxillin; activation of the MEK-ERK pathway both reduced localisation of EPLIN to sites of focal adhesions and abolished paxillin interaction (Tsurumi et al., 2014). A recent study by Zhang *et al*., (Zhang et al., 2013) illustrated that this ERK-mediated phosphorylation of EPLIN is itself regulated by EGF and revealed how targeting this signalling cascade can be manipulated to reduce epithelial-mesenchymal transition (EMT) and thus prostate cancer invasiveness (Zhang et al., 2013). EGF is also capable of promoting EPLIN protein turnover *in vitro* and *in vivo,* targeting it for polyubiquitination and proteomsome degradation, enhancing EPLIN downregulation and also inducing downregulation of E-Cadherin (Zhang et al., 2013). This suggests EGF is a primary driver around EPLIN protein regulation, and could be a reason why EPLIN is lost in aggressive cancer, as EGFR and EGF and generally overexpressed in cancer cells (Normanno et al., 2006). Recently, the human phosphatase CDC14A has been shown to counteract EGF-induced EPLIN phosphorylation by ERK; CDC14A dephosphorylates EPLIN at Ser362 and Ser604, invoking changes to the actin cytoskeleton and regulating cellular migration and adhesion (Chen et al., 2017). These data suggest several molecules are functionally related to EPLIN and provide a critical regulatory role for appropriate actin dynamics and may have implications in cancer progression. Furthermore, ERK is an established kinase for the association of paxillin and FAK via paxillin phosphorylation (Liu et al., 2002). How EPLIN associates with these molecules is currently unknown, but it could be via a specific phosphorylation event, which in itself could be ERK-dependant or ERK-independent. Phosphorylation events have proved to be crucial for cell signalling and actin association in FAK (Westhoff et al., 2004) and for cell matrix adhesion

dynamics in paxillin (Zaidel-Bar et al., 2007), so it seems reasonable that they may be important for EPLIN function and dynamics.

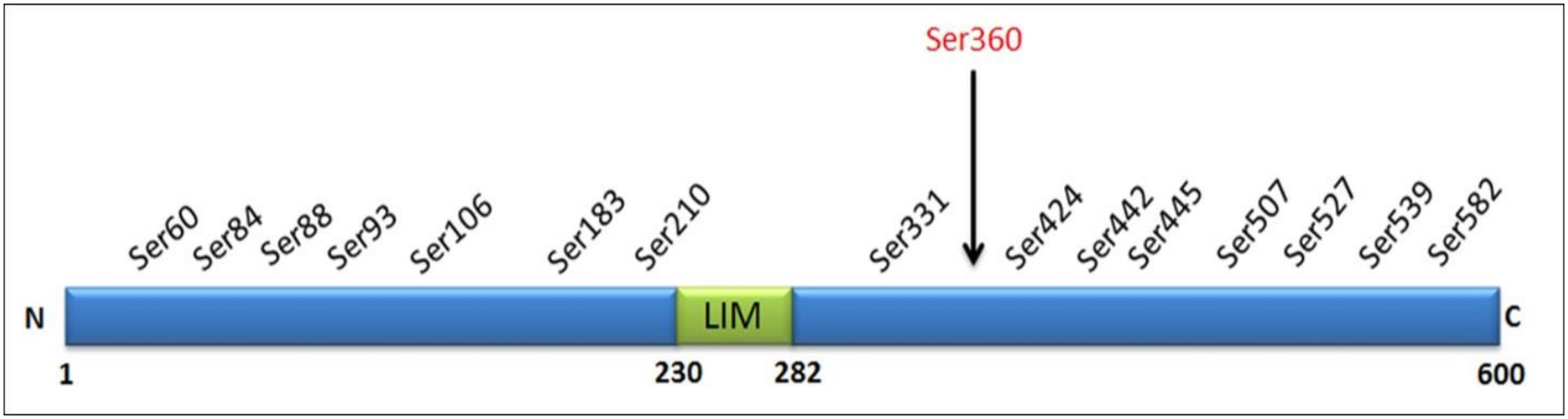

Figure 1.17 Predicted phosphorylation sites in EPLINα.

The protein structure of human EPLINα has multiple putative phosphorylation sites at all regions of the protein, including various sites where Serine kinases would likely act. Predicted Threonine and Tyrosine phosphorylation sites not shown. Highlighted in red is the phosphorylated residue suggested in (Han et al., 2007). Phosphorylation status predicted using NetPhos 2.0 software.

1.2.6 The role of EPLIN in cancer

Cancer progression involves various cellular, morphological and molecular alterations which result in a transformed cellular phenotype, ultimately having the potential to invade surrounding tissue and disseminate throughout the body. Cancer treatment options remain largely unspecific and create various undesired side effects, though more targeted approaches are emerging. Therefore, elucidating a molecular target for treating cancer, in addition to understanding the mechanism of cancer development is crucial. EPLINα first received attention for its involvement in cancer in 1999 where EPLINα down-regulation was described in various cancer cell lines (Maul and Chang, 1999). Altogether, low levels of EPLINα transcript were found in 8/8 oral cancer cell lines, 5/6 breast cancer cell lines and 4/4 prostate cancer cell lines (Maul and Chang, 1999). Using PC-3 and DU-145 prostate cancer cell lines, EPLINα expression was significantly reduced compared to primary prostate epithelial cells (PrEC), whereas aggressive cell lines LNCaP and LAPC4 failed to express EPLINα at all (Maul and Chang, 1999). This notion of EPLINα loss was also seen in breast cancer where EPLINα expression in cell lines BT-20, SKBr-3, MCF-7, T-47D and MDA-MB-231 was either reduced or completely lost (Maul and Chang, 1999). Lastly, the authors demonstrated that EPLINα was a putative tumour suppressor molecule, where overexpression of EPLINα in osteosarcoma cells altered cell morphology and caused a reduction in cancer cell proliferation (Maul and Chang, 1999). Interestingly, when EPLINα was depleted in breast cancer cell lines, EPLINβ either remained consistent or actually increased (Maul and Chang, 1999). This illustrates the potential cancer protective effects the EPLINα isoform may exert in various cancer cell systems. EPLIN overexpression has also proved effective in

altering the proliferation phenotype and morphology in additional cell systems including anchorage-independent NIH3T3 transformed cells (Song et al., 2002). Using a soft agar assay and utilising the activated Cdc42 or the chimeric nuclear oncogene EWS/Fli-1 to transform NIH3T3 cells, EPLIN overexpression resulted in a ~80% decrease in colony formation for Cdc42 transformed cells, with a similar proliferation decrease in EWS/Fli-1 transformed cells (Song et al., 2002). Interestingly, EPLIN displayed heterogeneous staining throughout Ras cells rather than localisation to the actin cytoskeleton (Song et al., 2002). This implies oncogenic transformation affects the EPLIN/actin architecture and thus, the localisation of EPLIN to the actin cytoskeleton may be important to exert its suppressive ability (Song et al., 2002).

1.2.7 EPLIN in cancer: development, progression and identification as a tumour suppressor

1.2.7.1 Prostate cancer

There is increasing evidence to suggest EPLIN is implicated in the development of prostate cancer and also the process of EMT. Metastatic cancer cells rely on assembly and disassembly of the actin cytoskeleton in order to move, therefore expression of certain cytoskeletal proteins at cell junctions is crucial. EMT is a process where polarised epithelial cells are down regulated and subjected to biochemical and morphological changes which ultimately can contribute to prostate cancer (Serrano-Gomez et al., 2016). Epithelial cells become transformed to a mesenchymal cell phenotype, losing their cell polarity and cell adhesion at cellular junctions (Kalluri and Weinberg, 2009). The converted mesenchymal cell phenotype has a reorganised cytoskeleton and experience alterations in cell signalling which

engenders enhanced migratory and invasiveness capabilities and increased resistance to apoptosis (Lamouille et al., 2014, Kalluri and Weinberg, 2009). During these cellular changes, the actin molecular architecture is disrupted and protein complexes like the cadherin-catenin complex and epithelial markers are lost (Figure 1.18) (Zhang et al., 2011). E-cadherin is a key epithelial marker and has implications in EMT where down regulation or loss of E-cadherin is frequently observed in tumour cell progression (Acs et al., 2001). As discussed, EPLIN is associated with the cadherin-catenin complex and contributes to functional cytoskeletal dynamics (Abe and Takeichi, 2008). Zhang and co-workers (Zhang et al., 2011) used biochemical and functional approaches to demonstrate EPLIN is a negative regulator of EMT and invasiveness in prostate cancer cells. EPLIN was significantly decreased in cells of more mesenchymal morphology (known as the Androgen Refractory Cancer of the Prostate (ARCaPM) cell lineage model), suggesting EPLIN down regulation is implicated in EMT, along with the cadherin-catenin complex (Zhang et al., 2011). Depletion of EPLIN also provokes various other morphological changes including disassembly of AJ, increased migratory and invasive potential of cells *in vitro*, activation of β-catenin signalling, increased expression of vimentin, increased chemo resistance and decreased expression and nuclear translocation of E-cadherin (Zhang et al., 2011). The authors also demonstrated that altered EPLIN expression affects a host of downstream genes involved in not only EMT, but various other biochemical processes including Wnt signalling, actin cytoskeleton regulation, proliferation factor signalling and functions important for cancer cell survival and progression (Zhang et al., 2011). Lastly, the authors used immunohistochemistry (IHC) to show that EPLIN downregulation is correlated with cancer progression in multiple cancer models including lymph node metastasis in prostate cancer, where EPLIN expression was

significantly reduced (Zhang et al., 2011). Altogether this illustrates that EPLIN may be involved in the regulation of EMT and prostate cancer progression and loss of EPLIN can lead to diverse downstream cellular and molecular effects. EPLIN in prostate cancer has also been evaluated by our laboratory using the prostate cancer cell line, PC-3. Using IHC analysis, EPLIN displayed a significant decrease in staining intensity in tumour cells in comparison to normal (Figure 1.19) (Sanders et al., 2011). This was accompanied by quantification of staining intensity within the cohort, where lower levels of EPLIN staining were associated with cancerous and higher tumour grade samples (Sanders et al., 2011). Overexpression analysis of EPLINα resulted in decreased proliferation rate in tumour cells *in vitro*, along with reduced invasiveness and cell adhesion to the ECM (Sanders et al., 2011). Mice injected with PC-3 cells overexpressing EPLINα developed tumours at a markedly decreased rate in comparison to control (Sanders et al., 2011). Furthermore, cells overexpressing EPLINα displayed a greater staining pattern for the focal adhesion targeting protein, paxillin, implying EPLIN may also be present at these plaques or play a role in regulating paxillin (Sanders et al., 2011, Maul and Chang, 1999). Altogether these results demonstrate the potential of EPLIN in regulating prostate cancer progression and how it can be manipulated to suppress prostate cancer and EMT via impeding cancerous traits.

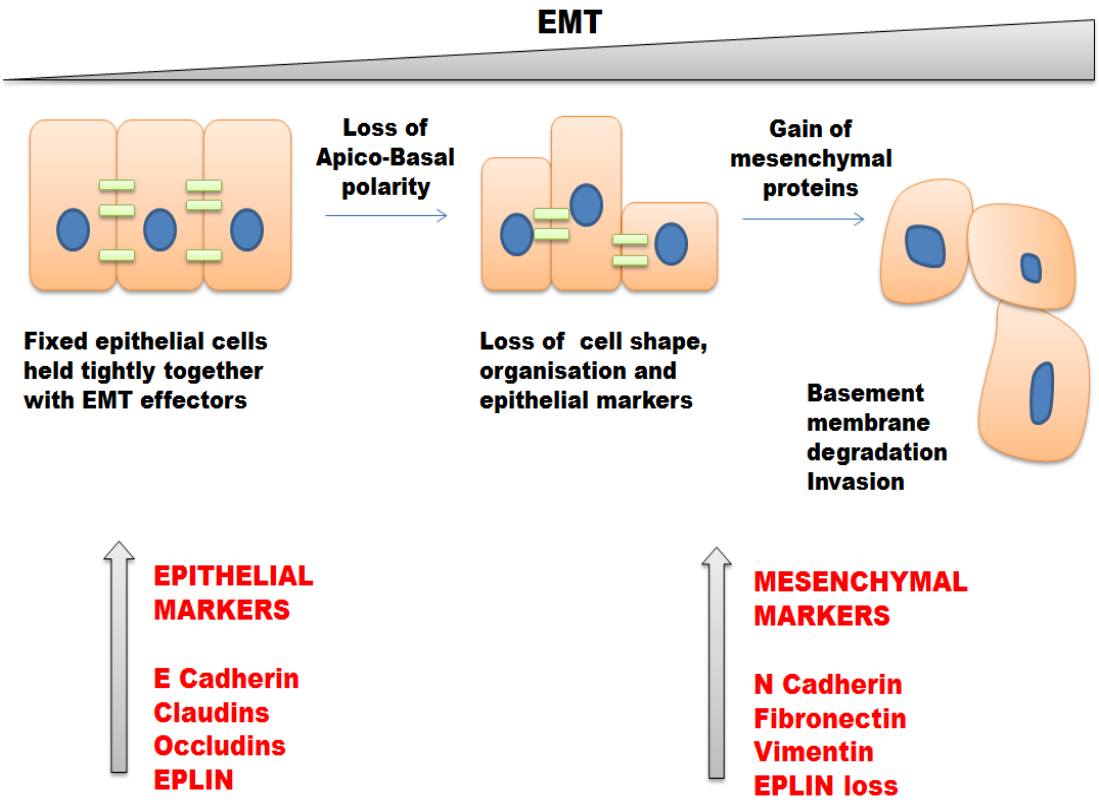

Figure 1.18 Schematic representation of early stages involved in Epithelial Mesenchymal Transition (EMT).

EMT is a process where epithelial cells lose polarity and have a less organised and compact morphology. This change is both morphological and biochemical where molecules like E-Cadherin, Claudins, Occludins and EPLIN are lost and pro-mesenchymal molecules are increased, including N-Cadherin, Fibronectin and Vimentin. This results in the degradation of the basement membrane of epithelial cells, and potential migration and invasion of cells. Adapted from (Micalizzi et al., 2010).

1.2.7.2 Breast cancer

EPLIN was first investigated in breast cancer by Maul and Chang (Maul and Chang, 1999) where EPLINα expression was either reduced or completely lost in breast cancer cell lines BT-20, MCF-7, T-47D and MDA-MB-231(Maul and Chang, 1999). Our lab has also evaluated EPLINs involvement in breast cancer progression by comparing EPLIN staining in normal vs. tumour sections using IHC analysis. EPLIN was found to be substantially weaker in tumour cells than in normal epithelial cells (Figure 1.19) (Jiang et al., 2008). This correlated with lower EPLIN transcript in tumour samples compared to normal samples (Figure 1.19E) with lower EPLIN levels being associated with higher tumour grade, a poorer patient prognosis and reduced overall survival rates (Figure 1.19.F G, H) (Jiang et al., 2008). IHC analyses in breast cancer from additional research groups also show EPLIN loss as the tumour becomes more aggressive, specifically comparing EPLIN immunointensity of primary tumours vs. tumours with lymph node metastases (Zhang et al., 2011). Lastly, *in vitro* and *in vivo* overexpression analysis of EPLINα highlighted significant reductions in cell proliferation and cell invasion using transfected breast cancer cell lines, and also highly significant reductions in tumour size were observed in nude mice inoculated with EPLINα transfected vs. control MDA-MB-231 breast cancer cells (Jiang et al., 2008). This further strengthens the use EPLIN has as a tumour suppressive molecule and how it may be employed as a therapeutic agent in cancer.

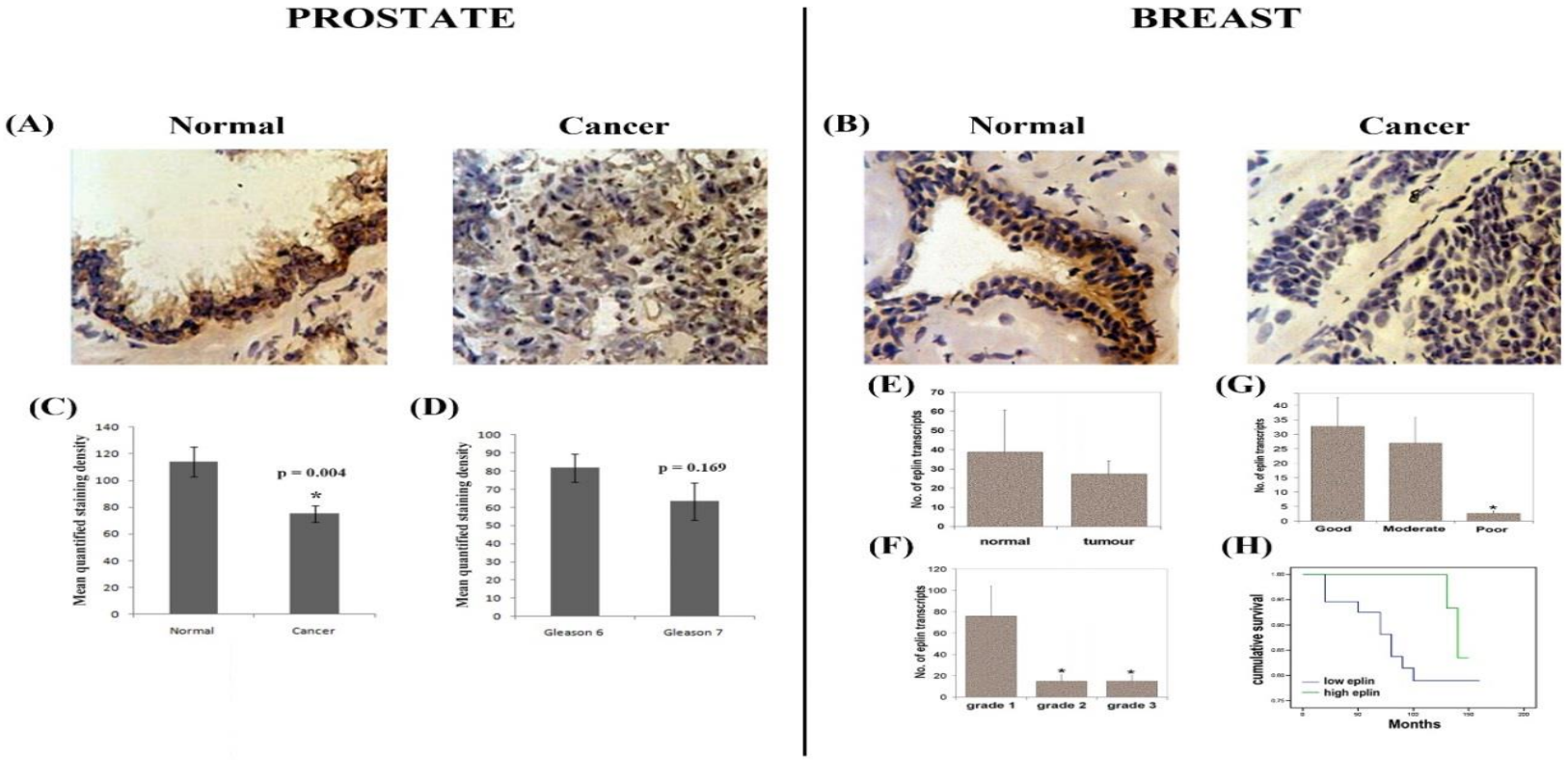

Figure 1.19 EPLIN profile in prostate and breast cancer.

Immunohistochemical staining (X20 objective magnification) of normal and cancerous (A) prostate and (B) breast clinical samples demonstrating EPLIN localisation and expressional differences. (C & D) Semi-quantitative analysis of EPLIN staining within prostate clinical cohort demonstrates lower levels of EPLIN staining are associated with cancerous and higher grade samples. (E) Within a clinical breast cancer cohort, lower transcript expression of EPLIN is seen in tumour samples compared to normal breast tissue and was associated with a higher grade (F), a poorer patient prognosis (G) and reduced overall survival rates (H). Figure modified from (Jiang et al., 2008, Sanders et al., 2011).

1.2.7.3 Oesophageal cancer

In oesophageal cancer, Q-PCR analysis displayed reduced expression of EPLIN for both cancerous tissue and cancer cell models (Liu et al., 2012a). With regard to tumour histological grade, TNM status, nodal status and survival status, EPLIN transcript generally decreased with levels significantly lower in patients who ultimately died from the cancer, suggesting EPLIN is implicated in oesophageal cancer progression and may give an indication for oesophageal cancer prognosis (Liu et al., 2012a). Overexpression analysis of EPLINα in the KYSE150 cell line resulted in decreased proliferation and invasiveness compared to control KYSE150 cells, suggesting EPLINα has tumour suppressive ability by regulating cellular aggressiveness in oesophageal cancer (Liu et al., 2012a).

1.2.7.4 Lung cancer

In a pulmonary cancer cohort also conducted within our lab, Q-PCR analysis showed a reduction of EPLIN expression in tumour vs. normal samples, where EPLIN was also reduced in later TNM stages and cancers with lymph node involvement (Liu et al., 2012b). Using the SKMES-1 cell line, overexpression of EPLINα via transfection in the pEF6 expression vector inhibited cell proliferation and cell motility (Liu et al., 2012b) in comparison to control SKMES-1 cells and again highlighting a role for EPLIN in regulating lung cancer progression.

1.2.7.5 Ovarian Cancer

Further work by our research group has also demonstrated EPLIN may be involved in the progression of ovarian cancer and has clinical potential as a prognostic marker

(Liu et al., 2016). Using knockdown models of EPLINα in epithelial ovarian cancer (EOC) cells SKOV3 and COV504, the loss of EPLINα was shown to have a significant pro-metastatic effect on cell proliferation (Liu et al., 2016). This trend was also seen on cell adhesion, invasion and motility using respective cell function assays with significant effects on cancer cell characteristics, with EPLINα knockdown and loss of expression causing the more metastatic phenotype (Liu et al., 2016). This data is in agreement with previous reports of EPLIN loss in cancer, with more aggressive traits associated with loss of EPLIN. This study further supports EPLIN's role as a potential prognostic marker for cancer development, and highlights how the molecule may contribute in the monitoring of cancer.

1.2.7.6 Additional cancer implications and renal disease

In addition to the apparent molecular loss of EPLIN in various cancers, EPLIN also appears to be reduced at the protein level for colorectal cancer and Squamous Cell Carcinoma of the Head and Neck (SCCHN), where IHC analysis revealed EPLIN is decreased in cancers with lymph node metastases vs. primary tumours (Zhang et al., 2011). Lastly, in addition to the implication of EPLIN in the spread and progression of cancer, a recent publication provides a link between EPLIN and renal diseases where patients with either membranoproliferative glomerulonephritis (MPGN) or IgA nephropathy had a decreased expression profile for EPLIN via IHC analysis (Tsurumi et al., 2014). This advocates the idea that EPLIN may be involved in the pathology of various disease states.

Collectively, these studies suggest two potential clinical roles for EPLIN: 1) as a clinical, prognostic indicator for cancer progression and development and 2) as a

tumour suppressive molecule in the regulation of cancer progression. Both these clinical options will be evaluated further throughout this study.

1.2.7.7 Tumour angiogenesis

Angiogenesis is the formation of new blood vessels from pre-existing vessels and is essential for wound healing and normal proliferation and development. The angiogenic process is frequently utilised by cancer cells, by a means of metastasis and tumour angiogenesis, to support advanced tumour proliferation and as a means to reach secondary sites around the body and develop secondary tumours. Angiogenesis is therefore a critical factor when targeting cancer therapies and an active area of research. Molecular components are crucial for tumour angiogenesis and various drugs have been established targeting angiogenic molecules. VEGF is an established angiogenic molecule and therapies including Bevacizumab (Avastin), Aflibercept (Sanofi Aventis) and Sunitinib (Sutent) are all approved cancer therapies targeting VEGF and angiogenesis (Mukherji et al., 2013). EPLINα has been shown to have a suppressive role in angiogenesis, where overexpression in the HECV endothelial cell line resulted in a reduced capacity to generate tubular structures in a Matrigel tubule formation assay when compared to vector controls (Sanders et al., 2010). This regulatory effect was also apparent *in vivo* where mice injected with HECV cells overexpressing EPLINα in conjunction with cancer cells developed tumours significantly slower than controls (Sanders et al., 2010). Forced expression also appears to exert an effect on cell matrix adhesion and migration capabilities in this cell line where cells overexpressing EPLINα both migrated at a significantly slower rate and were significantly less able to adhere to the Matrigel basement membrane (Sanders et al., 2010). This suppressive role in angiogenesis illustrates

EPLIN has potentially various regulatory mechanisms for reducing cancer metastasis and could be an effective strategy for cancer therapy.

1.3 Conclusions and outlook

The interaction of EPLIN and actin has provided an excellent model for investigating multiple aspects of cancer progression over the last decade. The discovery of EPLIN led to a subtle paradigm shift in structural view and organisation of cytoskeletal dynamics, with the acknowledgment that various actin-related molecules contribute to multiple dynamic processes underlying cellular migration and invasion. There is an established link between EPLIN and cancer progression with frequent down regulation of EPLIN in more aggressive cell lines, reduced staining in cancerous tissue samples and reduced proliferation potentials when there is forced expression of the EPLINα isoform *in vitro* and *in vivo*. EPLIN is functionally linked to molecules like actin and potentially paxillin and has been implicated in a number of potential pathways to enhance metastatic potential (outlined in Figure 1.20). However, the precise mechanistic action of EPLIN and subsequently how EPLIN loss contributes to the development of cancer remains elusive. Mechanistic investigations in this PhD study will therefore be crucial to elucidate the full importance of EPLIN in cancer pathophysiology.

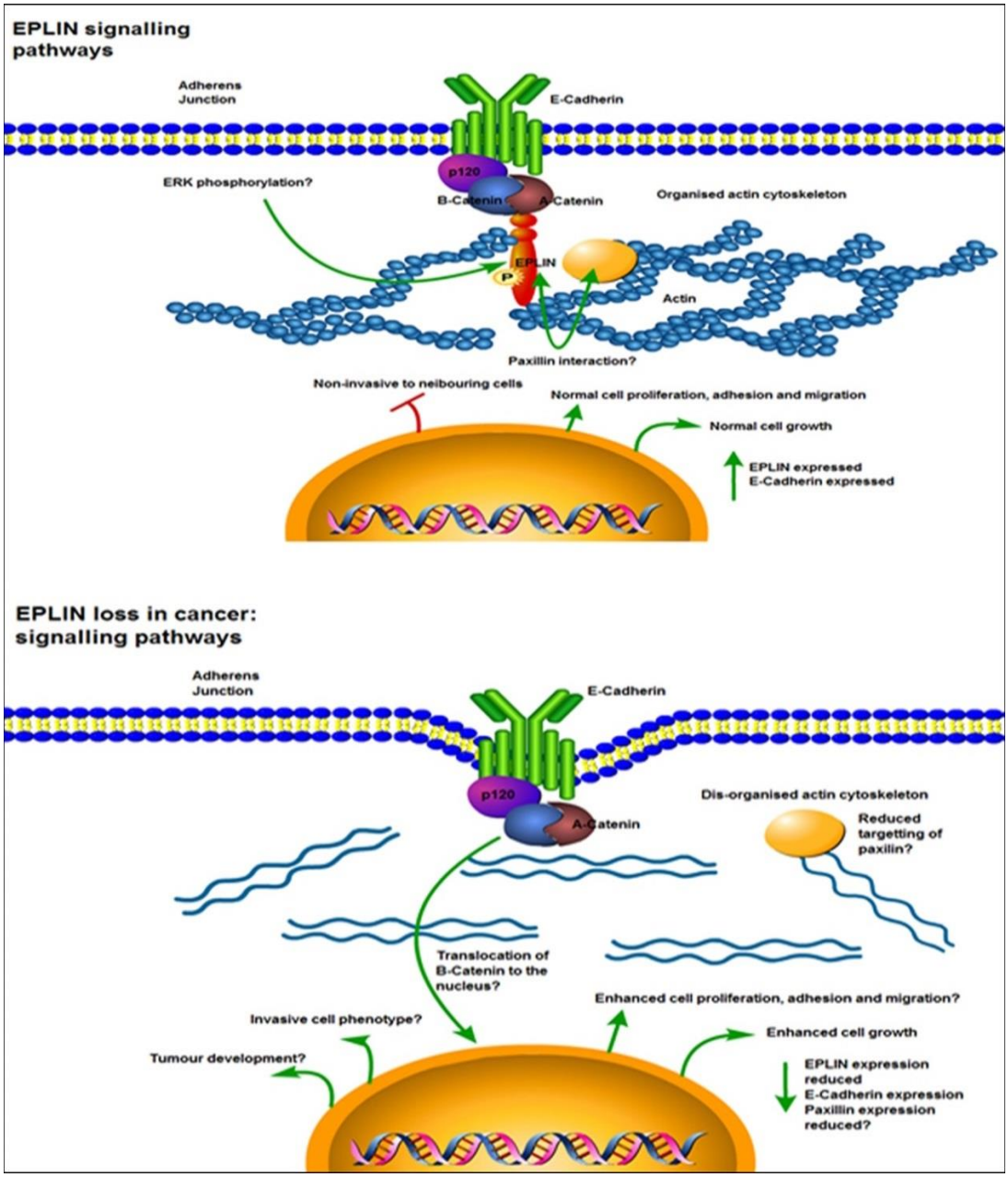

Figure 1.20 Proposed EPLIN signalling pathways and implications for loss in cancer.

In non-cancerous epithelial cells, EPLIN associates with the actin cytoskeleton linking the cadherin-catenin complex to F-actin via interaction with α-catenin. The signal transduction protein, paxillin, interacts with EPLIN in the cytoplasm and this complex likely stabilises actin dynamics. ERK phosphorylates EPLIN regulating cell motility and migration. In cancerous cells EPLIN is lost, the actin cytoskeleton becomes less organised and this induces membrane ruffling. Paxillin targeting is likely lost reducing focal adhesion between the cadherin-catenin complex and actin. These molecular, cellular and morphological consequences may result in increased metastatic potential including enhanced cell migration and motility. Signalling pathways summarised from: (Han et al., 2007, Zhang et al., 2011, Tsurumi et al., 2014, Sanders et al., 2011). Image generated using Pathway Builder 2.0 software.

1.4 PhD Thesis Aims and Objectives

EPLIN is a cytoskeletal molecule involved in actin dynamics and has associations with cancer development. As previously stated, EPLIN localises to epithelial cell junctions and interacts with various proteins to co-ordinate cell function. The role of EPLIN in cancer development is an active research area and thus altered expression of EPLIN is periodically being established in various cancer types. To date, altered expression of EPLIN has been illustrated by our research group in breast, oesophageal, lung, ovarian and prostate cancer, in addition to providing evidence of EPLIN as a potential tumour suppressive molecule and in cancer prognosis. This PhD will aim to build on previous work in this area and elucidate the functional role of EPLIN in prostate cancer metastasis. It is hypothesised that loss of EPLIN will correlate clinically with later stage, metastatic tumours, more aggressive *in vitro* cancer cell traits which will occur through a variety of mechanisms including paxillin and FAK. Specific aims of this PhD study are:

1. Determining the expression level and distribution of EPLIN in human prostate cancer using prostate cancer cell lines by RT-PCR, Q-PCR and Western Blotting. In order to demonstrate a potential link of EPLIN to clinical outcome, EPLIN expression in a larger cohort of prostate cancer and comparison of expression to clinical pathological information will be undertaken.
2. Evaluating the *in vitro* functional effects of forced expression of EPLINα in prostate cancer cell lines PC-3 and LNCaP. Manipulated EPLINα expression will be investigated in various *in vitro* functional assays including cell proliferation, cell adhesion, cell invasion and cell motility.

3. The effect of EPLINα manipulation on the establishment of bone metastases will be evaluated. This will be done by A) using an *in vitro* bone like environment, utilising Bone Matrix Extract (BME), and B) using a co-culture method utilising a human osteoblast cell line hFOB1.19, to assess any implications for EPLINα in prostate cancer metastasis to bone tissue.
4. Establishing and clarifying potential links of EPLINα to associated molecules paxillin and FAK. Determine how EPLINα expression effects FAK and paxillin transcript and protein expression in prostate cancer cell lines, in addition to the effect of EPLINα expression on FAK/paxillin phosphorylation status.
5. Explore the mechanistic relationship between EPLINα and FAK/paxillin and determine if the suppressive effect of EPLINα in cancer progression is linked to FAK and paxillin biology.
6. Explore other molecular avenues relating to EPLINα's mechanism of action and related signalling pathways. Determine any functional and mechanistic significance of these potential associations, and further clarify the mechanism behind EPLINα's functional role in prostate cancer progression and development.

Chapter II: Materials and Methods

2.1 Materials and solutions

2.1.1 Solutions for cell culture

All standard chemicals and reagents used in this study, unless otherwise specified, were obtained from Sigma (Dorset, UK).

0.05M Ethylene Diaminetetraacetic Acid (EDTA) trypsin

A stock solution of 10x trypsin-EDTA solution was purchased from Sigma-Aldrich, Inc. (Dorset, UK) and was diluted to a working concentration of 1x with sterile water. This solution was aliquoted into 25ml universal containers and stored at -20°C until required.

Antibiotics

A stock solution of 100x antibiotic solution (A5955) was purchased from Sigma-Aldrich, Inc. (Dorset, UK). This was aliquoted into 5ml aliquots and stored in universal containers at -20°C until required. One 5ml aliquot of antibiotics was added to each 500ml media bottle required prior to use.

Foetal Calf Serum (FCS)

FCS was purchased from Sigma-Aldrich, Inc. (Dorset, UK) and aliquoted into 25ml aliquots in universal containers and stored at -20°C until required. Two 25ml aliquots of FCS was added to each 500ml media bottle required giving a final volume of 10% FCS.

Phosphate buffered saline (PBS)

A stock solution of 10x phosphate buffered saline (P5943) was purchased from Sigma-Aldrich, Inc. (Dorset, UK) and autoclaved for cell culture use. This was then diluted with sterile water to reach a working concentration of 1x PBS. This solution was aliquoted into 25ml sterile universal containers and stored at room temperature until required.

2.1.2 Primers

Primers were designed using either Beacon software (PREMIER Biosoft international, California, USA) or Primer BLAST (National Center for Biotechnology Information, Bethesda, USA) and synthesised by Sigma (Sigma-Aldrich, Inc., Dorset, UK). Primer sequences are outlined in Table 2.1

Table 2.1 Primers used in this study.

The Z sequence for Q-PCR reactions are highlighted in bold and italicised.

Target	Application	Primer	Sequence (5' – 3')
LIMA1 (EPLIN)	PCR/Q-PCR	Forward (F8)	TCAAACTAAGATTCTCCGGG
LIMA1 (EPLIN)	PCR	Reverse (R8)	CAATAGGGGCATCTTCTACC
LIMA1 (EPLIN)	PCR/Q-PCR	Forward (F9)	AATGAAGAAGTTTCAGGCAC
LIMA1 (EPLIN)	PCR	Reverse (R9)	TTGTTTTGCCAGGTTGTTTT
LIMA1 (EPLIN)	Q-PCR	Reverse (ZR8)	***ACTGAACCTGACCGTACA***CTCCGAGTCAAATGTAGAAGA
LIMA1 (EPLIN)	Q-PCR	Reverse (ZR9)	***ACTGAACCTGACCGTACA***GACTGAGTTTGTTGTTGCAA
LIMA1 (EPLINβ)	PCR/Q-PCR	Forward (F1)	TCTCCATTTAATAGACGGCAA
LIMA1 (EPLINβ)	PCR	Reverse (R1)	TTCGGTGTTACTTCTCTTCTT
LIMA1 (EPLIN)	PCR/Q-PCR	Forward (F2)	TTAATAGACGGCAATGGACC
LIMA1 (EPLIN)	PCR	Reverse (R2)	TGCAGAAATCTTTTCCCCTT
LIMA1 (EPLIN)	Q-PCR	Reverse (ZR1)	***ACTGAACCTGACCGTACA***TTCGGTGTTACTTCTCTTCTT
LIMA1 (EPLIN)	Q-PCR	Reverse (ZR2)	***ACTGAACCTGACCGTACA***GTTTGTTTCTTCAGCTGCTT
LIMA1 (EPLIN)	PCR	Forward (F3)	CATTTAATAGACGGCAATGGA
LIMA1 (EPLIN)	PCR	Reverse (R3)	CCGGAGAATCTTAGTTTGAGT
LIMA1 (EPLIN)	PCR – for full coding sequence	Forward (ExF1)	ATGGAAAATTGTCTAGGAGAA
LIMA1 (EPLIN)	PCR – for full coding sequence	Reverse (ExR1)	TCACTCTTCATCCTCATCCTC
FAK	PCR	Forward (F22)	CTATCCAGGTCAGGCATCT
FAK	PCR	Reverse (R22)	CGATTTTACTGGACATCTCG

Paxillin	PCR	Forward	CTGACGAAAGAGAAGCCTAA
Paxillin	PCR	Reverse	CTTTTCACAGTAGGGCTGTC
GAPDH	PCR	Forward (F8)	GGCTGCTTTTAACTCTGGTA
GAPDH	PCR	Reverse (R8)	GACTGTGGTCATGAGTCCTT
GAPDH	Q-PCR	Forward (F2)	CTGAGTACGTCGTGGAGTC
GAPDH	Q-PCR	Reverse (ZR2)	***ACTGAACCTGACCGTACA***CAGAGATG ATGACCCTTTTG
PDPL	Q-PCR	Forward (F8)	GAATCATCGTTGTGGTTATG
PDPL	Q-PCR	Reverse (ZR8)	***ACTGAACCTGACCGTACA***CTTTCATTT GCCTATCACAT
T7F	PCR - Coding sequence orientation checking	Forward	TAATACGACTCACTATAGGG
BGHR	PCR - Coding sequence orientation checking	Reverse	TAGAAGGCACAGTCGAGG

2.1.3 Antibodies

Antibodies used in this study are outlined in Table 2.2 below.

Table 2.2 Antibodies used in this study for Western Blotting.

Antibody name	Host species	Molecular weight	Final Concentration	Supplier and catalogue number
EPLIN (20) sc-136399	Mouse	90kDa / 110kDA	1:200	Santa Cruz Biotechnology (Sc-136399)
EPLIN	Rabbit	90kDa / 110kDA	1:200	Bethyl Laboratories (A300-103A)
GAPDH (0411)	Mouse	37kDa	1:300	Santa Cruz Biotechnology (Sc-47724)
Paxillin	Mouse	68kDa	1:200	BD Biosciences (610051)
pPaxillin Tyr31	Rabbit	68kDa	1:150	Santa Cruz Biotechnology (Sc-14035R)
pPaxillin Tyr118	Rabbit	68kDa	1:200	Santa Cruz Biotechnology (Sc-14036R)
FAK	Mouse	125kDa	1:200	BD Biosciences (610087)
pFAK Tyr397 (2D11)	Mouse	125kDa	1:200	Santa Cruz Biotechnology (Sc-81493)
pFAK Tyr 397	Rabbit	125kDa	1:150	Santa Cruz Biotechnology (Sc-11765R)
pFAK Tyr925	Goat	125kDa	1:200	Santa Cruz Biotechnology (Sc-11766)
c-Src	Rabbit	60kDa	1:500	Abcam (Ab109381)
p-c-Src Tyr 419	Rabbit	60kDa	1:500	Abcam (Ab185617)
p-c-Src Tyr 530	Mouse	60kDa	1:200	Santa Cruz Biotechnology (Sc-166860)
ITGB1	Rabbit	135kDa	1:500	Abcam (Ab52971)
ERK1/2	Mouse	42kDa / 44kDa	1:150	Santa Cruz Biotechnology (Sc-514302)
pERK1/2 T202/Y204	Rabbit	42kDa / 44kDa	1:200	Cell signalling (#9101)
Anti-Mouse IgG	Mouse	N/A	1:500	Sigma Aldrich (A9044)
Anti-Rabbit IgG	Rabbit	N/A	1:500	Sigma Aldrich (A0545)

2.1.4 Solutions for microbiological methods

Luria Bertani (LB) agar

LB agar was made by dissolving 10g of LB Broth low salt granulated powder (Melford Laboratories Ltd., Suffolk, UK) and 7.5g of agar (A1296) (Sigma-Aldrich, Inc., Dorset, UK) in 500ml of distilled water. This was adjusted to pH value 7.0 prior to autoclaving. The final solution was allowed to cool and stored at room temperature. LB agar solidifies at room temperature, so was microwaved to melt the agar prior to each use.

LB broth

A solution of LB broth was made consisting of 8g LB Broth low salt granulated powder (Melford Laboratories Ltd., Suffolk, UK) and dissolving in 400ml sterile water. This solution was pH adjusted to 7.0 prior to autoclaving. The solution was allowed to cool and stored at room temperature until required.

Ampicillin

A 100mg/ml Ampicillin solution was prepared by dissolving 1g of ampicillin (Melford Laboratories Ltd., Suffolk, UK) in 10ml of sterile PBS. This was kept at 4°C for short term or -20°C for longer term storage.

2.1.5 Solutions for use in RNA and DNA molecular biology

Diethyl pyrocarbonate (DEPC) treated water

A solution of DEPC water was made by mixing 250µl diethyl pyroncarbonate (DEPC) and 4750µl of distilled water. The final solution was autoclaved prior to use and subsequently stored at room temperature.

Tris-Boric-Acid-EDTA (TBE)

10x concentrated TBE buffer was purchased from Sigma-Aldrich, Inc. (Dorset, UK) and diluted in sterile water to make a final 1x concentration of TBE. The solution was kept at room temperature on the PCR bench until required.

2.1.6 Solutions for protein analysis and Western Blotting

Lysis Buffer

A 1L volume of protein lysis buffer was made consisting of 8.76g of NaCl (150mM), 6.05g of Tris (50mM), 200mg Sodium azide (0.02%, w/v), 5g Sodium deoxycholate (0.5%, w/v) and 15ml Triton X-100 (1.5%, v/v) in sterile water and stored at 4°C in the fridge until required. A 50ml aliquot was taken and used to dissolve one tablet of cOmplete Tablets EASYpack protease inhibitor cocktail tablets (Roche Diagnostics, Mannheim, Germany) to ensure the blocking of protease activity in the lysis buffer for protein extraction. The 50ml was allowed to mix in a falcon tube on a rotating wheel for 15 minutes before further aliquoting into 1ml Eppendorf tubes (Greiner Bio-One Ltd, UK). 1ml aliquots were stored at -20°C until required. For screening of phospho-proteins, 100mM of Na_3VO_4 was added into the pre-made lysis buffer at the working concentration of 1mM prior to extraction.

10% Ammonium Persulfate (APS)

A solution of 10% APS was made by dissolving 2g of ammonium persulfate in 20ml of distilled water and stored at 4˚C until it was required.

Tris-Glycine-SDS running buffer

A 10x stock solution of Tris-Glycine-SDS buffer (T7777) (Sigma, Dorset, UK) was diluted 1/10 mixing 1L 10x solution with 9L distilled water. This was stored at room temperature until required.

Tris-Glycine transfer buffer

Transfer buffer was made up using 1L 10x solution of Tris-Glyine-Buffer (T4904) (Sigma, Dorset, UK), 2L of methanol (Fisher Scientific UK, Loughborough, UK) and 9L distilled water. This was stored at room temperature until required.

10X Tris Buffered Saline (TBS)

A 10x TBS stock solution (Sigma, Dorset, UK) was diluted 1/10 by mixing 1L 10x solution with 9L distilled water and stored at room temperature until required.

Resolving gel buffer

1L resolving gel buffer (161-0798) at pH 8.8 was purchased from Bio-Rad (Bio-Rad, Hertfordshire, UK) and used neat for use in gel preparation. Solutions were stored at 4°C.

Stacking gel buffer

1L stacking gel buffer (161-0799) at pH 6.8 was purchased from Bio-Rad (Bio-Rad, Hertfordshire, UK) and used neat for use in gel preparation. Solutions were stored at 4°C.

2.1.7 Solutions for protein microarray analysis

100mM Tris buffer was made by dissolving 6.0g of Tris powder in 1.5L sterile water. A 50ml Tris buffer was made using one cOmpleteTM, EDTA-free protease inhibitor cocktail tablet (Roche Diagnostics, Mannheim, Germany), 5ml of 2-mercaptoethonal (10%, v/v), nonident P-40 (1%, v/v) and 5ml of 500mM NaFl (50mM). This solution was allowed to mix and subdivided into further 1ml aliquots and stored at -20°C prior to use.

2.2 Cell lines and cell culture

All cell culture work was carried out in class II microflow cabinets under sterile conditions using aseptic techniques.. All cells were cultured in an incubator at 37˚C, 5% carbon dioxide and 95% humidity with the exception of the hFOB1.19 human osteoblast cell line which was cultured at 34˚C.

2.2.1 Cell lines

The human prostate cancer cell lines PC-3, LNCaP, VCaP, DU-145 and CA-HPV-10, immortalised ‘normal’ prostate cell line PZ-HPV-7, and a human osteoblast cell line hFOB1.19 were used for this study and obtained from ATCC. The majority of the study focused on prostate cell lines, whereas the hFOB1.19 cell line was used as part of a co-culture assay as part of functional testing. PC-3 and LNCaP cell lines

chosen as the focus of the majority of the experimental work. Full details of cell lines used are provided in Table 2.3. For functional analysis using cell lines transfected with the pEF6 control or EPLINα overexpression plasmid (see section 2.5), PC-3 and LNCaP cells were designated PC-3^{pEF6} and LNCaP^{pEF6} once transfected with the empty vector plasmid control, and PC-3$^{EPLIN\ EXP}$ and LNCaP$^{EPLIN\ EXP}$ once transfected with the EPLINα expression sequence. The plasmid used for this PhD study was the pEF6/V5-His-TOPO TA (see section 2.5).

2.2.2 Preparation of proliferation media

Cell lines PC-3, DU-145, VCaP and CA-HPV-10 were routinely cultured in Dulbecco's Modified Eagle's Medium (DMEM / Ham's F-12 with L-Glutamine (PAA Laboratories, Somerset, UK), supplemented with streptomycin (Streptomycin Sulphate salt, Sigma-Aldrich Co), penicillin (Benzylpenicillim, Britannia, Pharmaceutical, Ltd.) and 10% heat inactivated foetal calf serum (Invitrogen, Paisley, UK). Cells transfected with the pEF6/V5-His TOPO TA plasmid vector (with or without the EPLINα expression sequence) were first cultured for 6-14 days in selection media containing 5µg/ml Blasticidin S (Melford Laboratories Ltd., Suffolk, UK). Following the selection period the cells were transferred to maintenance media containing 0.5µg/ml Blasticidin S where they remained until they reached suitable confluence for RNA and protein extraction. LNCaP cells were routinely cultured in RPMI-1640 medium (Sigma-Aldrich Co) supplemented with streptomycin (Streptomycin Sulphate salt, Sigma-Aldrich Co), penicillin (Benzylpenicillim, Britannia, Pharmaceutical, Ltd.) and 10% heat inactivated foetal calf serum (Invitrogen, Paisley, UK). PZ-HPV-7 cells were routinely cultured in keratinocyte serum free medium supplemented with 0.05mg/ml BPE and 5ng/ml

EGF (Life Technologies, Paisley, UK). hFOB1.19 cells were routinely cultured in Ham's F12 Medium Dulbecco's Modified Eagle's Medium, with 2.5 mM L-glutamine (without phenol red) (Life Technologies, Paisley, UK) with 0.3 mg/ml G418 (Melford Laboratories Ltd., Suffolk, UK); foetal bovine serum to a final concentration of 10%.

Table 2.3 Cell lines in use.

Cells were grown in culture flasks and incubated at 37°C or 34°C and 5% carbon dioxide in a humidified incubator. Mycoplasma contamination in cell cultures was estimated using EZ-PCR Mycoplasma Test Kit (Biological Industries, Israel). Cell lines validated through short tandem repeat profiling.

Cell Line	Tissue	Morphology	Features	Medium used
PC-3	prostate; derived from metastatic site: bone	Epithelial	Grade IV, adenocarcinom, osteolytic	Dulbecco's Modified Eagle Medium (DMEM) (+10% FCS)
DU-145	prostate; derived from metastatic site: brain	Epithelial	Carcinoma	Dulbecco's Modified Eagle Medium (DMEM) (+10% FCS)
LNCaP	prostate; derived from metastatic site: left supraclavicular lymph node	Epithelial	Carcinoma, Osteolytic and osteoblastic	RPMI-1640 (+10% FCS)
VCaP	prostate; derived from metastatic site: vertebral metastasis	Epithelial	Carcinoma, osteoblastic	Dulbecco's Modified Eagle Medium (DMEM) (+10% FCS)
PZ-HPV-7	prostate; epithelium	Epithelial	Prostate epithelium transformed with human papillomavirus 18	Keratinocyte serum free medium (+ 0.05mg/ml BPE, 5ng/ml EGF)
CA-HPV-10	prostate	Epithelial	Adenocarcinoma	Dulbecco's Modified Eagle Medium (DMEM) (+10% FCS)
hFOB1.19	bone	Osteoblast	Bone	Ham's F12 Medium Dulbecco's Modified Eagle's Medium, with 2.5 mM L-glutamine (without phenol red) with 0.3 mg/ml G418; 10% FCS

2.2.3 Maintenance of cells

Cell lines were maintained in a cell culture incubator and maintained in supplemented media as described above. Cells were grown to confluence in either 25cm^2 (T25) or 75cm^2 (T75) tissue cultured flasks loosely capped (Greiner Bio-One Ltd., Gloucestershire, UK) at 37°C in 5% carbon dioxide and 95% humidification. All cell culture work was carried out following aseptic techniques inside a class II laminar flow cabinet and autoclaved instruments to keep conditions sterile.

2.2.4 Trypsinization of cells

All cell lines were grown in incubators until they reached approximately 80-90% confluence. Cells were checked for confluence under a light microscope. The culture medium was removed using a sterile glass pipette under vacuum and briefly rinsed in sterile PBS to remove excess serum. Trypsin–EDTA (1-2ml) was added to the cells by pipetting and incubated for 5-15 minutes depending on cells used. LNCaP cells, for example, required less time to detach, so only required a 5 minute incubation. PC-3 cells take longer so were incubated for approximately 15 minutes to allow full detachment of cells. The detached cell suspension was transferred to a 20ml universal container (Greiner Bio-One Ltd., Gloucestershire, UK) and an equal volume of cell media was added to neutralise the trypsin before centrifuging at 1400 rpm for 8 minutes to pellet the cells. The supernatant was discarded and the cells were resuspended in appropriate cell culture medium in a volume dependant on the size of the pellet. The cells were then re-seeded into new tissue culture flasks, counted for immediate experimental work or stored by freezing in liquid nitrogen.

2.2.5 Cell counting

Cell number was determined by counting using a Neubauer haemocytometer counting chamber (Mod-Fuchs Rosenthal, Hawksley, UK) using an Olympus CKX31 microscope at an objective magnification of X10 (Olympus, Tokyo, Japan).

2.2.6 Cell storage in liquid nitrogen

For long term storage, the cell lines were stored in liquid nitrogen. Cells were resuspended and stored in culture medium containing 10% Dimethylsulphoxide (DMSO) (Sigma-Aldrich, Gillingham, Dorset, UK). The volume of resuspension medium was dependant on how many samples were frozen. 1ml of cells was transferred into pre-labelled 1ml CRYO.STM tubes (Greiner Bio-One Ltd,. Gloucestershire, UK). Tubes were wrapped in 3 layers of tissue paper and stored overnight at -80°C in a deep freezer before storage in liquid nitrogen tanks for long term storage.

2.2.7 Cell revival

Frozen cells were removed from storage and allowed to thaw at room temperature. After completely thawing the cell suspension was transferred to a universal container containing 10 ml of pre-warmed medium before being centrifuged at 1400 rpm for 8 minutes to pellet the cells. The supernatant was aspirated, the pellet resuspended in 1ml of pre-warmed medium and placed into a fresh T25 tissue culture flask and incubated at 37°C (34°C for hFOB1.19), 95% humidification and 5% CO_2. The following day, the flask was examined under a light microscope to ensure a sufficient number of healthy adherent cells had survived the cell revival and subjected to a media change to remove any dead cells

2.3 Methods for detecting mRNA

2.3.1 Total RNA isolation

Cells were grown until they reached appropriate confluence (80-90%). Following this, cell media was aspirated, cells were washed with PBS and 1ml of Sigma Total RNA Isolation (TRI) Reagent was added (Sigma-Aldrich, Dorset, UK). Total RNA was allowed to detach cells from cell flask and subsequently transferred into a 1.5ml Eppendorf (Greiner Bio-One Ltd, UK). To allow dissociation of nucleoprotein complexes, the RNA was left to stand for 5 minutes at room temperature. Following this, 0.2ml chloroform was added and vigorously mixed by inversion for 15 seconds before Hettich centrifugation (DJB Labcare Ltd, United Kingdom) at 12000g for 15 minutes at 4°C. The resultant homogenate forms 3 phases: a red organic phase (containing protein), an interphase (containing DNA), and a colourless upper aqueous phase (containing RNA). The upper aqueous phase was carefully removed and transferred in a clean Eppendorf before adding 500µl of 2-propanol and mixing via inversion for 15 seconds. The samples were then centrifuged for 10 minutes at 12000g and 4°C. The supernatant was removed and the RNA pellet was washed with 1ml of 75% ethanol (Fisher Scientific UK, Loughborough, UK) in DEPC water before vortexing and centrifugation at 7500*g* for 5 minutes at 4 °C. The supernatant was removed and the pellet was briefly dried for 10 minutes by air-drying. The final pellet was completely resuspended in 30µl DEPC water before quantification.

2.3.2 RNA quantification

The concentration of RNA was measured using an IMPLEN nanophotometer (Geneflow Ltd., United Kingdom) set to detect RNA in ng/µl. The RNA samples

were either stored at -80°C for further use or used immediately for reverse transcription (RT).

2.3.3 Reverse transcription-polymerase chain reaction (RT-PCR)

Once total RNA had been isolated and quantified, RT-PCR was carried out to generate complementary (cDNA) from the RNA template using GoScript™ Reverse Transcription System (Promega, UK). A 20µl RT-PCR reaction, containing 250ng of RNA was undertaken to generate cDNA according to the manufacturer's instructions. The RT reaction is a 2 step reaction. For the first step, the following components were added to a PCR tube:

- 250ng experimental RNA (volume depends on RNA concentration)
- 1µl Oligo(dT) primer (0.5µg/reaction)
- Nuclease free water to final volume of 5µl

The RNA, primer and water was then transferred to a thermocycler and heated to 70°C for 5 minutes. Following initial heating, the tubes were then transferred to ice for at least 5 minutes and centrifuged in a microcentrifuge before storing on ice until the reverse transcription mix was added. For the second step in the reaction, a following 15µl reaction was then made consisting of:

- 4µl GoScript™ 5X Reaction Buffer
- 1µl PCR Nucleotide Mix (final concentration 0.5mM each dNTP)
- 1.2µl MgCl (final concentration 1.5–5.0mM)
- 1 µl GoScript™ Reverse Transcriptase
- Nuclease-Free Water (to a final volume of 15µl)

The 15µl mix above was added to the 5µl RNA and primer reaction used in the first step. The reaction was then transferred to a thermocycler and the following conditions were input:

- 25˚C for 5 minutes
- 42˚C for 60 minutes
- 70˚C for 15 minutes

Following RT reaction, the mix was diluted 1:4 in Nuclease free water and stored at -20˚C until required.

2.3.4 Polymerase chain reaction (PCR)

PCR was carried out using GoTaq Green Master mix DNA polymerase protocol (Promega, Southampton, United Kingdom). A final reaction of 16µl was prepared for each sample, with each individual PCR sample containing:

- 8µl - GoTaq mastermix
- 1µl – specific forward primer
- 1µl – specific reverse primer
- 5µl – PCR water
- •1µl –cDNA

Primers were designed targeting different regions of the EPLINα and EPLINβ gene sequence and were synthesised by Sigma (Sigma-Aldrich, Dorset, UK). Both forward and reverse primers were diluted to 10pM prior to use in sterile water. The PCR reaction was initially set up by preparing a mastermix of all components common to the particular reaction/molecule of interest (for example GoTaq

mastermix, primers, water) in a 0.6ml tube with sufficient volume for the required number of PCR reactions. Once each ingredient was added, 15µl of mastermix solution was added to a PCR tube and 1µl of cDNA was added. These were then mixed, centrifuged and placed in an ABI thermocycler (Thermo Fisher Scientific, USA). PCR reactions were amplified under the following conditions:

- Step 1: Initial denaturing period: 94 °C for 5 minutes.
- Step 2: Denaturing step: 94 °C for 30 seconds.
- Step 3: Annealing step: 55°C for 30 seconds.
- Step 4: Extension step: 72°C for 40 seconds.
- Step 5: Final extension period: 72°C for 10 minutes.

Steps 2, 3 and 4 were repeated over 30 cycles.

Products were separated on 1% agarose gel stained with SYBR Safe Gel Stain (Invitrogen, Paisley, UK) according to size and visualised using a U:Genius3 gel doc system (Syngene, Cambridge, UK). A negative control was included where cDNA was replaced with sterile water.

2.3.5 Agarose gel electrophoresis

Amplified PCR products were separated according to size on 1% agarose gels. Agarose gels were made by adding the required amount of agarose powder (Sigma-Aldrich, Dorset, UK) to TBE solution. The mixture was heated in a microwave to dissolve the agarose and 5-10µl of SYBR® Safe DNA Gel Stain (Invitrogen, Paisley, United Kingdom) was added to allow staining of DNA bands. The gel mixture was poured into gel tanks with an electrophoresis cassette and plastic comb

already loaded. Gels were allowed to set for 30 minutes. Once set, TBE buffer was poured into the electrophoresis tank, the comb removed and 8µl of the PCR products loaded each resultant well. To a separate well, 5µl of a 1Kb ladder (Geneflow, United Kingdom) was added to allow identification of resultant band sizes. Samples were electrophoretically separated using a electrophoresis power pack at 100V for 40 minutes to allow sufficient DNA band separation.

2.3.6 Real-time quantitative polymerase chain reaction (RT-QPCR)

RT-QPCR was performed to detect and quantify transcript copy number of target genes using Precision 2X Q-PCR Mastermix (Primer Design, UK) and Amplifluor™ Uniprimer™ (Uniprobe) Universal system (Intergen company®, New York, USA). The amplifluor probe consists of a 3' region specific to the Z-sequence, ACTGAACCTGACCGTACA, which presents on the target specific primers and a 5' hairpin structure labelled with a fluoresent tag (FAM). Ten microliter reactions were set up and added to MicroAmp® Fast Optical 96-Well Reaction Plates with Barcode (Life Technologies, Paisley, UK). GAPDH copy number was also included within these samples to allow standardisation and normalisation of the samples. Each reaction was set up as follows:

- Forward primer - 0.3µl (10pmol/µl)
- Reverse primer (containing Z sequence) - 0.3µl (1pmol/µl)
- Q-PCR Master Mix -5µl
- Uniprobe – 0.3µl (10pmol/µl)
- PCR water – 3µl
- cDNA - 1µl

The reverse primers in each reaction contain a sequence called the Z-sequence (ACTGAACCTGACCGTACA). This is a unique sequence that is present in both the reverse primers and also the uniprobe primer. During the reaction, the Z sequence contained on the reverse primer becomes incorporated into the PCR product sequence over the initial rounds of amplification. Subsequently, as the reverse primer, containing the Z sequence, is a limiting factor, in later stages the uniprobe primer anneals to the incorporated Z sequence. Ultimately, this causes extension of the uniprobe primer, causing a conformational change leading to florescence which can be directly measured. The intensity of fluorescence within each sample compared to a range of standards of known transcript copy number allows the calculation of transcript copy number within each sample. PCR amplification was performed using Applied Biosystems® Real-Time PCR Thermocycler (Life Technologies, Paisley, United Kingdom) under the following conditions:

- Step 1: Initial denaturing period: 94˚C for 10 minutes.
- Step 2: Denaturing step: 94˚C for 10 seconds.
- Step 3: Annealing step: 55˚C for 30 seconds.
- Step 4: Extension step: 72˚C for 10 seconds.

Steps 2, 3 and 4 were repeated over 100 cycles.

Expression of the target sequence was detected alongside a known standard transcript (PDPL) that is used to generate a standard curve to allow the calculation of transcript copy number in each target sample. Lastly, the transcript copy number of target genes were normalised by the detected copy number of GAPDH.

2.4 Methods for detecting protein

2.4.1 Cell lysis and protein extraction

Cells were grown in T75 cell culture flasks until appropriate confluency (~90%) and the cell monolayer washed 2X with PBS before being removed from the base of the cell culture flask using a disposable plastic cell scraper. The detached cells were then transferred to a sterile 30ml universal container and centrifuged for 5 minutes at 1800rpm. The supernatant was discarded and the protein pellet resuspended in 300µl lysis buffer. This solution was then transferred to a1.5ml Eppendorf tube and placed on a Labinco rotating wheel (Wolf Laboratories, York , UK) at 25rpm, 4°C for 45 minutes.. The solution was then centrifuged for 15 minutes at 13000rpm to pellet insoluble protein and the supernatant placed into a fresh Eppendorf tube before freezing at -20°C. For smaller cell flasks (T25) or 6 well plates, the same procedure was performed but were resuspended in lower volumes of lysis buffer (150µl for T25, 100µl 6 well plates).

2.4.2 Protein quantification

Protein concentration of samples was determined using a Bio-Rad DC protocol (Bio-Rad laboratories, Hammelhempstead, UK). Protein samples were compared to a known concentration of Bovine Serum Albumin (BSA) of 100mg/ml serially diluted to 0.029mg/ml (Sigma, Dorset, UK). Samples and standards were pipetted into a 96-well plate at a volume of 5µl before adding 25µl of ‘working reagent A’ and 200µl of reagent B. Solutions were allowed to stand for 15 minutes to allow the colorimetric reactions to develop. Absorbance of both standards and samples were read at 620nm using an ELx800 plate reading spectrophotometer (Bio-Tek, Wolf

laboratories, York, UK). Using the BSA known concentrations, a standard protein curve was created to establish each sample concentration. All samples were normalised to working concentrations of 2mg/ml by diluting in cell lysis buffer before further dilution in 2x Lamelli buffer (Sigma-Aldrich, Dorset, UK) in a 1:1(v/v) ratio of diluted sample and 2x Lamelli buffer. Samples were boiled at 100°C for 5 minutes before being stored at -20°C until required.

2.4.3 Protein extraction, fluorometric protein quantification for KinexusTM antibody microarrays

In order to acquire high concentration protein lysate, each cell type was cultured in two T75 flask until reaching ~80% confluency. Upon protein extraction, cells were washed with sterile PBS twice and scraped from the flask using a sterile cell scraper in 5ml sterile PBS. Cell suspensions from both flasks were combined in a 30ml universal container using a glass pipette and centrifuged at 2000rpm for 10 minutes. The pellet was then resuspended in 600µl lysis buffer and transferred to a 1.5ml Eppendorf tube. This was subsequently placed on a Labinoco rotating wheel at 25rpm for 1 hour at 4°C. The solution was then centrifuged at 13000rpm and the supernatant (containing protein lysate) was transferred into a fresh, pre-labelled eppendorf tube and stored at -20°C until required. For the Kinexus microarray, the standard Bio-Rad protein assay kit is unsuitable and not compatible with 2-mercaptoethanol, which is part of the lysis buffer. Fluorescamine acetone was made by dissolving 15mg of fluorescamine (F9015) (Sigma-Aldrich, Inc., Dorset, UK) in 5ml absolute acetone (10162180) (Fisher Scientific UK, Loughborough, UK) in a glass vial and stored at 4°C until required. A serial dilution of BSA standard samples was made, ranging from 10mg/ml to 0.078mg/ml, by mixing the appropriate amount

of BSA original stock and PBS. The extracted protein samples were diluted 1 in 10 by adding 50µl of protein sample in 450µl of PBS. Following this, 150µl of each serially diluted BSA standard samples and the 10x diluted protein extracted samples were aliquoted into a 96-well plate in triplicates prior to adding 50µl of fluorescamine acetone and being shaken for 1 minute. The fluorescence signal was then determined using a GloMax®-Multi Microplate Multimode Reader (Promega Biosystems Inc., Sunnyvale, CA, USA) with a 365nm excitation and 410-460nm emission filter. Protein concentration was based on the standard curve before being normalised to the desired concentration of 4mg/ml through the addition of an appropriate amount of lysis buffer to make 300µl stock followed by being stored at -20°C. The quantified protein samples were then sent to KinexusTM antibody microarray analysis (Kinexus Bioinformatics, Vancouver, British Columbia, Canada).

2.4.4 SDS gel assembly and gel electrophoresis

Acrylamide gels were assembled at 8-10% concentration depending on the molecule screened (proteins in the range of 20KDa to 120KDa are detected at these concentrations). Two solutions were made up; a 15ml resolving gel and a 5ml stacking gel and these solutions were prepared in a universal container. The components of the 8% resolving and 5% stacking gel are listed below:

Table 2.4 Western Blot gel preparation

Component	8% Resolving gel (ml)	Stacking gel (ml)
Water	5.9	3.4
30% acrylamide mix	5	0.83
1.0M Tris	3.8 (pH 8.8)	0.63 (pH 6.8)
10% SDS	0.15	0.05
10% Ammonia Persulphate	0.15	0.05
TEMED	0.006	0.005

SDS-PAGE was undertaken using an OmniPAGE VS10 vertical electrophoresis system (OminPAGE, Wolf Laboratories, York, UK). Once resolving and stacking gels were prepared, the resolving gel was added to the glass plates using a disposable plastic pipette until the solution reached a level just below where the plastic comb would make contact with the solution. The solution was then covered with ethanol ensuring the gel sets evenly leaving a smooth surface for addition of the stacking gel and left to set for 15 minutes. Following this time, the ethanol was removed and the stacking gel was added in place of the ethanol and plastic combs were gently inserted inside, creating wells for protein insertion. This solution was allowed to set for an additional 15 minutes. Once the stacking gel had set, the loading cassettes were inserted into an electrophoresis tank and the tank was filled with 1x running buffer (see section 2.1.6). The plastic combs were removed carefully and samples were loaded to the tank using a flat tipped needle at equal volumes of 12-18µl. A molecular weight marker (Geneflow Limited, Fradley, Staffordshire, UK) was included with the samples and loaded at a volume of 8µl

.

2.4.5 Poly acrylamide gel electrophoresis

Total protein was allowed to separate at power settings 120V, 150mA and 50W for approximately 2 hours. The gels were run using a EV243 power consort (Topac Inc., Cohasset, MA, USA).

2.4.6 Preparation of membrane and gel transfer

Once the gel had successfully run and proteins size separated, the gel products were next transferred onto PVDF nitrocellulose membrane (Millipore UK, United Kingdom) using electroblotting. Gels were removed from electrophoresis tanks, the glass plates separated and the stacking gel removed. PVDF membrane was cut into 7cm x 8cm rectangles and the top right of the membrane was cut off for orientation purposes. The membranes were immersed initially in 100% methanol (Fisher Scientific UK, Loughborough, UK) (30 seconds), followed by washing with water and then left in transfer buffer (see section 2.1.6) for 10 minutes. Following this, a 'sandwich' was created of filter paper (Sigma-Aldrich, Inc., Dorset, UK), membrane, gel and a second filter paper. The sandwich was inserted into a SD10 SemiDry Maxi System blotting unit (Wolf Laboratories, York, UK) and air bubbles removed by rolling. Electroblotting was performed at 15V, 500mA and 50W for 50 minutes. Membranes were then placed in 0.2% milk blocking solution (0.2% milk, 0.1% polyoxyethylene (20) sorbitan monolaurate (Tween 20) in TBS) prior to antibody staining.

2.4.7 Blocking/wash buffer preparation

A 200ml solution of blocking buffer and a 400ml solution of wash buffer was made in sterile 1L bottles. For the blocking buffer, 400mg milk powder and 200µl Tween 20 was mixed with 200ml TBS. For the wash buffer, 400µl Tween 20 was mixed with 400ml TBS. Both buffers were mixed by inversion and kept at room temperature until required.

2.4.8 Preparation for antibody solutions for western blotting

Antibodies were prepared at 1/5 dilution of the original concentration (in 0.1%BSA/PBS), aliquoted and stored at -20˚C until required. Diluted antibody solutions were prepared at varying working concentrations (see Table 2.2) for each Western Blot reaction by making to a final volume of 3ml in blocking buffer made as described above.

2.4.9 Snap id® 2.0 protein detection system

Once antibody solutions were made, any protein that was electroblotted onto the membrane was probed using a SNAP id® 2.0 Protein Detection System (Merck Millipore Ltd., Feltham, UK). First, the membrane holder was rinsed with distilled water and the membrane was placed protein side down inside, rolling out any air bubbles using a roller. The system holding frame was opened and the membrane placed inside protein side up before closing and locking the frame. Once the membrane was in place, 30ml of blocking solution (PBS 0.1% Tween 0.2% milk powder) was added, the frame pressed down and the system turned on to apply the vacuum. When the membrane appeared dry, the vacuum was turned off. Primary antibody solutions were then added at a volume of 3ml per membrane and incubated

at room temperature for 15 minutes. After the incubation period, the frame was pressed down and the vacuum turned on to pull through residual antibody solution. The membrane was then washed using wash solution (PBS 0.1% Tween) by adding 30ml to the membrane with the vacuum continuously running and repeating 3 times before turning the vacuum off. When the membrane was completely dry, 3ml of secondary antibody were added to the membrane and incubated for 10 minutes. Following the incubation, the vacuum was turned on to pull through residual secondary antibody. When the membrane was completely dry, the membrane was washed a second time with a total of 4 wash steps as above. Finally, the vacuum was turned off, the membrane removed from the holder and incubated with EZ-ECL protein detection reagent (GeneFlow Ltd., Staffordshire, UK) before visualising on a G:BOX Chemi XRQ protein detection system (Syngene, Cambridge, UK).

2.4.10 Semi-quantitative analysis on western blot results by densitometry

Image J v1.50c software was utilised for the semi-quantitative analysis of Western blot results. The rectangular selection tool was used to select a set area for each band on the Western blot image and the value of the integrated density for the selected area was then measured. The density of the protein of interest was then normalised by dividing the density value of the protein band of interest by the density value of the GAPDH control band.

2.4.11 Tissue Microarray (TMA) analysis of prostate cancer tissue

Tissue Microarrays (TMA) were purchased to explore EPLIN expression in normal prostate tissue and prostate cancer tissue. TMA's were purchased from US Biomax **(**US Biomax, Inc., Rockville, USA) and tissues were collected under HIPPA

approved protocols by the manufacturer**.** TMA's were stored and logged according to local HTA regulations with double locking under restricted access. TMA1 was labelled HPro-Ade96Sur-01 and TMA2 was labelled PR8011a, according to the US Biomax reference numbers for each TMA. The details of each TMA are shown in Table 2.5 and Table 2.6 and such details were used in relation to the staining analysis, though no pathology support was available within our department to confirm specified clinical information. Following staining of TMAs (as described below in 2.4.12), images were captured over a range of magnifications. Staining intensities of EPLIN in each section were classified, by three independent researchers, as negative staining (0), weak staining (1), moderate staining (2) or strong staining (3) within epithelial components of the tissues. Staining intensities were subsequently aligned to patient/sample clinical information to identify differential staining patterns between groups.

2.4.12 Immunohistochemical staining (IHC) of prostate sample tissues

Prior to staining, slides were placed in an oven set at 45°C for 48 hours to aid the sections adherence to the slides. Following this, slides were de-waxed and re-hydrated by immersing in the following solutions for 5 minutes each: 100% xylene (x2), 50% xylene/50% ethanol, 100% ethanol (x2), 90% ethanol, 70% ethanol, 50% ethanol, distilled water and PBS buffer. An antigen retrieval buffer was made during the last immersion step using 1mM EDTA buffer (0.37g EDTA in 1000ml dH_2O, pH 8). Antigen retrieval was performed by placing slides in a plastic container and covering with the EDTA buffer. These were then placed in a microwave oven on full power for 20 minutes. After 10 minutes, the microwave was stopped and the slide rack was shaken to disperse air bubbles. The slides were then gradually cooled and

washed for 10 minutes using tap water. Following washing, excess fluid was removed from the sections and a ring of wax was applied. The sections were then incubated with blocking solution (10% horse serum/0.1% BSA/PBS) for at least 90 minutes. Slides were placed in a humidified box during incubations to prevent the sections from drying out.

Whilst the sections were blocking, the primary and secondary antibodies, as well as the tertiary ABC reagent were prepared in the same blocking solution. Primary antibody used was EPLIN (20) (Santa Cruz Biotechnology, Inc., Heidelberg, Germany) and was prepared to give a final concentration of 2µg/ml. A Vectastain Universal Elite ABC Kit (PK-6200) (Vector Laboratories Ltd., Peterborough, UK) was used for the secondary antibody and the tertiary ABC reagent. For the secondary antibody, two drops of secondary reagent (biotinylated horse anti-mouse/rabbit IgG) was added to 5ml blocking solution, and for the ABC reagent, two drops of Reagent A and two drops of Reagent B were added to 5ml blocking solution. Following the blocking incubation, the solution was removed and sections were covered with the primary antibody and incubated overnight at 4^{o}C. The following day, sections were washed three times for five minutes each in PBS buffer, and were then incubated with the biotinylated secondary antibody for 30 minutes. Sections were subsequently washed three times with PBS and finally incubated with ABC reagent for 30 minutes. Three more wash steps were made prior to development with DAB (diaminobenzidine) substrate (D5637) (Sigma-Aldrich, Dorset, UK) for 10 minutes. DAB was made in 5ml PBS (final concentration 1mg/ml) and 6µl Hydrogen peroxide was added immediately before use. Slides were washed briefly with water before counterstaining with Gill's Haematoxylin (Vector Laboratories Ltd,

Peterborough, UK) for 2 minutes, and then blued in running tap water for 5 minutes. Sections were then dehydrated for five minutes in each 50% ethanol, 70% ethanol, 90% ethanol, 100% ethanol (x2), 50% ethanol/50% xylene and cleared in xylene (x2). Finally, sections were mounted with DPX/Histomount and left to dry prior to analysis. Prior to running TMA staining, the EPLIN antibody was optimised using a number of non-essential tissue sections and such sections were also run alongside the TMA slides to serve as a negative control.

Table 2.5 Patient/Sample details for tissues present in TMA1 (HPro-Ade96Sur-01)

Position	Age	Organ	Pathology	Stage	Gleason score	TNM	Months	Type	PSA (ng/ml)	Residual tumour	Follow up (months)	Follow-up result	Cause of death
A1, A2	68	Prostate	Adenocarcinoma	III	9	T3bN0M0	.	Malignant	*	*	*	*	
A3, A4	64	Prostate	Adenocarcinoma	II	7	T2cN0M0	.	Malignant	30	R0	60	alive	
A5, A6	71	Prostate	Adenocarcinoma	III	9	T3bN0M0	.	Malignant	60.4	R1	55	alive	
A7, A8	64	Prostate	Adenocarcinoma	III	10	T3aN0M0	.	Malignant	7.4	R1	47	alive	
A9, A10	59	Prostate	Adenocarcinoma	III	9	T3bN0M0	.	Malignant	9.8	R1	44	alive	
A11, A12	65	Prostate	Adenocarcinoma	IV	8	T4N0M0	.	Malignant	34.9	R1	43	alive	
B1, B2	73	Prostate	Adenocarcinoma	II	7	T2cN0M0	.	Malignant	48.1	R1	42	alive	
B3, B4	69	Prostate	Adenocarcinoma	II	7	T2cN0M1	.	Malignant	10.6	R0	42	alive	
B5, B6	62	Prostate	Adenocarcinoma	II	7	T2cN0M1	.	Malignant	37.3	R1	39	alive	
B7, B8	66	Prostate	Adenocarcinoma	III	9	T3bN0M0	.	Malignant	1.2	R1	39	alive	
B9, B10	60	Prostate	Adenocarcinoma	III	9	T3bN0M0	.	Malignant	40	R1	39	alive	
B11, B12	70	Prostate	Adenocarcinoma	IV	7	T4N0M0	.	Malignant	7	R1	37	alive	
C1, C2	65	Prostate	Adenocarcinoma	III	9	T3bN0M1	.	Malignant	17.5	R1	23	dead	cancer
C3, C4	67	Prostate	Adenocarcinoma	IV	9	T3bN1M0	.	Malignant	13.1	R1	34	alive	
C5, C6	69	Prostate	Adenocarcinoma	III	7	T3bN0M0	.	Malignant	1.1	R1	33	alive	
C7, C8	69	Prostate	Adenocarcinoma	III	7	T3aN0M1	.	Malignant	17.6	R1	27	alive	
C9, C10	70	Prostate	Adenocarcinoma	III	7	T3aN0M1	.	Malignant	9	R1	26	alive	
C11, C12	58	Prostate	Adenocarcinoma	III	9	T3bN0M0	.	Malignant	5.8	R0	26	alive	
D1, D2	71	Prostate	Adenocarcinoma	II	7	T2cN0M0	.	Malignant	31.4	R1	24	alive	
D3, D4	70	Prostate	Adenocarcinoma	III	7	T3bN0M0	.	Malignant	14.4	R1	19	alive	

D5, D6	59	Prostate	Adenocarcinoma	II	6	T2bN0M0	.	Malignant	18.3	R0	18	alive	
D7, D8	63	Prostate	Adenocarcinoma	III	9	T3bN0M0	.	Malignant	16.6	R1	17	alive	
D9, D10	72	Prostate	Adenocarcinoma	III	9	T3bN0M0	.	Malignant	*	R1	16	alive	
D11, D12	66	Prostate	Adenocarcinoma	III	8	T3bN0M0	.	Malignant	10.8	R1	17	dead	cancer
E1, E2	70	Prostate	Adenocarcinoma	II	7	T2cN0M1	.	Malignant	*	R0	15	alive	
E3, E4	68	Prostate	Adenocarcinoma	III	8	T3bN0M0	.	Malignant	26.9	R1	15	alive	
E5, E6	63	Prostate	Adenocarcinoma	III	10	T3bN0M1	.	Malignant	*	R1	15	alive	
E7, E8	57	Prostate	Adenocarcinoma	III	7	T3bN0M0	.	Malignant	25	R1	15	alive	
E9, E10	72	Prostate	Adenocarcinoma	III	8	T2cN0M0	.	Malignant	16.8	R1	15	alive	
E11, E12	70	Prostate	Adenocarcinoma	III	8	T3bN0M0	.	Malignant	0.5	R1	15	alive	
F1, F2	75	Prostate	Adenocarcinoma	III	9	T3bN0M0	.	Malignant	98	R1	15	alive	
F3, F4	62	Prostate	Adenocarcinoma	III	9	T3bN0M0	.	Malignant	*	R1	15	alive	
F5, F6	63	Prostate	Adenocarcinoma	III	9	T3bN0M0	.	Malignant	91	R1	14	alive	
F7, F8	53	Prostate	Adenocarcinoma	III	9	T3bN0M0	.	Malignant	161	R1	17	dead	cancer
F9, F10	63	Prostate	Adenocarcinoma	III	8	T3bN0M0	.	Malignant	13	R1	13	alive	
F11, F12	44	Prostate	Adenocarcinoma	III	7	T3bN0M1	.	Malignant	*	R1	11	alive	
G1, G2	65	Abdominal wall	Metastatic adenocarcinoma from prostate	IV	.	M1	36	Malignant					
G3, G4	61	Bone	Metastatic adenocarcinoma from prostate	IV	.	M1	32	Malignant					
G5, G6	69	Bone	Metastatic adenocarcinoma from prostate	IV	.	M1	34	Malignant					
G7, G8	59	Bone	Metastatic adenocarcinoma	IV	.	M1	0	Malignant					

			from prostate					
G9, G10	69	Prostate	Normal (match of #8)	.	.	.	.	Nat
G11, G12	62	Prostate	Normal (match of #9)	.	.	.	.	Nat
H1, H2	65	Prostate	Normal (match of #13)	.	.	.	.	Nat
H3, H4	69	Prostate	Normal (match of #16)	.	.	.	.	Nat
H5, H6	70	Prostate	Normal (match of #17)	.	.	.	.	Nat
H7, H8	70	Prostate	Normal (match of #25)	.	.	.	.	Nat
H9, H10	63	Prostate	Normal (match of #27)	.	.	.	.	Nat
H11, H12	44	Prostate	Normal (match of #36)	.	.	.	.	Nat

Table 2.6 Patient/Sample details for details for tissues present in TMA2 (PR8011a)

Position	Age	Organ	Pathology	Grade	Stage	Gleason Grade	Gleason score	TNM	Type
A1	60	Prostate	Adenocarcinoma	1	II	1	1+2	T3aN0M0	Malignant
A2	71	Prostate	Adenocarcinoma	1	II	1	1+1	T2N0M0	Malignant
A3	72	Prostate	Adenocarcinoma	2	II	3	3+3	T2N0M0	Malignant
A4	74	Prostate	Adenocarcinoma	2	IV	2	2+3	T4N1M1c	Malignant
A5	60	Prostate	Adenocarcinoma	1	IV	1	1+2	T4N1M1c	Malignant
A6	70	Prostate	Adenocarcinoma	2	II	2	2+3	T2aN0M0	Malignant
A7	70	Prostate	Adenocarcinoma	2	IV	2	2+3	T2N1M1c	Malignant
A8	61	Prostate	Adenocarcinoma	2	IV	3	3+3	T3N1M0	Malignant
A9	65	Prostate	Adenocarcinoma	2	II	3	3+3	T2N0M0	Malignant
A10	76	Prostate	Adenocarcinoma	2	II	4	4+2	T2aN0M0	Malignant
B1	62	Prostate	Adenocarcinoma	2	IV	3	3+4	T3N1M1b	Malignant
B2	26	Prostate	Adenocarcinoma	3	II	4	4+4	T2N0M0	Malignant
B3	76	Prostate	Adenocarcinoma	3	IV	4	4+4	T3N1M0	Malignant
B4	81	Prostate	Adenocarcinoma	3	III	4	4+5	T3aN0M0	Malignant
B5	80	Prostate	Adenocarcinoma	2--3	IV	3--4	3+4	T2N1M1c	Malignant
B6	64	Prostate	Adenocarcinoma	2	II	3	3+3	T2N0M0	Malignant
B7	64	Prostate	Adenocarcinoma	3	IV	4	4+3	T3N0M1	Malignant
B8	75	Prostate	Adenocarcinoma	2	IV	3	3+3	T2N1M1c	Malignant
B9	73	Prostate	Adenocarcinoma	3	IV	4	3+4	T3N1M1	Malignant
B10	65	Prostate	Adenocarcinoma	3	IV	4	4+3	T2N1M1	Malignant
C1	75	Prostate	Adenocarcinoma	2	IV	2	2+3	T4N1M1	Malignant
C2	69	Prostate	Adenocarcinoma	1	III	1	1+2	T3bN0M0	Malignant
C3	82	Prostate	Adenocarcinoma	3	II	4	4+5	T2N0M0	Malignant

C4	72	Prostate	Adenocarcinoma	3	IV	4	4+5	T2N0M1	Malignant
C5	67	Prostate	Adenocarcinoma	3	IV	4	4+4	T2N2M0	Malignant
C6	60	Prostate	Adenocarcinoma	4	II	5	5+5	T2N0M0	Malignant
C7	40	Prostate	Adenocarcinoma	1	IV	1	1+2	T2N1M1	Malignant
C8	78	Prostate	Adenocarcinoma	4	IV	5	5+4	T4N1M1	Malignant
C9	69	Prostate	Adenocarcinoma	4	IV	5	5+5	T4N0M1	Malignant
C10	87	Prostate	Adenocarcinoma	4	II	5	5+5	T2N0M0	Malignant
D1	69	Prostate	Small acinous carcinoma	2	II	2	2+3	T2N0M0	Malignant
D2	70	Prostate	Small acinous carcinoma	3	II	4	4+4	T2N0M0	Malignant
D3	63	Costal bone	Metastatic adenocarcinoma	2--3	-	-	-	-	Metastasis
D4	62	Lymph node	Metastatic adenocarcinoma	3	-	-	-	-	Metastasis
D5	78	Prostate	Hyperplasia	-	-	-	-	-	Malignant
D6	67	Prostate	Hyperplasia	-	-	-	-	-	Malignant
D7	66	Prostate	Hyperplasia	-	-	-	-	-	Malignant
D8	72	Prostate	Hyperplasia	-	-	-	-	-	Malignant
D9	78	Prostate	Hyperplasia	-	-	-	-	-	Malignant
D10	56	Prostate	Hyperplasia	-	-	-	-	-	Malignant
E1	72	Prostate	Hyperplasia	-	-	-	-	-	Malignant
E2	65	Prostate	Hyperplasia	-	-	-	-	-	Malignant
E3	69	Prostate	Hyperplasia (adenocarcinoma)	1	-	-	-	-	Malignant
E4	73	Prostate	Hyperplasia	-	-	-	-	-	Malignant
E5	77	Prostate	Hyperplasia	-	-	-	-	-	Malignant
E6	56	Prostate	Hyperplasia	-	-	-	-	-	Malignant
E7	69	Prostate	Hyperplasia	-	-	-	-	-	Malignant
E8	60	Prostate	Hyperplasia	-	-	-	-	-	Malignant

E9	70	Prostate	Hyperplasia	-	-	-	-	-	Malignant
E10	64	Prostate	Hyperplasia	-	-	-	-	-	Malignant
F1	72	Prostate	Hyperplasia	-	-	-	-	-	Malignant
F2	70	Prostate	Hyperplasia	-	-	-	-	-	Malignant
F3	62	Prostate	Hyperplasia	-	-	-	-	-	Malignant
F4	74	Prostate	Hyperplasia	-	-	-	-	-	Malignant
F5	67	Prostate	Hyperplasia	-	-	-	-	-	Malignant
F6	69	Prostate	Hyperplasia	-	-	-	-	-	Malignant
F7	71	Prostate	Hyperplasia	-	-	-	-	-	Malignant
F8	68	Prostate	Hyperplasia	-	-	-	-	-	Malignant
F9	72	Prostate	Hyperplasia	-	-	-	-	-	Malignant
F10	71	Prostate	Hyperplasia	-	-	-	-	-	Malignant
G1	73	Prostate	Chronic inflammation	-	-	-	-	-	Inflammation
G2	84	Prostate	Chronic inflammation	-	-	-	-	-	Inflammation
G3	64	Prostate	Chronic inflammation	-	-	-	-	-	Inflammation
G4	69	Prostate	Chronic inflammation	-	-	-	-	-	Inflammation
G5	68	Prostate	Chronic inflammation	-	-	-	-	-	Inflammation
G6	82	Prostate	Chronic inflammation	-	-	-	-	-	Inflammation
G7	25	Prostate	Cancer adjacent prostate tissue	-	-	-	-	-	AT
G8	21	Prostate	Cancer adjacent prostate tissue	-	-	-	-	-	AT
G9	27	Prostate	Cancer adjacent prostate tissue	-	-	-	-	-	AT
G10	64	Prostate	Cancer adjacent prostate tissue	-	-	-	-	-	AT
H1	77	Prostate	Cancer adjacent prostate tissue	-	-	-	-	-	AT
H2	80	Prostate	Cancer adjacent prostate	-	-	-	-	-	AT

			tissue						
H3	40	Prostate	Prostate tissue	-	-	-	-	-	Normal
H4	37	Prostate	Prostate tissue	-	-	-	-	-	Normal
H5	33	Prostate	Prostate tissue	-	-	-	-	-	Normal
H6	35	Prostate	Prostate tissue	-	-	-	-	-	Normal
H7	28	Prostate	Prostate tissue	-	-	-	-	-	Normal
H8	40	Prostate	Prostate tissue	-	-	-	-	-	Normal
H9	35	Prostate	Prostate tissue (smooth muscle)	-	-	-	-	-	Normal
H10	45	Prostate	Prostate tissue	-	-	-	-	-	Normal

2.5 Generation of EPLINα overexpression plasmid

2.5.1 Generation of full length EPLINα expression sequence

Full length EPLINα was targeted and amplified using primers previously designed in (Jiang et al., 2008) and a Platinum® Taq DNA Polymerase High Fidelity PCR reaction mix (Life Technologies, Paisley, UK). EPLINα was found to be highly expressed in the PZ-HPV-7 cell line and thus used to generate the full length sequence of EPLINα. It was initially attempted to amplify EPLINα from tissue cDNA, however this was not possible due to lack of sufficient tissue quality at time of cloning and PZ-HPV-7 cells were therefore used as a template. The reaction was set up as follows:

- 45µl Platinum Supermix master mix
- 1.5µl EPLIN forward primer (ExF1)
- 1.5µl EPLIN reverse primer (ExR1)
- 2µl PZ-HPV-7 cDNA

These primers, together with PZ-HPV-7 cDNA, were used in a PCR reaction with the following parameters:

- Step 1: Initial denaturing period: 94˚C for 2 minutes.
- Step 2: Denaturing step: 94˚C for 40 seconds.
- Step 3: Annealing step: 60˚C for 50 seconds
- Step 4: Extension step: 72˚C for 120 seconds.
- Step 5: Final extension period: 72˚C for 10 minutes.

The reaction was repeated for 36 cycles. The resultant product was electrophoretically run on a 1% agarose gel to confirm full length EPLIN band size. When EPLINα was confirmed this was then used for TOPO TA plasmid cloning.

2.5.2 Cloning of EPLINα expression sequence into plasmid vector

The pEF6/V5-His TOPO TA Expression system (Figure 2.1) is a one-step cloning strategy that provides an efficient, 5 minute, one-step cloning protocol for the insertion of Taq polymerase-amplified PCR products into a plasmid vector for high-level expression in mammalian cells. This cloning strategy requires no ligase, post-PCR procedures or PCR primers containing specific sequences. Once cloned, analyzed, and transfected into a mammalian host cell line, the PCR product can be constitutively expressed. The pEF6/ V5-His TOPO TA plasmid vector (Invitrogen, Inc., Paisley, UK) was used in the current study in accordance with the protocol provided (Figure 2.2). The TOPO cloning reaction was set up in a pre-labelled PCR tubes for each expression sequence used:

- PCR product (EPLINα expression sequence): 3µl
- Salt solution: 1µl
- TOPO vector: 1µl

The reaction was mixed gently and then left for 5 minutes at room temperature. Chemically competent *Escherichia coli* cells were removed from the deep freezer and allowed to thaw on ice. Five microlitres of the cloning reaction was transferred into chemically competent *Escherichia coli* (One Shot TOP10 *E.coli*, Life Technologies., Paisley, UK) and mixed gently by stirring with the pipette tip. The suspension was then placed on ice for 30 minutes before a 30 second heat shock at

42°C in a pre-heated water bath. The suspension was then immediately transferred back to ice for 2-5minutes. Following this, 250µl of pre-warmed SOC medium was added. The cells were incubated for 1 hour at 37°C with shaking at 200rpm on an orbital shaker. After one hour incubation, cells were spread onto agar plates (containing 100µg/ml ampicillin) at one high volume and one low volume to allow suitable colony proliferation and allowed to grow overnight at 37°C in an incubator.

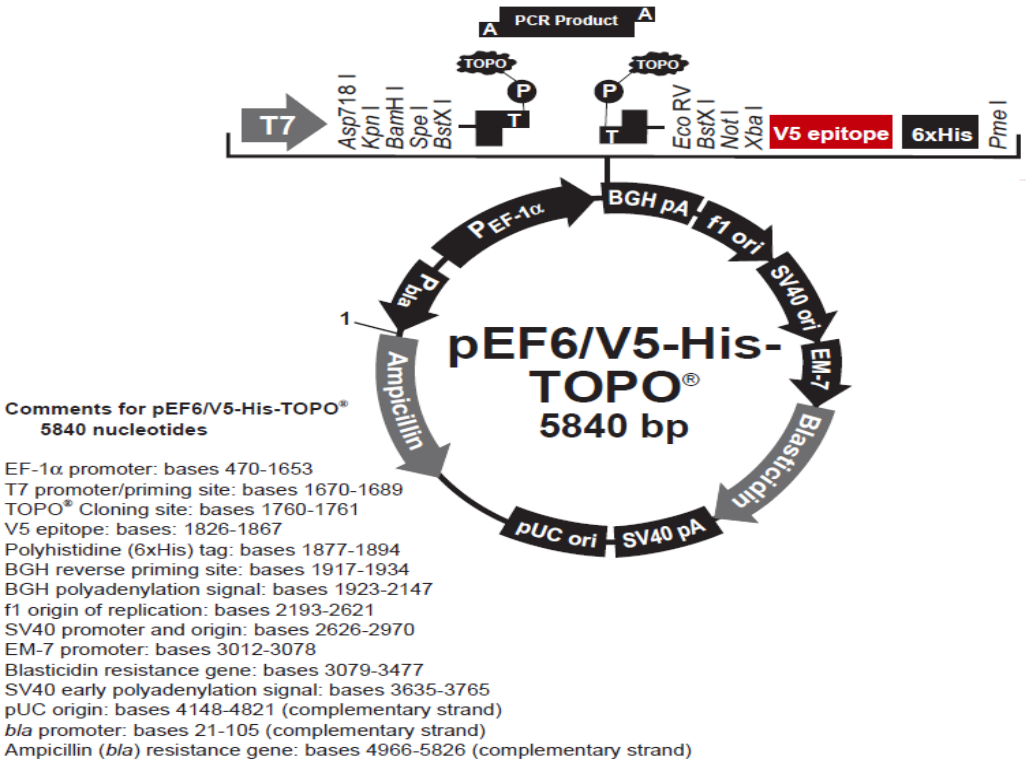

Comments for pEF6/V5-His-TOPO®
5840 nucleotides

EF-1α promoter: bases 470-1653
T7 promoter/priming site: bases 1670-1689
TOPO® Cloning site: bases 1760-1761
V5 epitope: bases: 1826-1867
Polyhistidine (6xHis) tag: bases 1877-1894
BGH reverse priming site: bases 1917-1934
BGH polyadenylation signal: bases 1923-2147
f1 origin of replication: bases 2193-2621
SV40 promoter and origin: bases 2626-2970
EM-7 promoter: bases 3012-3078
Blasticidin resistance gene: bases 3079-3477
SV40 early polyadenylation signal: bases 3635-3765
pUC origin: bases 4148-4821 (complementary strand)
bla promoter: bases 21-105 (complementary strand)
Ampicillin (*bla*) resistance gene: bases 4966-5826 (complementary strand)

Figure 2.1 Map of pEF6/ V5-His TOPO TA plasmid vector

Experimental Outline

The flow chart below outlines the experimental steps necessary to clone and express your PCR product

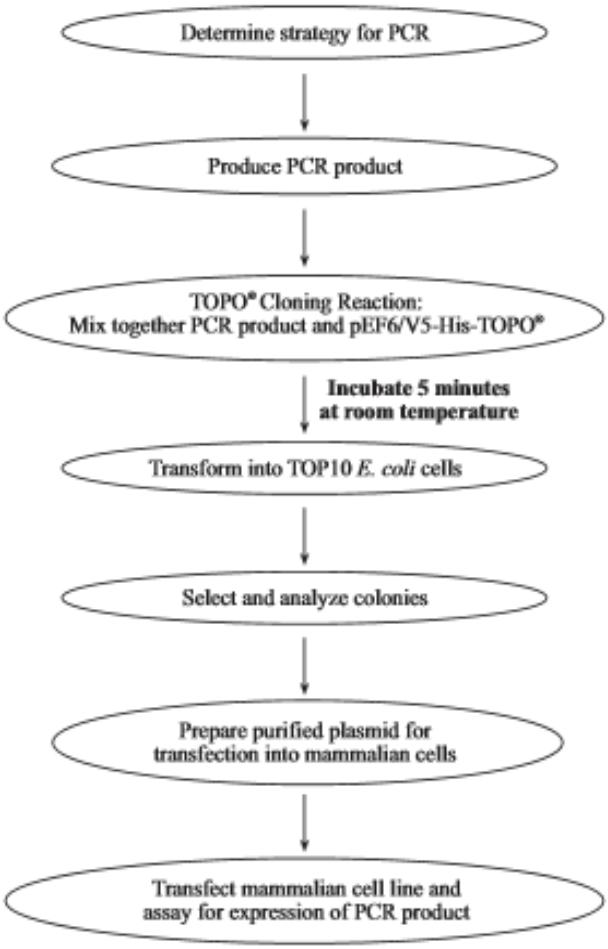

Figure 2.2 Experiment flow chart of pEF6/ V5-His TOPO TA plasmid vector cloning procedure

2.5.3 Selection and orientation analysis of positive colonies and colony PCR

Colonies grown on agar plates should contain the pEF6/ V5-His TOPO TA plasmid vector due to antibiotic resistance sites within the vector. Colonies were selected and analysed to check correct orientation of the insert. Fifteen colonies for EPLINα expression sequences were randomly selected for PCR amplification and amplified using vector-specific forward and reverse primers, T7F and BGHR, or EPLIN-specific primers, F8 and R8. Colonies were selected by touching the selected colony using a sterile pipette tip and placed into a PCR reaction mixture ready for amplification of the desired sequence. This resultant PCR gave products indicating either wrong orientation, right orientation, or mixed orientation. The colony PCR for expression sequences are as follows:

PCR product insertion primer pair mix

- 8µl - GoTaq Green master mix
- 1µl - T7F plasmid specific forward primer
- BGHR plasmid specific reverse primer
- 5µl - PCR water
- 1µl – Expression plasmid DNA

EPLINα overexpression ‘negative’ orientation reaction:

- 8µl – GoTaq® DNA Polymerase Reaction mix
- 5µl – PCR water
- 1µl – T7F plasmid specific forward primer
- 1µl – EPLIN sequence specific forward primer (F8)

- 1µl – Expression plasmid DNA

EPLINα overexpression 'positive' orientation reaction:

- 8µl – GoTaq® DNA Polymerase Reaction mix
- 5µl – PCR water
- 1µl – T7F plasmid specific forward primer
- 1µl – EPLIN sequence specific forward primer (R8)
- 1µl – Expression plasmid DNA

Each reaction was subjected to the following conditions:

- Step 1: Initial denaturing period: 94˚C for 10 minutes.
- Step 2: Denaturing step: 94˚C for 60 seconds.
- Step 3: Annealing step: 55˚C for 60 seconds.
- Step 4: Extension step: 72˚C for 60 seconds.
- Step 5: Final extension period: 72 ˚C for 10 minutes.

Steps 2, 3 and 4 were repeated over 32 cycles. The PCR products were run on a 1% gel. If the 'negative' reactions produced a positive result, it means the plasmid from that colony was in the wrong orientation and wasn't suitable. If the 'positive' reactions produced a positive result, it means the plasmid from that colony was in the right orientation and was suitable. Colonies in the right orientation at the expected product size were selected, taken from the agar plate and was used to inoculate 10 ml of ampicillin selective LB broth in universal containers and were horizontally shaken at 225 rpm overnight.

2.5.4 Plasmid extraction, purification and quantification (Miniprep)

Plasmid extraction was carried out using Sigma GenElute Plasmid MiniPrep Kit (Sigma-Aldrich, Dorset, UK), according to the provided protocol. Colony cultures were removed from incubator and centrifuged at 3000 rpm for 10 minutes to obtain a pellet of bacteria. The supernatant was discarded and the pellet fully resuspended in 200µl of Resuspension Solution (containing RNAase A) and mixed through pipetting and vortexing. To lyse samples, 200µl of Lysis Solution was added and mixed 6-8 times by inversion and followed immediately by adding 350µl Neutralisation/Binding Solution and then centrifuged at 12,000g for 10 minutes in a micro centrifuge. Mini Spin Columns were then prepared by adding 500µl Column Preparation Solution and centrifuged for 12000g for 30 seconds. The cell lysate was then transferred into prepared Mini Spin Columns centrifuged at 12000 x g for 1 minute. The flow-through was discarded and 750µl Wash Solution was added to the column before centrifuging at 12,000g for 1 minute. The flow-through was discarded and an additional spin was carried out to remove excess Wash Solution. The Mini Spin Column was transferred to a clean collection tube and the plasmid DNA eluted in 100µl Elution Solution by centrifugation at 12,000g for 1 minute. The plasmid DNA was then run on a 1% gel to check both plasmid purity and product size.

2.5.5 Transfection of mammalian cells using electroporation

Following purification, quantification and verification of plasmids, 10µg of overexpression plasmid, and 5µg control pEF6 plasmid, was used to transfect prostate cancer cell lines, PC-3 and LNCaP. Once cells reached confluence, wild type cells were detached from cell flasks using trypsin EDTA, pelleted and resuspended as previously described. Electroporation cuvettes were removed from

packaging and 1ml of cells (at a density of $1x10^6$ cells/ml) added with the purified plasmid. The cuvette was loaded into a Cell Pulser Xcell™ Total System (BioRad, Hertfordshire, UK) and was pulsed with electricity (see table below for electroporation conditions). The electrical pulse causes cell membrane perforation and integration of plasmid DNA. Transfection conditions consisted of 310V and 1500μA for PC-3 cells, and 290V and 1500 μA for LNCaP cells. The mixture was immediately transferred into 5ml of prewarmed media in a T25 flask and placed in an incubator under standard incubation conditions overnight. Cells were selected the following morning for 6-14 days (6 for LNCaP cells, 14 for PC-3 cells) in appropriate cell line media containing 5μg/ml Blasticidin S (Melford, Suffolk, UK). Cells were subsequently maintained in 0.5μg/ml Blasticidin. Once cells reached sufficient confluence, RNA and protein was extracted as above.

2.5.6 Plasmid sequencing

To confirm and verify presence of full length EPLINα sequence in pEF6/ V5-His TOPO TA plasmid vector, plasmid samples were analysed using Sanger sequencing. This was done using an external company called Source BioScience (Source BioScience, Nottingham, UK) and samples were prepared at a concentration of 100ng/μl prior to sending in accordance with the companies guidelines.

2.6 *In vitro* tumour cell functional assays

2.6.1 Bone matrix extract (BME) preparation for functional assays

BME was employed in tumour functional assays to generate an *in vitro* bone-like environment. BME was prepared using fresh human bone tissues obtained post hip replacement. Bones were crushed at ice cold temperature prior to processing using a

Bone Mill (Splerings Orthopaedics B.V., The Netherlands) and subsequently a BioRuptor (Wolf Laboratories, York, UK) to solubilise and extract matrix proteins in PBS buffer. This was prepared, aliquoted and used previously in (Davies and Jiang, 2010). For functional assays in section 4 and 5, an aliquot of stock BME (at concentration 2mg/ml) was removed from the freezer and allowed to thaw at room temperature. BME was required at a final concentration of 50µg/ml and 100µg/ml. This was done by making a working concentration of 100µg/ml and 200µg/ml (2x concentrated) which was subsequently diluted 1:1 with prostate cancer cells (PC-3 or LNCaP cells). The volume made was dependant on the functional assay and number of wells required.

2.6.2 FAK inhibitor treatment to determine inhibitor concentration

Prostate cancer cells were pre-seeded to approximately 60% confluence into 6 well plates one day prior to FAK treatment. PC-3 cells were treated overnight with four separate FAK inhibitor (CAS4506-66-5) (Santa Cruz Biotechnology, Inc., Heidelberg, Germany) concentrations to determine optimal concentration for functional assay testing. The concentrations chosen were 100nM, 500nM, 1µM and 5µM. FAK inhibitor solutions were made up in DMEM medium with sufficient volume for each concentration. The following day, protein was extracted as in section 2.4.1 but with a reduced volume of lysis buffer (100µl). Protein concentration was determined as in section 2.4 and samples were stored at -20°C until required for functional assays.

2.6.3 Src inhibitor (dasatinib) treatment to determine inhibitor concentration

The same procedure was employed for determining optimal inhibitor concentration of dasatinib as in section 2.6.2. The chosen inhibitor concentrations were 100nM, 500nM and 1µM. Following treatment, protein was extracted as in section 2.4.1 but with a reduced volume of lysis buffer (100µl). Protein concentration was determined as in section 2.4 and samples were stored at -20°C until required for functional assays.

2.6.4 FAK inhibitor preparation for functional assays

FAK inhibitor was prepared at final concentrations of 1µM and 5µM. This concentration was chosen following treatment to PC-3 cells overnight followed by Western Blot (see Chapter6). This deduced optimal inhibition of FAK Y397 in both cell lines. The stock inhibitor was stored at 10mM concentration and diluted 1:1000 to give a working concentration of 10µM, then diluting by half depending on volume requirements for appropriate functional assays required.

2.6.5 Src inhibitor (dasatinib) preparation for functional assays

Dasatinib inhibitor (Axon1392) (Axon Medchem, Groningen, Netherlands) was prepared at a final concentration of 500nM. This concentration was chosen following treatment to PC-3 and LNCaP cells overnight followed by Western Blot (see Chapter 7). This deduced optimal inhibition of Src Y419 in both cell lines. The stock inhibitor was stored at concentration 1mM and diluted 1:1000 to give a working concentration of 1µM, then diluting by half depending on volume requirements for appropriate functional assays required.

2.6.6 *In vitro* tumour cell proliferation assay

Cell proliferation was measured using an *in vitro* tumour proliferation assay. Cells were seeded into a 96-well plate (Nunc, Fisher Scientific, Leicestershire, UK) at 3000 and 10,000 cells per well in 200µl of cell medium for PC-3 and LNCaP, respectively. In total, three plates were seeded to obtain proliferation readings at time points of Day 1, Day 3 and Day 5. Plates were seeded approximately 16 hours prior to the start of the first time point (Day 1). Cell proliferation of each sample was then compared at Day 3 and Day 5 time points and compared to the control (Day 1). For each experiment, samples were run in triplicate. After each incubation period (Day 1, 3 or 5), cells were fixed in 4% formalin for 10 minutes before staining for 10 minutes with 0.5% (w/v) crystal violet in distilled water. The plates were washed with water and the cells extracted using 10% acetic acid (v/v). Absorbance was measured at a wavelength of 540nm on an ELx800 plate reading spectrophotometer (Bio-Tek, Wolf laboratories, York, UK). The percentage of cell proliferation was determined using the following equation:

$$Percentage\ Increase = \frac{Day\ 3\ or\ 5\ Absorbance - Day\ 1\ Average\ Absorbance}{Day\ 1\ Average\ Absorbance} \times 100$$

The doubling time of PC-3 and LNCaP Wild-Type cells is 25hrs and 60hrs respectively (ATCC). Doubling time of PC-3/LNCaP$^{pEF6/EPLIN\ EXP}$ was established at Day 5. This was done using the following equation:

$$Doubling\ time = \frac{Duration\ between\ Day\ 1\ and\ Day\ 5\ (hrs) - \log(2)}{\log(Day\ 5\ cell\ count) - \log(Day\ 1\ cell\ count)}$$

In addition to untreated PC-3 and LNCaP cells, cell proliferation assay were performed in the presence of BME and FAK inhibitor. Use of BME was performed to establish the effects on cell proliferation in an *in vitro* bone-like environment, and the FAK inhibitor was used to establish the effect of FAK inhibition in conjunction with EPLINα over expression on PC-3 and LNCaP cells.

2.6.7 *In vitro* tumour cell matrigel invasion assay

The invasive capacity of the cells used in this study was assessed using an *in vitro* tumour cell Matrigel invasion assay. The assay measures the capability of cells to penetrate and invade through an artificial basement membrane created using Matrigel (MatrigelTM, BD Bioscience,Oxford, UK). Cell culture inserts containing 8µM pores were placed into a 24-well plate and coated in 50µg Matrigel. A solution of Matrigel was initially made of concentration 0.5mg/ml in Serum Free Media (SFM) and 100µl was added to each of the inserts and allowed to dry in an incubator at 55˚C for 2-3 hours. Once dry, the inserts were rehydrated in 100µl of SFM for 30 minutes. The media was then aspirated and the cells were seeded in the inserts on top of the basement membrane. Cells were seeded in 200µl at 15,000 for PC-3 cells and 60,000 for LNCaP cells in each well. Once cells were seeded, 500µl of cell media was added to the well (outside of the insert) to support invading cells. The plates were then incubated for 3 days at 37˚C with 5% CO_2. Following the incubation period, the inserts were rinsed and subject to cleaning inside of the insert using cotton buds to remove excess media and non-invaded cells. The cells which had invaded through the pores and penetrated the Matrigel were fixed in 500µl formalin solution for 10 minutes before staining in 0.5% crystal violet (w/v) in distilled water. Inserts were left overnight to dry before being visualized under the microscope under

X20 objective magnification. Of each insert, 4 random fields were counted and an average taken to evaluate cellular invasion of each sample. In addition to untreated PC-3 and LNCaP cells, cellular invasion was assessed in the presence of BME and an FAK inhibitor. Use of BME was performed to establish the effects on cellular invasion in an *in vitro* bone-like environment, and the FAK inhibitor was used to establish the effect of FAK inhibition in conjunction with EPLINα overexpression on PC-3 and LNCaP cells.

2.6.8 *In vitro* cell-matrix adhesion assay

The adhesive capacity of the cells used in this study was assessed using an *in vitro* tumour cell Matrigel adhesion assay. Matrigel was made using a concentration of 0.05mg/ml in SFM and 100µl added to the wells of a 96-well plate. The plates were allowed to dry in the oven at 55˚C for 2-3 hours. Once dry, the inserts were rehydrated in 100µl of SFM for 30 minutes. The media was then aspirated and the cells were seeded in the inserts on top of the basement membrane. Cells were seeded in 200µl at varying density for varying incubation times depending on cell line as indicated in Table 2.7.

Table 2.7 *In vitro* cell-matrix adhesion assay conditions

Cell line	Cell seed density	Incubation time
PC-3	40,000	45 minutes
LNCaP	60,000	60 minutes

LNCaP cell lines were incubated longer to ensure sufficient cellular attachment for measurement. Incubations were done at 37˚C with 5% CO_2. After the incubation

period, the medium was aspirated and cells fixed in 4% formalin for 10 minutes before being stained in 0.5% crystal violet (w/v) in distilled water. The number of adherent cells were counted from 4 random fields per well, with 3 triplicate wells per sample, under a microscope at X20 objective magnification. In addition to untreated PC-3 and LNCaP cells, cellular adhesion was assessed in the presence of BME and an FAK inhibitor. Use of BME was performed to establish the effects on cellular adhesion in an *in vitro* bone-like environment, and the FAK inhibitor was used to establish the effect of FAK inhibition in conjunction with EPLINα overexpression on PC-3 and LNCaP cells.

2.6.9 *In vitro* scratch/wound healing assay

Cellular migration was evaluated across a wounded surface of a confluent monolayer of PC-3 cells. PC-3 cells were seeded at a seeding density of 100,000 cells per well in a 24 well plate the day before the scratch assay was planned to commence. Upon reaching a confluent monolayer, the cells were vertically scraped using a 10µl pipette tip, creating a wound. The cell media was then removed and fresh media and/or treatment was added to the PC-3 cells. Photos were taken on a Leica DM IRB microscope (Leica GmbH, Bristol, UK) at x20 magnification and designated as 0 hour. Cell plates were placed back in the incubator to keep a constant temperature of 37°C and further photographs were taken at 1 hour intervals, over a course of 4 hours. Cell migration was analysed using ImageJ software by measuring the distance between the two wounded fronts of each well at 4 separate points per incubation. The distance between the migrating fronts at each 1 hour time point was determined by comparing the time point to Time 0, and subtracting the distance between the two fronts at the specific intervals with the original time point. The cellular migration of

PC-3 cells transfected with the pEF6 plasmid the EPLINα overexpression plasmid was determined, in addition to treatments used for the experiment. In addition to untreated PC-3 cells, cellular migration was assessed in the presence of BME and an FAK inhibitor. Use of BME was performed to establish the effects on cellular migration in an *in vitro* bone-like environment, and the FAK inhibitor was used to establish the effect of FAK inhibition in conjunction with EPLINα overexpression on PC-3.

2.6.10 *In vitro* transwell migration assay

A transwell migration assay was performed on LNCaP cells to assess cellular migration. Unlike PC-3 cells, LNCaP cells are less adherent and thus a scratch assay wasn't suitable. The assay measures the capability of cells to migrate through cell culture inserts containing 8μm pores. Cells were seeded in 200μl at a density of 60,000 LNCaP cells in each well. A chemoattractant media of was used to ensure suitable migration through the pores (2% FCS on top of the inserts, 10% FCS in the wells). The plates were then incubated for 3 days at 37˚C with 5% CO_2. Following the incubation period, the inserts were washed and blotted with cotton buds to remove excess media. The cells which had migrated through the pores and were fixed in 500μl formalin solution for 10 minutes before staining in 0.5% crystal violet (w/v) in distilled water. Inserts were left overnight to dry before being visualized under the microscope under X20 magnification. Of each insert, 4 random fields were counted and an average taken to evaluate cellular migration of each sample. In addition to untreated LNCaP cells, cellular migration was assessed in the presence of BME and an FAK inhibitor. Use of BME was performed to establish the effects on cellular migration in an *in vitro* bone-like environment, and the FAK inhibitor was

used to establish the effect of FAK inhibition in conjunction with EPLINα overexpression on LNCaP cells.

2.6.11 *In vitro* co-culture invasion assay with human osteoblasts

This assay was set up in a similar way to the *in vitro* Matrigel invasion assay as described in section 2.6.7; however this included the incubation with human hFOB1.19 osteoblast cells, to determine the impact of EPLINα overexpression on cellular invasion in an *in vitro* bone-like environment. hFOB1.19 cells were seeded at a seeding density of 40,000 cells per well in a 24 well plate one day prior to the start of the experiment. PC-3/LNCaP^{pEF6} and PC-3/LNCaP$^{EPLIN\ EXP}$ cells were seeded in inserts pre-covered with a layer of Matrigel as in section 2.6.7. PC-3 cells were seeded at 15,000 cells per insert, and LNCaP at 60,000 cells per insert in 200µl. Inserts containing PC-3 or LNCaP cells were then transferred to the 24 well plates pre-seeded with human osteoblasts, and to a plate containing no osteoblasts. The plates were then placed in the incubator and left for 3 days. Following the incubation, plates were fixed in formalin and stained using crystal violet before being visualised on the microscope. Cellular invasion was compared for PC-3/LNCaP^{pEF6} and PC-3/LNCaP$^{EPLIN\ EXP}$ cells +/- osteoblasts. In addition to untreated PC-3 and LNCaP cells, cellular invasion was assessed in the presence of BME and an FAK inhibitor. Use of BME was performed to establish the effects on cellular invasion in an *in vitro* bone-like environment, and the FAK inhibitor was used to establish the effect of FAK inhibition in conjunction with EPLINα overexpression on PC-3 and LNCaP cells.

2.7 Data analysis for Kinexus™ protein microarray

The protein microarray determined the change in expression of certain molecules in response to EPLINα overexpression in PC-3 cells. Protein samples for PC-3^{pEF6} and PC-$3^{EPLIN\ EXP}$ were prepared and quantified as described in section 2.4.3 before being sent to Kinexus Bioinformatics, Canada for processing and analysis. The Kinexus microarray utilises several key parameters for data analysis and these include 1) Globally Normalised Signal Intensity, 2) Z ratio and 3) % Change From Control (CFC). The Globally Normalised Signal intensity is calculated by totalling the net signal median values for a particular sample. The Z ratio is a comparison between two Z scores, by dividing the Z score differences by the standard deviation of all the differences in the comparison. A Z ratio greater than 1.64 is considered statistically significant for a molecule which has showed upregulation (in response to EPLINα overexpression) and a Z ratio less than -1.64 is considered statistically significant for a molecule that is downregulated (in response to EPLINα overexpression). The %CFC is a percentage calculation for a change in normalised signal intensity from the specified control. If a molecule is upregulated from the specified control, it will have a positive %CFC, and if a molecule is downregulated from the specified control, it will have a negative %CFC. This method has been described previously in (Owen et al., 2016).

2.8 Statistical analysis

Statistical analysis was performed using the SigmaPlot 11 statistical software package (Systat Software Inc., London, UK). Comparison between test groups was performed using a two sample, two tailed t-test or a Mann Whitney U test depending on data parameters. All experiments were carried out a minimum of three

independent times. Values of $p < 0.05$ were regarded as statistically significant. All figures annotated using *, ** or *** indicate $p<0.05$, $p<0.01$ and $p<0.001$ respectively.

Chapter III: Expression profile for EPLIN in cells and tissues and generation of model systems

3.1 Introduction

Gene dysregulation or loss is a primary indicator for potential association in disease progression in molecular biology and is frequently used as a tool for identifying cancer-related genes. EPLIN is widely expressed in various tissues including the kidney, placenta, ovaries, spleen, heart and prostate, however, EPLIN expression markedly diminishes during cancer progression (Maul and Chang, 1999). This loss was first identified in 1999 where the EPLINα isoform was downregulated or lost in various cancers, including oral, breast and prostate cancer (Maul and Chang, 1999). In later years this lead to various research groups evaluating EPLIN as a potential marker in cancer progression and as a possible therapeutic target. In prostate cancer specifically, subsequent publications have demonstrated a progressive loss of EPLIN in more advanced staged cancers, in addition to EPLIN loss being associated with pro-metastatic features including EMT transition, and has clinical implications linking to prognosis (Sanders et al., 2011, Zhang et al., 2011). EPLIN has key links to the globular protein actin and has been shown to have actin binding capacity within its structure (Maul et al., 2003), and although this indicates EPLIN may have roles in cell movement and migration, the direct function of EPLIN remains elusive. This chapter aims to gain a further understanding of the expression profile of EPLIN in human prostate cancer, utilising prostate cancer cell lines and clinical prostate cancer tissue representative of various stages of prostate cancer progression to determine if EPLIN loss correlated with metastatic capacity and aggressiveness. Additionally, plasmid constructs were generated including the EPLINα full length expression sequence (for EPLINα overexpression) to gain further insight into the cell function and mechanism of action of manipulated EPLINα expression. EPLINα

expression plasmids were transfected into PC-3 and LNCaP cell lines, and verified for overexpression by PCR and Western Blotting. These stably transfected cells were used in later chapters of this thesis for cell functional and mechanistic investigations. The current chapter explores the expression profile of EPLIN in a range of cell lines and prostate tissues and describes the generation of these expression plasmids and EPLINα manipulated cell lines in addition to the verification of EPLINα overexpression at both transcript and protein level.

3.2 Material and methods

3.2.1 Materials

All primers used were manufactured and provided by Sigma (Sigma Aldrich, Gillingham, UK). Antibodies and primer sequences used for this study are listed in section 2.1.2 and 2.1.3.

3.2.2 Cell lines

The human prostate cancer cell lines PC-3, LNCaP, VCaP, DU-145 and CA-HPV-10, immortalised 'normal' prostate cell line PZ-HPV-7 and a human osteoblast cell line hFOB1.19 were used for this study. For cell line media and incubation conditions, please see section 2.2.

3.2.3 RNA extraction and cDNA synthesis

RNA extraction was carried out on cells according to TRI reagent protocol (Sigma-Aldrich, Dorset, UK). Reverse transcription was carried out using GoScript™ Reverse Transcription System (Promega, UK). For full procedure please refer to section 2.3.3.

3.2.4 Polymerase Chain Reaction (PCR)

PCR was carried out on cDNA from PC-3, LNCaP, VCaP, DU-145, PZ-HPV-7, CA-HPV-10 and hFOB1.19. Levels of EPLINα and EPLINβ transcript were established. For full procedure please refer to section 2.3.4.

3.2.5 Real-Time Quantitative Polymerase Chain Reaction (RT-QPCR)

RT-QPCR was performed using Precision Q-PCR 2X qPCR Mastermix (Primer Design, UK). Quantitative PCR data were analysed and normalised to the housekeeping gene, GAPDH. Primer sequences used for this study are listed in section 2.1.2. For the full procedure, please refer to section 2.3.6.

3.2.6 SDS-polyacrylamide gel electrophoresis (SDS-PAGE) and Western blotting

Protein expression was established by SDS-PAGE and Western Blotting. This was done using an OmniPAGE VS10 vertical electrophoresis system (OminPAGE, Wolf Laboratories, York, UK) and a SD10 SemiDry Maxi System blotting unit (Wolf Laboratories, York, UK) for electroblotting. Protein was detected using SNAP i.d.® 2.0 Protein Detection System (Merck Millipore Ltd., Feltham, UK). For full procedure please refer to section 2.4.

3.2.7 Generation of full length EPLINα overexpression plasmid

Amplification of the EPLINα coding sequence was carried out using a Platinum® PCR SuperMix kit (Thermo Fisher Scientific,USA) using primers capable of amplifying the full length sequence of human EPLINα from PZ-HPV-7 cell line cDNA. Full length EPLINα was cloned into a pEF6/V5-His TOPO® TA cloning vector and extracted and verified. For full procedure please refer to section 2.5.

3.2.8 Transfection of pEF6/V5-HIS TOPO TA vector containing EPLINα overexpression plasmids into prostate cancer cell lines

pEF6/V5-HIS TOPO TA vectors containing EPLIN overexpression plasmid or empty pEF6/V5-HIS TOPO TA vector were used to transfect PC-3 or LNCaP cells

by electroporation. Following transfection cells were selected for 6-14 days (6 days for LNCaP, 14 days for PC-3) in appropriate cell line media containing 5μg/ml Blasticidin S (Melford, Suffolk, UK). Cells were subsequently maintained in 0.5μg/ml Blasticidin S. For full procedure please refer to section 2.5.5.

3.2.9 EPLIN expression analysis in prostate cancer tissues and related secondary tissues

EPLIN expression was evaluated in clinical prostate cancer using two TMA's labelled HPro-Ade96Sur-01 and PR8011a (see section 2.4.11). IHC analysis was performed on sections of normal prostate and prostate cancer tissue. For full procedure please refer to sections 2.4.11 and 2.4.12. Patient/sample information for sections present on the TMA's is shown in Table 2.5 and Table 2.6.

3.2.10 Statistical analysis

Statistical comparisons were made between different groups using a two sample, two tailed t-test or a Mann Whitney U test dependant on data normality using SigmaPlot 11 software. All experiments were carried out a minimum of three independent times and $p < 0.05$ regarded as statistically significant.

3.3 Results

3.3.1 Expression profile of EPLIN in prostate cancer cells

EPLIN expression was evaluated in prostate cancer, normal prostate and bone like cells lines by RT-PCR, Q-PCR and Western blotting (Figure 3.1A-C). EPLIN transcript was expressed in all cell lines with highest levels in CA-HPV-10, PZ-HPV-7 and hFOB1.19, high levels were also observed in the DU-145 prostate cancer cell line. EPLINβ transcript was expressed at low levels and remained relatively consistent throughout the cell lines. Lowest levels of EPLIN transcript were seen in more aggressive cell lines PC-3, LNCaP and VCaP. Given the relatively consistent levels of EPLINβ transcript within all samples, PC-3, LNCaP and VCaP also had lowest levels of EPLINα expression. For Q-PCR analysis, EPLIN remained highly expressed in CA-HPV-10, and had low transcript expression in PC-3, DU-145, LNCaP and VCaP (Figure 3.1B). Samples were normalised to the CA-HPV-10 sample for Q-PCR data analysis. EPLIN transcript was significantly reduced in PC-3 ($p=0.003$), DU-145 ($p=0.005$), LNCaP ($p=<0.001$) and VCaP ($p=0.002$) when compared to EPLIN expression in CA-HPV-10. A similar EPLIN profile was seen during the protein analysis, with high expression of EPLINα and β in CA-HPV-10 and hFOB1.19 and moderate expression of EPLINα in PZ-HPV-7. Low EPLINα expression was seen for DU-145 and VCaP, whilst EPLINβ was negative was these cell lines. For PC-3 and LNCaP, both EPLIN isoforms were negative (Figure 3.1C). GAPDH was run alongside each PCR, Q-PCR and Western Blot reaction as a control.

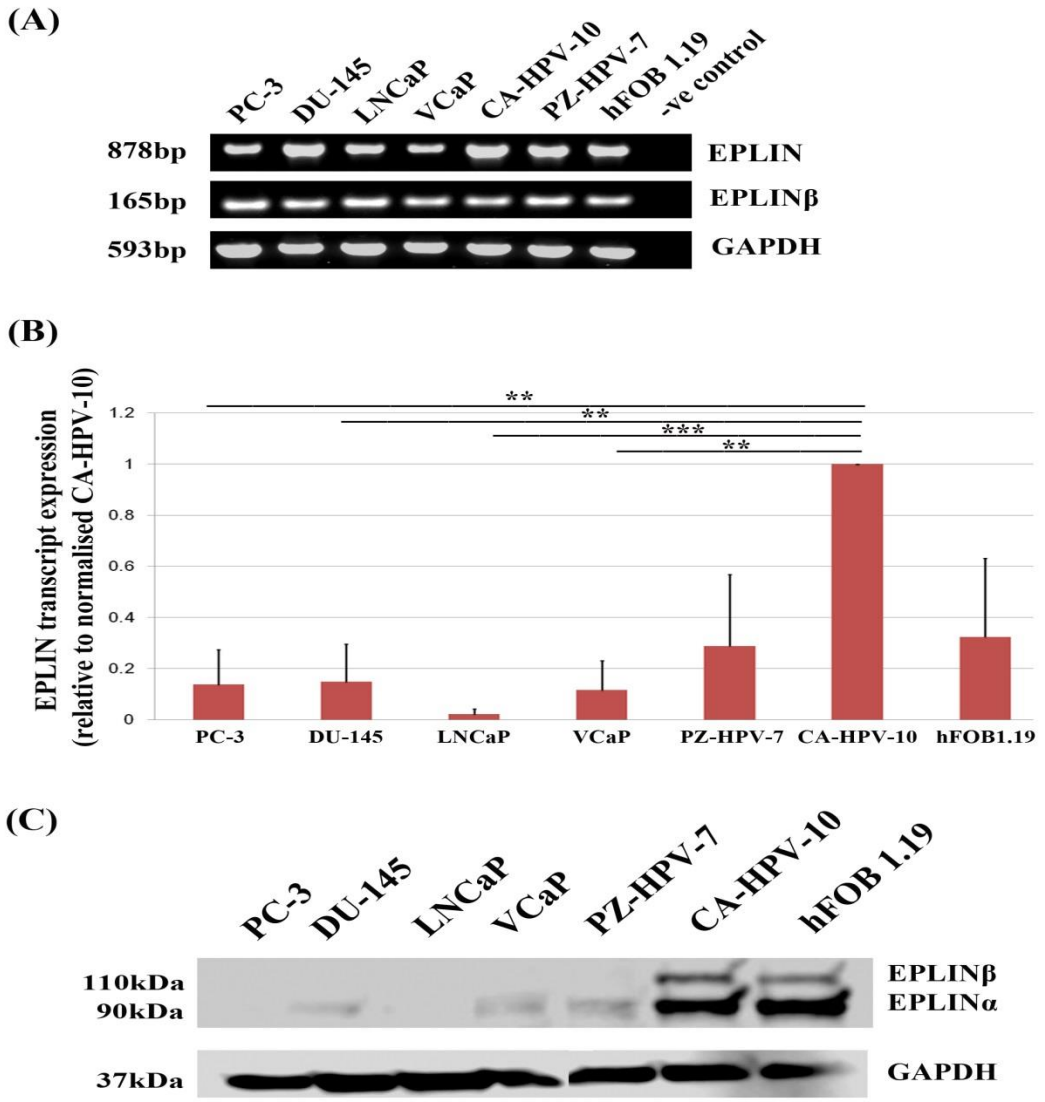

Figure 3.1– EPLIN expression profile in prostate cancer cells lines.

(A) PCR analysis of prostate cell lines showing EPLINα, EPLINβ and GAPDH transcript expression. (B) q-PCR analysis of EPLIN transcript in prostate cell lines. Samples were normalised and compared to the CA-HPV-10 cell line. Error bars represent SE of the mean. (C) Western Blot protein analysis of EPLIN protein in prostate cell lines. GAPDH was used alongside each experiment as a control. Gel images and graphs are representative of n=3 repeats for each experiment. ** = $p<0.01$, *** = $p<0.001$. Statistical test performed for this analysis was a two sample, two tailed t-test using SigmaPlot software.

3.3.2 Generation of EPLINα overexpression plasmid

To assess the effect of increased or sustained EPLINα expression on prostate cancer cell characteristics, a plasmid was constructed which included the EPLINα full length coding sequence (Figure 3.2). EPLINα transcript was initially derived and isolated from PZ-HPV-7 cell cDNA previously shown to express human EPLIN. Primers known to target a region of EPLINα (EPLIN F8/EPLIN R8) were also used alongside as a positive control, and produced a PCR band of 878bp, confirming the presence of EPLIN in PZ-HPV-7 (Figure 3.2B). Primers targeting the full EPLINα CDS were utilised to isolate a 1.8kb band using a high fidelity PCR procedure before progressing onto cloning steps (Figure 3.2C). EPLINα expression sequences were then cloned into a pEF6/V5-His TOPO® TA vector and transformed into competent *E.coli* cells. Colonies were selected from plates and the orientation of the insert was checked by PCR using plasmid specific primers (T7F and BGHR) and EPLIN specific primers (F8 and R8). 'Correct orientation' PCR reactions produced strong bands at approximately 2kb (T7F vs BGHR) and 1.1kb (T7F vs EPLIN R8) and 'incorrect orientation' PCR reactions produced no band (T7F vs EPLIN F8/ (-)). This confirmed presence of the human EPLINα sequence and correct orientation in the plasmid. Further sequence analysis was implemented by sequencing the plasmid and confirmed presence of EPLINα when comparing the sequencing product to the mRNA structure of EPLINα using a NCBI reference sequence (Figure 3.2E). These plasmids were then used for subsequent transfection procedures to mammalian prostate cancer cell lines.

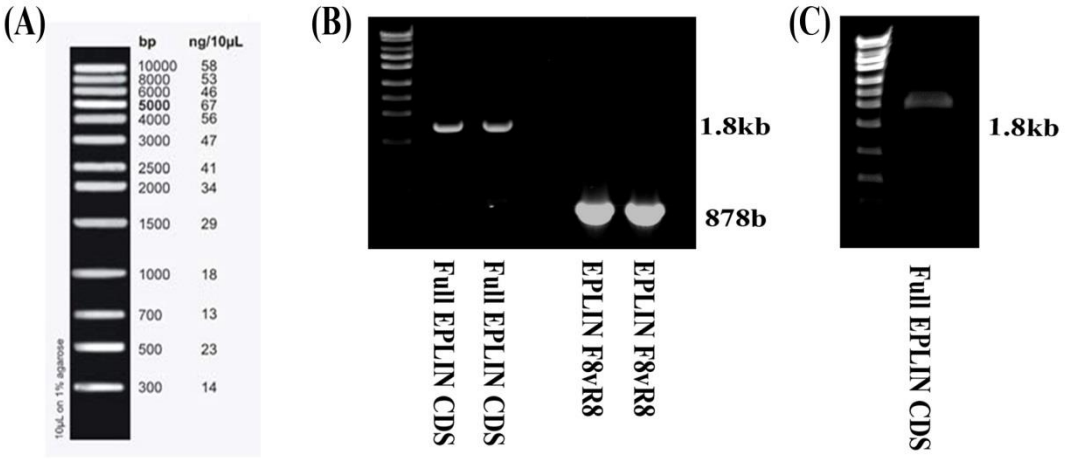

(D)

.....gaagtaaaaaaATGGAAAATTGTCTAGGAGAATCCAGGCATGAAGTAGAAAAATCAGAAATC
AGTGAAAACACAGATGCTTCGGGCAAAATAGAGAAATATAATGTTCCGCTGAACAGGCTTAAGATGATGTTTGAGAAA
GGTGAACCAACTCAAACTAAGATTCTCCGGGGCCCAAAGCCGAAGTGCAAGTGGAAGGAAGATCTCTGAAAACAGCT
ATTCTCTAGATGACCTGGAAATAGGCCCAGGTCAGTTGTCATCTTCTACATTTGACTCGGAGAAAAATGAGAGTAGA
CGAAATCTGGAACTTCCACGCCTCTCAGAAACCTCTATAAAGGATCGAATGGCCAAGTACCAGGCAGCTGTGTCCA
AACAAAGCAGCTCAACCAACTATACAAATGAGCTGAAAGCCAGTGGTGGCGAAATCAAAATTCATAAAATGGAGCAA
AAGGAGAATGTGCCCCCAGGTCCTGAGGTCTGCATCACCCATCAGGAAGGGGAAAAGATTTCTGCAAATGAGAATA
GCCTGGCAGTCCGTTCCACCCCTGCCGAAGATGACTCCCCAGGTGACTCCCAGGTTAAGAGTGAGGTTCAACAGC
CTGTCCATCCCAAGCCACTAAGTCCAGATTCCAGAGCCTCCAGTCTTTCTGAAAGTTCTCCTCCCAAAGCAATGAAG
AAGTTTCAGGCACCTGCAAGAGAGACCTGCGTGGAATGTCAGAAGACAGTCTATCCAATGGAGCGTCTCTTGGCCA
ACCAGCAGGTGTTTCACATCAGCTGCTTCCGTTGCTCCTATTGCAACAACAAACTCAGTCTAGGAACATATGCATCTT
TACATGGAAGAATCTATTGTAAGCCTCACTTCAATCAACTCTTTAAATCTAAGGGCAACTATGATGAAGGCTTTGGGC
ACAGACCACACAAGGATCTATGGGCAAGCAAAAATGAAAACGAAGAGATTTTGGAGAGACCAGCCCAGCTTGCAAA
TGCAAGGGAGACCCCTCACAGCCCAGGGGTAGAAGATGCCCCTATTGCTAAGGTGGGTGTCCTGGCTGCAAGTAT
GGAAGCCAAGGCCTCCTCTCAGCAGGAGAAGGAAGACAAGCCAGCTGAAACCAAGAAGCTGAGGATCGCCTGGC
CACCCCCCACTGAACTTGGAAGTTCAGGAAGTGCCTTGGAGGAAGGGATCAAAATGTCAAAGCCCAAATGGCCTC
CTGAAGACGAAATCAGCAAGCCCGAAGTTCCTGAGGATGTCGATCTAGATCTGAAGAAGCTAAGACGATCTTCTTCA
CTGAAGGAAAGAAGCCGCCCATTCACTGTAGCAGCTTCATTTCAAAGCACCTCTGTCAAGAGCCCAAAAACTGTGT
CCCCACCTATCAGGAAAGGCTGGAGCATGTCAGAGCAGAGTGAAGAGTCTGTGGGTGGAAGAGTTGCAGAAAGGA
AACAAGTGGAAAATGCCAAGGCTTCTAAGAAGAATGGGAATGTGGGAAAAACAACCTGGCAAAACAAAGAATCTAA
AGGAGAGACAGGGAAGAGAAGTAAGGAAGGTCATAGTTTGGAGATGGAGAATGAGAATCTTGTAGAAAATGGTGCA
GACTCCGATGAAGATGATAACAGCTTCCTCAAACAACAATCTCCACAAGAACCCAAGTCTCTGAATTGGTCGAGTTT
TGTAGACAACACCTTTGCTGAAGAATTCACTACTCAGAATCAGAAATCCCAGGATGTGGAACTCTGGGAGGGAGAA
GTGGTCAAAGAGCTCTCTGTGGAAGAACAGATAAAGAGAAATCGGTATTATGATGAGGATGAGGATGA
AGAGTGAcaaatt.....

(E)

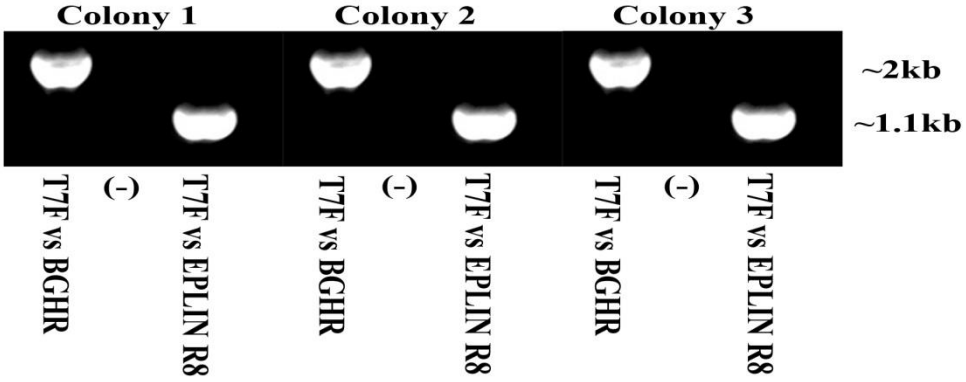

(F)

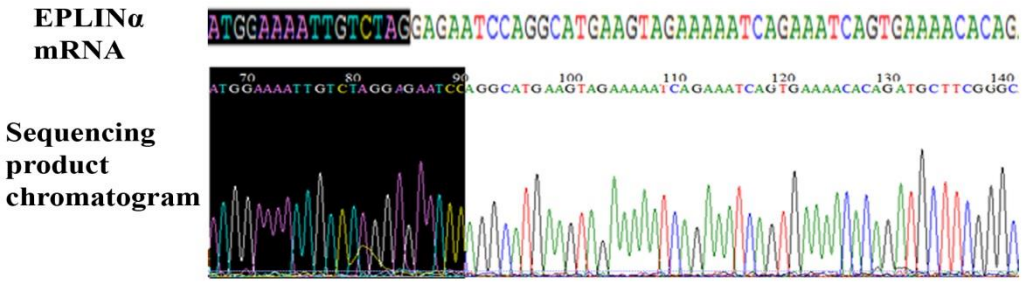

Figure 3.2 EPLINα overexpression plasmid generation and verification.

(A) Geneflow HighRanger 1kb DNA Ladder. (B) Confirmation of EPLINα expression and primer suitability in PZ-HPV-7 cell line. Bands at 1.8kb represent the full CDS of EPLINα that were amplified by primers targeting the start and end of the EPLINα sequence. Bands at approximately 878bp represent a region of EPLINα recognised by EPLIN-specific primers F8 and R8. PCR reactions run in duplicate. (C) PCR reaction using High Fidelity PCR kit to generate full EPLINα coding sequence for cloning reaction. (D) EPLINα full CDS region. Primers used for PCR amplification highlighted in bold. (E) PCR amplification of plasmids following cloning and plasmid extraction utilising EPLIN-specific primers (F8 and R8) and vector-specific primers (T7F). Positive orientation of sequence indicated by 1.1kb band in T7F vs EPLIN R8 whereas a negative result in T7F vs EPLIN F8 represents the absence of incorrectly orientated sequences. (F) Sequence chromatogram of sequencing products following sequencing from Source Biosciences. Start region of EPLINα mRNA depicted alongside start region of sequencing product.

3.3.3 Transfection of EPLINα expression sequence into PC-3 cells and verification of stable transfectants

Following successful plasmid extraction, the mammalian prostate cancer cell line PC-3 was transfected with the EPLINα expression plasmid by electroporation. This was subsequently named PC-3$^{EPLIN\ EXP}$. Plasmid control cells were generated by transfecting PC-3 Wild-Type cells with an empty pEF6 plasmid which was designated PC-3^{pEF6}. After electroporation and recovery, the cells were subjected to selection in Blasticidin S (5µg/ml) for 14 days. Following selection periods, RNA and protein were extracted from each cell line and verified for successful incorporation of the plasmid and enhancement of EPLIN expression. Successful forced expression was confirmed using PCR and Western Blotting (Figure 3.3). EPLIN transcript ($P<0.001$) and protein expression ($P=0.004$) was significantly increased in cells containing the EPLINα expression plasmid compared to cells containing empty pEF6 vector following semi-quantitative analysis of band intensities. PC-3^{pEF6} cells had comparable EPLIN expression to PC-3 Wild-Type cells, displaying low levels of EPLIN transcript expression and negligible EPLIN protein expression (data not shown). The EPLINβ isoform increased at the protein level (Figure 3.3C) but this increase was not seen at the transcript level (Figure 3.3A). GAPDH was used as a housekeeping gene/protein for both PCR and Western Blotting reactions and for standardizing levels of cDNA and protein within the samples.

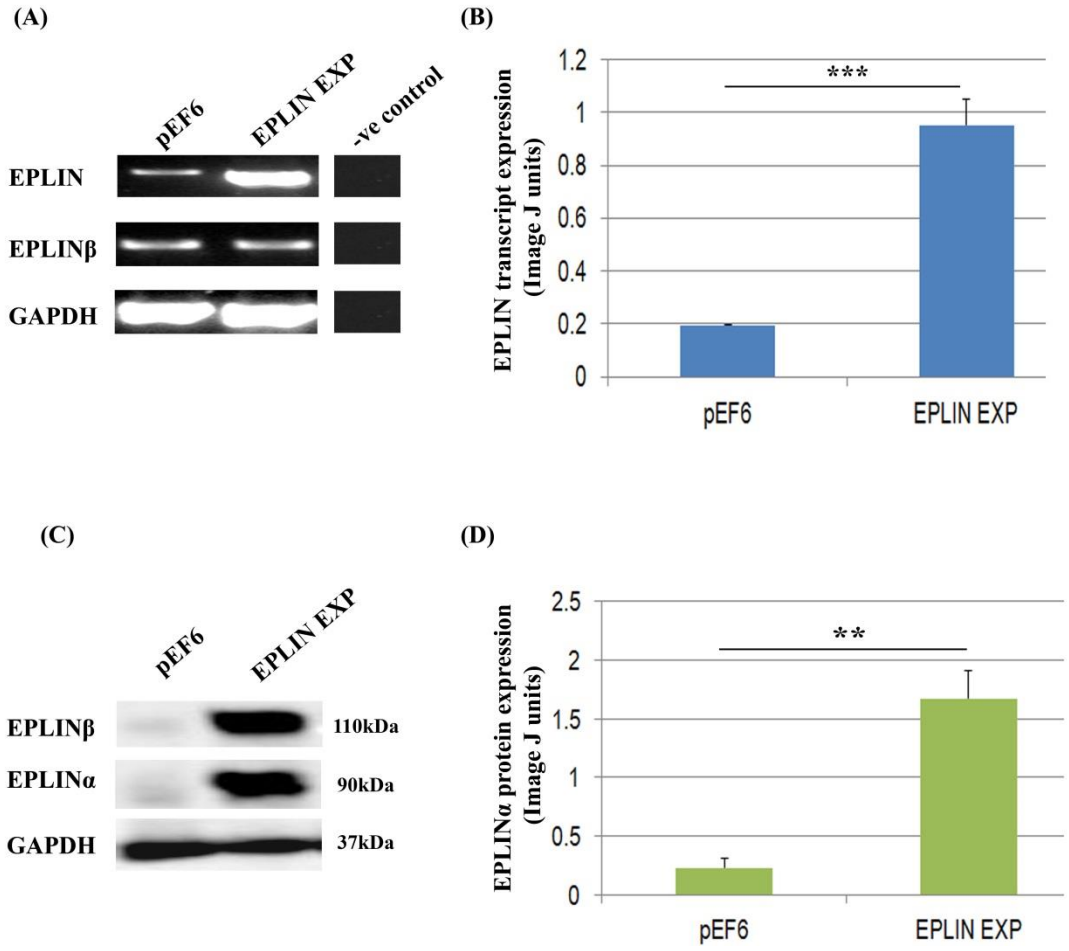

Figure 3.3 EPLINα overexpression in PC-3 cells.

(A) EPLIN and EPLINβ PCR reaction. EPLINα transcript was substantially enhanced in PC-3$^{EPLIN\ EXP}$ cells compared to PC-3^{pEF6} cells. (B) Semi-quantitative analysis of EPLINα band intensity from PCR reaction demonstrated a significant enhancement of EPLINα expression in PC-3$^{EPLIN\ EXP}$ cells compared to PC-3^{pEF6} cells (C) EPLINα and EPLINβ Western Blot reaction. The EPLINα isoform was markedly increased in PC-3$^{EPLIN\ EXP}$ cells compared to PC-3^{pEF6} (D) Semi-quantitative analysis of EPLINα band intensity from Western Blot reaction demonstrated a significant enhancement of EPLINα expression in PC-3$^{EPLIN\ EXP}$ cells compared to PC-3^{pEF6} cells. Samples normalised to GAPDH for all experiments. Representative images shown, semi-quantitative analysis shows mean values of n=3 repeats. Error bars represent SE of the mean. ** = $p<0.01$, *** = $P<0.001$. Statistical test performed for semi-quantitative analysis was a two sample, two tailed t-test using SigmaPlot software.

3.3.4 Transfection of EPLINα expression sequence into LNCaP cell line and verification of stable transfectants

Following successful plasmid extraction, the mammalian prostate cancer cell line LNCaP was transfected with the EPLINα expression plasmid by electroporation. This was subsequently named LNCaP$^{EPLIN\ EXP}$. A control was used by transfecting LNCaP Wild-Type cells with an empty pEF6 plasmid control which was designated LNCaP^{pEF6}. After electroporation and recovery the cells were subjected to a selection period in Blasticidin S (5µg/ml) for 6 days. Following selection periods, RNA and protein were extracted from each cell line and verified successful incorporation of the plasmid and enhancement of EPLIN expression using PCR and Western Blotting (Figure 3.4). Transfection of LNCaP cells with the EPLINα expression plasmid enhanced transcript expression of EPLIN, and to a lesser extent, EPLINβ (Figure 3.4A), though the overexpression of EPLIN transcript in LNCaP$^{EPLIN\ EXP}$ compared to LNCaP^{pEF6} did not quite reach statistical significance following semi-quantitative band analysis. For protein analysis, EPLINα was significantly increased in cells containing the EPLINα expression plasmid compared to cells containing empty pEF6 vector (P=0.047) (Figure 3.4D). LNCaP^{pEF6} cells had comparable EPLIN expression to LNCaP Wild-Type cells, displaying low EPLIN transcript expression and negligible EPLIN protein expression (data not shown). An increase in the EPLINβ isoform was also seen at protein level in LNCaP (Figure 3.4C). GAPDH was used as a housekeeping gene/protein for both PCR and Western Blotting reactions and standardized levels of cDNA and protein within the samples.

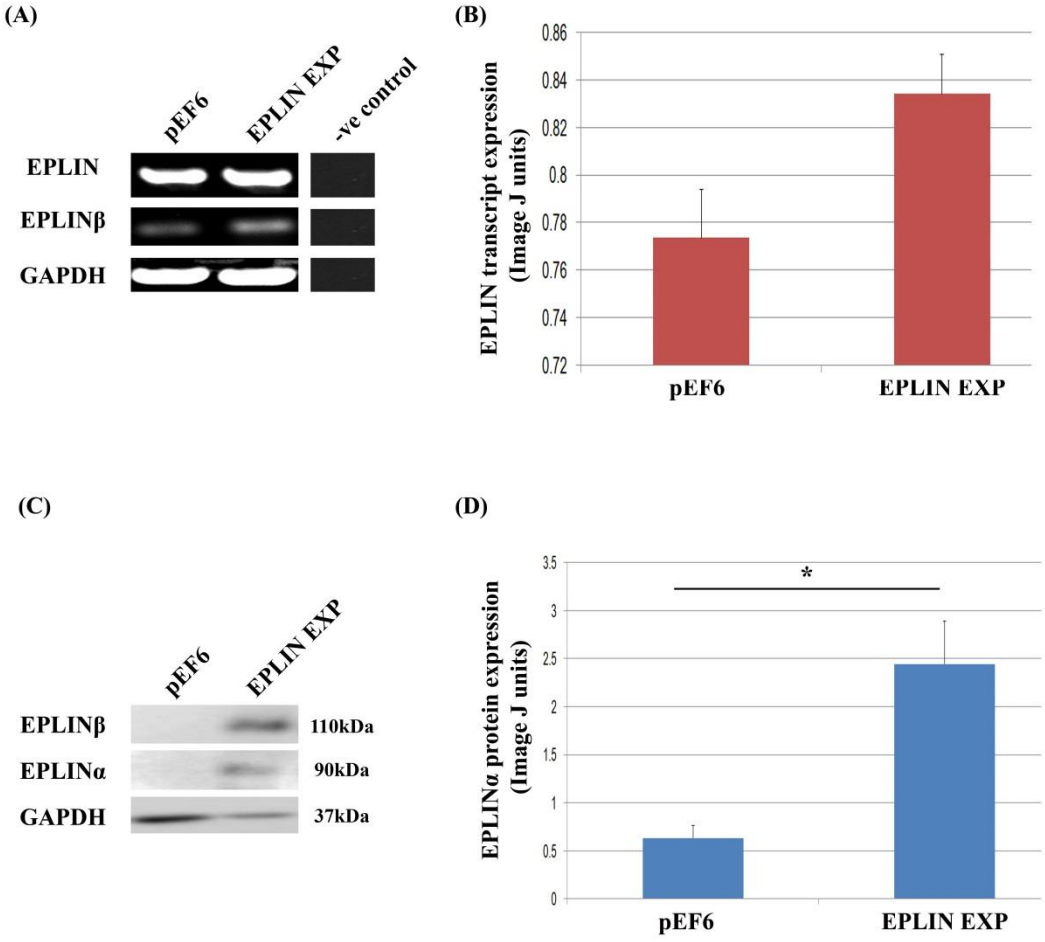

Figure 3.4 EPLINα overexpression in LNCaP cells.

(A) EPLIN and EPLINβ PCR reaction in LNCaP^{pEF6} and LNCaP$^{EPLIN\ EXP}$ cells. (B) Semi-quantitative analysis of EPLIN band intensity from PCR reaction demonstrating slight increase in EPLIN expression in LNCaP$^{EPLIN\ EXP}$ cells compared to LNCaP^{pEF6} cells. (C) EPLINα and EPLINβ Western Blot reaction. The EPLINα isoform was markedly increased in LNCaP$^{EPLIN\ EXP}$ cells compared to LNCaP^{pEF6}. (D) Semi-quantitative analysis of EPLINα band intensity from Western Blot reaction demonstrated a significant enhancement of EPLINα expression in LNCaP$^{EPLIN\ EXP}$ cells compared to LNCaP^{pEF6} cells. Semi-quantitative analysis carried out using Image J software. Samples normalised to GAPDH for all experiments. Representative images shown, semi-quantitative analysis shows mean values of n=3 repeats. Error bars represent SE of the mean. * = $p<0.05$. Statistical test performed for semi-quantitative analysis was a two sample, two tailed t-test using SigmaPlot software.

3.3.5 Expression analysis of EPLIN transcript levels in PCa tissues using the Gene Expression Omnibus (GEO) repository

EPLIN expression in prostate cancer tissue has been previously evaluated where similar trends were seen to prostate cell line data demonstrated in this study. Using GEO profiles extracted from NCBI, EPLIN continually scored lower in cancerous tissue compared to normal prostate, with significant reductions in highly metastatic cancer tissues across cohorts (Figure 3.5). For the GDS2865 / 217892_s_at cohort, highly metastatic cancer tissue scored significantly lower for EPLIN expression than poorly metastatic ($p<0.05$) cancer tissue (Figure 3.5A). For the GDS1439 / 222457_s_at cohort, metastatic prostate cancer tissue scored significantly less for EPLIN compared to Benign Prostate Tissue ($p<0.01$) and Primary Prostate Cancer ($p<0.001$) (Figure 3.5B). A similar trend was seen for the GDS1439 / 217892_s_at GEO profile where metastatic prostate cancer tissue scored significantly less for EPLIN compared to Benign Prostate Tissue ($p<0.05$) and Primary Prostate Cancer ($p<0.01$) (Figure 3.5C).

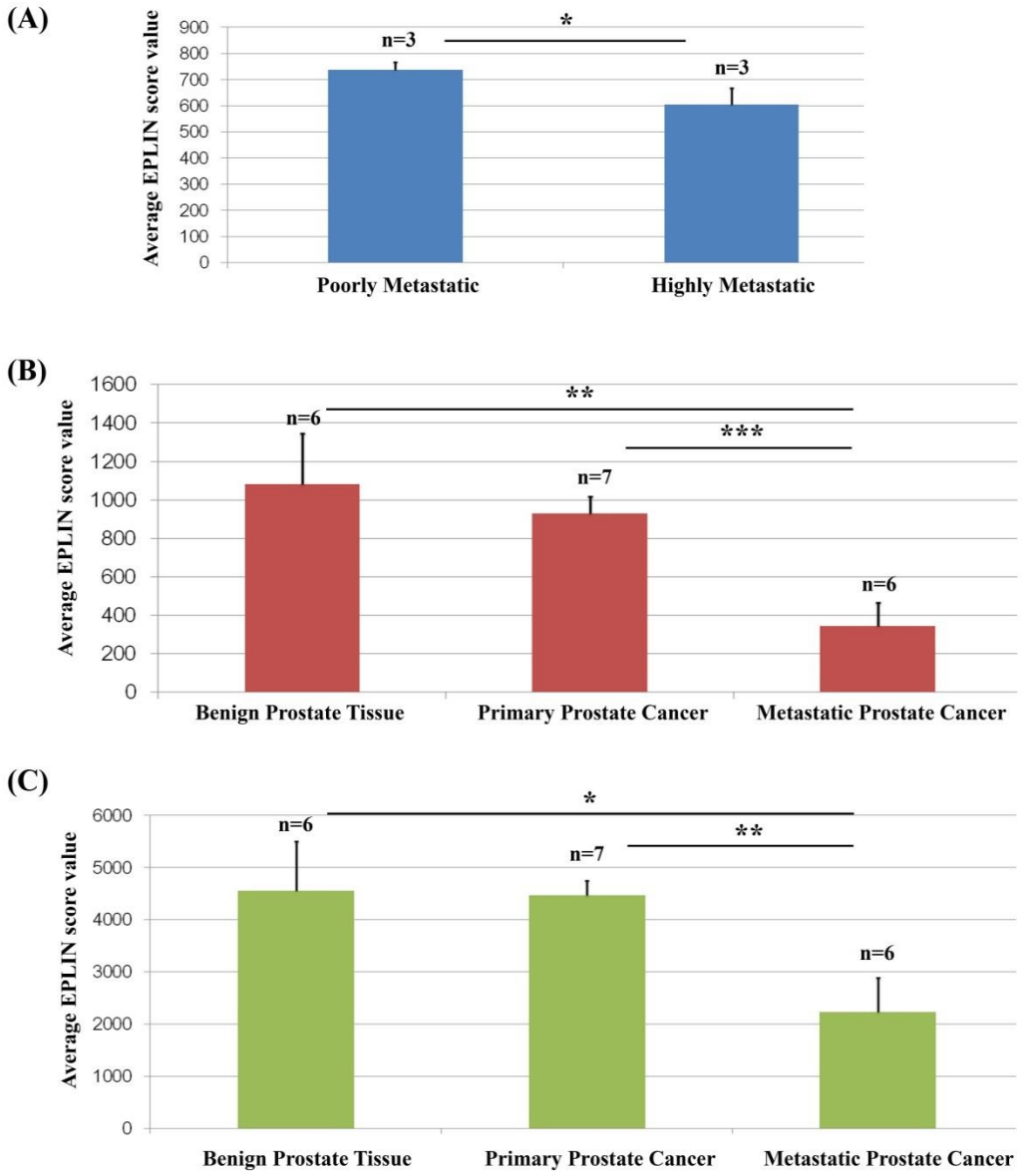

Figure 3.5 Gene Expression Omnibus (GEO) profiles of EPLIN score values from various cancer cohorts extracted from NCBI.

(A) Profile GDS2865 / 217892_s_at; EPLIN score value in poorly metastatic tissue and highly metastatic tissue. (B) Profile GDS1439 / 222457_s_at; EPLIN score value in benign prostate tissue, primary prostate cancer and metastatic prostate cancer. (C) Profile GDS1439 / 217892_s_at; EPLIN score value in benign prostate tissue, primary prostate cancer and metastatic prostate cancer. Statistical test performed for analysis was a two sample, two tailed t-test using SigmaPlot software.

3.3.6 Expression analysis of EPLIN in prostate cancer tissues

EPLIN expression was evaluated in clinical prostate cancer tissue using two TMAs (Figure 3.6). Several clinical parameters were evaluated for EPLIN staining in terms of cancer progression, these included cancer tissue vs. normal, cancer stage, Gleason score, chronic inflammation, cancers in adjacent to prostate tissue and cancer type (hyperplasia and adenocarcinoma). In the first TMA (HPro-Ade96Sur-01), EPLIN expression was reduced in cancer tissue compared to normal tissue (Figure 3.7). EPLIN expression in normal tissue was predominately expressed in the epithelial portion of the sections. EPLIN expression was also reduced in higher stage cancers, specifically stage III and IV compared to stage II (Figure 3.8). A reduction of EPLIN expression was also seen with increasing Gleason score samples, with EPLIN downregulation observed in Gleason 8, 9 and 10, compared to Gleason 6 and 7 (Figure 3.9), though none of these trends reached statistical significance. In the second TMA (PR8011a), EPLIN expression was significantly reduced in patients with prostate cancer hyperplasia ($p=<0.001$) and adenocarcinoma ($p=0.005$) compared to normal prostate tissue (Figure 3.10). EPLIN was also highly expressed in the epithelial portion of normal tissue sections. A significant reduction in EPLIN expression was also seen in hyperplasia samples compared to adjacent prostate tissue ($p=0.003$). A general reduction in EPLIN expression was also seen between adjacent tissue and adenocarcinoma, and between normal prostate tissue and chronic inflammation, though these didn't quite reach statistical significance ($p=0.054$ for adjacent tissue vs. adenocarcinoma; $p=0.071$ for normal prostate tissues vs. chronic inflammation). No significant differences were seen in EPLIN expression between normal prostate tissues and adjacent prostate tissue ($p=0.422$) (Figure 3.10).

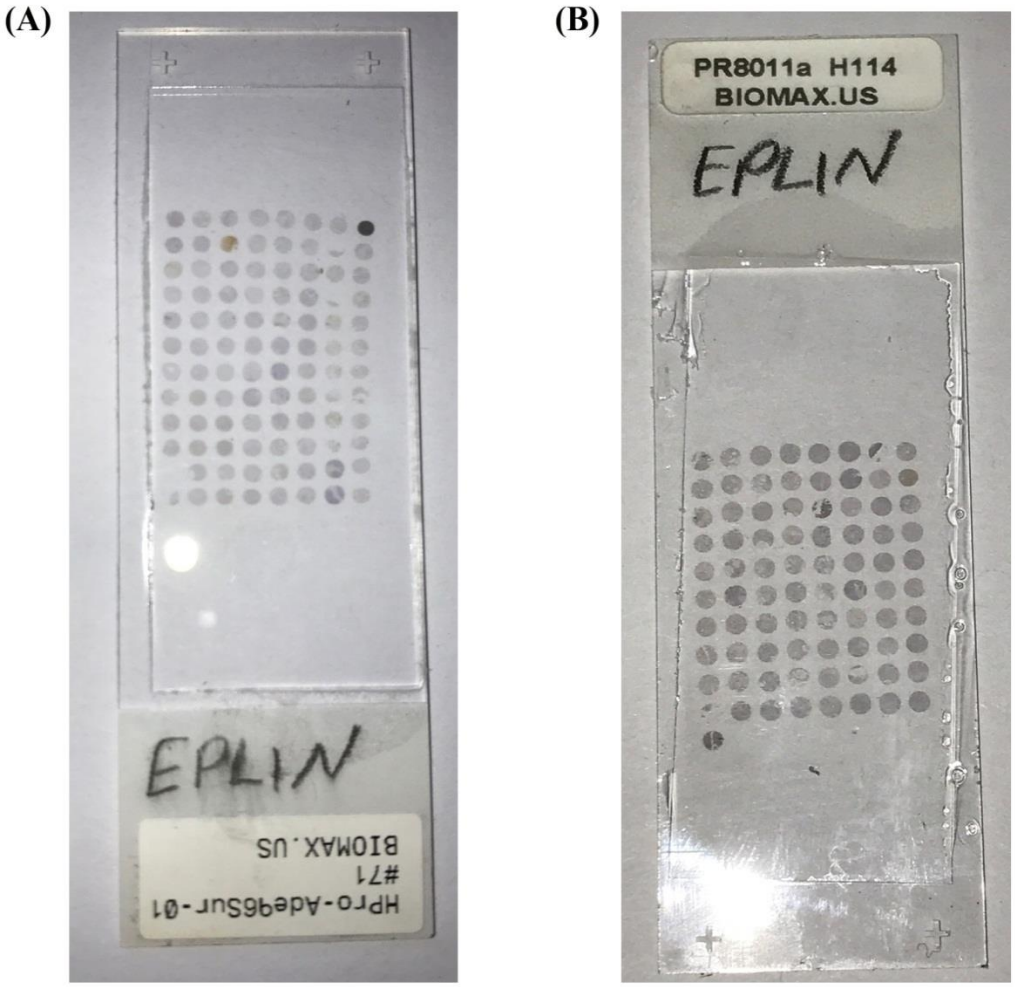

Figure 3.6 TMA slides used for IHC analysis of EPLIN staining.

(A) Photograph taken of TMA1; HPro-Ade96Sur-01. (B) Photograph taken of TMA2; PR8011a.

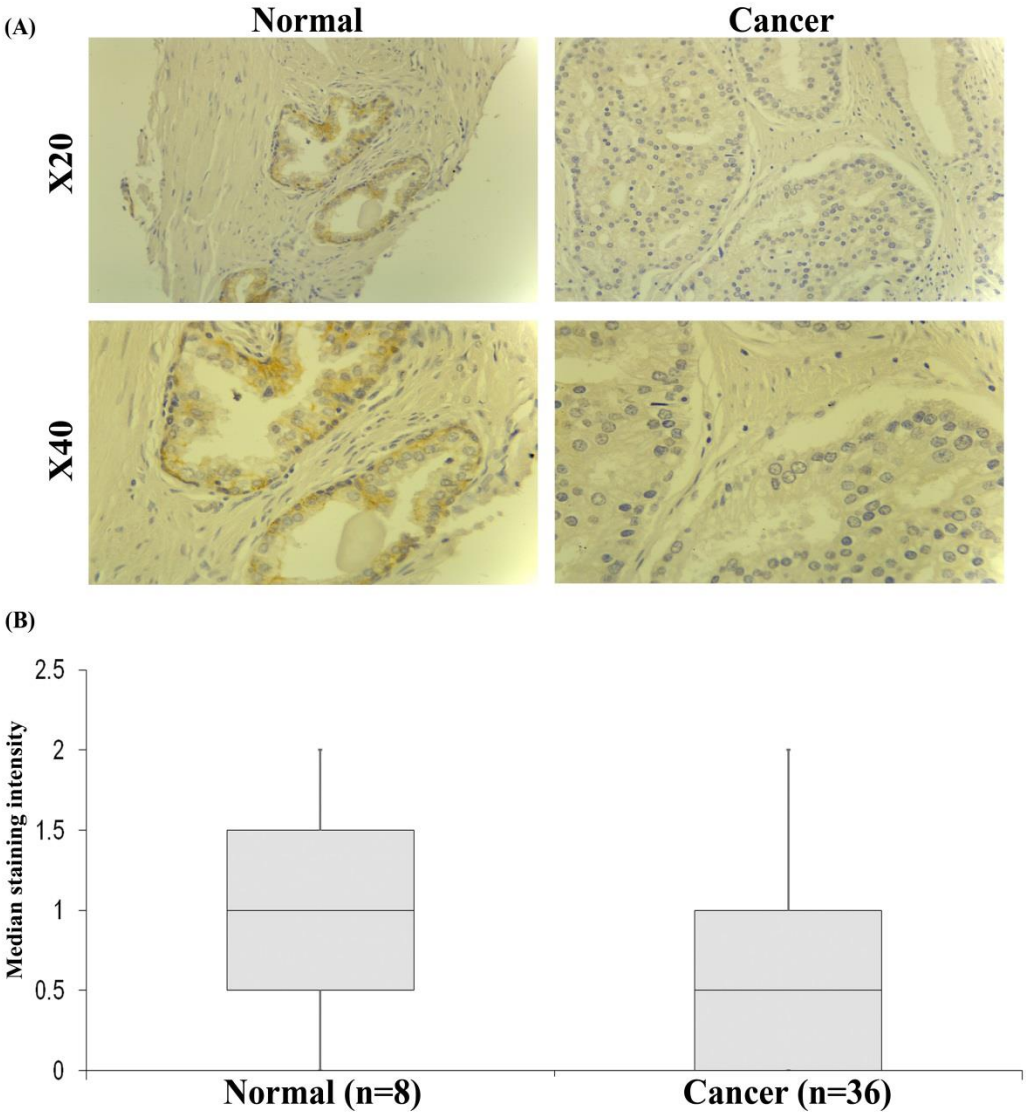

Figure 3.7 EPLIN IHC staining in normal prostate tissue and cancer tissue from TMA1 (HPro-Ade96Sur-01).

(A) Representative images of EPLIN IHC staining from normal (n=8) and prostate cancer (n=36) samples at X10 and X20 objective magnification. Representative images are grid numbers G9 (Normal) and C8 (Cancer). Refer to Table 2.5 for full details. (B) Boxplot representations of (A) showing Median, Q1 and Q3 staining intensity. Whiskers represent minimum and maximum staining intensity. Staining intensity was determined by three independent operators using 0, 1, 2 and 3 as scoring intensities before taking an average of each score. The larger the number between 0-3, indicates the degree of brown protein staining.

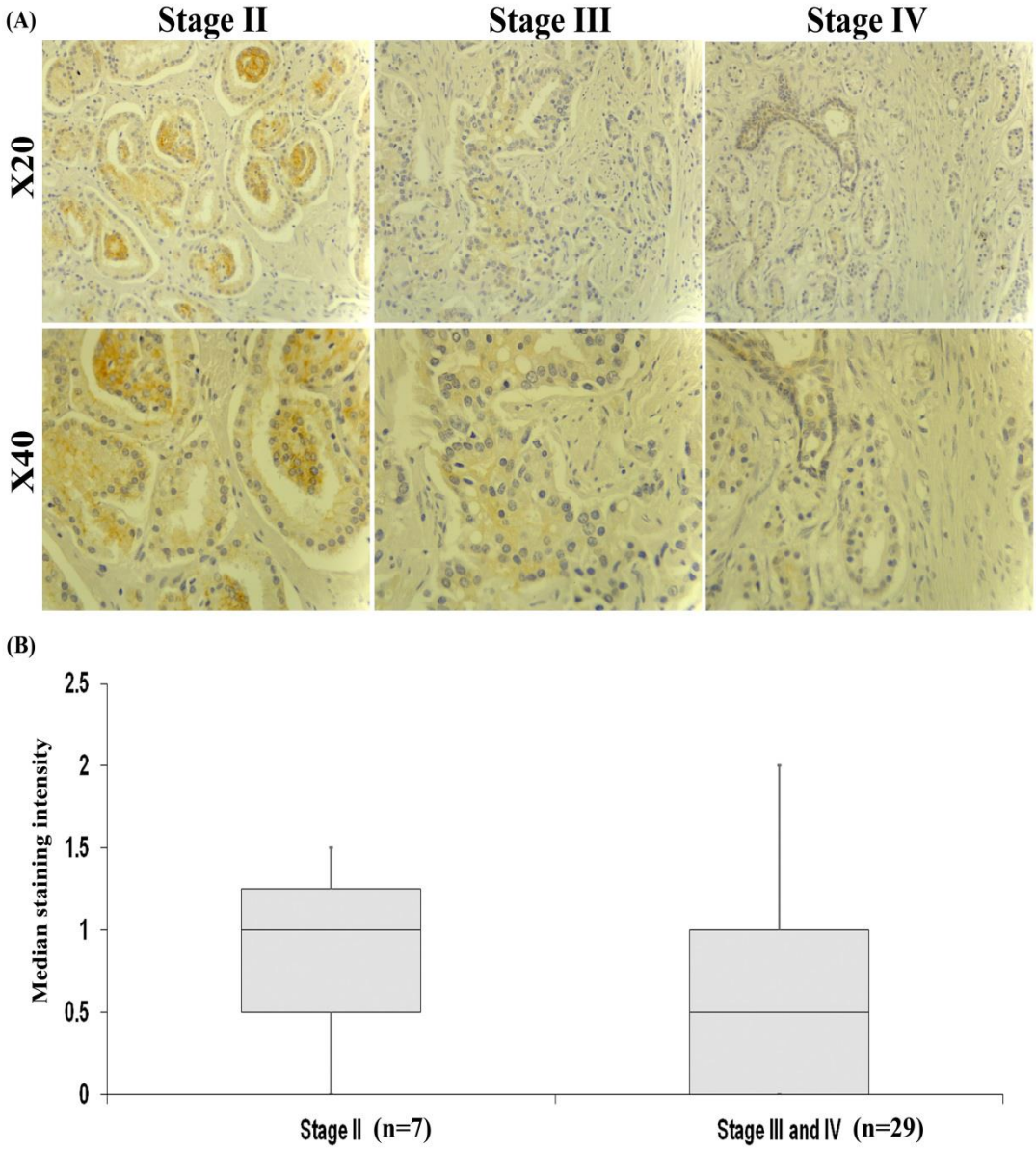

Figure 3.8 EPLIN IHC staining in cancer samples of Stage II, III and IV from TMA1 (HPro-Ade96Sur-01).

(A) Representative images of EPLIN IHC staining from cancer samples of Stage II (n=7), III (n=26) and IV (n=3) at X10 and X20 objective magnification. Representative images are grid numbers B5 (Stage II), C7 (Stage III) and B11 (Stage IV). Refer to Table 2.5 for full details. (B) Boxplot representations of (A) showing Median, Q1 and Q3 staining intensity. Box plot data shows Stage II (n=7) vs. combined Stage III and IV (n=29). Whiskers represent minimum and maximum staining intensity. Staining intensity was determined by three independent operators using 0, 1, 2 and 3 as scoring intensities before taking an average of each score. The larger the number between 0-3, indicates the degree of brown protein staining.

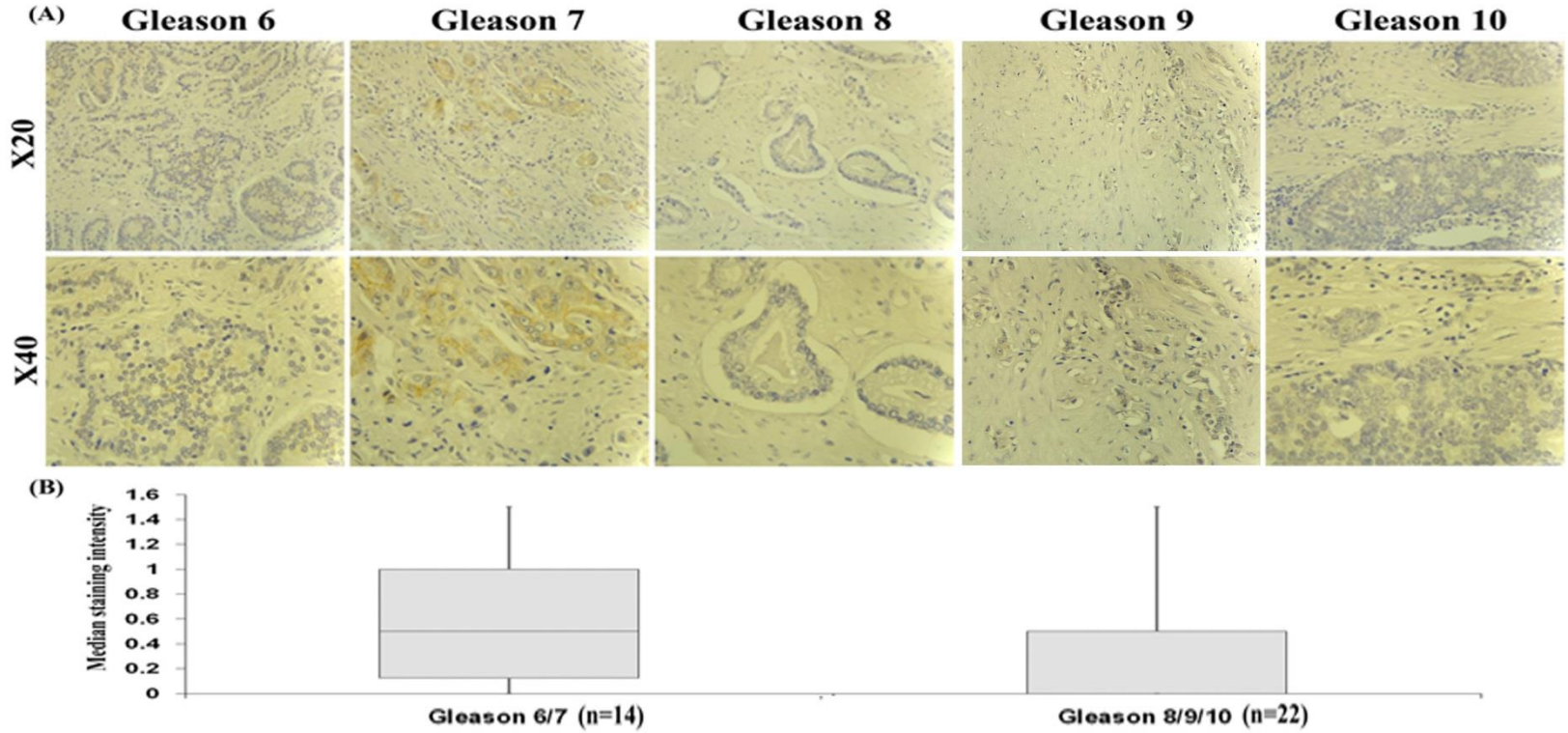

Figure 3.9 EPLIN IHC staining in cancer samples Gleason 6, 7, 8, 9 and 10 from TMA1 (HPro-Ade96Sur-01).

(A) Representative images of EPLIN IHC staining from cancer samples of Gleason 6 (n=1), 7 (n=13), 8 (n=6), 9 (n=14) and 10 (n=2) at X10 and X20 objective magnification. Representative images are grid numbers D5 (Gleason 6), B4 (Gleason 7), D12 (Gleason 8), A9 (Gleason 9) and E5 (Gleason 10). Refer to Table 2.5 for full details. (B) Boxplot representations of (A) showing Median, Q1 and Q3 staining intensity. Box plot data shows combined Gleason 6/7 (n=14) vs. combined Gleason 8/9/10 (n=22). Whiskers represent minimum and maximum staining intensity. Staining intensity was determined by three independent operators using 0, 1, 2 and 3 as scoring intensities before taking an average of each score. The larger the number between 0-3, indicates the degree of brown protein staining.

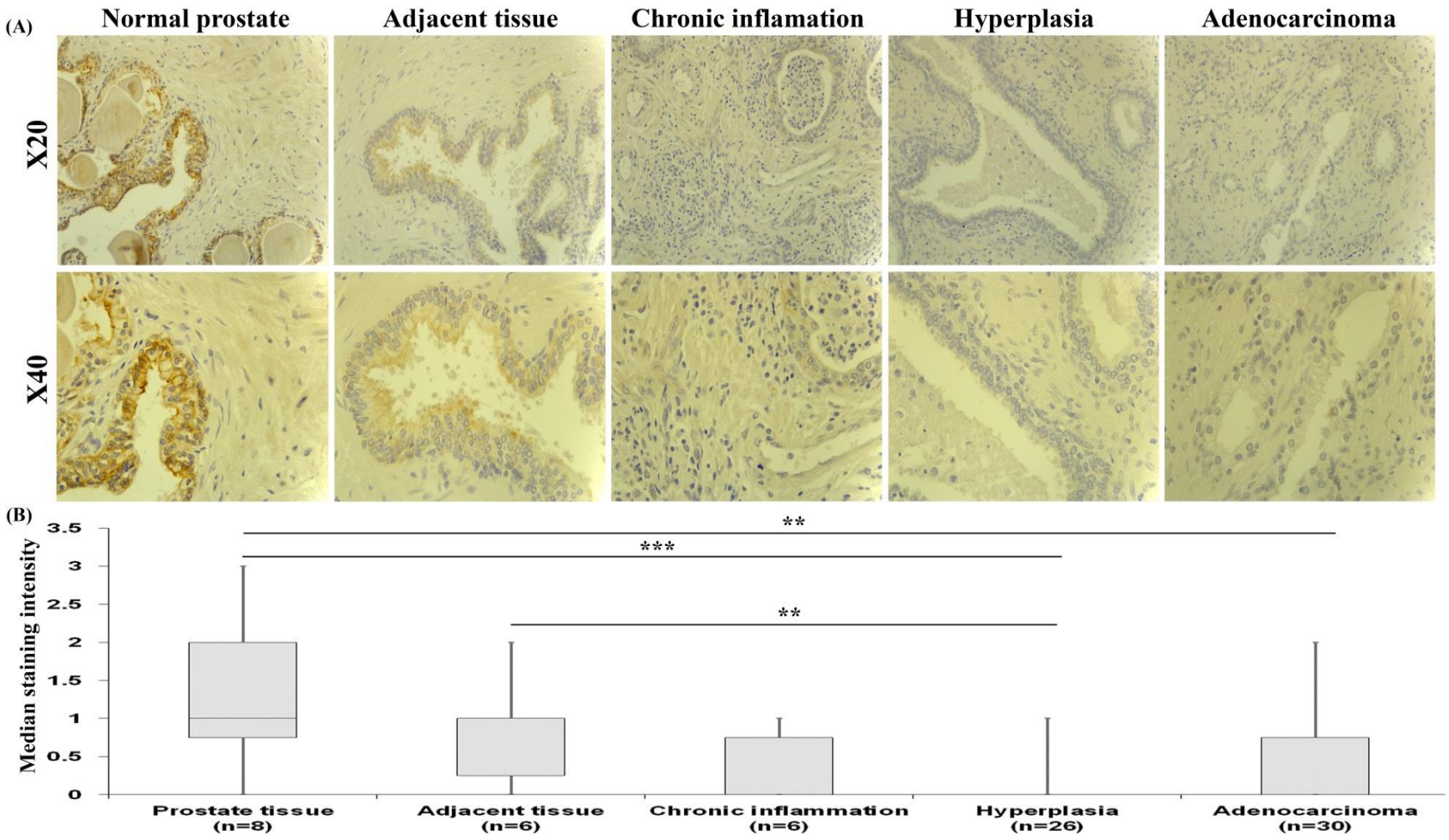
(A)
Normal prostate
Adjacent tissue
Chronic inflamation
Hyperplasia
Adenocarcinoma
X20
X40
(B)
Median staining intensity
3.5
3
2.5
2
1.5
1
0.5
0
**
***
**
Prostate tissue (n=8)
Adjacent tissue (n=6)
Chronic inflammation (n=6)
Hyperplasia (n=26)
Adenocarcinoma (n=30)

Figure 3.10 EPLIN IHC staining in normal prostate tissue, tissue with adjacent cancers, chronic inflammation, hyperplasia and adenocarcinoma from TMA2 (PR8011a).

(A) Representative images of EPLIN IHC staining from normal prostate tissue (n=8), tissue with adjacent cancers (n=6), chronic inflammation (n=6), hyperplasia (n=26) and adenocarcinoma (n=30) at X20 and X40 objective magnification. Representative images are grid numbers H3 (Normal Prostate), G8 (Adjacent Tissue), G4 (Chronic Inflammation), F10 (Hyperplasia) and C3 (Adenocarcinoma). Refer to Table 2.6 for full details. (B) Boxplot representations of (A) showing Median, Q1 and Q3 staining intensity. Staining intensity was determined by three independent operators using 0, 1, 2 and 3 as scoring intensities before taking an average of each score. The larger the number between 0-3, indicates the degree of brown protein staining. Whiskers represent minimum and maximum staining intensity. ** = $p<0.01$ and *** = $p<0.001$. Comparison between test groups was performed using a Mann Whitney U test.

3.4 Discussion

This study aimed to create an expression profile for EPLIN in human prostate cancer, utilising prostate cancer cell lines and clinical prostate cancer tissue. EPLIN was initially identified as a protein with differential expression between normal and HPV immortalized oral keratinocytes (Chang et al., 1998) and this study sought to build on previous work utilising further prostate cancer cell lines and tissue. The initial cell line screen determined that EPLIN is differentially expressed in prostate cancer cell lines at the transcript level, with lowest expression in PC-3, LNCaP and VCaP. This notion was also comparable to protein data, where EPLIN was negative for both PC-3 and LNCaP. On the other hand, EPLIN transcript and protein was strongly expressed in the PZ-HPV-7 and CA-HPV-10 cell lines. This suggests that EPLIN is lost progressively as prostate cancer develops and becomes more aggressive, as PC-3, LNCaP and VCaP are cell lines derived from an aggressive form of prostate cancer which has metastasised, whereas PZ-HPV-7 is derived from normal prostate tissue, and CA-HPV-10 is derived from a non-metastatic adenocarcinoma. EPLINβ was expressed equivalently at low levels at the transcript level for all cell lines tested, however was negative for all prostate cell lines except for CA-HPV-10. These findings for EPLIN expression in prostate cancer concur with previous studies using PC-3, DU-145 and LNCaP models where EPLIN expression was low or abolished compared to non-cancerous controls (Maul and Chang, 1999). This is the first known study where the VCaP model has been used to evaluate EPLIN expression in prostate cancer and demonstrates comparable expression to the PC-3 and LNCaP models, supporting the concept that EPLIN is lost as prostate cancer progresses, as VCaP is a metastatic derived cell line from

vertebral metastases and is a more aggressive form of cancer compared to CA-HPV-10 and PZ-HPV-7 (Korenchuk et al., 2001). It's interesting to note that the lowest EPLIN expression profile was seen in cell lines derived from secondary bone sites (PC-3, VCaP), or secondary regions in the vicinity of bone sites (LNCaP), suggesting EPLIN expression may be at its weakest when in a most aggressive form of metastasised bone cancer. This potential relationship between EPLIN and development of bone metastasis will be investigated further in later chapters.

To evaluate EPLIN expression in clinical cancer, the global transcriptome database GEO was searched for EPLIN expression in various cancers. Analyses of three independent sets of microarray data on clinical prostate cancer demonstrated that metastatic and highly metastatic cancer correlated with markedly low EPLIN scores. Further to this, EPLIN expression was determined in two separate TMA experiments. EPLIN expression was markedly reduced in cancer samples compared to normal, and EPLIN loss correlated with increasing cancer stage and Gleason score. EPLIN expression was also reduced in cancer tissue samples with hyperplasia and adenocarcinoma with highly significant reductions compared to normal prostate tissue. This emphasises the importance of EPLIN expression in cancer progression and further suggests a cumulative loss of EPLIN in more aggressive prostate cancer types. This substantiates previous work evaluating EPLIN expression in clinical cancer, and demonstrates a potential use of EPLIN in diagnostic/prognostic testing of prostate cancer development and progression (Sanders et al., 2011, Jiang et al., 2008, Zhang et al., 2011, Liu et al., 2016). Interestingly, in the second TMA study, EPLIN was reduced in samples with chronic inflammation compared to normal prostate, which may also suggest a novel association of EPLIN expression in immune

response in cancer. Though, due to low sample number, this must be considered with caution and requires validation. In addition to low sample number, there are possible issues which could affect the level of protein staining in the tissues and these include antibody performance issues, processing, and embedding or antigenicity/antigen retrieval issues. This could help explain the reasons for poor staining of the sections. This TMA was also purchased commercially; therefore the ability to modify processing of the samples was unavailable. Further work is therefore required using a larger sample number and additional degrees of prostate cancer aggressiveness.

Lastly, this study successfully generated a plasmid construct containing a full length EPLIN expression sequence for overexpression work in later chapters. Plasmids were transfected into PC-3 and LNCaP cells and EPLIN expression was verified by PCR and Western Blotting. In these two cell lines, EPLIN was successfully overexpressed and showed significant increase in EPLINα expression in both PC-3 and LNCaP cells transfected with the expression plasmid compared to plasmid control cells, thus establishing suitable cell models for later chapters evaluating cell function in relation to manipulated EPLINα expression and potential mechanisms of action. Following EPLINα overexpression, PC-3 cells tended to show a more flattened, cobblestone morphology, opposed to a more spherical morphology of control pEF6-transfected PC-3 cells. LNCaP cells remained relatively unchanged morphologically following transfection. Changes in morphology following manipulated EPLINα expression has been previously seen using osteosarcoma cells, where cells became more spindle forming with cytoplasmic extensions (Maul and Chang, 1999). Both PC-3 and LNCaP cells overexpressing EPLINα also required longer incubations times for cells to be detached using trypsin, suggesting changes in

cell-matrix interaction with increased EPLINα and changes to cell adhesion. This will be discussed further in later chapters. Notably from this analysis, EPLINβ expression also increased alongside EPLINα overexpression. The reason for this is unknown; however it could be due to a potential stabilising effect of increased EPLINα on EPLINβ. As no significant increase was seen at the transcript level of EPLINβ for either PC-3 or LNCaP (Figure 3.3/Figure 3.4), this effect on EPLINβ must be acting post-transcriptionally. Little work has been presented and focused on the relationship between EPLINα and EPLINβ expression in cancer (Sanders et al., 2010, Jiang et al., 2008, Liu et al., 2012a) nor has EPLINβ been comprehensively evaluated for implication in cancer in the literature, so it's difficult to decipher if this increase is specific to prostate cancer cell lines PC-3 and LNCaP, or is a regulatory effect in other cell systems. On a side note, we have overexpressed the EPLINα isoform in the pancreatic cancer cell line PANC-1 previously, and no subsequent increase in EPLINβ was seen (unpublished, data not shown), therefore it may be that this increase is specific to prostate cancer cell lines. Lastly, this increase of EPLINβ cannot be directly from the expression plasmid itself, as EPLIN sequenced plasmid products contains only EPLINα promoter regions and everything upstream of the EPLINα promoter and hence, the start of EPLINβ sequence is missing from the sequenced plasmid.

Based on the findings of this study, it supports the conclusion that EPLIN is downregulated or lost in prostate cancer, with largest reductions in expression of aggressive cancer cell lines or aggressive metastatic prostate cancer tissue. As other studies have reported, this demonstrates the potential of EPLIN as a prognostic

marker protein and could be used to envisage the aggressive nature of prostate cancer.

Chapter IV: Functional impact of EPLINα expression in a osteolytic PC-3 cell model of prostate cancer

4.1 Introduction

With the discovery of EPLIN loss in cancer, a key research area emerged to elucidate its role in carcinogenesis and progression. Although there are indications of functional links of EPLIN to actin dynamics (Maul et al., 2003), the functional role of EPLIN in cancer development remains elusive. Several studies have illustrated that manipulation of the EPLINα isoform may have potential for cancer therapy and treatment, where enhanced EPLINα expression proved to be advantageous in suppressing metastatic characteristics including cellular invasion, adhesion, proliferation and motility, whereas inhibition of EPLINα expression resulted in a more aggressive phenotype across a number of cancer types (Sanders et al., 2011, Jiang et al., 2008, Liu et al., 2012a, Liu et al., 2016). In addition to EPLIN's association to actin, there are highlighted links to various other signalling molecules including paxillin and FAK (Sanders et al., 2010). The majority of work carried out on the molecular characteristics of EPLIN in prostate cancer biology has utilised the classical prostate cell line PC-3 and this chapter aims to further explore EPLIN's role using this cell model. In this chapter, PC-3 cells previously transfected with a EPLINα overexpression plasmid (see Chapter 3) were used to evaluate any functional importance of EPLINα by employing a number of *in vitro* functional techniques. In addition, cells were treated BME, and used in a co-culture osteoblast model, in order to highlight any change in metastatic potential of cells when in a bone like environment and to evaluate any potential role for EPLIN in establishment or development of bone metastasis. The aim of this chapter is to further explore the importance of EPLINα in the PC-3 osteolytic model of prostate cancer and to evaluate potential roles for EPLINα in regulating bone metastasis *in vitro*.

4.2 Material and methods

4.2.1 Materials

All primers used were manufactured and provided by Sigma-Aldrich (Dorset, UK). Antibodies and primer sequences used for this study are listed in section 2.1.2 and 2.1.3. For this section, BME was used in *in vitro* functional assays. For preparation and dilution conditions, please see section 2.6.1.

4.2.2 Cell lines

The prostate cancer cell line PC-3 was used for this section of the study. PC-3 cells were cultured in DMEM as described in section 2.2. For the co-culture invasion assay with human osteoblasts, hFOB1.19 cells were used with a specialist medium of DMEM without phenol red supplemented with 10% FCS, 1% antibiotics and 0.3mg/ml G418.

4.2.3 *In vitro* tumour cell proliferation assay

Cells were seeded into 96 well plates for varying incubation times to evaluate cell proliferation. Absorbance was measured to determine cell number and proliferation rate. The proliferation of both control PC-3^{pEF6} cells and PC-3$^{EPLIN\ EXP}$ cells was determined in addition to any treatments used. For full procedure please refer to section 2.6.6.

4.2.4 *In vitro* tumour cell Matrigel adhesion assay

Cells were seeded into a 96 well plate which was pre-covered with layer of Matrigel. Following an appropriate incubation period, the number of cells that had adhered to the artificial basement membrane was counted. The adhesion of both control PC-

3^{pEF6} cells and PC-$3^{EPLIN\ EXP}$ cells was determined in addition to any treatments used. For full procedure please refer to section 2.6.8.

4.2.5 *In vitro* tumour cell invasion assay

Cells were seeded into 24 well plates containing cell culture inserts coated with a Matrigel layer. Following a 3 day incubation period, the number of cells which had penetrated and invaded the artificial basement membrane was stained and visualised on the microscope. The invasive capacity of both control PC-3^{pEF6} cells and PC-$3^{EPLIN\ EXP}$ cells was determined in addition to any treatments used. For full procedure please refer to section 2.6.7.

4.2.6 *In vitro* tumour migration/wound healing assay

Cells were seeded into 24 well plates one day prior to day of experiment ensuring sufficient cells to reach a confluent monolayer. A wound healing assay was performed over four hours and photos were taken at each one hour interval. Migratory potential both control PC-3^{pEF6} cells and PC-$3^{EPLIN\ EXP}$ cells was then determined. For full procedure please refer to section 2.6.9

4.2.7 *In vitro* co-culture invasion assay with human osteoblasts

Human osteoblast hFOB1.19 cells were seeded into 24 well plates one day prior to the beginning of the experiment to ensure sufficient confluence. Once seeded, an invasion assay was set up as in section 2.6.7. Cell invasion was determined in both control PC-3^{pEF6} cells and PC-$3^{EPLIN\ EXP}$ cells in an *in vitro* bone environment in presence of human osteoblasts. For full procedure please see section 2.6.11

4.2.8 Statistical analysis

Statistical comparisons were made between different groups using a two sample, two tailed t-test or a Mann Whitney U test dependant on data normality. SigmaPlot 11.00 software was used to conduct statistical analysis and $p < 0.05$ regarded as statistically significant

4.3 Results

4.3.1 Effect of EPLINα overexpression on PC-3 cell proliferation

The functional effect of EPLINα overexpression was determined in the osteolytic PC-3 cell line using an *in vitro* tumour cell proliferation assay. Forced EPLINα expression significantly reduced the cell proliferation of PC-3 cells at Day 3 ($p=0.005$) and at Day 5 ($p=0.023$), when comparing PC-$3^{EPLINEXP}$ and PC-3^{pEF6} cells (Figure 4.1A). The approximate doubling time of PC-3^{pEF6} cells at Day 5 was 35 hours. The approximate doubling time of PC-$3^{EPLIN\ EXP}$ cells at Day 5 was 41 hours. The effect of BME, at 50µg/ml and 100µg/ml concentrations, was also determined in both PC-3^{pEF6} and PC-$3^{EPLINEXP}$ cells to deduce the potential effect of EPLINα expression on cell proliferation in an *in vitro* bone-like environment (Figure 4.1B/C). BME had no apparent effect on PC-3 cell proliferation for both PC-3^{pEF6} and PC-$3^{EPLIN\ EXP}$ cells at either concentration tested (50µg/ml and 100µg/ml).

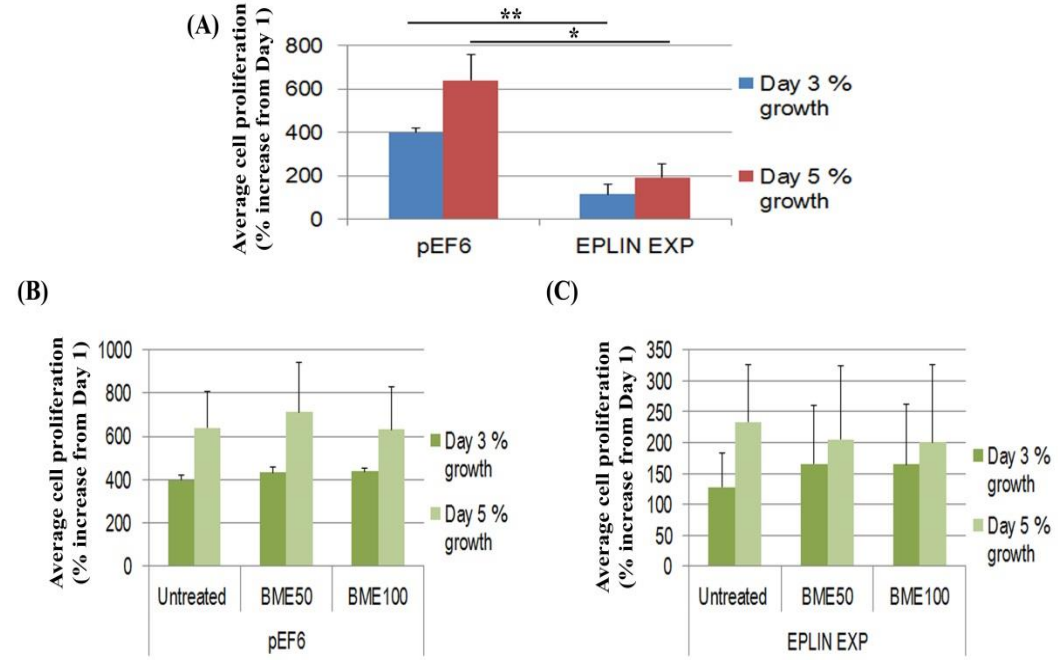

Figure 4.1 Cell proliferation assay in PC-3 cells.

(A) Average cell proliferation (% change from Day 1) of PC-3^{pEF6} (pEF6) and PC-3$^{EPLIN\ EXP}$ (EPLIN EXP) cells at 3 day and 5 day time points. (B) Effect of BME at 50µg/ml and 100µg/ml concentrations upon PC-3^{pEF6} (pEF6) cells at 3 day and 5 day time points (% change from Day 1). (C) Effect of BME at 50µg/ml and 100µg/ml concentrations upon PC-3$^{EPLIN\ EXP}$ (EPLIN EXP) cells at 3 day and 5 day time points (% change from Day 1). BME was added to tumour cell functional assays to represent an *in vitro* bone-like environment. Mean of three independent repeats (n=3) are shown. Error bars represent SE of the Mean. * = $p<0.05$, ** = $p<0.01$. Statistical analysis was performed using a two sample, two tailed t-test using SigmaPlot software.

4.3.2 Effect of EPLINα overexpression on tumour cell invasion

The capability for PC-3^{pEF6} and PC-3^{EPLINEXP} cells to invade surrounding tissue was evaluated using an *in vitro* Matrigel invasion assay (Figure 4.2). Forced EPLINα expression in PC-3^{EPLINEXP} cells caused a significant decrease in cellular invasion ($p=0.048$) (Figure 4.2A/B). The effect of BME, at 50µg/ml and 100µg/ml concentrations, was also determined in both PC-3^{pEF6} and PC-3^{EPLINEXP} cells to deduce the potential effect of EPLINα expression on cell invasion in an *in vitro* bone-like environment (Figure 4.2C/D). BME had no apparent effect on PC-3 cell invasion for PC-3^{pEF6} and PC-3$^{EPLIN\ EXP}$ cells at either concentration tested (50µg/ml and 100µg/ml).

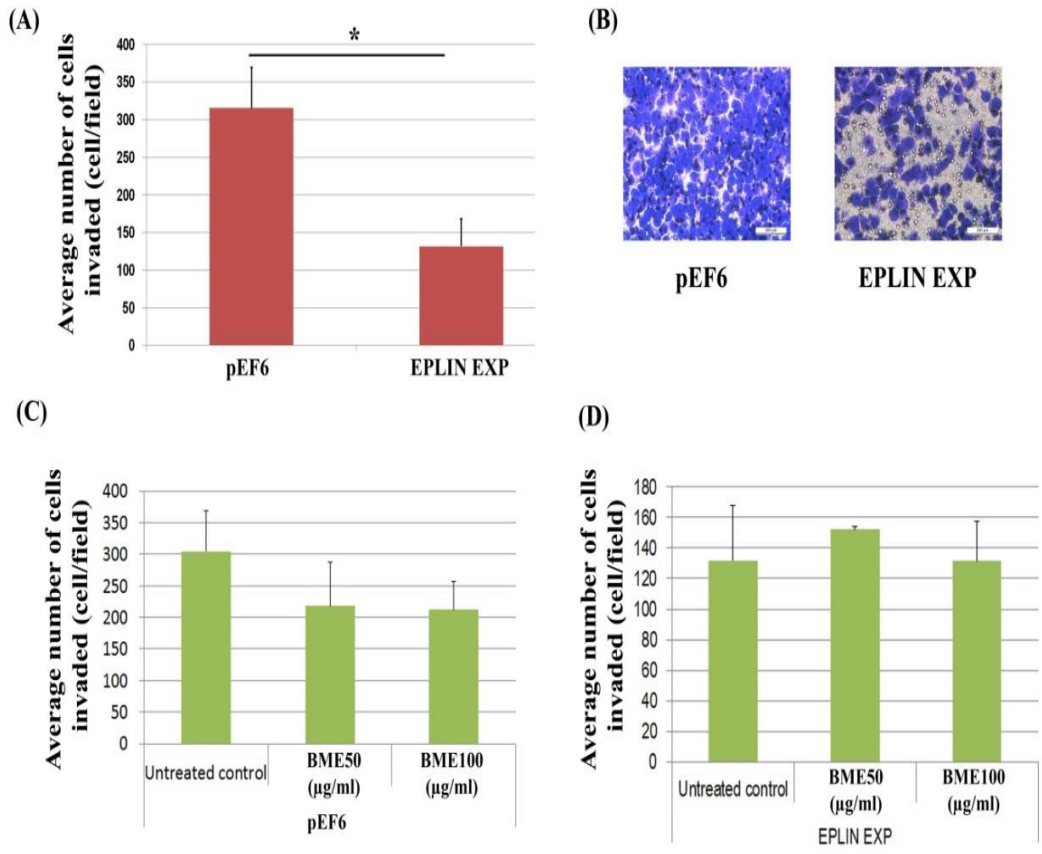

Figure 4.2 Cellular invasion assay in PC-3 cells.

(A) Average cell invasion of PC-3^{pEF6} and PC-3$^{EPLIN\ EXP}$ cells through Matrigel over a 3 day incubation period. (B) Representative microscope image of PC-3^{pEF6} (pEF6) and PC-3$^{EPLIN\ EXP}$ (EPLIN EXP) cell invasion images taken at X20 objective magnification. (C) Effect of BME addition at 50µg/ml and 100µg/ml concentrations on the invasiveness of PC-3^{pEF6} cells. (D) Effect of BME addition at 50µg/ml and 100µg/ml concentrations on the invasiveness of PC-3$^{EPLIN\ EXP}$ cells. BME was added to tumour cell functional assays to represent an *in vitro* bone-like environment. Mean of three independent repeats (n=3) are shown. Error bars represent SE of the Mean. * = $p<0.05$. Statistical analysis was performed using a two sample, two tailed t-test using SigmaPlot software.

4.3.3 Effect of EPLINα overexpression on tumour cell adhesion

The ability of PC-3^{pEF6} and PC-3^{EPLINEXP} cells to adhere to the matrix was evaluated using an *in vitro* Matrigel adhesion assay. Forced expression of EPLINα caused a significant increase in the cells ability to adhere to the cell matrix (P=0.034) (Figure 4.3A/B). The effect of BME at 50µg/ml and 100µg/ml concentrations was also determined in both PC-3^{pEF6} and PC-3^{EPLINEXP} cells to deduce the potential effect of EPLINα expression on adhesion in an *in vitro* bone-like environment (Figure 4.3C/D). BME had no apparent effect on PC-3 cell adhesion for PC-3^{pEF6} and PC-3$^{EPLIN\ EXP}$ cells at either concentration tested (50µg/ml and 100µg/ml).

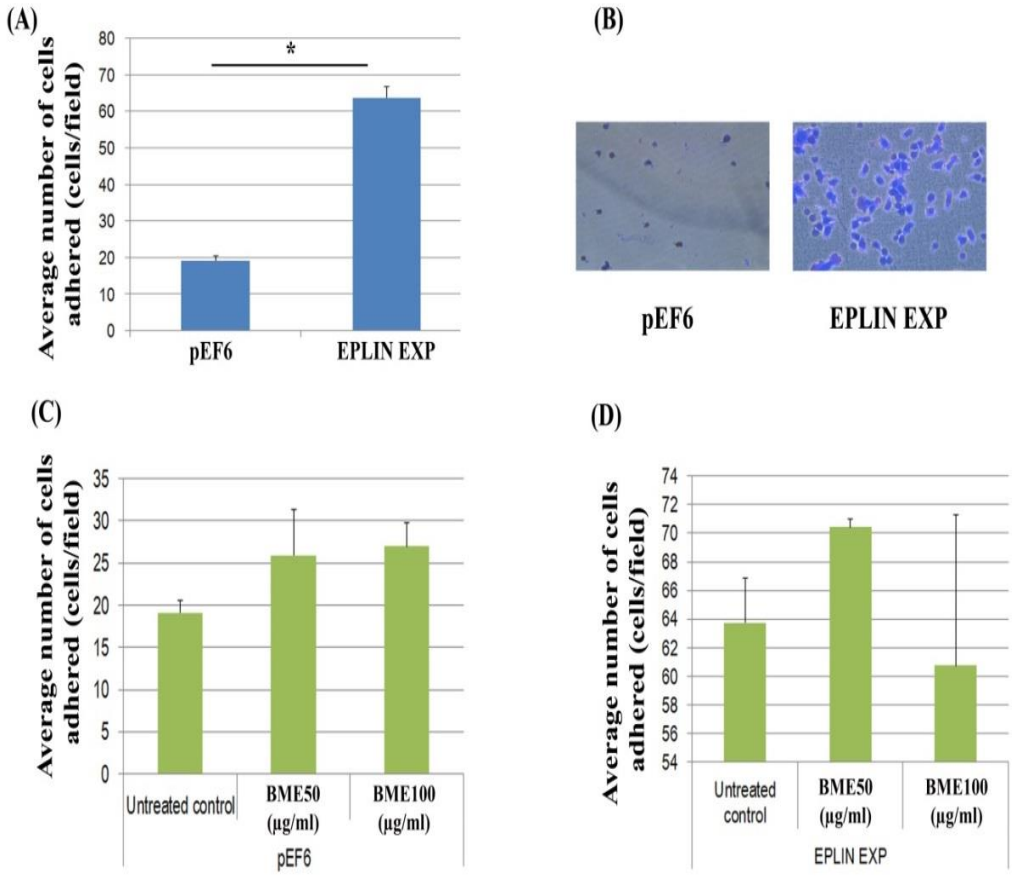

Figure 4.3 Cellular adhesion assay in PC-3 cells.

(A) Average cell adhesion of PC-3^{pEF6} and PC-3$^{EPLIN\ EXP}$ cells to Matrigel matrix. (B) Representative microscope image of PC-3^{pEF6} (pEF6) and PC-3$^{EPLIN\ EXP}$ (EPLIN EXP) cell adhesion, images taken at X20 objective magnification. (C) Effect of BME addition, at 50µg/ml and 100µg/ml concentration, on matrix adhesion of PC-3^{pEF6} cells. (D) Effect of BME addition, at 50µg/ml and 100µg/ml concentration, on matrix adhesion of PC-3$^{EPLIN\ EXP}$ cells. BME was added to tumour cell functional assays to represent an *in vitro* bone-like environment. Mean of three independent repeats (n=3) are shown. Error bars represent SE of the Mean. * = $p<0.05$. Statistical analysis was performed using a two sample, two tailed t-test using SigmaPlot software.

4.3.4 Effect of EPLINα overexpression on tumour cell migration using a scratch/wound healing assay

To determine the effect of EPLINα expression on cell migration, an *in vitro* scratch/wound healing assay was performed on PC-3^{pEF6} cells and PC-3^{EPLINEXP} cells (Figure 4.4). Cell migration was measured at 4 time points (1 hour, 2 hours, 3 hours and 4 hours) and compared to a control at Time 0 (0 hour). EPLINα overexpression resulted in a significant decrease in cell migration at the 2 hour time point (p=0.011), 3 hour time point (p=0.004) and the 4 hour time point (p=0.005), with highly significant reductions in cell migration being seen at the later time points (Figure 4.4A/B). The effect of BME, at 50µg/ml and 100µg/ml concentrations, was also determined in both PC-3^{pEF6} and PC-3^{EPLINEXP} cells to deduce the potential effect of EPLINα expression on cell migration in an *in vitro* bone environment (Figure 4.4C/D). In PC-3^{pEF6} cells, BME had no apparent effect on PC-3^{pEF6} cell migration at either concentration tested (50µg/ml and 100µg/ml). In PC-3^{EPLINEXP} cells, the lower, 50µg/ml, BME concentration enhanced the migration rate of PC-3^{EPLINEXP} cells throughout each time point; with a significant increase in cellular migration at the 2 hour time point (p=0.043), in comparison to the untreated PC-3$^{EPLIN\ EXP}$. The higher, 100µg/ml BME concentration had no significant effects on PC-3^{EPLINEXP} cells at any time point tested when compared to untreated PC-3$^{EPLIN\ EXP}$ cells (Figure 4.4D).

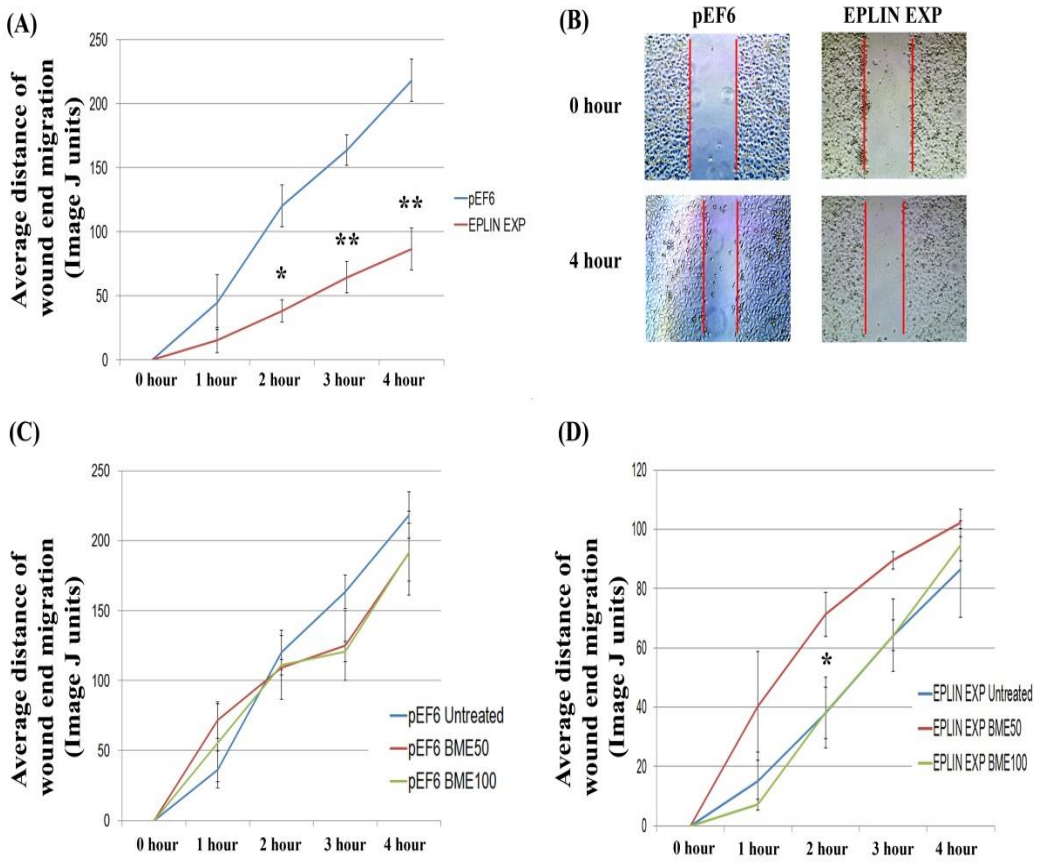

Figure 4.4 Cell migration assay in PC-3 cells.

(A) Average cell migration of PC-3^{pEF6} and PC-3$^{EPLIN\ EXP}$ cells over 4 hours. (B) Representative images of PC-3^{pEF6} (pEF6) and PC-3$^{EPLIN\ EXP}$ (EPLIN EXP) wounds at initial and end points, images taken at X10 objective magnification. (C) Effect of BME addition, at 50µg/ml (BME 50) and 100µg/ml (BME 100) concentration, on the migration rates of PC-3^{pEF6} cells. (D) Effect of BME addition, at 50µg/ml (BME 50) and 100µg/ml (BME 100) concentration, on the migration rates of PC-3$^{EPLIN\ EXP}$ cells. BME was added to tumour cell functional assays to represent an *in vitro* bone-like environment. Mean of three independent repeats (n=3) are shown. Error bars represent SE of the Mean. * = $p<0.05$, ** = $p<0.01$. Statistical test performed for analysis was a two sample, two tailed t-test using SigmaPlot software.

4.3.5 Effect of EPLINα overexpression on cell invasion using a co-culture human osteoblast model

To further determine the effect of EPLINα overexpression in the bone environment, cell invasion was established in the presence of human hFOB1.19 osteoblasts in an *in vitro* co-culture assay (Figure 4.5). Two 24 well plates were set up, one cultured with osteoblasts and the other without osteoblasts and Matrigel coated transwell inserts (containing 8µm pores) were placed over the top of the empty wells and those containing hFOB1.19 osteoblast cells in a similar fashion to that in the invasion assay. The presence of osteoblasts generally increased cellular invasion for both PC-3^{pEF6} and PC-$3^{EPLINEXP}$ cells. For the PC-3^{pEF6} cells, presence of osteoblasts significantly increased cellular invasion ($P<0.001$ vs. mono-cultured PC-3^{pEF6} cells). For PC-$3^{EPLINEXP}$ cells, presence of osteoblasts slightly increased invasion, however the change was not significant ($p=0.400$), suggesting EPLINα expression may protect against pro-invasive signals secreted by osteoblasts at the bone environment. EPLINα overexpression significantly reduced cellular invasion in absence of osteoblasts ($p=<0.001$) when compared to the equivalent PC-3^{pEF6} group. When osteoblasts were present, EPLINα overexpression reduced cellular invasion, however this didn't reach significance when compared to PC-3^{pEF6} cells (in presence of osteoblasts) ($p=0.100$) (Figure 4.5A/B). The effect of 50µg/ml BME was also determined in both PC-3^{pEF6} and PC-$3^{EPLINEXP}$ cells, for osteoblast positive and osteoblast negative culture conditions. In PC-3^{pEF6} cells, BME enhanced cell invasion for osteoblast positive and osteoblast negative culture conditions, with the highest amount of cell invasion seen in conditions where both osteoblasts and BME were present (Figure 4.5C). Although BME treatment increased cellular invasion when compared to PC-3^{pEF6} cells, this increase was not statistically significant

(p=0.094 for osteoblast negative condition, p=0.730 for osteoblast positive condition). In PC-3$^{EPLIN\ EXP}$ cells, a similar trend was seen, where BME increased cell invasion when compared to untreated controls, with highest invasion seen in the presence of osteoblasts (Figure 4.5D). Although BME treatment increased cellular invasion when compared to PC-3^{EPLINEXP} cells, this increase was not statistically significant (p=0.204 for osteoblast negative condition, p=0.229 for osteoblast positive condition).

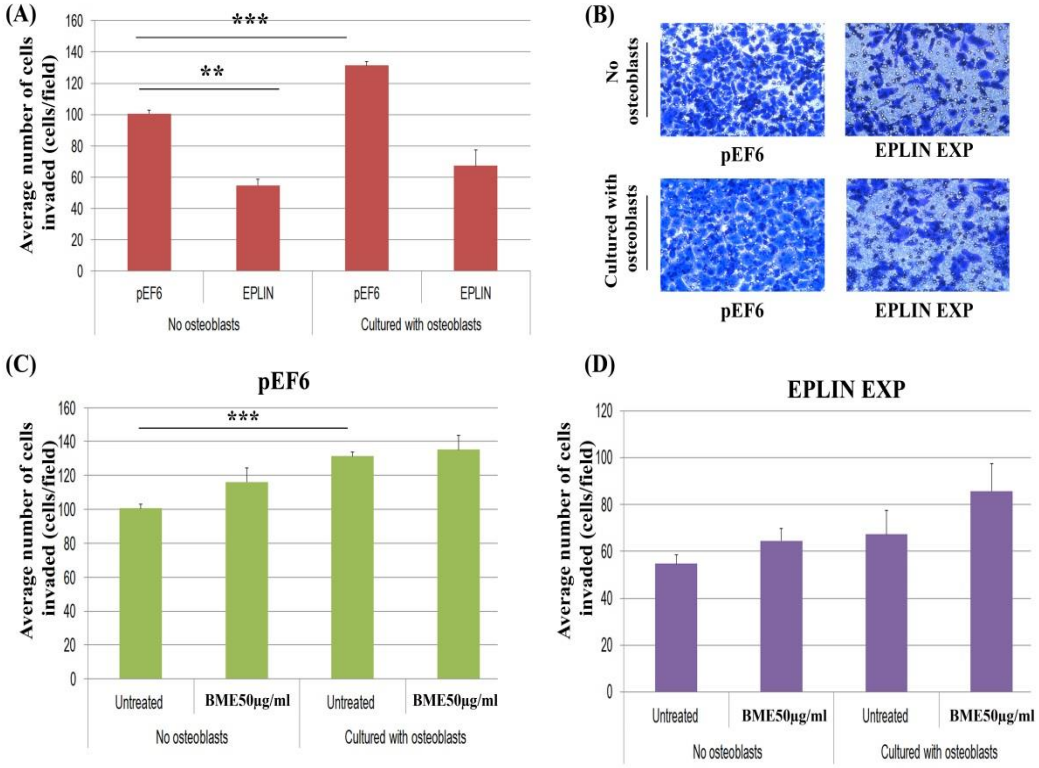

Figure 4.5 Co-culture invasion assay with human hFOB1.19 osteoblasts and PC-3 cells.

(A) Average cell invasion of PC-3^{pEF6} and PC-3$^{EPLIN\ EXP}$ cells with and without osteoblasts. (B) Representative images, taken at X20 objective magnification, of invaded PC-3^{pEF6} (pEF6) and PC-3$^{EPLIN\ EXP}$ (EPLIN EXP) cells following culture in the presence or absence of hFOB1.19 osteoblasts. (C) Effect of 50µg/ml BME addition on the invasiveness of PC-3^{pEF6} cells cultured with and without osteoblasts. (D) Effect of 50µg/ml BME addition on the invasiveness of PC-3$^{EPLIN\ EXP}$ cells cultured with and without osteoblasts. BME was added to tumour cell functional assays to represent an *in vitro* bone-like environment +/- human osteoblasts. Mean of three independent repeats (n=3) are shown. Error bars represent SE of the Mean. ** = $p<0.01$, *** = $p<0.001$. Statistical test performed for semi-quantitative analysis was a two sample, two tailed t-test using SigmaPlot software.

4.4 Discussion

This study has demonstrated the functional impact of EPLINα expression using an osteolytic cell line model, PC-3. The functional effect of EPLINα overexpression was established in PC-3 by employing various *in vitro* functional assays. EPLINα overexpression resulted in a less aggressive PC-3 phenotype in terms of cell proliferation, invasion and migration. Forcing EPLINα expression led to PC-3 cells displaying reduced invasiveness, proliferation rates and motility. EPLINα expression was also associated with enhanced matrix-adhesion of PC-3 cells to Matrigel. These functional effects agree with previous reports in prostate cancer (Sanders et al., 2011), breast cancer (Jiang et al., 2008), oesophageal cancer (Liu et al., 2012a) and ovarian cancer (Liu et al., 2016) that EPLINα expression is able to influence various cell functions and demonstrates a key role for EPLINα in regulating cancer progression as a tumour suppressive molecule. The enhanced adhesive ability of PC-3 cells overexpressing EPLINα also strengthens the putative link to FAK, as FAK is an established molecule for inducing focal adhesion via integrin signalling (Guan, 1997), and this is a relationship which will be explored in more detail in Chapter 6 of this thesis.

As EPLINα appears to have an anti-proliferative effect in PC-3 cells by the three day time point, which concurs with previous reports (Sanders et al., 2011), it's important to note that any other cellular effect visualised with a similar time point (for example the tumour invasion assay in Figure 4.2), could also be attributed, in part, to this anti-proliferative effect.

In addition to untreated PC-3^{pEF6} and PC-3$^{EPLIN\ EXP}$cells, *in vitro* tumour functional assays were carried out in presence of BME, to establish any effects EPLINα may have on cell function in a bone-like environment. BME contains proteins extracted from human femoral bones and thus provides a molecular environment for cancer cells when used in functional tests. BME appeared to have no significant effect on cell proliferation, adhesion, invasion or migration in PC-3^{pEF6} and PC-3$^{EPLIN\ EXP}$ cells. Notably, BME caused a slight increase in cell proliferation of PC-3^{pEF6} control cells but not PC-3$^{EPLIN\ EXP}$ cells and a reduction of cell invasion of PC-3^{pEF6} control cells but not PC-3$^{EPLIN\ EXP}$ cells. Further, an increase in matrix-adhesion of both PC-3^{pEF6} and PC-3$^{EPLIN\ EXP}$ cells was seen in response to BME addition. Interestingly, BME appeared to increase cell migration of PC-3$^{EPLIN\ EXP}$ cells in earlier stages of the experiment compared to untreated PC-3$^{EPLIN\ EXP}$ cells, with a significant increase at the 2 hour time point, yet PC-3^{pEF6} cells were unresponsive to BME. Lastly, in order to further elucidate if the potential tumour suppressive effect of EPLINα has any potential in the bone environment and in the development of bone metastasis, an *in vitro* co-culture model was established using PC-3 cells and human hFOB1.19 osteoblasts with and without BME. PC-3 cells with forced EPLINα expression were capable of significantly reducing cell invasion outside the bone-like environment. Whereas untreated PC-3^{pEF6} cells were highly invasive, and at their most aggressive within a bone-like environment, PC-3$^{EPLIN\ EXP}$ cells displayed no significant difference when they moved from a non-bone-like environment to a bone-like environment. Currently, there are no published articles that have examined the impact of EPLIN in regards to the homing of prostate cancer cells to the bone or in the development of bone metastasis. This early study highlighted some subtle differences in how PC-3^{pEF6} and PC-3$^{EPLIN\ EXP}$ cells responded to BME, though these

were generally not significant. Furthermore, it has demonstrated that EPLINα overexpression may be capable of reducing the pro-invasive effect brought about by the presence of osteoblasts. Hence the current data suggests that EPLINα may have some role in regulating the responsiveness of PC-3 cells to factors present within the bone matrix or secreted by bone cells present in the environment and may thus play a role in cancer dissemination or establishment in such environments.

Collectively, this study addresses the functional importance of EPLINα in prostate cancer, specifically utilising an osteolytic cell line model and has identified early indications of EPLINα biology in a bone-like environment. To compliment this data, further functional and mechanistic evidence is required from additional models of prostate cancer to provide and clarify EPLIN's role in cancer progression. The following chapter of this thesis will examine the impact of EPLINα overexpression in the LNCaP cell line, a model suggested forming mixed osteolytic/osteoblastic metastasis.

Chapter V: Functional impact of EPLINα expression in a mixed osteoblastic/osteolytic LNCaP cell model of prostate cancer

5.1 Introduction

Previous reports have utilised the "classic" PC-3 cell line to demonstrate the functional anti-cancer effects of EPLIN (Sanders et al., 2011, Maul and Chang, 1999). Whilst a previous study has explored the functional impact of EPLIN in LNCaP using an *in vitro* invasion assay (Zhang et al., 2011), a comprehensive study elucidating EPLINα's potential exploiting the LNCaP model is yet to be undertaken. The LNCaP model is an androgen-dependant model of prostate cancer utilising metastatic prostate cancer cells derived from the left supraclavicular lymph node of human prostatic adenocarcinoma (Horoszewicz et al., 1983). Prostate cancer cells nearly always form osteoblastic lesions when metastasised to bone, unlike breast, kidney and lung cancer cells which tend to form osteolytic lesions (Logothetis and Lin, 2005). PC-3 cells tend to form osteolytic lesions, whereas LNCaP cells form a mixture of osteoblastic and osteolytic lesions. LNCaP cells are therefore useful for evaluating prostate cancer in the laboratory due to the close association of the clinical disease. Importantly, a key aim of this thesis was to evaluate any potential links EPLINα may have on the establishment of bone metastases, therefore making the LNCaP cell line useful for functional analysis. In this chapter, LNCaP cells that were previously transfected with the EPLINα overexpression plasmid (see Chapter 3) were used in various *in vitro* functional techniques to assess the effect of forced EPLINα expression on cancer cell characteristics in a mixed osteolytic/osteoblastic cell model. These functional assays were carried out in presence of BME to provide a bone-like environment for the cancer cells. The aims of this chapter is to deduce if forced EPLINα expression can influence LNCaP cells and potentially mitigate the

characteristics associated with metastatic cancer cells within this mixed osteoblastic/osteolytic prostate cancer cell model.

5.2 Material and methods

5.2.1 Materials

All primers used were manufactured and provided by Sigma-Aldrich (Dorset, UK). Antibodies and primer sequences used for this study are listed in section 2.1.2 and 2.1.3. BME was prepared and used as described in Section 2.6.1.

5.2.2 Cell lines

The human prostate cancer cell line LNCaP and the human hFOB1.19 osteoblast cell line were used for this section of the study. LNCaP cells were cultured in RPMI-1640 media. For the co-culture invasion assay with human osteoblasts, hFOB1.19 cells were used with a specialist medium of DMEM without phenol red supplemented with 10% FCS, 1% antibiotics and 0.3mg/ml G418.

5.2.3 Polymerase Chain Reaction (PCR)

PCR was carried out on cDNA previously reverse transcribed from LNCaP RNA. EPLIN expression was determined in LNCaP^{pEF6} cDNA and LNCaP$^{EPLIN\ EXP}$ cDNA. For full procedure please refer to section 2.3.4.

5.2.4 SDS PAGE and Western Blotting

Western blotting was carried out on LNCaP protein extracted from cells previously transfected with the pEF6 vector or the EPLINα expression plasmid. EPLIN protein levels were determined and changes in expression were evaluated. For full procedure please refer to section 2.4.

5.2.5 *In vitro* tumour cell proliferation assay

Cells were seeded into quadruplicate 96 well plates for varying incubation times to evaluate cell proliferation as described in section 2.6.6. Absorbance was measured to determine cell number and proliferation rate. The proliferation rates of both control LNCaP^{pEF6} cells and LNCaP$^{EPLIN\ EXP}$ cells were determined in addition to any treatments used. For full procedure please refer to section 2.6.6.

5.2.6 *In vitro* tumour cell Matrigel adhesion assay

Cells were seeded into a 96 well plate which was pre-covered with layer of Matrigel (5µg). Following an incubation period, the number of cells that had adhered to the artificial basement membrane was fixed, stained and counted. The adhesion capacities of both control LNCaP^{pEF6} cells and LNCaP$^{EPLIN\ EXP}$ cells were determined in addition to any treatments used. For full procedure please refer to section 2.6.8.

5.2.7 *In vitro* tumour cell invasion assay

Cells were seeded into 24 well plates containing cell culture inserts, containing 8µm pores, with a Matrigel layer (50µg). Following a 3 day incubation period, the number of cells which had penetrated and invaded the artificial basement membrane was fixed, stained and visualised on the microscope. The invasive capacities of both control LNCaP^{pEF6} cells and LNCaP$^{EPLIN\ EXP}$ cells were determined in addition to any treatments used. For full procedure please refer to section 2.6.7.

5.2.8 *In vitro* tumour transwell migration assay

A transwell migration assay was performed using cell culture inserts, containing 8µm pores utilising a chemoattractant cell medium .Cell migration was visualised by counting and measuring the number of cells that migrated through the 8µm pores of the cell culture inserts after a 3 day incubation period on the microscope. The migration capacities of both control LNCaP^{pEF6} cells and LNCaP$^{EPLIN\ EXP}$ cells were determined in addition to any treatments used. For full procedure please refer to section 2.6.10.

5.2.9 *In vitro* co-culture invasion assay with human osteoblasts

Human osteoblast hFOB1.19 cells were seeded into 24 well plates one day prior to the beginning of the experiment to ensure sufficient confluence. Once seeded, an invasion assay was set up as in section 2.6.7. Cell invasion was determined in both control LNCaP^{pEF6} cells and LNCaP$^{EPLIN\ EXP}$ cells in an *in vitro* bone environment in presence of human osteoblasts. For full procedure please see section 2.6.11.

5.2.10 Statistical analysis

Statistical comparisons were made between different groups using a two sample, two tailed t-test or a Mann Whitney U test dependant on data normality. SigmaPlot 11 software was used to conduct statistical analysis and $p < 0.05$ regarded as statistically significant.

5.3 Results

5.3.1 Effect of EPLINα overexpression on LNCaP cell proliferation

The functional effect of EPLINα overexpression was determined in the LNCaP cell line using an *in vitro* tumour cell proliferation assay. Forced EPLINα expression in LNCaP cells displayed a similar trend to PC-3 cells with a reduction of cell proliferation in $LNCaP^{EPLIN\ EXP}$ compared to $LNCaP^{pEF6}$ cells, at both day 3 ($p=0.114$) and day 5 ($p=0.329$) time points, however this reduction didn't reach significance (Figure 5.1A). The approximate doubling time of $LNCaP^{pEF6}$ cells at Day 5 was 40 hours. The approximate doubling time of $LNCaP^{EPLIN\ EXP}$ cells at Day 5 was 62 hours. The effect of BME, at 50µg/ml and 100µg/ml concentrations, was also determined in both $LNCaP^{pEF6}$ and $LNCaP^{EPLIN\ EXP}$ cells to deduce the potential effect of EPLIN**α** expression on cell proliferation in an *in vitro* bone-like environment (Figure 5.1B/C). BME had no apparent effect on LNCaP cell proliferation for both $LNCaP^{pEF6}$ and $LNCaP^{EPLIN\ EXP}$ cells at either concentration tested (50µg/ml and 100µg/m l).

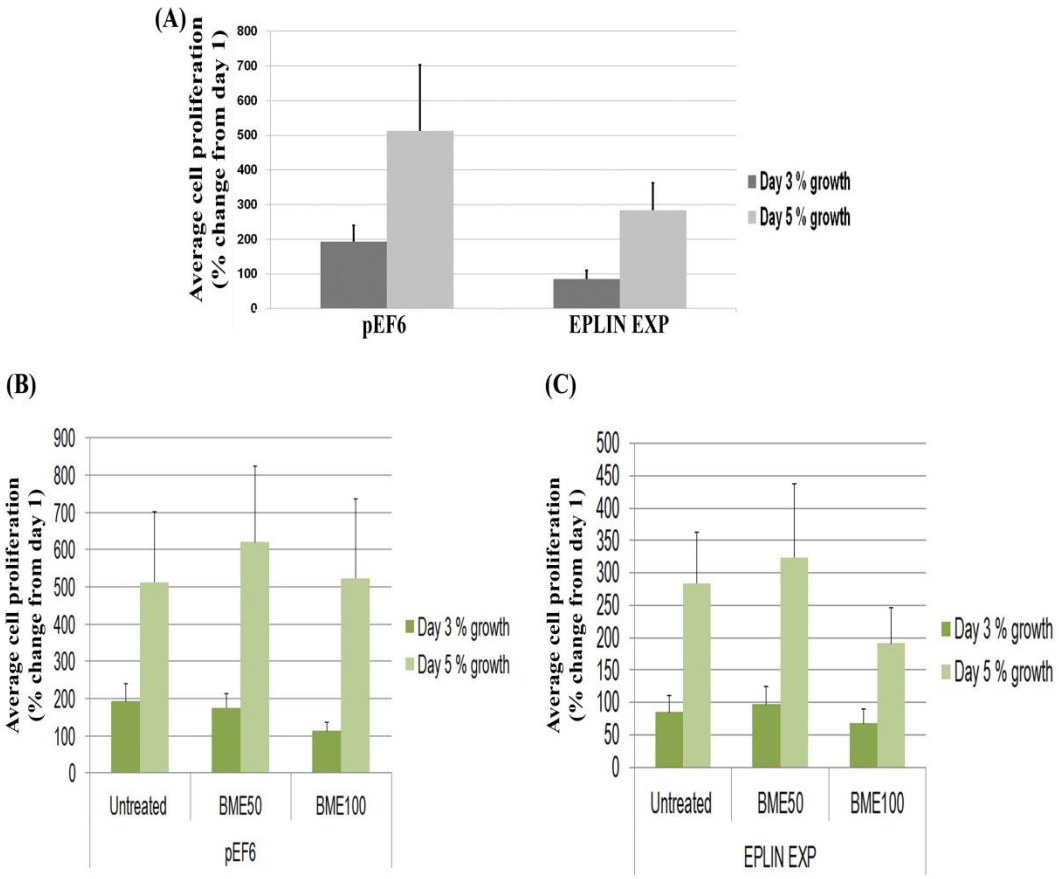

Figure 5.1 Cell proliferation assay in LNCaP cells.

(A) Average cell proliferation of LNCaP^{pEF6} and LNCaP$^{EPLIN\ EXP}$ cells at 3 day and 5 day time points (% change from Day 1). (B) Effect of BME addition, at 50µg/ml (BME 50) and 100µg/ml (BME 100) concentrations, to LNCaP^{pEF6} cells at 3 day and 5 day time points (% change from Day 1). (C) Effect of BME addition, at 50µg/ml (BME 50) and 100µg/ml (BME 100) concentrations, to LNCaP$^{EPLIN\ EXP}$ cells at 3 day and 5 day time points (% change from Day 1). BME was added to tumour cell functional assays to represent an *in vitro* bone-like environment. Mean of three independent repeats (n=3) are shown. Error bars represent SE of the Mean. Statistical test performed for analysis was a two sample, two tailed t-test using SigmaPlot software.

5.3.2 Effect of EPLINα overexpression on LNCaP cell invasion

The invasive capability of LNCaP^{pEF6} and LNCaP$^{EPLIN\ EXP}$ cells was evaluated using an *in vitro* Matrigel invasion assay (Figure 5.2). Forced EPLINα expression in LNCaP$^{EPLIN\ EXP}$ cells caused a reduction in cellular invasion, however this didn't reach significance (p=0.194) (Figure 5.2A/B). The effect of BME, at 50µg/ml and 100µg/ml concentrations, was also determined in both LNCaP^{pEF6} and LNCaP$^{EPLIN\ EXP}$ cells to deduce the potential effect of EPLINα expression on cell invasion in an *in vitro* bone-like environment. BME had no apparent effect on LNCaP cell invasion for LNCaP^{pEF6} and LNCaP$^{EPLIN\ EXP}$ cells at either concentration tested (50µg/ml and 100µg/ml).

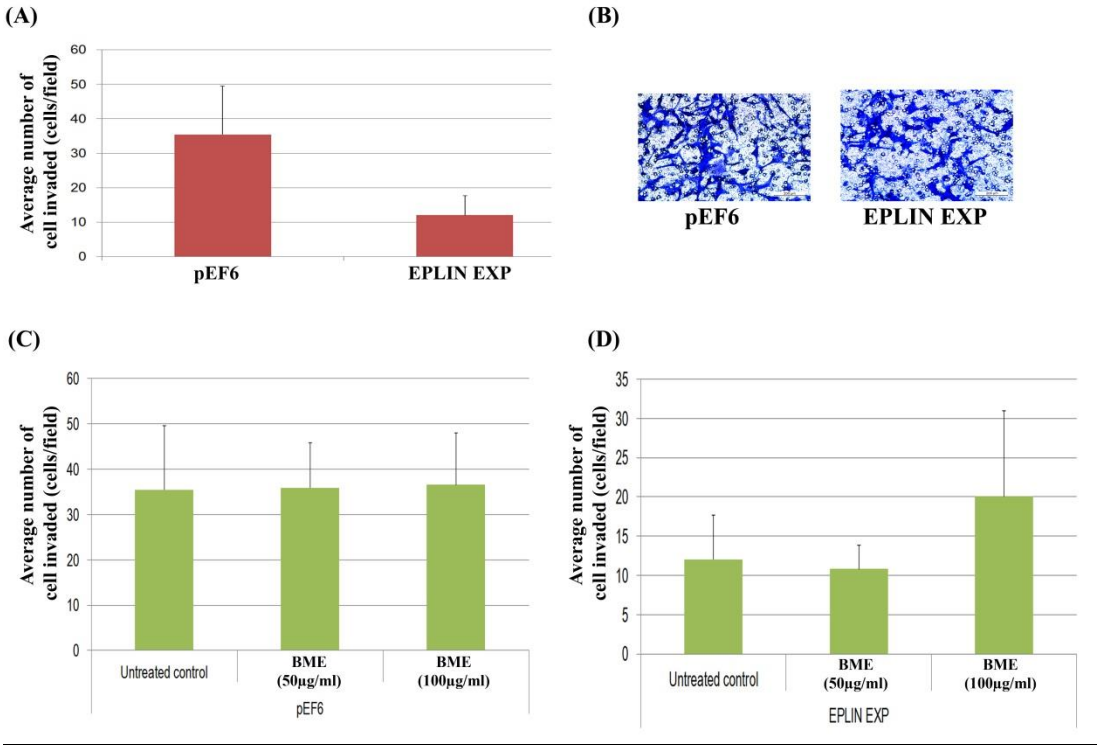

Figure 5.2 Cell invasion assay in LNCaP cells.

(A) Average cell invasion of LNCaP^{pEF6} and LNCaP$^{EPLIN\ EXP}$ cells following 3 day incubation. (B) Representative microscope image of LNCaP^{pEF6} (pEF6) and LNCaP$^{EPLIN\ EXP}$ (EPLIN EXP) cell invasion, images taken at X20 objective magnification. (C) Effect of BME addition, at 50µg/ml and 100µg/ml concentrations, on the invasiveness of LNCaP^{pEF6} cells. (D) Effect of BME addition, at 50µg/ml and 100µg/ml concentrations, on the invasiveness of LNCaP$^{EPLIN\ EXP}$ cells. BME was added to tumour cell functional assays to represent an *in vitro* bone-like environment. Mean of three independent repeats (n=3) are shown. Error bars represent SE of the Mean. Statistical test performed for analysis was a two sample, two tailed t-test using SigmaPlot software.

5.3.3 Effect of EPLINα overexpression on LNCaP cell adhesion

The ability of LNCaP^{pEF6} and LNCaP$^{EPLIN\ EXP}$ cells to adhere to the Matrigel matrix was evaluated using an *in vitro* Matrigel adhesion assay. Forced expression of EPLINα caused a significant increase in the cells ability to adhere to the cell matrix (P=0.006) (Figure 5.3A/B). The effect of BME, at 50µg/ml and 100µg/ml concentrations, was also determined in both LNCaP^{pEF6} and LNCaP$^{EPLIN\ EXP}$ cells to deduce the potential effect of EPLINα expression on matrix-adhesion in an *in vitro* bone-like environment (Figure 5.3C/D). In LNCaP^{pEF6} cells, BME had no apparent effect on LNCaP cell adhesion for LNCaP^{pEF6} and LNCaP$^{EPLIN\ EXP}$ cells at either concentration tested (50µg/ml and 100µg/ml). For LNCaP$^{EPLIN\ EXP}$ cells, no apparent change was seen at the lower concentration of BME tested (50µg), but a significant increase in cellular adhesion was seen for the higher concentration (100µg) tested.

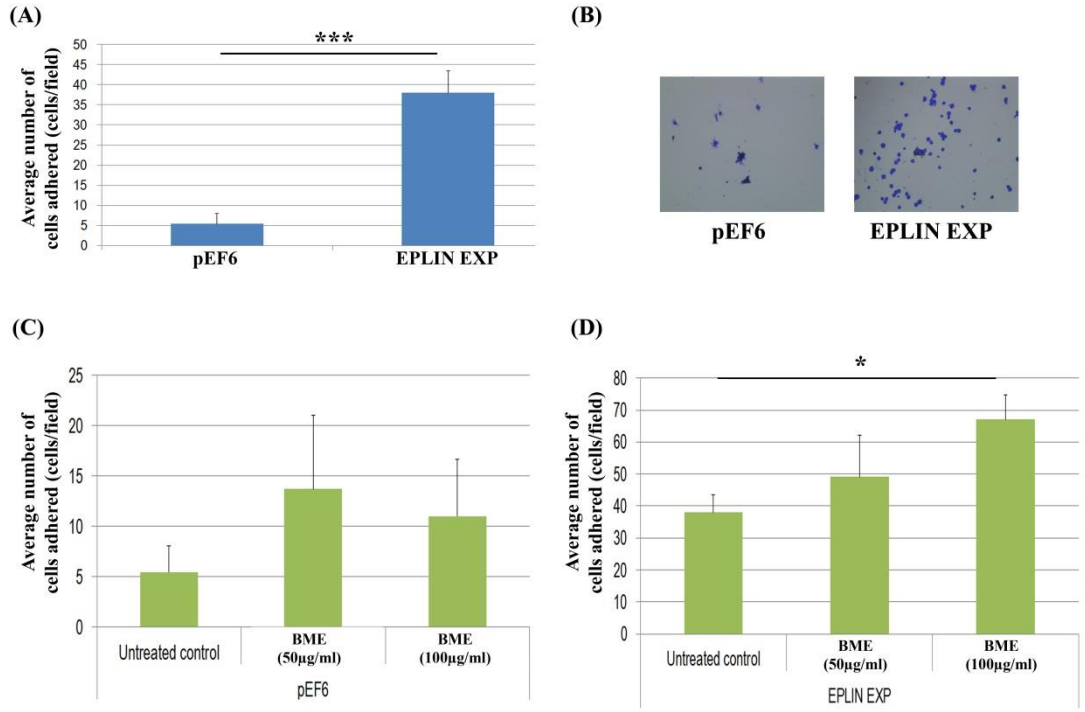

Figure 5.3 Cell adhesion assay in LNCaP cells.

(A) Average cell adhesion of LNCaP^{pEF6} and LNCaP$^{EPLIN\ EXP}$ cells. (B) Representative microscope image of LNCaP^{pEF6} (pEF6) and LNCaP$^{EPLIN\ EXP}$ (EPLIN EXP) cell adhesion, images taken at X20 objective magnification. (C) Effect of BME addition, at 50µg/ml and 100µg/ml concentrations, on the cell-matrix adhesion of LNCaP^{pEF6} cells. (D) Effect of BME addition, at 50µg/ml and 100µg/ml concentrations, on the cell-matrix adhesion of LNCaP$^{EPLIN\ EXP}$ cells. BME was added to tumour cell functional assays to represent an *in vitro* bone-like environment. Mean of three independent repeats (n=3) are shown. Error bars represent SE of the Mean. * = $p<0.05$, *** = $p<0.001$. Statistical test performed for analysis was a two sample, two tailed t-test using SigmaPlot software.

5.3.4 Effect of EPLINα overexpression on LNCaP cell transwell migration

To assess the effect EPLINα exerts on tumour cell migration in the LNCaP cell line, an *in vitro* transwell migration assay was undertaken (Figure 5.4). Forced EPLINα expression reduced the ability of LNCaP cells to migrate through the pores of the transwell inserts and reduced cell migration when compared to $LNCaP^{pEF6}$ cells, however this didn't reach significance (p=0.381) (Figure 5.4A/B). To establish if the presence of a bone-like environment effected cell migration and/or EPLINα's effect on cell migration, the assay was carried out in presence of BME at a concentration of 50µg/ml (Figure 5.4C). BME had no apparent effect on LNCaP cell migration for $LNCaP^{pEF6}$ and $LNCaP^{EPLIN\ EXP}$ cells at concentration 50µg BME.

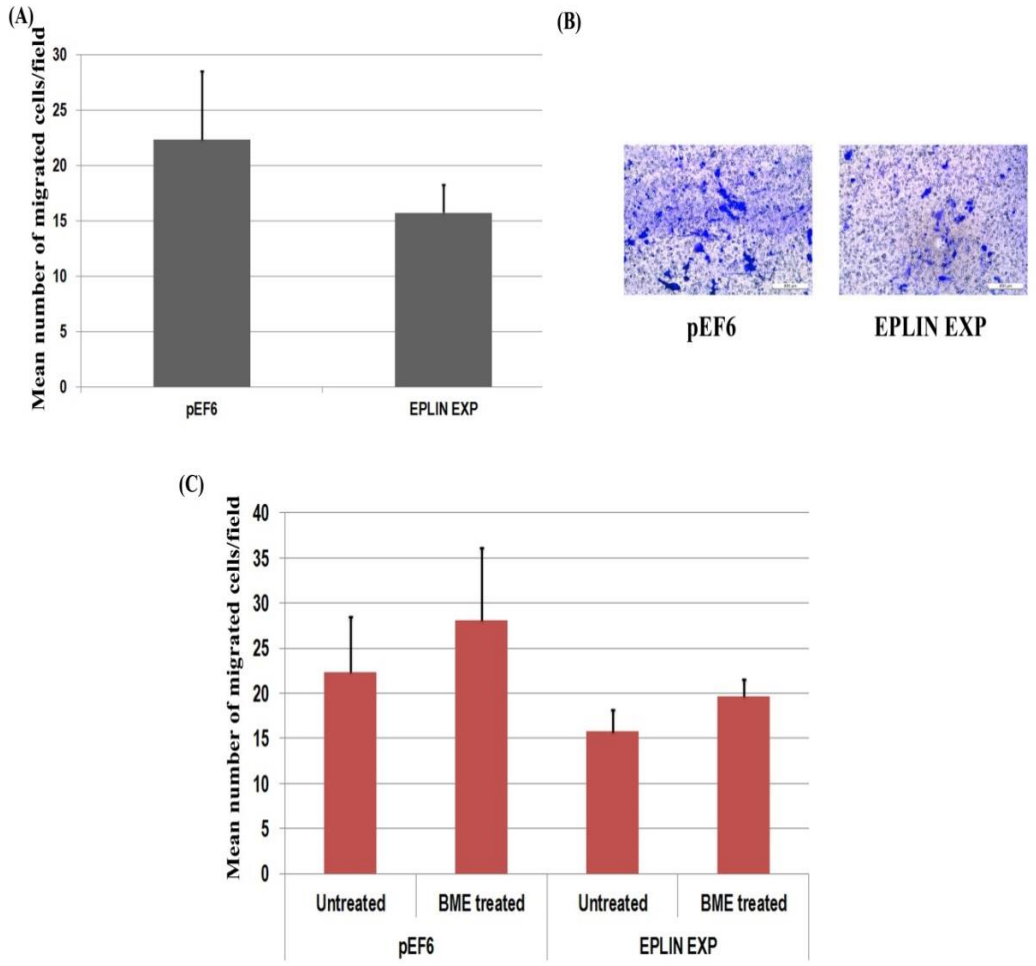

Figure 5.4 Transwell cell migration assay in LNCaP cells.

(A) Average cell migration of LNCaP^{pEF6} and LNCaP$^{EPLIN\ EXP}$ cells. (B) Representative images of LNCaP^{pEF6} (pEF6) and LNCaP$^{EPLIN\ EXP}$ (EPLIN EXP) cells, images taken at X20 objective magnification. (C) Effect of BME (50µg/ml) addition on LNCaP^{pEF6} and LNCaP$^{EPLIN\ EXP}$ cell migration. BME was added to tumour cell functional assays to represent an *in vitro* bone-like environment. Mean of three independent repeats (n=3) are shown. Error bars represent SE of the Mean.

5.3.5 Effect of EPLINα overexpression on cell invasion using a co-culture human osteoblast model

To determine the effect of EPLINα overexpression in the bone environment, cell invasion was established in the presence of human hFOB1.19 osteoblasts in an *in vitro* co-culture assay (Figure 5.5). Duplicate 24 well plates were set up, one cultured with osteoblasts and the other without osteoblasts. For LNCaP cells, the presence of an osteoblast environment appeared to have little effect on overall invasive capacity and this was seen for both LNCaP^{pEF6} and LNCaP$^{EPLIN\ EXP}$ cells. For both experiments (with and without osteoblasts) EPLINα overexpression caused a reduction in cellular invasion, but this change didn't reach significance (p=0.054 without osteoblast co-culture, p=0.400 with osteoblast co-culture) (Figure 5.5A/B). The effect of 50µg/ml BME was also determined in both LNCaP^{pEF6} and LNCaP$^{EPLIN\ EXP}$ cells, both in the presence and absence of osteoblast cells (Figure 5.5 C/D). BME had no apparent effect on LNCaP cell invasion for LNCaP^{pEF6} and LNCaP$^{EPLIN\ EXP}$ cells at concentration 50µg BME +/- osteoblasts.

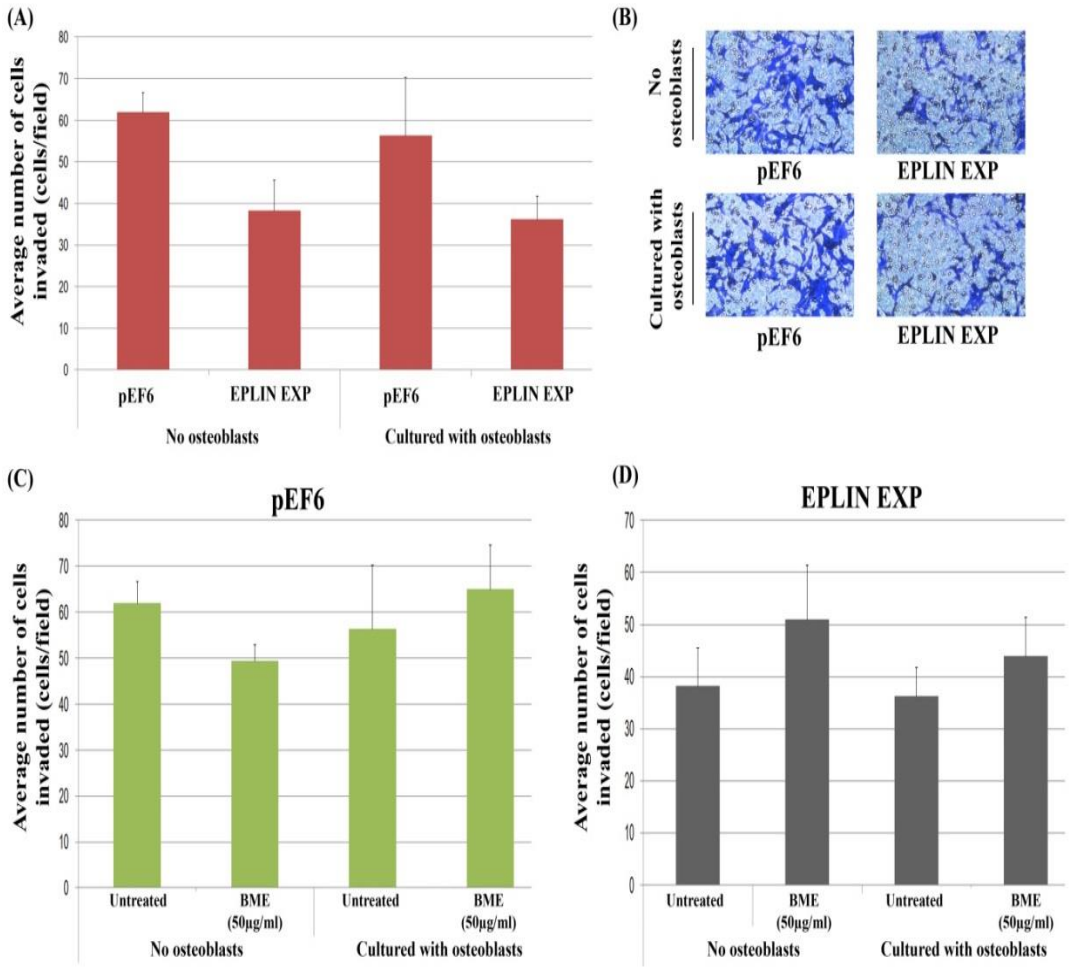

Figure 5.5 Cell co-culture assay with human hFOB1.19 osteoblasts in LNCaP cells.

(A) Average cell invasion of LNCaP^{pEF6} (pEF6) and LNCaP$^{EPLIN\ EXP}$ (EPLIN EXP) cells with and without osteoblasts. (B) Representative images of LNCaP^{pEF6} and LNCaP$^{EPLIN\ EXP}$ cells with and without osteoblasts, images taken at X20 objective magnification. (C) Effect of 50µg/ml BME addition on cellular invasion of LNCaP^{pEF6} cells with and without osteoblasts. (D) Effect of 50µg/ml BME addition on cellular invasion of LNCaP$^{EPLIN\ EXP}$ cells with and without osteoblasts. BME was added to tumour cell functional assays to represent an *in vitro* bone-like environment +/- human osteoblasts. Mean of three independent repeats (n=3) are shown. Error bars represent SE of the Mean.

5.4 Discussion

The aim of this chapter was to utilise the LNCaP prostate cancer cell model to evaluate the functional effects of EPLINα expression in prostate cancer. EPLINα expression appeared to influence several key traits of LNCaP cells, including cell proliferation, adhesion, invasion and migration. Similar to the PC-3 model, EPLINα expression reduced cell proliferation, invasion and migration, although this change was not as profound as in PC-3 and significance was not reached. EPLINα expression significantly enhanced LNCaP cells ability to adhere to Matrigel membrane using the cell adhesion assay. Taken together, these data support previous findings on the notion that EPLINα can function as a tumour suppressive molecule in cancer through impeding metastatic traits (Sanders et al., 2011, Jiang et al., 2008, Liu et al., 2012a, Maul and Chang, 1999). Specifically, in a previous LNCaP experiment (Zhang et al., 2011), the *in vitro* invasion assay utilised EPLIN depletion using siRNA knock-down, rather than EPLINα overexpression, and caused enhanced cellular invasion, whereas this study shows the opposite effect with increased expression. This suggests EPLIN expression may be able to act as a regulatory molecule to control prostate cancer cell invasion in the LNCaP cell line.

To establish the effects of EPLINα overexpression within the LNCaP cell model in a bone-like environment, BME was used in these functional assays and its effects on LNCaP cells compared to untreated cells. BME appeared to have no significant effect on LNCaP cell function for proliferation, migration and invasion. However, the treatment of BME affected LNCaP$^{EPLIN\ EXP}$ cells' ability to adhere to Matrigel membrane, with a significant increase in cell adhesion when BME was introduced at

the higher 100µg/ml BME concentration, suggesting increased EPLINα may enhance LNCaP cells matrix-adhesion when in the vicinity of bone ECM.

Lastly, to further assess the potential impact of EPLINα overexpression in the LNCaP cell model in an *in vitro* bone-like environment, a co-culture invasion assay was performed using LNCaP^{pEF6} and LNCaP$^{EPLIN\ EXP}$ cells in presence of human hFOB1.19 osteoblasts. EPLINα overexpression lead to a reduction of cellular invasion both without osteoblasts and when co-cultured with osteoblasts, however the reduction was not significant. BME also had no significant effect on cell invasion without osteoblasts or in presence of osteoblasts. Taken in combination with data generated in the PC-3 model, this may suggest that EPLINα expression is more influential as a general metastasis suppressor, and is less related to the bone environment, especially when utilising the LNCaP prostate cancer cell model.

This chapter aimed to establish the functional effects of EPLINα using the LNCaP prostate cancer cell model and addresses this using several *in vitro* tumour functional assays. This study supports the notion that EPLINα is a tumour suppressor in cancer, and can influence various metastatic characteristics of prostate cancer cells. Principally, this study provides a novel and comprehensive outlook evaluating EPLINα biology using the LNCaP cell model for the progression of prostate cancer. This chapter also suggests that the significance of EPLINα at the bone environment may be somewhat cell type specific as highlighted by the differential responses of PC-3 and LNCaP cells to EPLINα overexpression. The remainder of the thesis will focus on elucidation of potential mechanisms through which EPLINα exerts its tumour suppressive functions seen using these two cancer cell models.

Chapter VI:
Investigation into the potential mechanistic links of EPLINα with paxillin and FAK

6.1 Introduction

In the last decade, it has become established that EPLIN is a molecule involved in regulating cell junctional integrity of adherens junctions, specifically through providing a molecular link from the cadherin-catenin complex to filamentous actin (Chervin-Petinot et al., 2012, Abe and Takeichi, 2008). This has built on further work that EPLIN is an actin-binding protein, and functions to regulate actin cell dynamics by cross linking, bundling and stabilising actin filaments (Maul et al., 2003). This suggests EPLIN is likely involved in various key processes of cancer cells, namely cellular adhesion and migration. Although information is available on EPLIN's association to the molecular architecture of cell-cell adherens junctions, significantly less is known on the importance of EPLIN in cell-matrix adhesion and interaction. More recent reports have provided insights to this, where EPLIN associated with the focal adhesion protein PINCH-1 at focal adhesion sites in keratinocytes (Karakose et al., 2015). Our research group have previously reported a link between EPLINα and paxillin (Sanders et al., 2011) and others have demonstrated the two molecules physically bind by means of co-precipitation (Tsurumi et al., 2014). Paxillin is a phosphotyrosine containing protein involved in focal adhesion and integrin signalling and has several implications in cancer (Salgia et al., 1999, Deakin et al., 2012). FAK operates alongside paxillin in its signalling pathway and forms a physical complex with paxillin in addition to having diverse functions in cancer progression (Hu et al., 2014). Both paxillin and FAK are established molecules in the field of cancer biology and have important regulatory functions including influencing cellular adhesion and migration. This chapter aims to establish the potential associations of these signalling molecules to EPLINα, to

determine any mechanistic effects of EPLINα expression on cell function, such as the importance of EPLINα in regulating cell-matrix integrity, and determine if this association is mechanistically linked in prostate cancer progression. Paxillin and FAK transcript and protein levels were analysed in PC-3 and LNCaP cells lines which had demonstrated EPLINα overexpression to establish the effect of EPLINα expression on paxillin and FAK expression levels. The status of paxillin and FAK phosphorylation was also explored to evaluate the effect of EPLINα expression on key phosphorylated residues within these molecules. Several functional assays were also performed in presence of an FAK inhibitor to outline the effect of FAK inhibition in combination with EPLINα overexpression on cancer cell function.

6.2 Material and methods

6.2.1 Materials

All primers used were manufactured and provided by Sigma-Aldrich (Dorset, UK). Antibodies and primer sequences used for this study are listed in section 2.1.2 and 2.1.3. For this section, an inhibitor known to inhibit FAK at region Y397 (FAK inhibitor 14, Santa Cruz Biotechnology, U.S.A) was used at concentration 1μM and 5μM, following an initial inhibitor screen. For FAK inhibitor dilution and preparation please see section 2.6.2.

6.2.2 Polymerase Chain Reaction (PCR)

PCR was carried out on cDNA previously reverse transcribed from PC-3 and LNCaP RNA. EPLIN, FAK and paxillin transcript expression was determined in PC-3 /LNCaP^{pEF6} cDNA and PC-3/LNCaP$^{EPLIN\ EXP}$ cDNA. For full procedure please refer to section 2.3.4.

6.2.3 Western Blotting

Western blotting was performed on PC-3 and LNCaP protein extracted from cells previously transfected with the pEF6 expression vector or the EPLINα expression plasmid. EPLIN, FAK and paxillin protein levels were determined and changes in expression were evaluated. For full procedure please refer to section 2.4.

6.2.4 *In vitro* tumour cell proliferation assay

Cells were seeded into 96 well plates for varying incubation times to evaluate cell proliferation. Absorbance was measured to determine cell number and proliferation rate. The proliferation of control PC-3/LNCaP^{pEF6} cells and PC-3/LNCaP$^{EPLIN\ EXP}$

cells was determined at Day 3 and Day 5 time points in addition to the proliferation rates of PC-3/LNCaP^{pEF6} cells and PC-3/LNCaP$^{EPLIN\ EXP}$ cells treated with FAK inhibitor. For full procedure please see section 2.6.6.

6.2.5 *In vitro* tumour cell Matrigel adhesion assay

Cells were seeded into a 96 well plate which was pre-covered with layer of Matrigel Following an incubation period, the number of cells that had adhered to the artificial basement membrane was counted. The adhesion of both control PC-3/LNCaP^{pEF6} cells and PC-3/LNCaP$^{EPLIN\ EXP}$ cells was determined in addition to PC-3/LNCaP^{pEF6} cells and PC-3/LNCaP$^{EPLIN\ EXP}$ cells treated with FAK inhibitor. For full procedure please see section 2.6.8.

6.2.6 *In vitro* tumour cell invasion assay

Cells were seeded into 24 well plates containing cell culture inserts with a Matrigel layer. Following a 3 day incubation period, the number of cells which had penetrated and invaded the artificial basement membrane was stained and visualised on the microscope. The invasive capacity of both control PC-3/LNCaP^{pEF6} cells and PC-3/LNCaP$^{EPLIN\ EXP}$ cells was determined in addition to PC-3/LNCaP^{pEF6} cells and PC-3/LNCaP$^{EPLIN\ EXP}$ cells treated with FAK inhibitor. For full procedure please see section 2.6.7.

6.2.7 *In vitro* scratch/wound healing migration assay

PC-3 cells were seeded into 24 well plates one day prior to day of experiment ensuring sufficient cells to reach a confluent monolayer. A wound healing assay was performed and photos were taken at each one hour interval over a four hour

experiment. Migratory potential of the cells was then determined for PC-3/LNCaP^{pEF6} cells and PC-3/LNCaP$^{EPLIN\ EXP}$ cells both with and without the addition of FAK inhibitor. For full procedure please see section 2.6.9

6.2.8 *In vitro* tumour transwell migration assay

LNCaP cells were seeded into cell culture inserts utilising a chemo attractant media . Following 3 day incubation, the number of cells which had migrated through the pores of the insert were stained and visualised on the microscope. The migratory capacity of both control PC-3/LNCaP^{pEF6} cells and PC-3/LNCaP$^{EPLIN\ EXP}$ cells was determined in addition to PC-3/LNCaP^{pEF6} cells and PC-3/LNCaP$^{EPLIN\ EXP}$ cells treated with FAK inhibitor. For full procedure please see section 2.6.10.

6.2.9 *In vitro* co-culture invasion assay with human osteoblasts

Human osteoblast cells were seeded into 24 well plates one day prior to the beginning of the experiment to ensure sufficient confluence. Once seeded, an invasion assay was set up as in section 2.6.7 Cell invasion was determined of both control PC-3/LNCaP^{pEF6} cells and PC-3/LNCaP$^{EPLIN\ EXP}$ in an *in vitro* bone environment in presence of human osteoblasts. The effect of FAK inhibition was also established. For full procedure please see section 2.6.11.

6.2.10 Statistical analysis

Statistical comparisons were made between different groups using a two sample, two tailed t-test or a Mann Whitney U test dependant on data normality using SigmaPlot 11 software. All experiments were carried out a minimum of three independent times and $p < 0.05$ regarded as statistically significant.

6.3 Results

6.3.1 Establishment of FAK/paxillin expression and phosphorylation states in the PC-3 cell model following EPLINα overexpression

6.3.1.1 FAK

To determine any potential link between EPLINα and the focal adhesion protein FAK, the level of FAK transcript and FAK protein was evaluated by PCR and Western Blotting in cell lines which have been verified to overexpress EPLINα. In PC-3 cDNA, FAK transcript was significantly upregulated when EPLINα was overexpressed, demonstrated by PCR (Figure 6.1A/B). For PC-3 protein, FAK total protein was also increased when EPLINα was overexpressed (Figure 6.1C/D). GAPDH was used as a housekeeping gene/protein for both PCR and Western Blotting reactions and to standardize levels of cDNA and protein within the samples. Semi-quantification analysis (Figure 6.1B/D) was carried out utilising Image J software and confirmed a significant increase in total FAK transcript ($p=0.01$). Semi-quantification analysis on FAK total protein also quantified an increase when EPLIN is overexpressed in PC-3, but this increase didn't reach significance ($p=0.400$) (Figure 6.1D).

6.3.1.2 Paxillin

To determine any potential link between EPLINα and paxillin, the level of paxillin transcript and protein was evaluated by PCR and Western Blotting in cell lines which have been verified to overexpress EPLINα. In PC-3 cDNA, EPLINα overexpression didn't affect the level of paxillin transcription and the level of paxillin transcript was comparable in PC-3^{pEF6} cDNA and in PC-$3^{EPLIN\ EXP}$ cDNA

(Figure 6.2A/B). At the protein level, paxillin was significantly upregulated when EPLINα was overexpressed (Figure 6.2C/D). GAPDH was used as a housekeeping gene/protein for both PCR and Western Blotting reactions and to standardize levels of cDNA and protein within the samples. Semi-quantification analysis (Figure 6.2B/D) was carried out utilising Image J software and confirmed increased paxillin protein expression following EPLINα overexpression ($p<0.001$ vs. PC-3^{pEF6}).

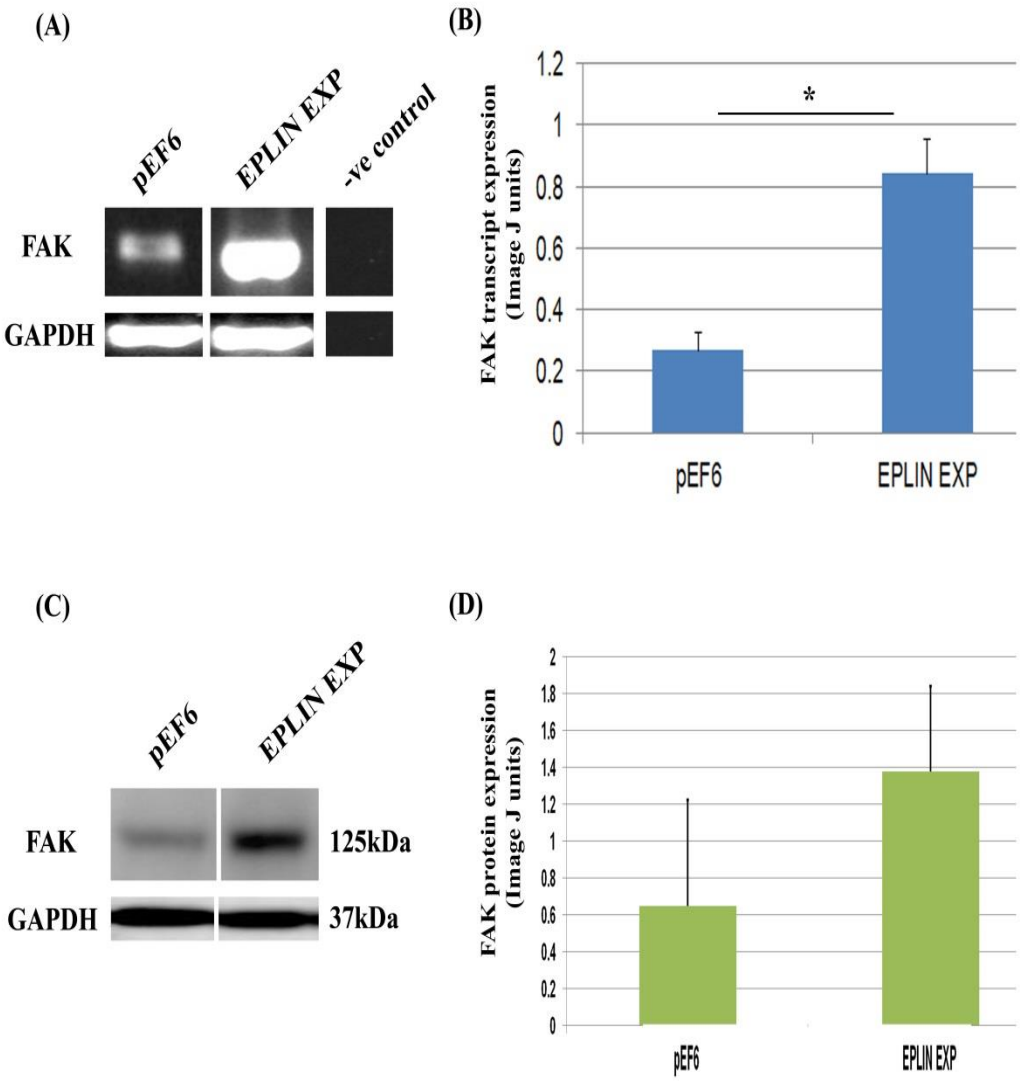

Figure 6.1 FAK expression in PC-3 cells overexpressing EPLIN*α*.

(A) FAK PCR reaction in PC-3^{pEF6} and PC-3$^{EPLIN\ EXP}$ cells cDNA. (B) Semi-quantitative analysis of FAK band intensity from PCR reaction. (C) FAK Western Blot reaction. (D) Semi-quantitative analysis of FAK band intensity from Western Blot reaction. Semi-quantitative analysis carried out using Image J software. Samples normalised to GAPDH for all experiments. Representative images are shown, semi-quantitative analysis represents mean of a minimum of three (n=3) independent band intensities, error bars represent Standard Error of the mean. * = $p < 0.05$. Statistical test performed for semi-quantitative analysis was a two sample, two tailed t-test using SigmaPlot software.

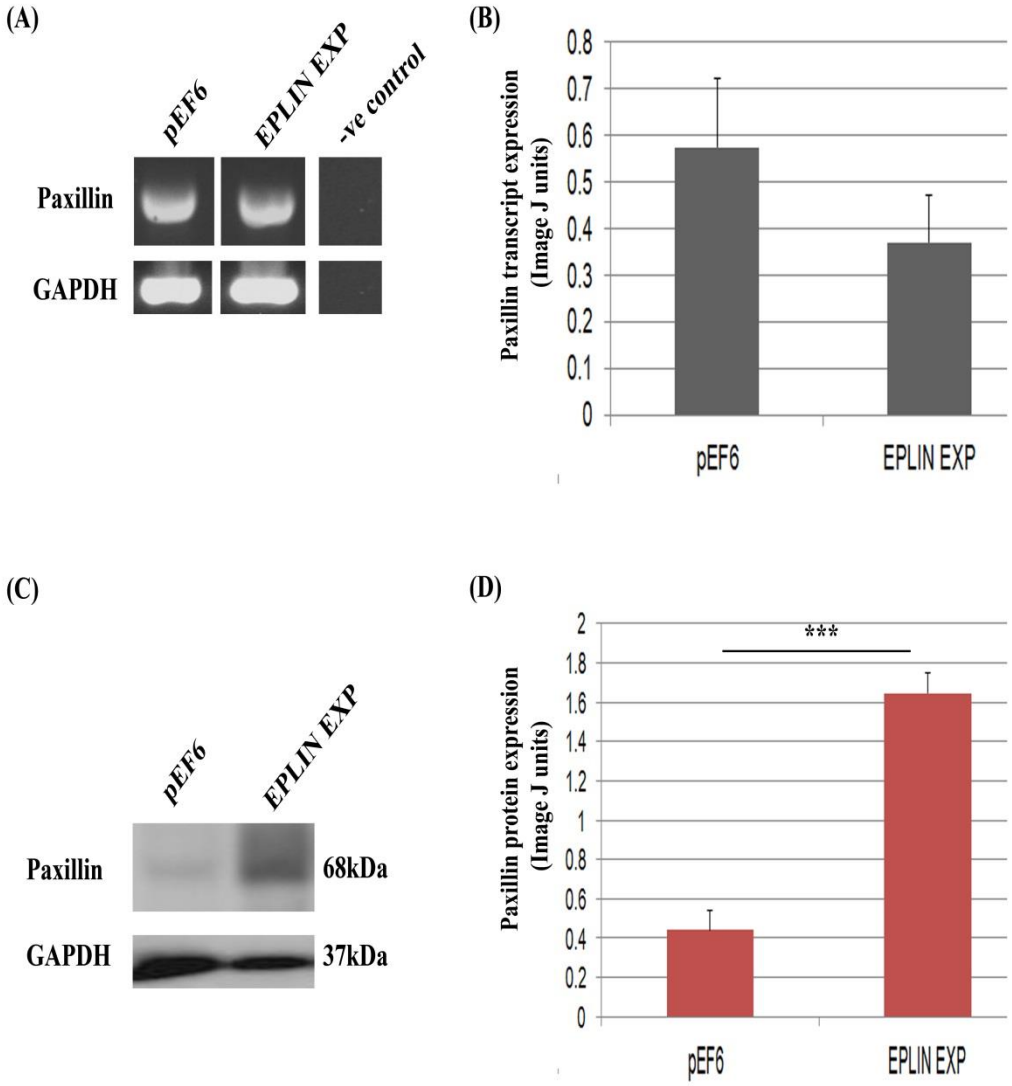

Figure 6.2 Paxillin expression in PC-3 cells overexpressing EPLINα.

(A) Paxillin PCR in PC-3^{pEF6} and PC-3$^{EPLIN\ EXP}$ cell cDNA. (B) Semi-quantitative analysis of paxillin band intensity from PCR reaction. (C) Paxillin Western Blot reaction. (D) Semi-quantitative analysis of paxillin band intensity from Western Blot reaction. Semi-quantitative analysis carried out using Image J software. Samples normalised to GAPDH for all experiments. Representative images are shown, semi-quantitative analysis represents mean of a minimum of three (n=3) independent band intensities, error bars represent SE of the mean. *** = P<0.001. Statistical test performed for semi-quantitative analysis was a two sample, two tailed t-test using SigmaPlot software.

6.3.1.3 pFAK status

FAK phosphorylation was determined at two FAK phosphorylation sites in PC-3 protein samples which had verified EPLINα overexpression to establish whether EPLINα expression exerted any effect on FAK phosphorylation and thus FAK function. Two FAK phosphorylation residues were screened in PC-3 protein samples using Western Blotting and these sites targeted Tyr397 and Tyr925. EPLINα overexpression resulted in an increase in phosphorylation of FAK at Tyr397 and in Tyr925 in PC-3 (Figure 6.3A/B). GAPDH was used as a housekeeping protein for Western Blotting reactions and to standardize levels of protein within the samples. Semi-quantification analysis was carried out utilising Image J software and this highlighted substantial enhances in phosphorylation of Tyr397 and Tyr925 following EPLINα overexpression, though only the enhancement of Tyr925 was found to be statistically significant in comparison to PC-3^{pEF6} controls ($p=0.01$).

6.3.1.4 pPaxillin status

The phosphorylation status of paxillin was determined in PC-3 protein which had verified EPLINα overexpression to establish whether EPLINα expression exerted any effect on paxillin phosphorylation and thus paxillin function. Two paxillin phosphorylation residues were screened in PC-3 protein using Western Blotting and these sites targeted Tyr31 and Tyr118. EPLINα overexpression resulted in an obvious increase in protein band intensities for these two phosphorylation sites in comparison to PC-3^{pEF6} control cells (Figure 6.3C/D). GAPDH was used as a housekeeping protein for Western Blotting reactions and to standardize levels of protein within the samples. Semi-quantification analysis was carried out utilising

Image J software and again highlighted a significant increase in Tyr31 and Tyr118 phosphorylated paxillin in PC-3$^{EPLIN\ EXP}$ compared to PC-3^{pEF6} samples ($p = 0.031$ and $p = 0.026$ respectively).

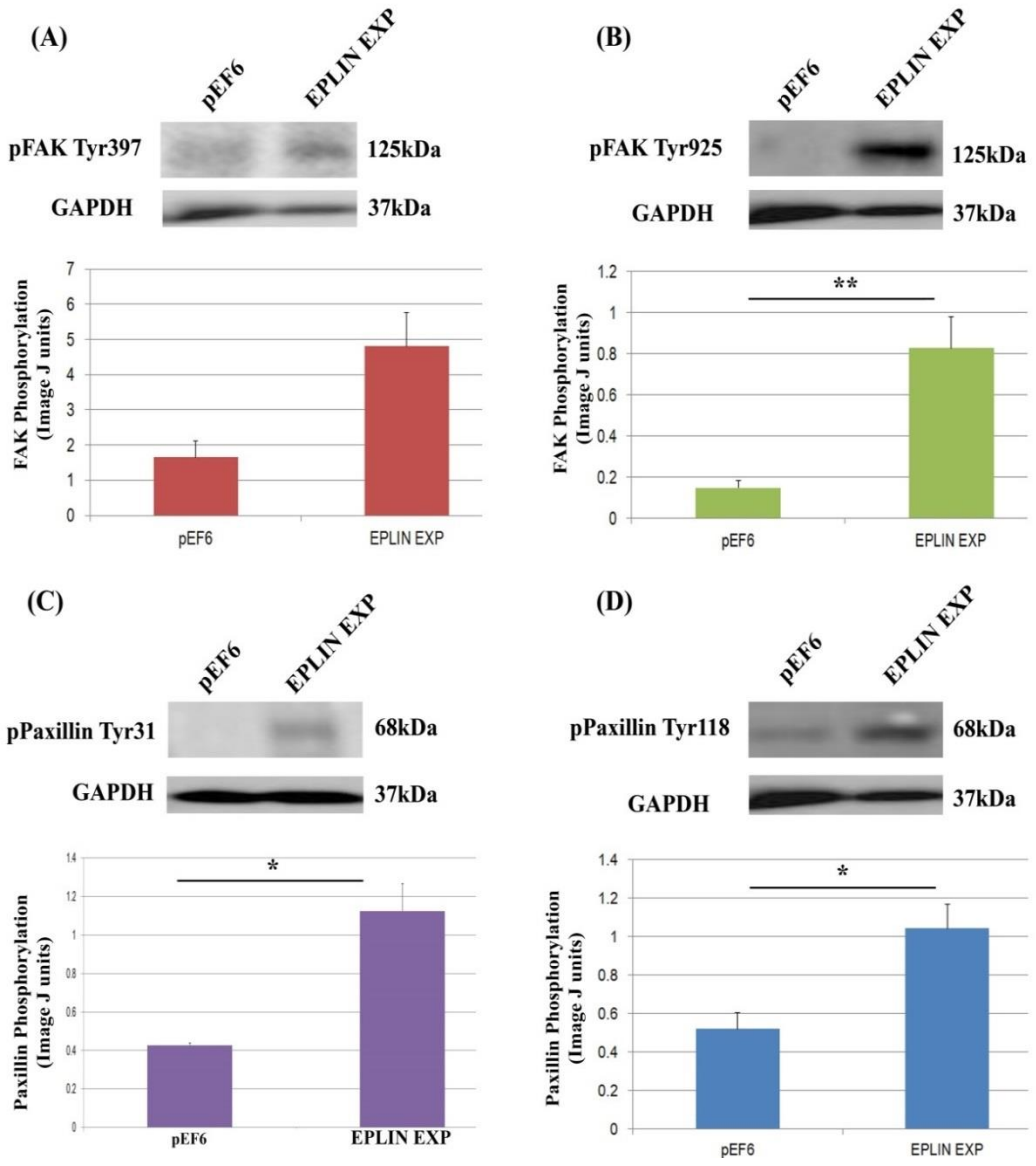

Figure 6.3 Phosphorylation status of FAK and paxillin in PC-3 cells overexpressing EPLINα.

(A) Level of FAK phosphorylation at Tyr397 in PC-3^{pEF6} (pEF6) and PC-3$^{EPLIN\ EXP}$ (EPLIN EXP) cells. (B) Level of FAK phosphorylation at Tyr925 in PC-3^{pEF6} (pEF6) and PC-3$^{EPLIN\ EXP}$ (EPLIN EXP) cells. (C) Level of paxillin phosphorylation at Tyr31 in PC-3^{pEF6} (pEF6) and PC-3$^{EPLIN\ EXP}$ (EPLIN EXP) cells. (D) Level of paxillin phosphorylation at Tyr118 in PC-3^{pEF6} (pEF6) and PC-3$^{EPLIN\ EXP}$ (EPLIN EXP) cells. Semi-quantitative analysis carried out using Image J software. Samples normalised to GAPDH for all experiments. Representative images are shown, semi-quantitative analysis represents mean of a minimum of three (n=3) independent band intensities, error bars represent SE of the mean.* = $p < 0.05$, ** = $p<0.01$. Statistical test performed for semi-quantitative analysis was a two sample, two tailed t-test using SigmaPlot software.

6.3.2 Establishment of FAK/paxillin expression and phosphorylation states in the LNCaP model following EPLINα overexpression

6.3.2.1 FAK

The level of FAK transcript and FAK protein was evaluated by PCR and Western Blotting in LNCaP cell lines which have been verified to overexpress EPLINα. In LNCaP cDNA and protein, FAK expression was increased, with notable increases in FAK band intensities at both the transcript and protein level observed in $LNCaP^{EPLIN\ EXP}$ compared to $LNCaP^{pEF6}$ samples, though this trend was found to be more apparent at the protein level (Figure 6.4A/C). GAPDH was used as a housekeeping gene/protein for both PCR and Western Blotting reactions and to standardize levels of cDNA and protein within the samples. Semi-quantification analysis (Figure 6.4 B/D) was carried out utilising Image J software and confirmed increased FAK expression in transcript and protein levels in $LNCaP^{EPLIN\ EXP}$ compared to $LNCaP^{pEF6}$ samples, though significance was not reached ($p=0.424$ for FAK transcript, $p=0.488$ for FAK protein).

6.3.2.2 Paxillin

The level of paxillin transcript and protein was evaluated by PCR and Western Blotting in LNCaP cell lines which have been verified to overexpress EPLINα. In LNCaP cDNA, EPLINα overexpression appeared to reduce paxillin transcript expression, with a loss of total paxillin transcript following forced EPLINα expression (Figure 6.5A/B). At the protein level, paxillin expression was increased slightly, in comparison to $LNCaP^{pEF6}$ controls, when EPLINα is overexpressed (Figure 6.5C/D) GAPDH was used as a housekeeping gene/protein for both PCR and

Western Blotting reactions and to standardize levels of cDNA and protein within the samples. Semi-quantification analysis (Figure 6.5B/D) was carried out utilising Image J software and demonstrated a significant reduction in total paxillin transcript expression in LNCaP$^{EPLIN\ EXP}$ samples compared to LNCaP^{pEF6} samples ($p=<0.001$), though no significant differences between the two LNCaP cell lines was seen at the protein level.

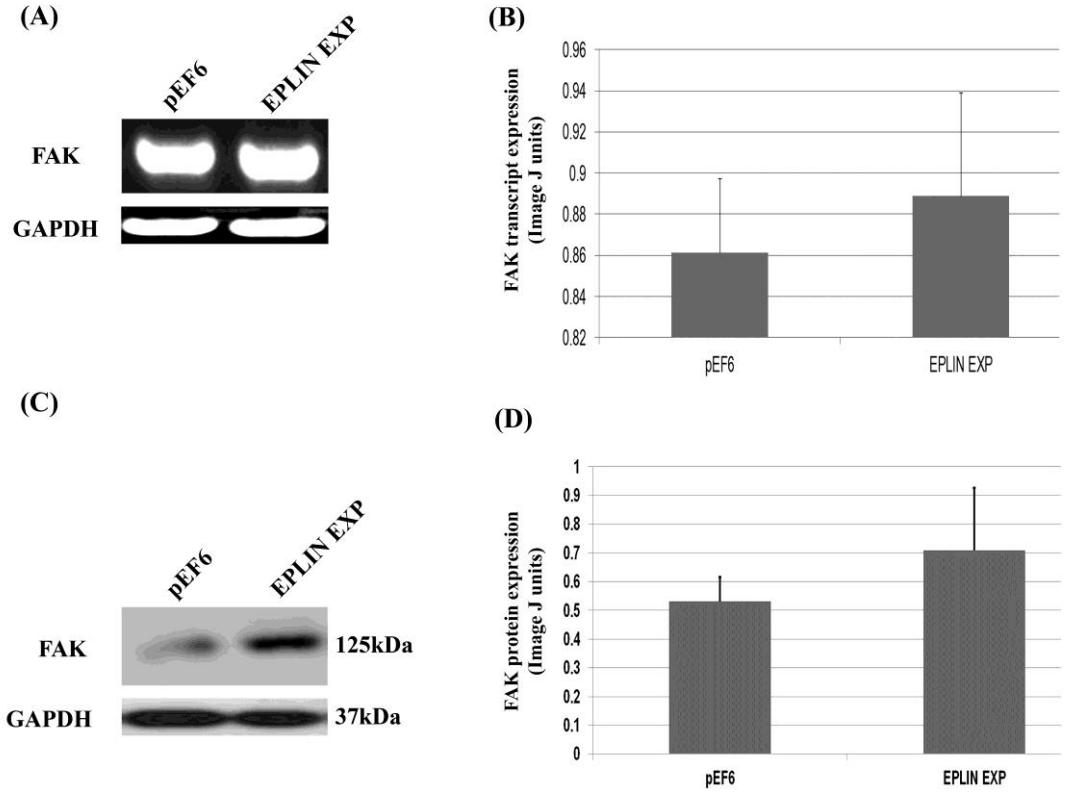

Figure 6.4 FAK expression in LNCaP cells overexpressing EPLINα.

(A) FAK PCR in LNCaP^{pEF6} and LNCaP$^{EPLIN\ EXP}$ cell cDNA. (B) Semi-quantitative analysis of FAK band intensity from PCR reaction. (C) FAK Western Blot reaction. (D) Semi-quantitative analysis of FAK band intensity from Western Blot reaction. Semi-quantitative analysis carried out using Image J software. Samples normalised to GAPDH for all experiments. Representative images are shown, semi-quantitative analysis represents mean of a minimum of three (n=3) independent band intensities, error bars represent SE of the mean.

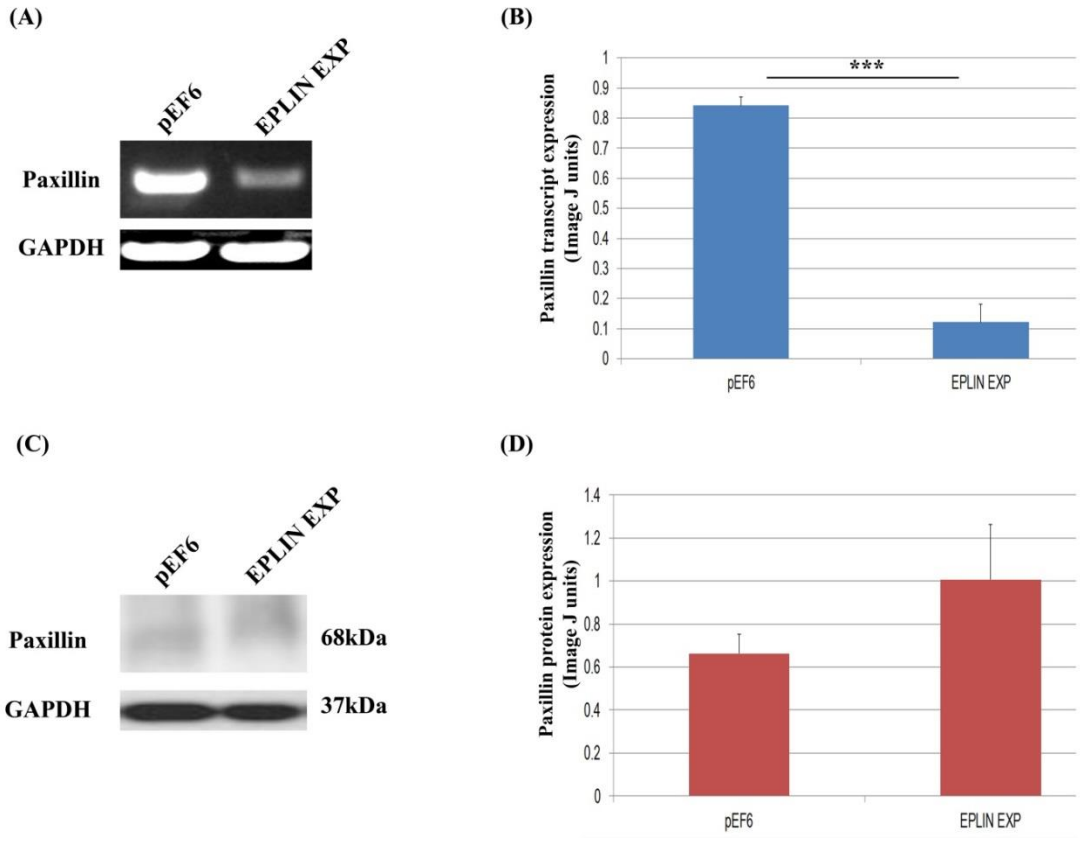

Figure 6.5 Paxillin expression in LNCaP cells overexpressing EPLIN*α*.

(A) Paxillin PCR in LNCaP^{pEF6} (pEF6) and LNCaP$^{EPLIN\ EXP}$ (EPLIN EXP) cell cDNA. (B) Semi-quantitative analysis of paxillin band intensity from PCR reaction. (C) Paxillin Western Blot reaction. (D) Semi-quantitative analysis of paxillin band intensity from Western Blot reaction. Semi-quantitative analysis carried out using Image J software. Samples normalised to GAPDH for all experiments. Representative images are shown, semi-quantitative analysis represents mean of a minimum of three (n=3) independent band intensities, error bars represent SE of the mean *** = $p<0.001$. Statistical test performed for semi-quantitative analysis was a two sample, two tailed t-test using SigmaPlot software.

6.3.2.3 pFAK status

FAK phosphorylation status was determined in LNCaP cells which demonstrated increased EPLINα expression at two phosphorylation sites; Tyr397 and Tyr925. Western Blot analyses revealed an obvious increase in the band intensity obtained for FAK Tyr397 in LNCaP$^{EPLIN\ EXP}$ cells compared to LNCaP^{pEF6} control cells and this increase was found to be statistically significant following semi-quantitative band analysis (Figure 6.6A; $p = 0.036$). FAK Tyr925 displayed only minimal expression in both LNCaP^{pEF6} or LNCaP$^{EPLIN\ EXP}$ cells and thus no significant change in this residue was seen following LNCaP EPLINα overexpression (Figure 6.6B; $p > 0.05$). GAPDH was used as a housekeeping protein for Western Blotting reactions and to standardize levels of protein within the samples. Semi-quantification analysis was carried out utilising Image J software.

6.3.2.4 pPaxillin status

Paxillin phosphorylation was also determined in LNCaP protein samples following EPLINα overexpression at two phosphorylation sites; Tyr31 and Tyr118. EPLINα overexpression had no significant impact on Tyr31 phosphorylation in LNCaP cells and was expressed at low levels in both LNCaP^{pEF6} and LNCaP$^{EPLIN\ EXP}$ cells (Figure 6.6C; $p > 0.05$). Conversely to the PC-3 cell line, EPLINα overexpression in LNCaP cells appeared to induce a reduction of paxillin phosphorylation at Tyr118 and, following semi-quantitative band analysis, significantly reduced levels of paxillin Tyr118 were seen in LNCaP$^{EPLIN\ EXP}$ cells compared to LNCaP^{pEF6}cells (Figure 6.6D; $p=0.023$). GAPDH was used as a housekeeping protein for Western Blotting

reactions and to standardize levels of protein within the samples. Semi-quantification analysis was carried out utilising Image J software.

A summary figure of all paxillin and FAK transcript and protein associations following EPLIN expression in PC-3 and LNCaP is provided in Figure 6.7.

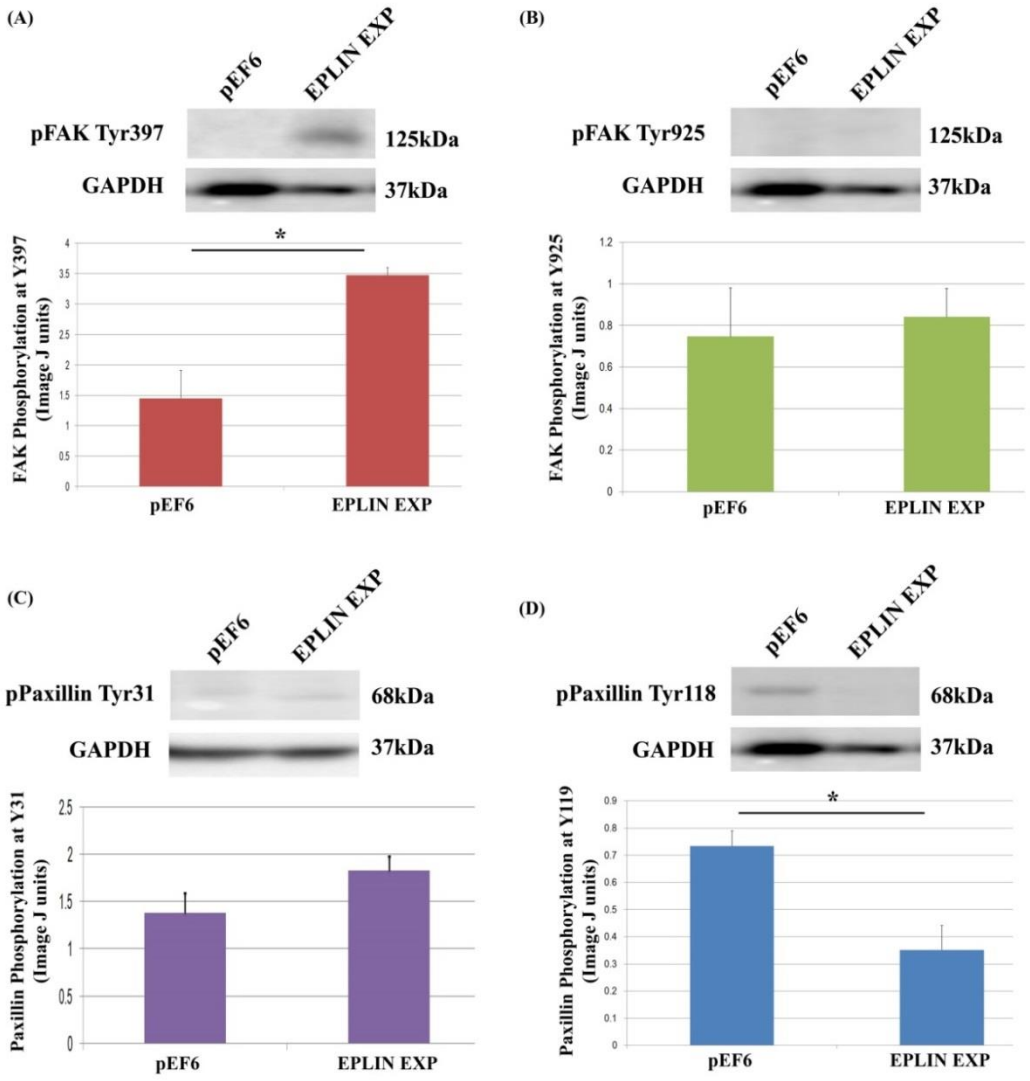

Figure 6.6 Phosphorylation status of FAK and paxillin in LNCaP cells following EPLINα overexpression.

(A) Level of FAK phosphorylation at Tyr397 in LNCaP^{pEF6} (pEF6) and LNCaP$^{EPLIN\ EXP}$ (EPLIN EXP) cells. (B) Level of FAK phosphorylation at Tyr925 in LNCaP^{pEF6} (pEF6) and LNCaP$^{EPLIN\ EXP}$ (EPLIN EXP) cells. (C) Level of paxillin phosphorylation at Tyr31 in LNCaP^{pEF6} and LNCaP$^{EPLIN\ EXP}$ (EPLIN EXP) cells. (D) Level of paxillin phosphorylation at Tyr118 in LNCaP^{pEF6} (pEF6) and LNCaP$^{EPLIN\ EXP}$ (EPLIN EXP) cells. Semi-quantitative analysis carried out using Image J software. Samples normalised to GAPDH for all experiments. Representative images are shown, semi-quantitative analysis represents mean of a minimum of three (n=3) independent band intensities, error bars represent SE of the mean * = $p < 0.05$. Statistical test performed for semi-quantitative analysis was a two sample, two tailed t-test using SigmaPlot software.

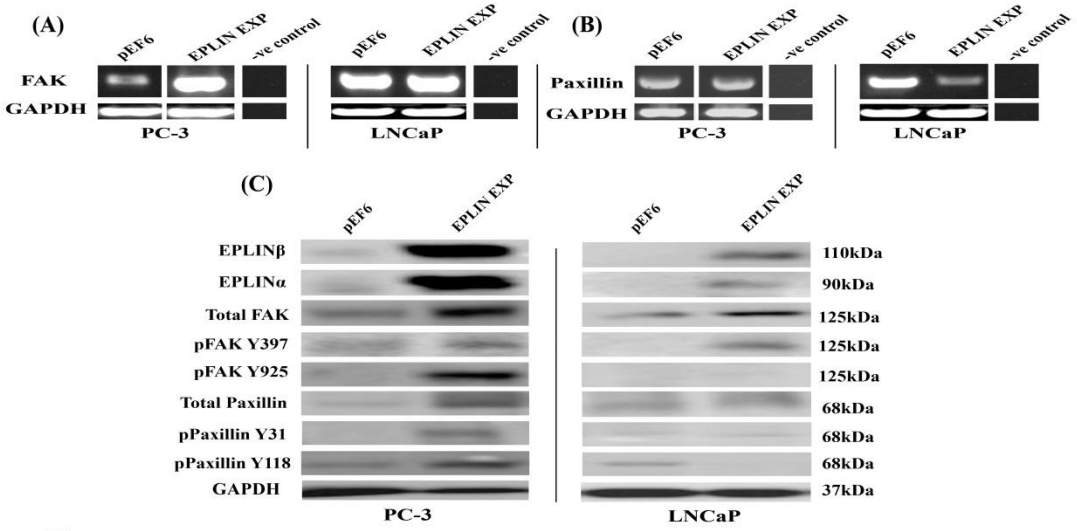

(D)

Cell Line	Transcript / Protein	Residue	Effect following EPLIN overexpression	Significant?
PC-3	Transcript	FAK	Increased	*Yes*
		Paxillin	No change	*No*
	Protein	Total FAK	Increased	*No*
		FAK Y397	Increased	*No*
		FAK Y925	Increased	*Yes*
		Total Paxillin	Increased	*Yes*
		Paxillin Y31	Increased	*Yes*
		Paxillin Y118	Increased	*Yes*
LNCaP	Transcript	FAK	No change	*No*
		Paxillin	Decreased	*Yes*
	Protein	Total FAK	Increased	*No*
		FAK Y397	Increased	*Yes*
		FAK Y925	No change	*No*
		Total Paxillin	No change	*No*
		Paxillin Y31	No change	*No*
		Paxillin Y118	Decreased	*Yes*

Figure 6.7 Summary of paxillin/FAK associations to EPLIN expression in PC-3 and LNCaP.

(A) PCR quantification of FAK transcript expression in PC-3/LNCaP^{pEF6} and PC-3/LNCaP$^{EPLIN\ EXP}$. (B) PCR quantification of paxillin transcript expression in PC-3/LNCaP^{pEF6} and PC-3/LNCaP$^{EPLIN\ EXP}$. (C) Western blot analysis of total FAK/paxillin expression and FAK/paxillin phospho-protein expression in control and EPLINα overexpression cell lines. Molecules screened were total FAK, p-FAK Y397, p-FAK Y925, total paxillin, p-paxillin Y31 and p-paxillin Y118. GAPDH was used alongside each experiment as a control. Representative images of a minimum of three independent repeats are shown. (D) Summary table showing the effects of EPLIN expression on FAK/Paxillin expression in PC-3 and LNCaP.

6.3.3 *In vitro* tumour cell functional assays with PC-3 cells using FAK inhibitor

6.3.3.1 FAK inhibitor titration to determine optimum inhibitory concentration

To further evaluate the link between EPLIN and FAK, a FAK inhibitor was used, in conjunction with EPLINα overexpression, in a number of cellular functional assays. To ascertain optimum inhibitory concentrations for the FAK inhibitor, a titration was set up to establish FAK Tyr397 expression in PC-3 cells following treatment with 100nM, 500nM, 1μM and 5μM concentrations of the FAK inhibitor (Figure 6.8). Western blot and semi-quantitative analysis demonstrate efficacy of the inhibitor at all concentrations, though 1μM and 5μM show the greatest efficacy and were thus, chosen for use in the functional assays.

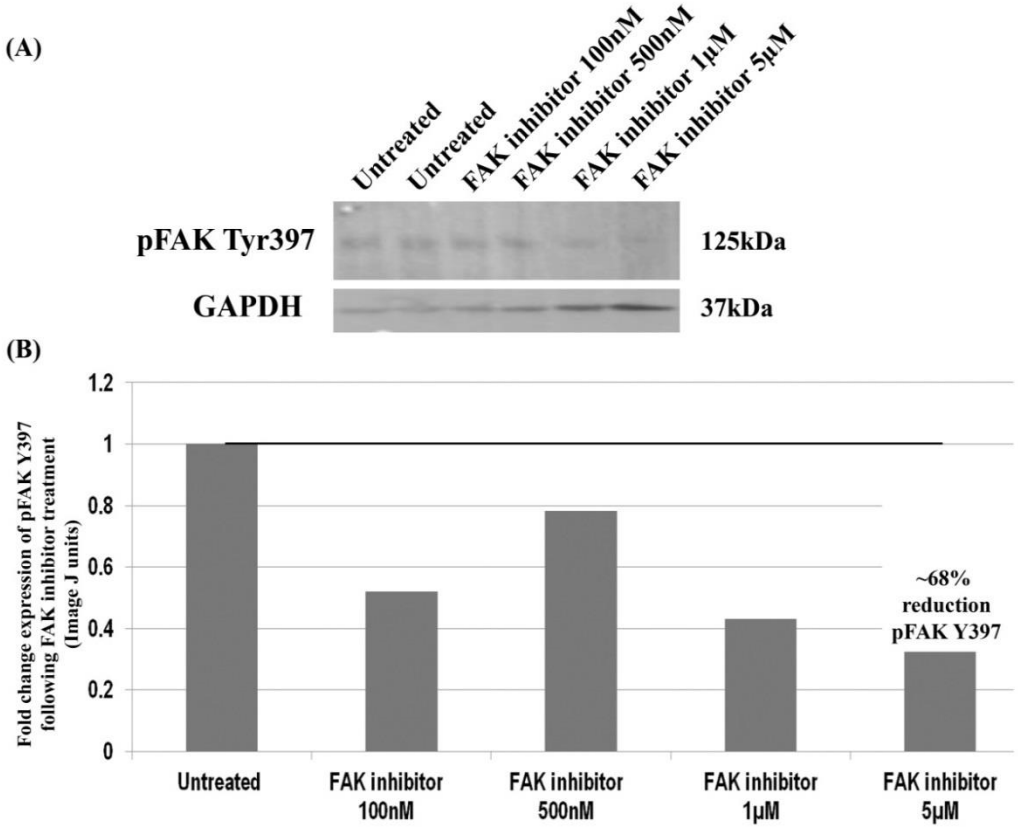

Figure 6.8 FAK inhibitor titration screen in PC-3 cells to determine optimum concentration for use in functional assays.

(A) Western blot image of concentrations tested for FAK inhibitor. PC-3 cells were treated with concentrations of 100nM, 500nM, 1µM and 5µM of the FAK inhibitor and tested for expression of pFAK Tyr397 via Western Blotting. GAPDH was used as a control protein. (B) Semi quantitative analysis of pFAK Tyr397 band intensities. Semi-quantitative analysis carried out using Image J software. Samples normalised to GAPDH.

6.3.3.2 Cell proliferation

A cell proliferation assay was carried out but in the presence of an FAK inhibitor, known to inhibit FAK phosphorylation at Tyr397, to evaluate the functional effect of EPLINα overexpression on cell proliferation when FAK is inhibited. In PC-3^{pEF6} and PC-3$^{EPLIN\ EXP}$ cells, FAK inhibition at 1 μM didn't affect cell proliferation and no significant differences were observed in cell proliferation when comparing FAK 1μM treated PC-3^{pEF6} and PC-3$^{EPLIN\ EXP}$ to the representative untreated samples. However at the 5μM FAK inhibitor concentration, cell proliferation was markedly reduced for both control PC-3^{pEF6} and PC-3$^{EPLIN\ EXP}$ cells, with a significant reduction of cell proliferation for PC-3^{pEF6} cells at Day 3 when compared with untreated equivalent lines (p=0.006) (Figure 6.9A/B). For PC-3$^{EPLIN\ EXP}$ cells, cell proliferation was reduced in FAK inhibitor treated cells at the 5μM concentration compared to untreated controls, however this didn't reach significance for either Day 3 or Day 5 (p=0.139 for Day 3, p=0.100 for Day 5). In the LNCaP cell model, FAK inhibition in LNCaP^{pEF6} cells at the lower 1μM concentration reduced cell proliferation, with a significant reduction of cell proliferation at day 3 for LNCaP^{pEF6} (p=0.041) (Figure 6.9C). By Day 5 however, no significant differences in cell proliferation were seen between FAK 1μM treated LNCaP^{pEF6} cells and untreated LNCaP^{pEF6} cells (p=0.431). For LNCaP$^{EPLIN\ EXP}$ cells, no significant differences in cell proliferation were observed between FAK 1μM treated LNCaP$^{EPLIN\ EXP}$ cells compared to untreated LNCaP$^{EPLIN\ EXP}$ cells at either time point (p=0.286 for Day 3, p=0.219 for Day 5) (Figure 6.9D). For the higher concentration of FAK inhibitor (5μM), an anti-proliferative effect was seen and LNCaP^{pEF6} cell proliferation was significantly reduced compared to untreated controls at Day 3 (p=0.009) and Day 5

($p=0.042$). For LNCaP$^{EPLIN\ EXP}$ cells, the higher 5μM concentration of FAK inhibitor lead to a significant reduction of cell proliferation at Day 3 ($p=0.007$) and Day 5 ($p=0.013$) (Figure 6.9D).

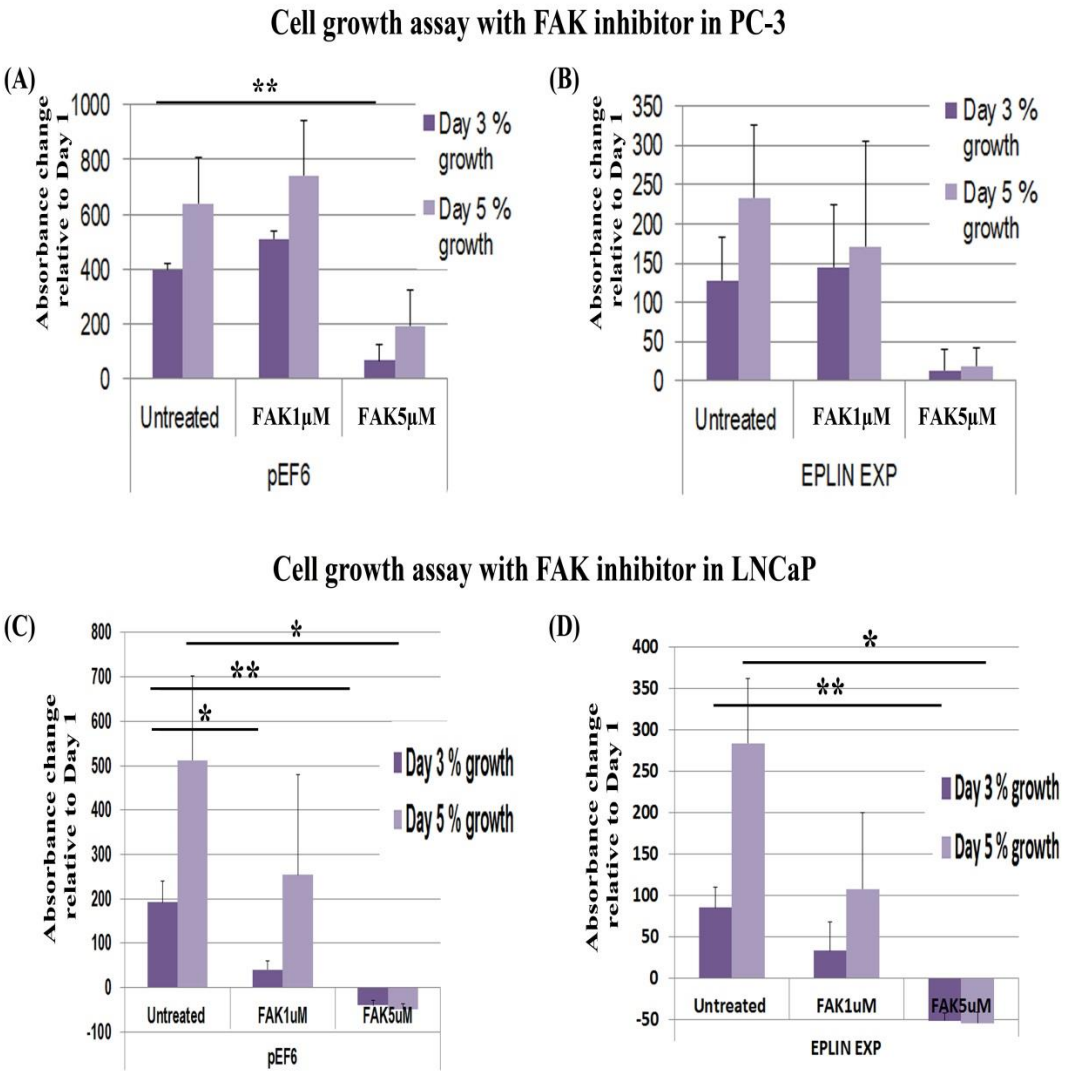

Figure 6.9 Effect of FAK Y397 inhibitor treatment on cell proliferation of PC-3 and LNCaP cells when EPLINα is overexpressed.

(A) Cell proliferation assay with PC-3^{pEF6} cells +/- FAK inhibitor at concentration 1µM and 5µM. (B) Cell proliferation assay with PC-3$^{EPLIN\ EXP}$ cells +/- FAK inhibitor at concentration 1µM and 5µM (C) Cell proliferation assay with LNCaP^{pEF6} cells +/- FAK inhibitor at concentration 1µM and 5µM. (D) Cell proliferation assay with LNCaP$^{EPLIN\ EXP}$ cells +/- FAK inhibitor at concentration 1µM and 5µM. Cell proliferation was measured at time points Day 3 and Day 5 and compared to Day 1. Values shown are mean of three independent repeats, error bars represent standard error of the mean. * = $p < 0.05$, ** = $p < 0.01$. Statistical test performed for analysis was a two sample, two tailed t-test using SigmaPlot software.

6.3.3.3 Cell adhesion

A cell adhesion assay was carried out in the presence of an FAK inhibitor, known to inhibit FAK phosphorylation at Tyr397, to evaluate the functional effect of EPLINα overexpression on cell adhesion when FAK is inhibited. The same concentrations of FAK were used as in the cell proliferation assay, 1µM and 5µM. In PC-3^{pEF6} cells, the lower concentration of FAK slightly increased the cells ability to adhere to the matrix and the higher concentration reduced the adhesive capacity of the cells, however neither concentration of treatment induced any significant changes to cell adhesion when compared to untreated PC-3^{pEF6} cells (p=0.130 for 1µM, p=0.085 for 5µM) (Figure 6.10A). For the PC-3$^{EPLIN\ EXP}$ cells, a dose dependant drop in cellular adhesion was visualised, with cellular adhesion gradually reducing with increasing FAK inhibitor concentration, however this was not significant (p=0.646 for 1µM, p=0.100 for 5µM) when compared to untreated controls (Figure 6.10B).

In LNCaP^{pEF6} cells, both concentrations of FAK inhibitor (1µM and 5µM) had no apparent effects on cellular adhesion when compared to untreated control LNCaP^{pEF6} cells (p=0.689 for 1µM, p=0.393 for 5µM) (Figure 6.10C). For the LNCaP$^{EPLIN\ EXP}$ cells, the lower concentration of FAK inhibitor had no apparent effects on cellular adhesion when compared to untreated control $^{LNCaPEPLIN\ EXP}$ cells. For the 5µM FAK inhibitor concentration, a decrease in cellular adhesion was seen compared to untreated control LNCaP$^{EPLIN\ \ EXP}$ cells, though this didn't reach statistical significance (p=0.064 for 5µM) (Figure 6.10D).

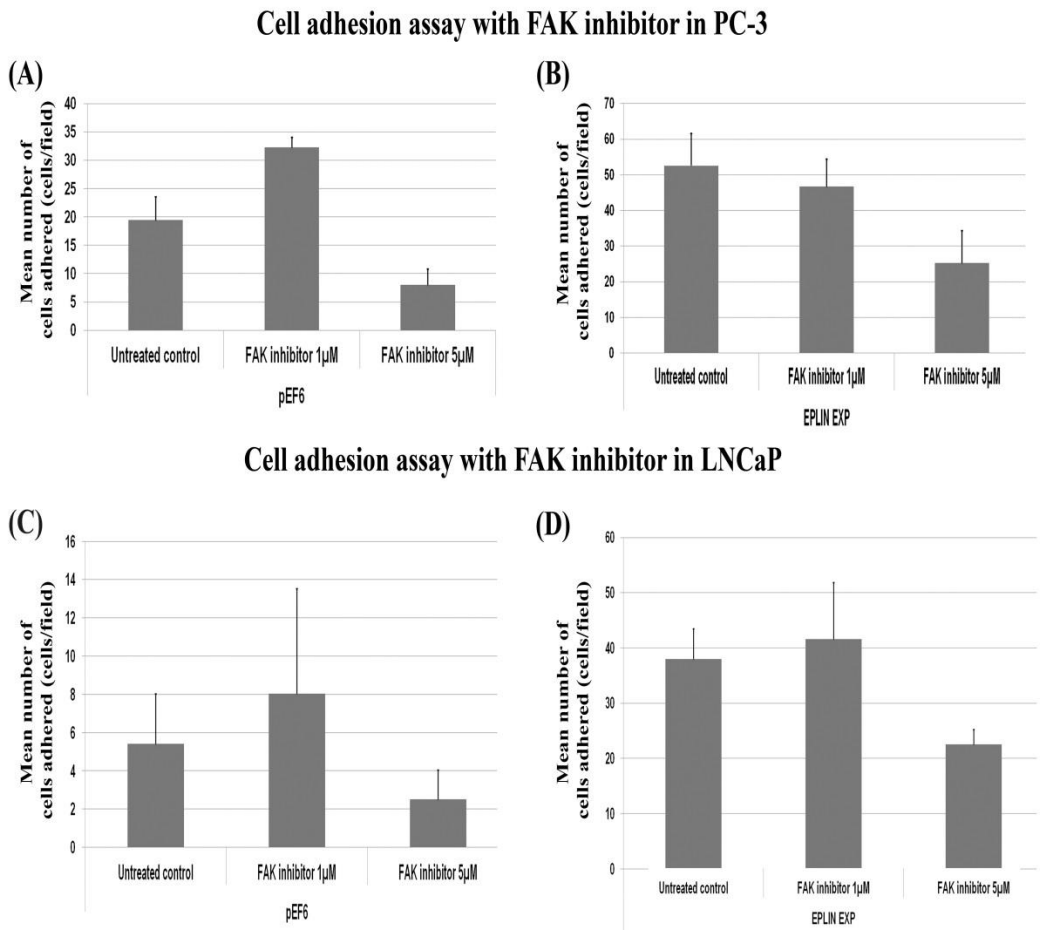

Figure 6.10 Effect of FAK Y397 inhibitor treatment on cell adhesion of PC-3 and LNCaP cells when EPLINα is overexpressed

(A) Cell adhesion assay with PC-3^{pEF6} cells +/- FAK inhibitor at concentration 1µM and 5µM. (B) Cell adhesion assay with PC-3$^{EPLIN\ EXP}$ cells +/- FAK inhibitor at concentration 1µM and 5µM. C) Cell adhesion assay with LNCaP^{pEF6} cells +/- FAK inhibitor at concentration 1µM and 5µM. (D) Cell adhesion assay with LNCaP$^{EPLIN\ EXP}$ cells +/- FAK inhibitor at concentration 1µM and 5µM. Values shown are mean of three independent repeats, error bars represent standard error of the mean.

6.3.3.4 Cell invasion

A cellular invasion assay was carried out in the presence of an FAK inhibitor, known to inhibit FAK phosphorylation at Tyr397, to evaluate the functional effect of EPLINα overexpression on cell invasion when FAK is inhibited. For PC-3^{pEF6} cells and PC-3$^{EPLIN\ EXP}$ cells, no significant differences were seen for the 1µM FAK inhibitor treatment (Figure 6.11A/B). For the higher concentration of FAK inhibitor (5µM), a significant reduction was seen on cell invasion to PC-3^{pEF6} cells (p=0.034) when compared to untreated PC-3^{pEF6} cells (Figure 6.11A). For PC-3$^{EPLIN\ EXP}$ cells, treatment with the FAK inhibitor at 5µM concentration also reduced cell invasion, however this didn't reach significance when compared to untreated PC-3$^{EPLIN\ EXP}$ cells (p=0.158) (Figure 6.11B). For LNCaP^{pEF6} cells and LNCaP$^{EPLIN\ EXP}$ cells, the FAK inhibitor caused a dose dependant reduction in cellular invasion (Figure 6.11C/D), though this didn't reach statistical significance for either LNCaP^{pEF6} cells or LNCaP$^{EPLIN\ EXP}$ cells (LNCaP^{pEF6} 1µM, p=0.582, 5µM, p=0.218, LNCaP$^{EPLIN\ EXP}$ 1µM, p=0.186m 5µM, p=0.114).

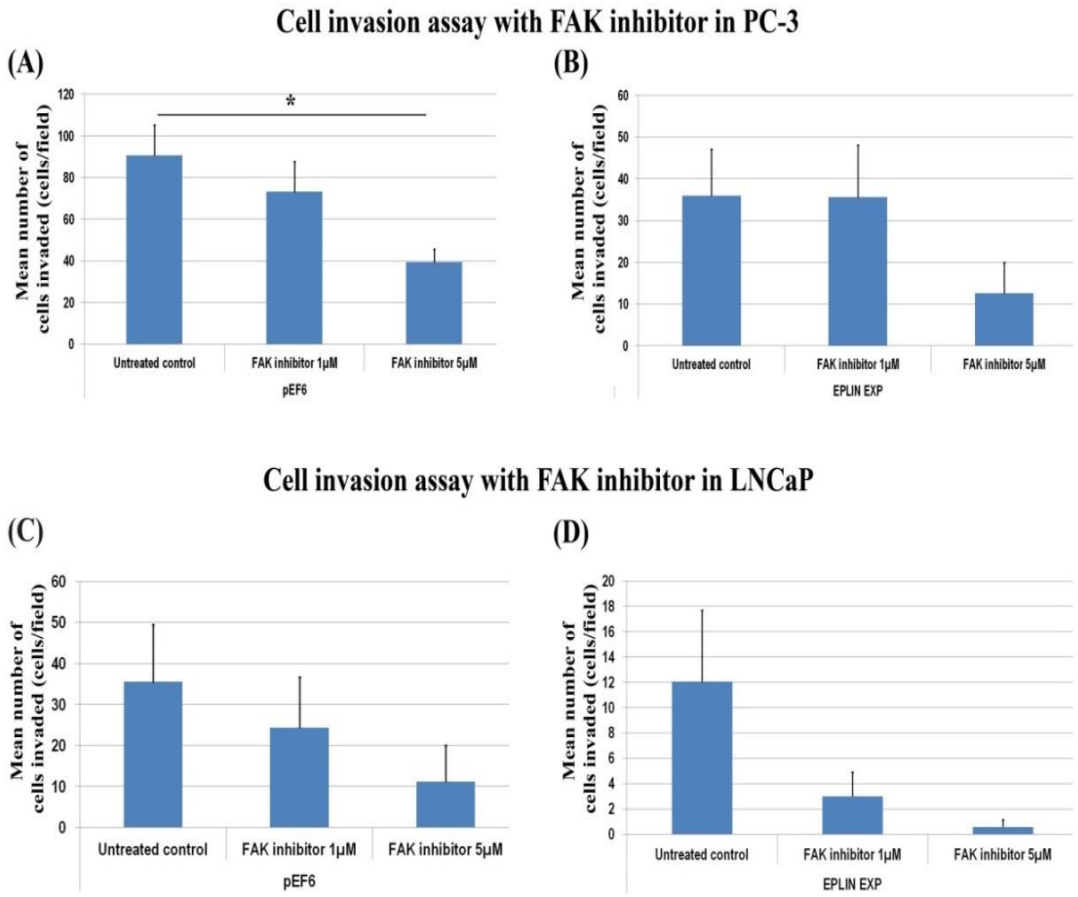

Figure 6.11 Effect of FAK Y397 inhibitor treatment on cell invasion of PC-3 and LNCaP cells when EPLINα is overexpressed

(A) Cell invasion assay with PC-3^{pEF6} cells +/- FAK inhibitor at concentration 1µM and 5µM. (B) Cell invasion assay with PC-3$^{EPLIN\ EXP}$ cells +/- FAK inhibitor at concentration 1µM and 5µM. (C) Cell invasion assay with LNCaP^{pEF6}cells +/- FAK inhibitor at concentration 1µM and 5µM. (D) Cell invasion assay with LNCaP$^{EPLIN\ EXP}$ cells +/- FAK inhibitor at concentration 1µM and 5µM. Values shown are mean of three independent repeats, error bars represent standard error of the mean. * = $p < 0.05$. Statistical test performed for analysis was a two sample, two tailed t-test using SigmaPlot software.

6.3.3.5 Cell migration

A wound healing assay was carried out but in the presence of an FAK inhibitor, known to inhibit FAK phosphorylation at Tyr397, to evaluate the functional effect of EPLINα overexpression on cell migration when FAK is inhibited in PC-3 cells. In PC-3^{pEF6} cells, both concentrations of FAK inhibitor rendered the cells less motile. For the lower concentration of FAK inhibitor used (1μM), inhibitor treatment significantly reduced cell migration at the 4 hour time point ($p=0.009$) compared to untreated PC-3^{pEF6} cells (Figure 6.12A). For the higher concentration of FAK inhibitor used (5μM), inhibitor treatment significantly reduced cellular migration at 2, 3 and 4 hour time points of the experiment ($p=0.003$, $p=0.002$ and $p=0.001$, respectively) when compared to untreated PC-3^{pEF6} cells (Figure 6.12A). For the PC-3$^{EPLIN\ EXP}$ cells, at the lower concentration of FAK inhibitor used (1μM), no significant differences were seen in cellular migration compared to untreated PC-3$^{EPLIN\ EXP}$ cells ($p>0.05$ at all time points) (Figure 6.12B). For the higher concentration of FAK inhibitor used (5μM), cell migration was significantly reduced at the 3 hour time ($p=0.034$) when compared to untreated PC-3$^{EPLIN\ EXP}$ cells, but no significant differences were seen at other time points measured (Figure 6.12B).

For LNCaP cells, a transwell migration assay was performed in presence of a FAK inhibitor at concentration 5μM, to deduce if EPLINα exercises any effect on cell migration in conjunction with FAK in LNCaP cells (Figure 6.12C). FAK inhibition reduced cell migration in LNCaP^{pEF6} cells and in LNCaP$^{EPLIN\ EXP}$ cells, with a significant reduction in cell migration observed for cells with forced EPLINα expression (LNCaP$^{EPLIN\ EXP}$ cells) ($p=0.01$ vs. untreated LNCaP$^{EPLIN\ EXP}$ cells) (Figure 6.12C).

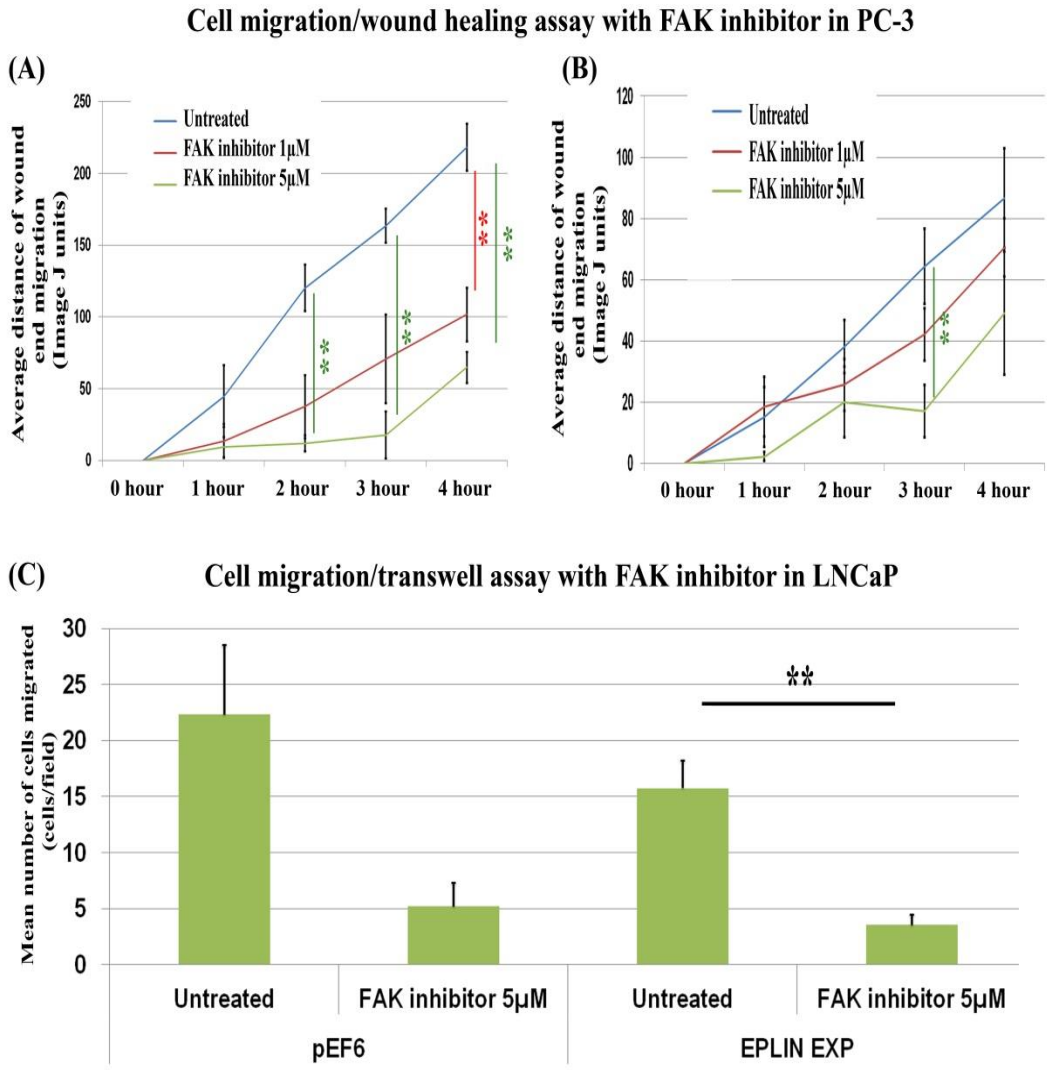

Figure 6.12 Effect of FAK Y397 inhibitor treatment to cell migration of PC-3 and LNCaP cells when EPLINα is overexpressed

(A) Cell migration/wound healing assay with PC-3^{pEF6} cells +/- FAK inhibitor at concentration 1μM and 5μM. Cell migration tested over 4 hours and normalised against to Time 0. (B) Cell migration/wound healing assay with PC-3$^{EPLIN\ EXP}$ cells +/- FAK inhibitor at concentration 1μM and 5μM. Cell migration tested over 4 hours and normalised against Time 0. (C) Cell migration/transwell assay with LNCaP^{pEF6}and LNCaP$^{EPLIN\ EXP}$ cells +/- FAK inhibitor at concentration 5μM. Values shown are mean of three independent repeats, error bars represent standard error of the mean. * = $p < 0.05$, ** = $p < 0.01$. Statistical test performed for analysis was a two sample, two tailed t-test using SigmaPlot software.

6.3.3.6 Co-culture with human osteoblasts

Co-culture invasion assays, conducted in the presence and absence of FAK inhibitor, were set up to explore EPLIN – FAK relationship in an *in vitro* bone like environment. For PC-3^{pEF6} cells, the FAK inhibitor significantly reduced cell invasion both for osteoblast positive and osteoblast negative cells ($p<0.001$ vs. equivalent control without FAK inhibitor) (Figure 6.13A). For PC-3$^{EPLIN\ EXP}$ cells, a similar trend was seen, where the FAK inhibitor significantly reduced cell invasion both for osteoblast positive and osteoblast negative cells, though this change was more significant in the osteoblast negative conditions ($p= <0.001$ vs. untreated PC-3$^{EPLIN\ EXP}$ cells without osteoblast) than the osteoblast positive conditions ($p=0.005$ vs. untreated PC-3$^{EPLIN\ EXP}$ cells with osteoblast) (Figure 6.13B). The lowest cell invasion for all samples tested was the PC-3$^{EPLIN\ EXP}$ cells which were treated with the FAK inhibitor, in the absence of osteoblasts. Although introducing osteoblasts slightly increased cell invasion, no significant changes were seen ($p>0.05$). For LNCaP^{pEF6} cells, the FAK inhibitor lead to a reduction of cellular invasion for both for osteoblast positive and osteoblast negative conditions, however this was only significant for osteoblast negative LNCaP^{pEF6} cells ($p=0.009$ vs. equivalent untreated osteoblast negative control) (Figure 6.13C) For LNCaP$^{EPLIN\ EXP}$ cells, the FAK inhibitor reduced cell invasion both for osteoblast positive and osteoblast negative cells, however this change was not significant for LNCaP$^{EPLIN\ EXP}$ cells ($p = 0.075$ vs. equivalent untreated control without osteoblasts, $p = 0.087$ vs. equivalent untreated control with osteoblast co-culture) (Figure 6.13D).

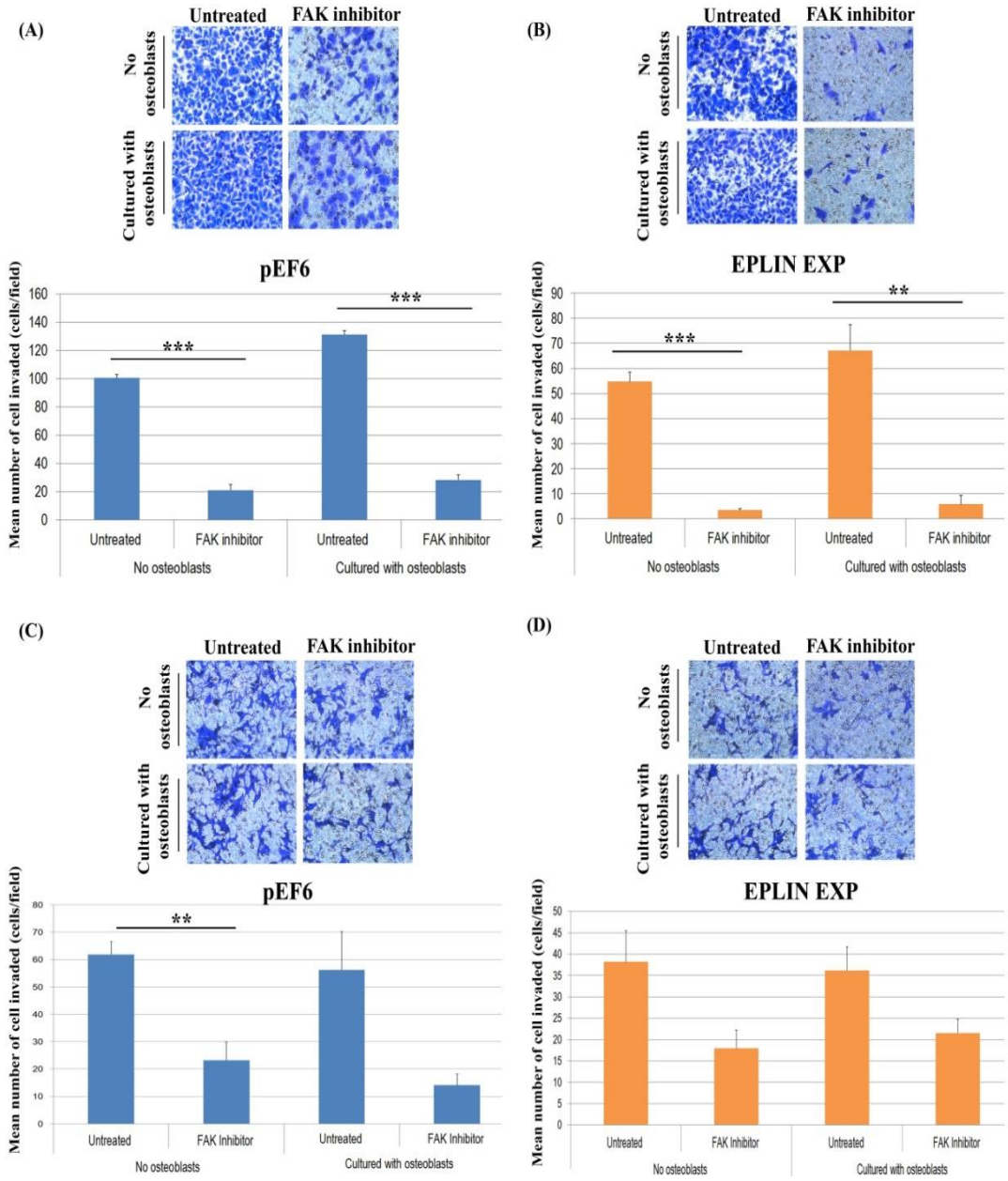

Figure 6.13 Effect of FAK inhibition on PC-3 and LNCaP invasion in an osteoblast co-culture environment.

(A) Effect of FAK inhibition on cellular invasion of co-cultured PC-3^{pEF6} cells +/- osteoblasts. (B) Effect of FAK inhibition on cellular invasion of co-cultured PC-$3^{EPLIN\ EXP}$ cells +/- osteoblasts. (C) Effect of FAK inhibition on cellular invasion of co-cultured LNCaP^{pEF6} cells +/- osteoblasts. (D) Effect of FAK inhibition on cellular invasion of co-cultured LNCaP$^{EPLIN\ EXP}$ cells +/- osteoblasts. PC-3 and LNCaP cells were co-cultured with human osteoblast cell line hFOB1.19. FAK inhibitor concentration for all assays used was 5µM. Representative images are shown. Values shown are mean of three independent repeats, error bars represent standard error of the mean. ** = $p < 0.01$, *** = $p < 0.001$. Statistical test performed for analysis was a two sample, two tailed t-test using SigmaPlot software.

6.4 Discussion

This chapter sought to establish and validate a putative link between EPLIN and focal adhesive molecules paxillin and FAK. Paxillin and FAK have wide implications in various cancers and several studies have now illustrated they both play key roles in cell migration and contribute to the dynamic assembly/disassembly of focal adhesions (Brown et al., 2005, Hanks et al., 2003). Paxillin and FAK directly interact with each other via the FAT domain of FAK, and this docking of FAK to paxillin orchestrates a host of signalling pathways and ultimately controls cell functions including cell motility and invasion (Hsia et al., 2003). To establish any link of EPLIN to paxillin and FAK, EPLINα was firstly overexpressed in the PC-3 cell line and this forced expression seemed to enhance expression of both FAK and paxillin. EPLINα overexpression was able to significantly increase transcript and protein level of FAK, whereas it was only able to increase protein expression of paxillin. The paxillin association concurs with previous work both in prostate cancer, where EPLINα overexpression created an enhanced staining profile for paxillin, and in human mesangial cells where EPLIN co-localised with paxillin in a protein complex (Sanders et al., 2011, Tsurumi et al., 2014). EPLINα overexpression also leads to a significant increase in the phosphorylation of paxillin at Tyr31 and Tyr118 in PC-3 cells. Both of these regions are critical for paxillin function and serve as sites of association to FAK (Bellis et al., 1995, Mitra et al., 2005). As EPLINα appears to increase paxillin phosphorylation at these residues, it could be that EPLINα expression in PC-3 causes a more stable complex between FAK and paxillin, to co-ordinate cell functions like cell adhesion, migration and invasion (Deramaudt et al., 2014). If this is the case, this could be the mechanism for the enhanced adhesion in

PC-3 cells seen when EPLINα is overexpressed (see Chapter 4), as weakening these interactions have been shown to reduce cell adhesion (Deramaudt et al., 2014), though it this mechanism does not appear to align with the other cellular implication of EPLINα overexpression, such as reduced motility and invasiveness, which will be investigated further in the following chapter of this thesis.

This is the first known study to comprehensively report and evaluate a molecular link of EPLINα and FAK. In addition to an increase in total FAK protein in response to EPLINα overexpression, an increase in Tyr925 phosphorylation was established in PC-3 cells. There was a slight increase also in FAK Tyr397, however this change wasn't significant. Both Tyr397 and Tyr925 are critical residues in FAK function and have implications in cancer. Tyr397 for example, is a major phosphosite for binding the Src family kinases via the SH2 domain, which upon autophosphorylaton regulate cell functions including cell migration (Xing et al., 1994). Therefore, it could be possible that EPLINα exerts its functional effect in tandem with FAK and Src-related signalling, a hypothesis that will be further elucidated in the following chapter. Additionally, Tyr925 phosphorylation in FAK is generally associated with focal adhesion disassembly, cell migration and protein turnover (Deramaudt et al., 2011). It could therefore be possible that EPLINα exerts its function in PC-3 cells partially through the action of FAK Tyr925. Specifically, if EPLINα causes an increase in Tyr925 which then reduces focal adhesion turnover, this could influence cell adhesion properties of PC-3 cells, resulting in a cell which is less effective at detaching form the matrix (Deramaudt et al., 2011). This may then provide insights into EPLINα's potential mechanism through the action of FAK for regulating cell functions like cell adhesion.

To further clarify molecular associations between EPLIN, paxillin and FAK, the LNCaP model was also used for potential interaction analysis between the molecules. Firstly, transcript and protein expression of paxillin and FAK was determined in LNCaP cDNA and protein with forced EPLINα expression. For FAK, increased EPLINα expression appeared to have no significant effect on FAK transcript expression in LNCaP. However, at the protein level, FAK total protein was significantly increased in LNCaP when EPLINα was overexpressed. This differs from the PC-3 cell line, where both FAK transcript and protein were significantly upregulated in conjunction with EPLINα expression. The reason for this could be due to EPLINα overexpression being more successful in the PC-3 cell line compared to LNCaP (see Chapter 3), which could partially explain the discrepancy of increased FAK transcript expression observed between the two lines. There is also a larger basal level of EPLINα transcript in PC-3 Wild-Type cDNA compared to LNCaP Wild-Type cDNA, so this could also be affecting the capacity of EPLINα overexpression within PC-3 over LNCaP, and thus FAK transcript. Secondly, FAK transcript is highly expressed in LNCaP^{pEF6} cDNA, whereas only low expression was seen in PC-3^{pEF6} cDNA, potentially meaning FAK transcript was already highly expressed within LNCaP, and hence increasing EPLINα may be less likely to bring about significant further enhances in FAK transcript levels. Finally, inherent differences between the PC-3 and LNCaP cell lines may also account somewhat for these observations and it may be that there are further, unknown, levels of regulation present in one cell but not the other, which may account for these discrepancies. Furthermore, EPLINα expression influenced the proportion of FAK phosphorylation at Tyr397 within LNCaP. FAK Tyr397 is an established auto phosphorylation site within FAK to provide a high-affinity binding site for Src homology 2 (SH2)

domains of Src family kinases and these include molecules like c-Src PI-3 Kinase (Schaller et al., 1994, Chen et al., 1996). This could imply that overexpression of EPLINα in LNCaP affects cell migratory properties due to enhanced FAK Tyr397 being generally associated as a promoter of cell migration (Zhao and Guan, 2011). This appears to be not the case with the LNCaP model, as EPLIN overexpression reduced cell migration rather than promoted migration, however this could potentially due to further downstream signalling factors which will be explored later. Phosphorylation of FAK at Tyr925, on the other hand, displayed no significant change in expression when EPLINα was overexpressed, in contrast to PC-3 where a significant increase in FAK Tyr925 was seen when EPLINα was overexpressed. It also could be that FAK Y925 is not expressed/minimally expressed in the LNCaP model, as no detectable band was present for either LNCaP^{pEF6} or LNCaP$^{EPLIN\ EXP}$ cells. FAK Y925 is responsible for cell migration, cell protrusion and focal adhesion turnover (Deramaudt et al., 2011), so this could be a reason why LNCaP cells are generally a less aggressive model of prostate cancer, which is also less migratory, compared to PC-3. It may also suggest that the mechanistic relationship between EPLINα and FAK differs between different prostate cancer cell lines.

For paxillin, transcript expression was significantly reduced when EPLINα was overexpressed in LNCaP and had no significant change at the protein level. This suggests the effect of EPLINα on paxillin expression is less pronounced in LNCaP compared to PC-3 cells. This notion differs from previous reports where EPLIN expression appears to be linked to paxillin via enhancing paxillin staining (Maul and Chang, 1999, Sanders et al., 2011) and by forming a protein complex with paxillin (Tsurumi et al., 2014). There was also a change in phosphorylation of paxillin in

LNCaP at Tyr118 when EPLINα was overexpressed; EPLINα overexpression lead to a significant reduction of Tyr118 phosphorylation, contrasting to what was seen in PC-3 where EPLINα overexpression significantly enhanced Tyr118 phosphorylation of paxillin. Both Tyr31 and Tyr118 are essential sites of association between paxillin and FAK (Bellis et al., 1995, Mitra et al., 2005) and altering these interactions can have diverse downstream effects on cell function including cell migration, adhesion and invasion (Deramaudt et al., 2014). Therefore, as EPLINα expression in LNCaP appears to reduce Tyr118 in paxillin, and the expression of paxillin Y31 is negligible for both LNCaP^{pEF6} and LNCaP$^{EPLIN\ EXP}$ cells, this could suggest EPLINα expression may reduce or disrupt the FAK/paxillin complex in LNCaP cells. This could result in reduced invasion and migration of LNCaP cells overexpressing EPLINα, as altering paxillin:FAK interaction has previously been shown to reduce cellular migration and invasion (Deramaudt et al., 2014) providing glances into the potential mechanistic links of EPLINα with regard to influencing cellular migration and invasion through FAK/paxillin.

As there has been previous reports addressing the putative link between EPLIN and paxillin (Sanders et al., 2011, Tsurumi et al., 2014) but little work done to establish a link between EPLIN and FAK, further clarification was sought between the two molecules, including use of an FAK inhibitor in combination with *in vitro* tumour functional assays. FAK inhibition was determined in PC-3 cells transfected with the pEF6 control plasmid and the EPLINα overexpression plasmid. This was done to evaluate if EPLINα exerts its functional capacity in conjunction with FAK or has any functional link to FAK in prostate cancer. In the cell proliferation assay, FAK significantly reduced cell proliferation of PC-3^{pEF6} control cells at 5µM

concentration, suggesting inhibition of FAK impairs cell proliferation of normal PC-3 cells at this concentration. This was expected as the FAK inhibitor has an established anti-proliferative effect on certain cancer cells (Golubovskaya et al., 2008). When EPLINα was overexpressed, FAK was still able to reduce cell proliferation; however this reduction was not significant suggesting EPLINα and FAK may be acting partially in tandem on cell proliferation in PC-3. This raises a number of possibilities, firstly, overexpression of EPLINα appears to somewhat enhance FAK protein and phosphorylation. As the FAK inhibitor acts through inhibition of Tyr397, then it is possible that, due to the enhanced levels of FAK and phospho-FAK in EPLINα overexpression PC-3 cells, the inhibitor is less effective than that in PC-3^{pEF6} cells expressing normal levels of FAK/phospho-FAK. Secondly, the FAK/paxillin complex activate and mediate a variety of downstream effector molecules and signalling pathways and it may hence be that EPLINα also exerts a level of regulation on these molecules/pathways, which would account for the loss of effect of upstream FAK inhibition. The second possibility will be explored further in the following chapter of this thesis. For LNCaP cells, the FAK inhibitor comparably reduced cell proliferation of both LNCaP^{pEF6} cells and LNCaP$^{EPLIN\ EXP}$ cells, potentially suggesting that the EPLINα FAK link for cell proliferation is not as significant in LNCaP cells as in PC-3 cells.

The FAK inhibitor also lead to a dose dependant drop in cellular invasion of LNCaP cells for both LNCaP^{pEF6} and LNCaP$^{EPLIN\ EXP}$ cells, although this change was not significant. Interestingly, in PC-3$^{EPLIN\ EXP}$ cells overexpression the FAK inhibitor at a concentration of 1μM had no apparent impact on the invasiveness of this overexpression line but did bring about some reduction in the LNCaP^{pEF6} control

line. This again supports the potential links between EPLINα and FAK discussed previously in the PC-3 cell line.

The most prominent effect on cellular adhesion was seen in LNCaP$^{EPLIN\ EXP}$ cells, where FAK inhibition significantly reduced cellular adhesion at the highest concentration. This could suggest that when FAK expression is blocked in LNCaP cells, it negates the effect of enhanced adhesion EPLINα has on LNCaP cells (see Chapter 5).

For the cellular migration assay, two separate experiments were set up for PC-3 and LNCaP cells; for PC-3 cells a scratch/wound healing assay, and for LNCaP cells, a transwell migration assay due to the ineffectiveness of the scratch assay with the LNCaP cell model. For PC-3 cells, the FAK inhibitor lead to a reduction in cellular migration of both LNCaP cells for both concentrations of FAK inhibitor tested, suggesting the FAK inhibitor renders PC-3 cells largely less motile. However, for the lower concentration tested (1μM), only PC-3^{pEF6} cells had a significantly reduced migratory potentials when compared to untreated PC-3^{pEF6} cells at the 4 hour time point of the experiment ($p=0.009$). For PC-3$^{EPLIN\ EXP}$ cells, the lower concentration of FAK inhibitor had no significant impact on cellular migration vs. untreated PC-3$^{EPLIN\ EXP}$ cells ($p>0.05$ for all time points tested). Similar trends were seen for the higher 5μM FAK inhibitor concentration, where migration was significantly reduced for PC-3^{pEF6} cells at hours 2, 3 and 4. Whereas for PC-3$^{EPLIN\ EXP}$ cells, only the 3 hour time point lead to a significant reduction of cellular migration. Given that the FAK inhibitor is more effective in reducing migration of PC-3^{pEF6} cells (where low levels of EPLIN are present), it could further suggest that EPLIN exerts its tumour suppressive functions on cell migration partially through the action of FAK,

especially since in PC-3$^{EPLIN\ EXP}$ cells (when EPLINα is expressed) only limited effects on cell migration were noted following FAK inhibition. This adds to the potential interactions between EPLINα and FAK as discussed previously and strengthens these hypothetical relationships between EPLINα and FAK and their impact on cellular functions like migration in PC-3 cells.

In the LNCaP transwell migration assay the FAK inhibitor markedly reduced cellular migration of LNCaP^{pEF6} and LNCaP$^{EPLIN\ EXP}$ cells, with a more apparent reduction in migration for LNCaP$^{EPLIN\ EXP}$ cells. This suggests that the effect of EPLINα overexpression on cellular migration in LNCaP cells may not be as tightly linked to the action of FAK, due to the substantial effect of FAK inhibition on LNCaP$^{EPLIN\ EXP}$ cells.

Finally, to evaluate the potential effects of FAK inhibition in combination with EPLINα overexpression in an *in vitro* bone like environment, a co-culture assay was performed on PC-3 and LNCaP cells with FAK treatment at 5μM. In the co-culture assay, the FAK inhibitor significantly reduced cellular invasion of PC-3^{pEF6} and PC-3$^{EPLIN\ EXP}$ cells. This reduction in invasion was also demonstrated when in presence of human osteoblasts, suggesting the presence of human osteoblasts or a bone-like environment has little effect on the EPLINα FAK interaction and their inhibitory effects on cell invasion. For the LNCaP cell model, the FAK inhibitor significantly reduced cellular invasion of LNCaP^{pEF6} cells, in the absence of osteoblasts, but no significant differences were seen following FAK inhibition when LNCaP^{pEF6} cells were cultured with osteoblasts. This may suggest, at least in LNCaP, that FAK inhibition is less efficient at reducing cellular invasion when in presence of a bone-like environment. However for LNCaP$^{EPLIN\ EXP}$ cells, significance was not reached

both in the presence and absence of osteoblasts. In general, as with previous analyses, addition of FAK inhibitor at 5μM concentrations again substantially reduced the invasiveness of pEF6 and EPLIN EXP transfected cells in both PC-3 and LNCaP models, though here a greater level of significance was noted, potentially due to the reduced inter-experimental variability seen in these assays. Of note was the apparent lack of significant impact here for the FAK inhibitor on LNCaP$^{\text{EPLIN EXP}}$ cells, though given the variability of such results with previous assays conducted throughout this chapter, these results must be interpreted cautiously. In addition, as discussed in Chapter 3, any effects observed here on the status of paxillin/FAK expression via enhanced EPLIN expression, could be due to the observed increase in EPLINβ in conjunction with EPLINα in PC-3 and LNCaP. The relationship between EPLINα and EPLINβ and their downstream effects on other molecules and/or cell function, therefore require further investigation for full validation.

This chapter evaluated several aspects of EPLINα associations to the signalling molecules paxillin and FAK and provides insights into EPLINα's mechanism of action in prostate cancer, specifically through phosphorylation of FAK and paxillin at key residues in PC-3 and LNCaP cell lines. Further work is needed to fully elucidate and unravel these interactions, and downstream effectors, and doing so will provide crucial indications into EPLINα's physiology in prostate cancer progression.

Chapter VII:
Investigations into potential mechanisms of action of EPLINα in prostate cancer

7.1 Introduction

EPLIN has been implicated in the progression of several cancers including prostate, colorectal and breast cancer where a gradual downregulation or loss of EPLIN is seen in more aggressive clinical cancer tissues (Zhang et al., 2011, Sanders et al., 2011, Jiang et al., 2008). EPLIN is also associated with the actin cytoskeleton and functions to assist, stabilise and control actin dynamics (Maul et al., 2003). In various cases, expression of the EPLINα isoform is able to suppress various cancer cell characteristics, like cell proliferation and invasion, suggesting a protective function for EPLIN in cancer progression as a suppressor of tumour metastasis. The mechanism(s) responsible for the suppressive effect of EPLIN in cancer, however, remain largely unknown. Several reports have hinted into the mechanism of EPLIN via the ERK pathway to control cell motility (Han et al., 2007) and EGF signalling (Zhang et al., 2013), in addition to having links to the tumour suppressor p53 (Ohashi et al., 2017, Steder et al., 2013). EPLIN has recently been shown to associate to the LIM-only domain protein PINCH1, and EPLIN appears to localise to integrin adhesion sites via interaction with PINCH1, suggesting potential roles in integrin signalling (Karakose et al., 2015). Our group have previously established a link between EPLIN and paxillin (Sanders et al., 2011) and this connection was evaluated further in the previous chapter. Currently, a comprehensive study elucidating the mechanism of action of EPLIN in cancer is yet to be undertaken, and the interactome encompassing EPLIN remains elusive in the literature. This chapter therefore aimed to substantiate this area, and sought to clarify the existing knowledge of EPLIN's mechanism of action in prostate cancer. This was done by performing a protein microarray on PC-3 cells transfected with the pEF6 plasmid

and the EPLINα overexpression plasmid, revealing several molecules whose expression activity was altered following EPLINα overexpression. The current chapter further sought to validate key candidates using conventional means and particularly focuses on the relationship between EPLINα and Src and their involvement in the process of tumour migration and invasion. Overall, this chapter provides mechanistic insights into the suppressive ability of EPLINα on tumour cell characteristics and suggests various avenues for future work on EPLINα signalling in prostate cancer.

7.2 Materials and Methods

7.2.1 Kinexus™ Antibody Microarray and data analysis

PC-3^{pEF6} and PC-3$^{EPLIN\ EXP}$ protein samples were extracted as outlined in section 2.4.3. These samples were subsequently sent to Kinexus Bioinformatics, Canada for protein microarray analysis. Data analysis was performed to determine which proteins were affected when EPLINα is overexpressed in PC-3 cells. For full procedure please see section 2.4.3 and 2.7. This method has also been previously described in (Owen et al., 2016).

7.2.2 Western Blotting verification of Kinexus protein microarray

Western blotting was performed on PC-3 and LNCaP protein extracted from cells previously transfected with the pEF6 vector or the EPLINα expression plasmid. Molecules selected from the Kinexus™ protein microarray were screened and expression levels were determined in PC-3 and LNCaP cell lines transfected with the pEF6 and EPLINα expression plasmids to validate the protein microarray. For full procedure please refer to section 2.4.

7.2.3 *In vitro* tumour invasion assay with dasatinib inhibitor

Cells were seeded into 24 well plates containing cell culture inserts with a Matrigel layer as described in section 2.6.7. Following a 3 day incubation period, the number of cells which had penetrated and invaded the artificial basement membrane was fixed, stained and visualised under the microscope. The invasive capacity of both control PC-3/LNCaP^{pEF6} cells and PC-3/LNCaP$^{EPLIN\ EXP}$ cells was determined in addition to PC-3/LNCaP^{pEF6} cells and PC-3/LNCaP$^{EPLIN\ EXP}$ cells treated with Src

inhibitor (dasatinib) at a concentration of 500nM. For full procedure and treatment calculations see section 2.6.7 and 2.6.5.

7.2.4 *In vitro* tumour migration/wound healing assay with dasatinib inhibitor

PC-3 cells were seeded into 24 well plates one day prior to the day of the experiment ensuring sufficient cells to reach a confluent monolayer. A wound healing assay was performed and photos were taken at each one hour interval over a four hour experiment. Migratory potential of the cells was then determined for PC-3/LNCaP^{pEF6} cells and PC-3/LNCaP$^{EPLIN\ EXP}$ cells both with and without the addition of Src inhibitor (dasatinib) at a concentration of 500nM. For full procedure and treatment calculations see section 2.6.9 and 2.6.5

7.2.5 *In vitro tumour* migration transwell assay with dasatinib inhibitor

LNCaP cells were seeded into cell culture inserts utilising a chemo attractant media Following 3 day incubation, the number of cells which had migrated through the pores of the insert were stained and visualised on the microscope. The migratory capacity of both control PC-3/LNCaP^{pEF6} cells and PC-3/LNCaP$^{EPLIN\ EXP}$ cells was determined in addition to PC-3/LNCaP^{pEF6} cells and PC-3/LNCaP$^{EPLIN\ EXP}$ cells treated with Src inhibitor (dasatinib) at a concentration of 500nM. For full procedure and treatment calculations see section 2.6.10 and 2.6.5

7.2.6 Statistical analysis

Comparisons between different groups were made using two sample t test where appropriate using the Sigmaplot 11 software package. All experiments were carried out a minimum of three independent times and $p< 0.05$ was regarded as statistically

significant. Micro array analysis of the Kinexus protein array chip was performed by Kinexus Bioinformatics. Within the chip analysis a z-ratio of > 1.64 or < -1.64 was deemed statistically significant.

7.3 Results

7.3.1 Protein microarray analysis and potential downstream signalling mechanisms

To evaluate potential mechanisms and signalling pathways of EPLINα, PC-3 samples transfected with the pEF6 plasmid and the EPLINα overexpression plasmid were sent to Kinexus Bioinformatics, Canada, for a protein microarray to be undertaken on the Kinexus850 platform. The microarray screens 877 commercial antibodies from various companies and deduces the change in expression (if any) of these molecules between control and treated samples (Figure 7.1). For this study, control samples were PC-3 cells transfected with the pEF6 plasmid and were compared to PC-3 cells transfected with the EPLINα overexpression plasmid. Antibodies screened by Kinexus include both Pan-specific (total) molecules and phospho-molecules. Tables 7.1-7.4 display the top molecules of interest from the microarray. Table 7.1 shows the top total molecules, detected by pan-specific antibodies, which are significantly upregulated in PC-3 when EPLINα is overexpressed. p53 was highlighted as a potential molecular of interest for further validation. Table 7.2 shows the top phospho-specific molecules which are significantly upregulated in PC-3 when EPLINα is overexpressed. PAK1/2/3, p53, ILK and ITGB1 were highlighted as potential molecules of interest for further validation. Table 7.3 shows the top total molecules, detected by pan-specific antibodies, which are significantly downregulated in PC-3 when EPLINα is overexpressed. ERK1 was highlighted as a potential molecule of interest for further validation. Table 7.4 shows the top phospho-specific molecules which are significantly downregulated in PC-3 when EPLINα is overexpressed. Src, ERK1 and ERK1/2 were highlighted as potential molecules of interest for further validation.

Highlighted rows indicate molecules of particular interest or with previous established links in the literature to EPLIN biology. Figure 7.2-Figure 7.4 are graphical representations of molecules which are significantly up/downregulated in response to EPLINα overexpression in PC-3 cells.

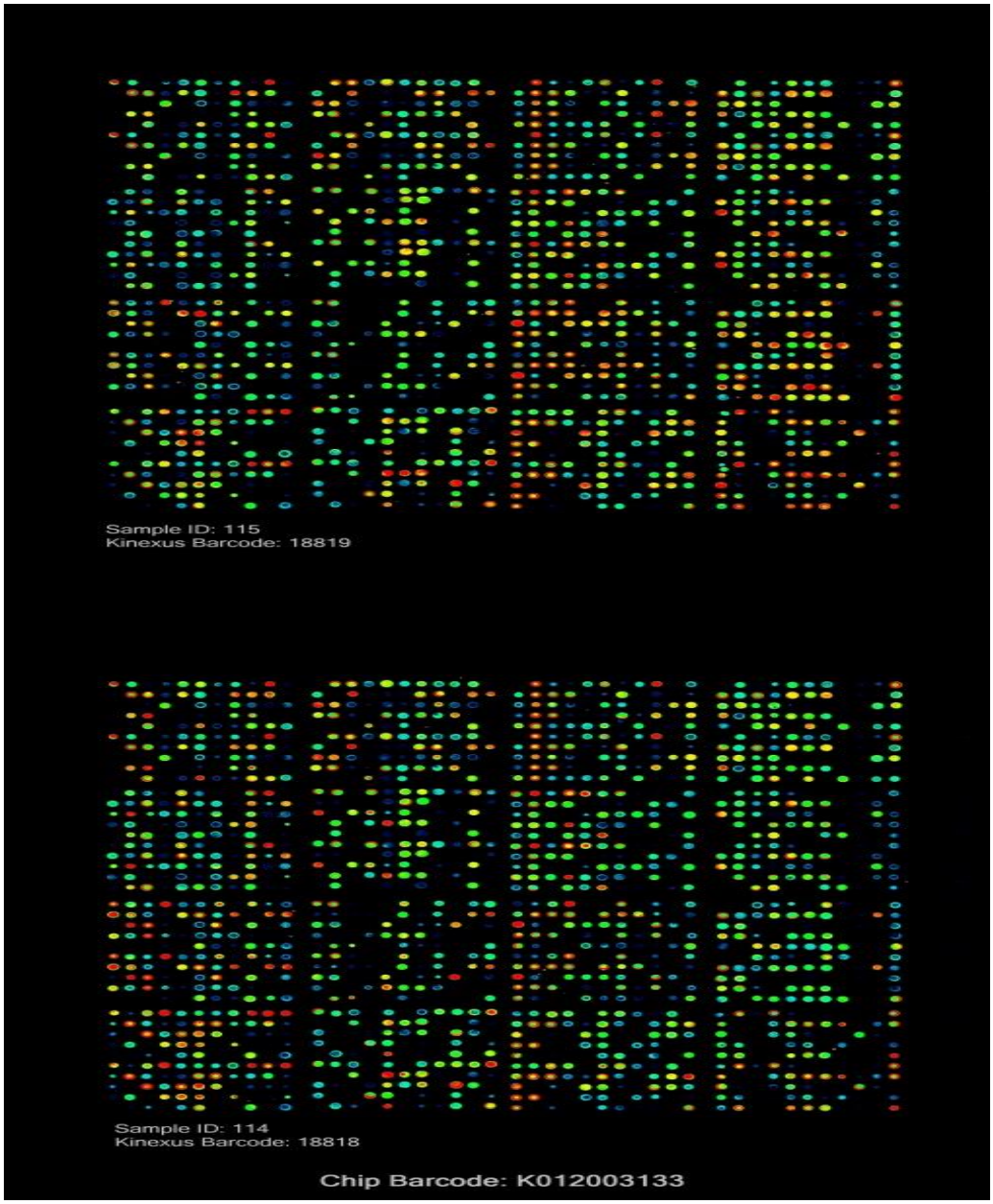

Figure 7.1 Sample image of Kinexus850 protein array.

Sample 114: $PC3^{pEF6}$ control cells (bottom); Sample 115: $PC3^{EPLIN\ EXP}$ cells (top). The level of protein expression correlates with the signal intensity of the antibody tested. Different colours represent different signal intensities and decreasing signal intensity corresponds with a red to orange to yellow to green to blue transition.

Table 7.1 Results from protein microarray. Total, pan-specific, molecules significantly upregulated in response to increased EPLINα expression.

Molecules of potential interest are highlighted in yellow.

Target Protein Name	Phospho Site (Human)	Full Target Protein Name	Globally Normalized - PC-3 pEF6	Globally Normalized - PC-3 EPLIN EXP	Z-ratio (pEF6 vs. EPLIN EXP)
PTEN	Pan-specific	Phosphatidylinositol-3,4,5-trisphosphate 3-phosphatase and protein phosphatase and tensin homolog deleted on chromosome 10	33	212	6.76
SNF1lK	Pan-specific	Serine/threonine-protein kinase SIK1	43	183	5.31
JNK1	Pan-specific	Jun N-terminus protein-serine kinase (stress-activated protein kinase (SAPK)) 1	184	337	2.37
p53	Pan-specific	Tumour suppressor protein p53 (antigenNY-CO-13)	3981	7542	2.23
Trail	Pan-specific	Tumour necrosis factor-related apoptosis-inducing ligand	5	9	2.18
p38d MAPK	Pan-specific	Mitogen-activated protein-serine kinase p38 delta (MAPK13)	11039	20477	2.08
SIK2	Pan-specific	Serine/threonine-protein kinase SIK2	10480	18463	1.91
PP2A/Ca	Pan-specific	Protein-serine phosphatase 2A - catalytic subunit - alpha isoform	356	566	1.83
PKD (PKCm)	Pan-specific	Protein-serine kinase C mu (Protein kinase D)	3580	5955	1.80

MEK4	Pan-specific	MAPK/ERK protein-serine kinase 4 (MKK4)	7179	11993	1.76
Cdc2 p34	Pan-specific	Cyclin-dependent protein-serine kinase 1	6018	9994	1.76
Cdc25A	Pan-specific	Cell division cycle 25A phosphatase	8252	13722	1.73
SHIP1	Pan-specific	Phosphatidylinositol-3,4,5-trisphosphate 5-phosphatase 1	7803	12868	1.71
MST1	Pan-specific	Mammalian STE20-like protein-serine kinase 1 (KRS2)	265	403	1.71
PP2B/Aa	Pan-specific	Protein-serine phosphatase 2B - catalytic subunit - alpha isoform	132	197	1.70
JNK3	Pan-specific	Jun N-terminus protein-serine kinase (stress-activated protein kinase (SAPKb) 3	6067	9795	1.66
MEK6	Pan-specific	MAPK/ERK protein-serine kinase 6 (MKK6)	198	294	1.64

Table 7.2 Results from protein microarray. Phospho-specific molecules significantly upregulated in response to increased EPLINα expression.

Molecules of potential interest are highlighted in yellow.

Target Protein Name	Phospho Site (Human)	Full Target Protein Name	Globally Normalized - PC-3 pEF6	Globally Normalized - PC-3 EPLIN EXP	Z-ratio (pEF6 vs. EPLIN EXP)
PLCg2	Y753	1-phosphatidylinositol-4,5-bisphosphate phosphodiesterase gamma-2	176	415	3.23
p38a MAPK	T180/Y182	Mitogen-activated protein-serine kinase p38 alpha	391	856	2.91
STAT3	Y704	Signal transducer and activator of transcription 3	919	2012	2.84
PAK1/2/3	S144/S141/S154	p21-activated kinase 1 (alpha) (serine/threonine-protein kinase PAK 1)	214	434	2.70
ALK	Y1507	Anaplastic lymphoma kinase	2681	5658	2.63
PYKSD8	pTyr	Phosphotyrosine residue located near kinase subdomain 8	17	31	2.55
4E-BP1	S65	Eukaryotic translation initiation factor 4E binding protein 1 (PHAS1)	238	450	2.45
IkBa	Y42	Inhibitor of NF-kappa-B alpha (MAD3)	225	418	2.39
IGF1R	Y1280	Insulin-like proliferation factor 1 receptor protein-tyrosine kinase	862	1626	2.34
IKKa	T23	Inhibitor of NF-kappa-B protein-serine kinase alpha (CHUK)	186	333	2.28
MKK3	S189	MAPK/ERK protein-serine kinase 3 beta isoform (MKK3 beta)	100	175	2.25

Dab1	Y198	Disabled homolog 1	537	968	2.22
IRS1	S639	Insulin receptor substrate 1	181	301	2.04
p53	S6	Tumour suppressor protein p53 (antigenNY-CO-13)	552	927	1.98
PTEN	S380/T382/T383	Phosphatidylinositol-3,4,5-trisphosphate 3-phosphatase and protein phosphatase and tensin homolog deleted on chromosome 10	172	279	1.96
p90 RSK	S352	Ribosomal S6 protein-serine kinase 1	284	461	1.92
GATA1	S142	Erythroid transcription factor	173	275	1.88
4G10	pTyr	Phosphotyrosine (Clone 4G10)	3925	6694	1.88
Fos	T232	Fos-c FBJ murine osteosarcoma oncoprotein-related transcription factor	564	901	1.81
ILK1	Y351	Integrin-linked protein-serine kinase 1	1631	2649	1.78
Integrin b1	S785	Integrin beta 1 (fibronectin receptor beta subunit, CD29 antigen)	757	1181	1.71
EGFR	T693	Epidermal proliferation factor receptor-tyrosine kinase	508	773	1.66
Smad2	T220	Mothers against decapentaplegic homolog 2	321	482	1.65
InsR	Y1189	INSR insulin receptor	1867	2915	1.64

Table 7.3 Results from protein microarray. Total, pan-specific, molecules significantly downregulated in response to increased EPLINα expression.

Molecules of potential interest are highlighted in yellow.

Target Protein Name	Phospho Site (Human)	Full Target Protein Name	Globally Normalized - PC-3 pEF6	Globally Normalized - PC-3 EPLIN EXP	Z-ratio (pEF6 vs. EPLIN EXP)
LIMK1	Pan-specific	LIM domain kinase 1	888	510	-1.68
ERK1	Pan-specific	Extracellular regulated protein-serine kinase 1 (p44 MAP kinase)	21383	13225	-1.69
Nek2	Pan-specific	NIMA (never-in-mitosis)-related protein-serine kinase 2	5		-1.71
CSF1R	Pan-specific	Macrophage colony-stimulating factor 1 receptor	25812	15740	-1.75
Catenin b	Pan-specific	Catenin (cadherin-associated protein) beta 1	3887	2260	-1.76
HSF4	Pan-specific	Heat shock transcription factor 4	657	362	-1.80
ROKa	Pan-specific	Rho-associated protein kinase 2	508	277	-1.81
RSK1	Pan-specific	Ribosomal S6 protein-serine kinase 1	180	95	-1.83
CrkL (32H4)	Pan-specific	Crk-like protein	9776	5582	-1.90
RONa	Pan-specific	Macrophage-stimulating protein receptor alpha chain	724	387	-1.91

Akt2 (PkBb)	Pan-specific	RAC-beta serine/threonine-protein kinase	56	27	-1.99
p70 S6K	Pan-specific	Ribosomal protein S6 kinase beta-1	197	95	-2.15
RIPK	Pan-specific	Receptor-interacting protein-serine kinase 1	1964	1001	-2.15
STAT3	Pan-specific	Signal transducer and activator of transcription 3 (acute phase response factor)	3322	1669	-2.24
VHR	Pan-specific	Dual specificity protein phosphatase 3	650	296	-2.44
PTP-PEST	Pan-specific	Protein tyrosine phosphatase, non-receptor type 12	125	45	-3.08
HspBP1	Pan-specific	Hsp70 binding protein 1	970	369	-3.09
Cofilin	Pan-specific	Cofilin 1	1399	537	-3.09

Table 7.4 Results from protein microarray. Phospho-specific molecules significantly downregulated in response to increased EPLINα expression.

Molecules of potential interest are highlighted in yellow.

Target Protein Name	Phospho Site (Human)	Full Target Protein Name	Globally Normalized - PC-3 pEF6	Globally Normalized - PC-3 EPLIN EXP	Z-ratio (pEF6 vs. EPLIN EXP)
ERK1	S74	Extracellular regulated protein-serine kinase 1 (p44 MAP kinase)	12481	7612	-1.69
VEGFR2	Y1059	Vascular endothelial proliferation factor receptor-tyrosine kinase 2 (Flk1)	1205	691	-1.72
PDGFRa	Y762	Platelet-derived proliferation factor receptor kinase alpha	50	27	-1.72
Rac1/cdc 42	S71	Ras-related C3 botulinum toxin substrate 1	576	324	-1.73
RSK1/2	S221/S2 27	Ribosomal S6 protein-serine kinase 1	1888	1085	-1.74
LIMK1/2	Y507/T5 08	LIM domain kinase 1	4315	2498	-1.78
Src	Y418	Src proto-oncogene-encoded protein-tyrosine kinase	901	488	-1.88
NMDAR 1	S896	N-methyl-D-aspartate (NMDA) glutamate receptor 1 subunit zeta	1098	595	-1.90
RSK1/2	S363/S3 69	Ribosomal S6 protein-serine kinase 1	789	423	-1.91
RSK1/2	S380/S3 86	Ribosomal S6 protein-serine kinase 1	757	405	-1.91

eIF2a	S52	Eukaryotic translation initiation factor 2 alpha	1688	895	-2.01
Huntingtin	S421	Huntington's disease protein	162	81	-2.01
B23 (NPM)	T234/237	B23 (nucleophosmin, numatrin, nucleolar protein NO38)	915	471	-2.06
NFKB p65	S536	NF-kappa-B p65 nuclear transcription factor	1432	738	-2.09
NFKB p65	S529	NF-kappa-B p65 nuclear transcription factor	488	230	-2.31
ERK1/2	T202	Extracellular regulated protein-serine kinase 1 (p44 MAP kinase) + Extracellular regulated protein-serine kinase 2 (p42 MAP kinase)	1356	630	-2.43
Raf1	S259	Raf1 proto-oncogene-encoded protein-serine kinase	227	98	-2.55
Cyclin E	T395	Cyclin E1	2328	1056	-2.56
TrkB	Y705	BNDF/NT3/4/5 receptor- tyrosine kinase	481	209	-2.57
BRCA1	S1423	Breast cancer type 1 susceptibility protein	1295	572	-2.61
ERK1/2	Y204	Extracellular regulated protein-serine kinase 1 (p44 MAP kinase) + Extracellular regulated protein-serine kinase 2 (p42 MAP kinase)	824	350	-2.70
MEK1	S298	MAPK/ERK protein-serine kinase 1 (MKK1)	47	11	-4.41

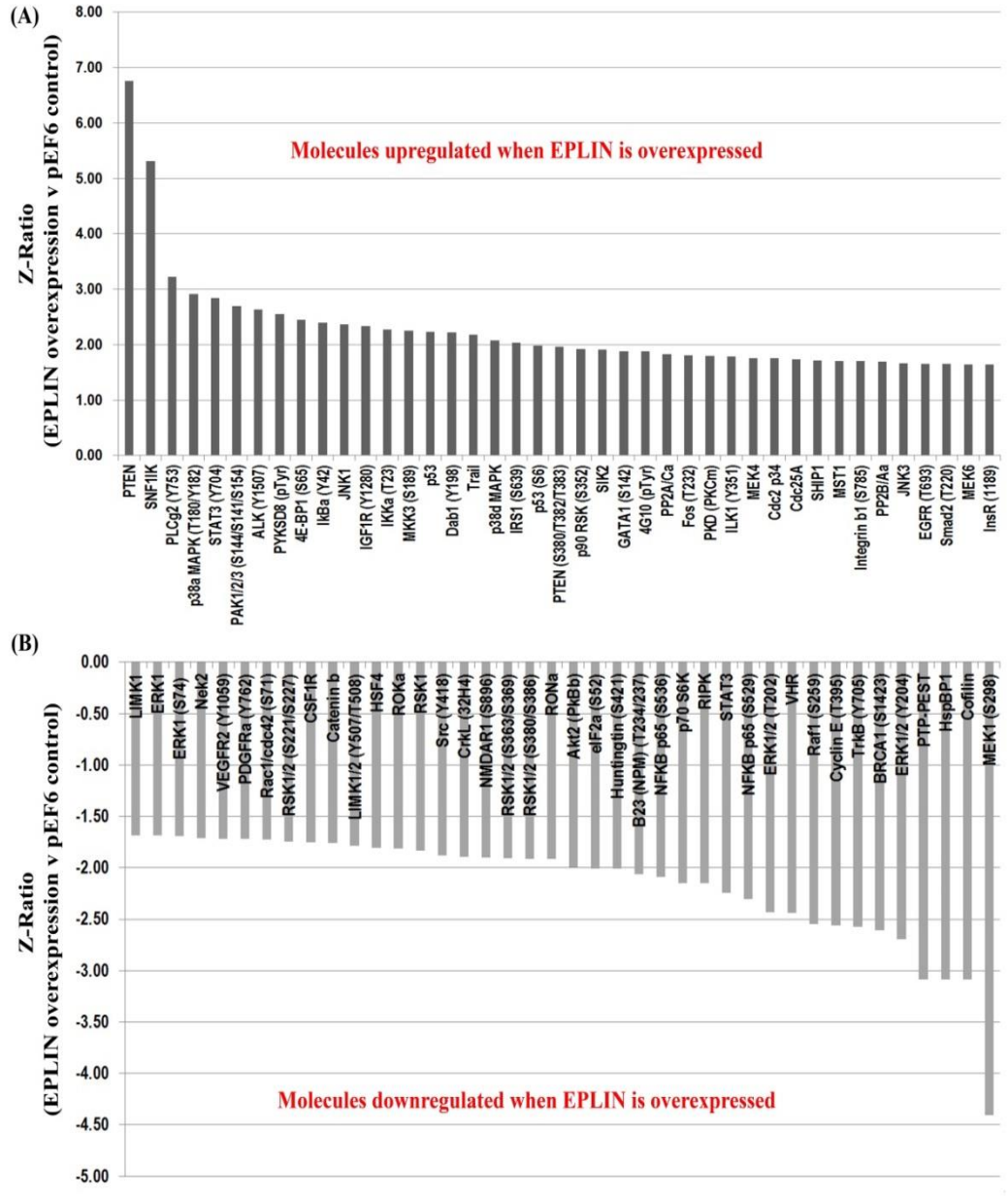

Figure 7.2 Protein microarray summary: top molecules (both total and phospho) significantly up/downregulated in response to EPLINα expression in PC-3.

(A) Molecules with highest significance upregulated in response to EPLINα expression in PC-3. (B) Molecules with highest significance downregulated in response to EPLINα expression in PC-3. Significance was determined used the z-ratio; a z-ratio of > 1.64 or < -1.64 was deemed statistically significant.

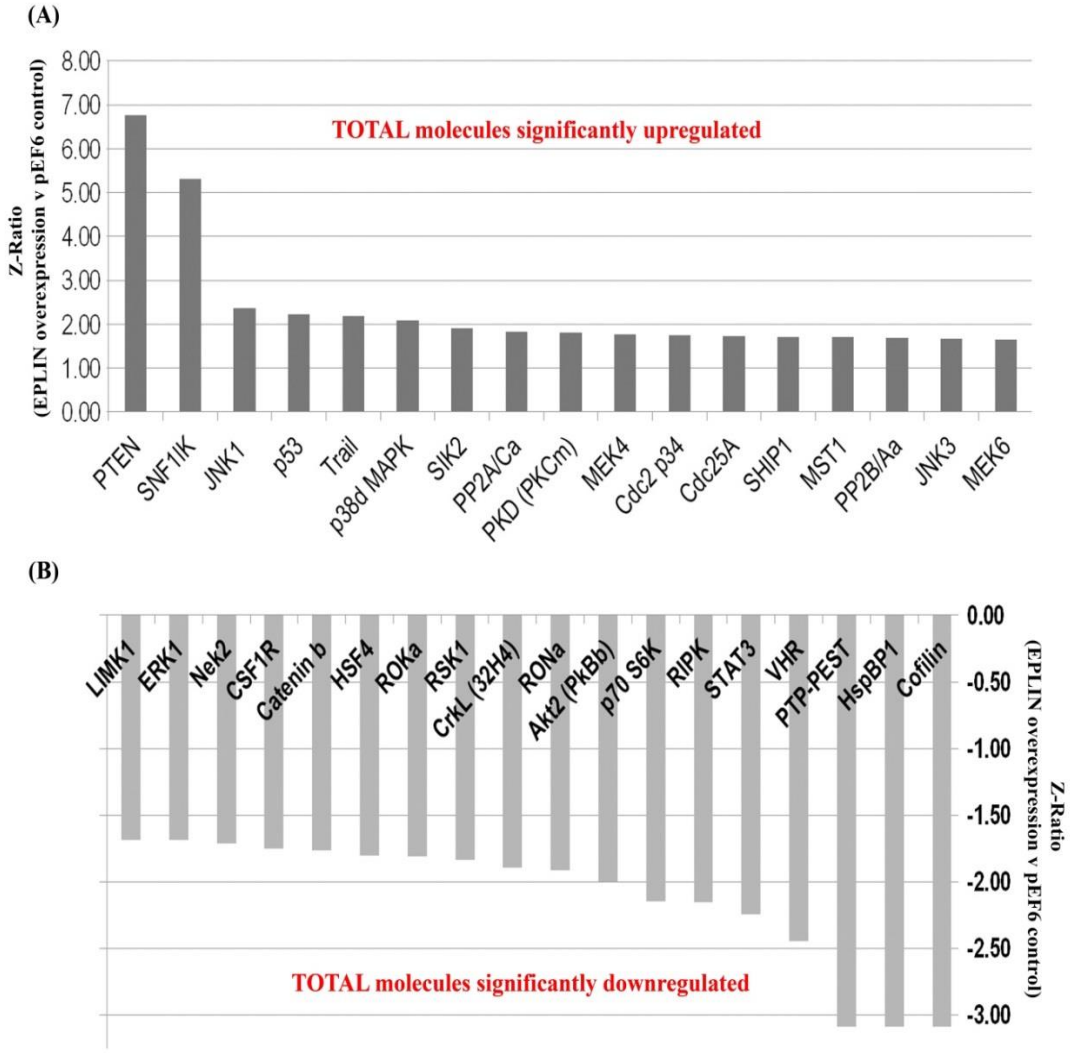

Figure 7.3 Top total molecules significantly up/downregulated in response to EPLINα expression in PC-3.

(A) Molecules with highest significance upregulated in response to EPLINα expression in PC-3. (B) Molecules with highest significance down regulated in response to EPLINα expression in PC-3. Significance was determined used the z-ratio; a z-ratio of > 1.64 or < -1.64 was deemed statistically significant.

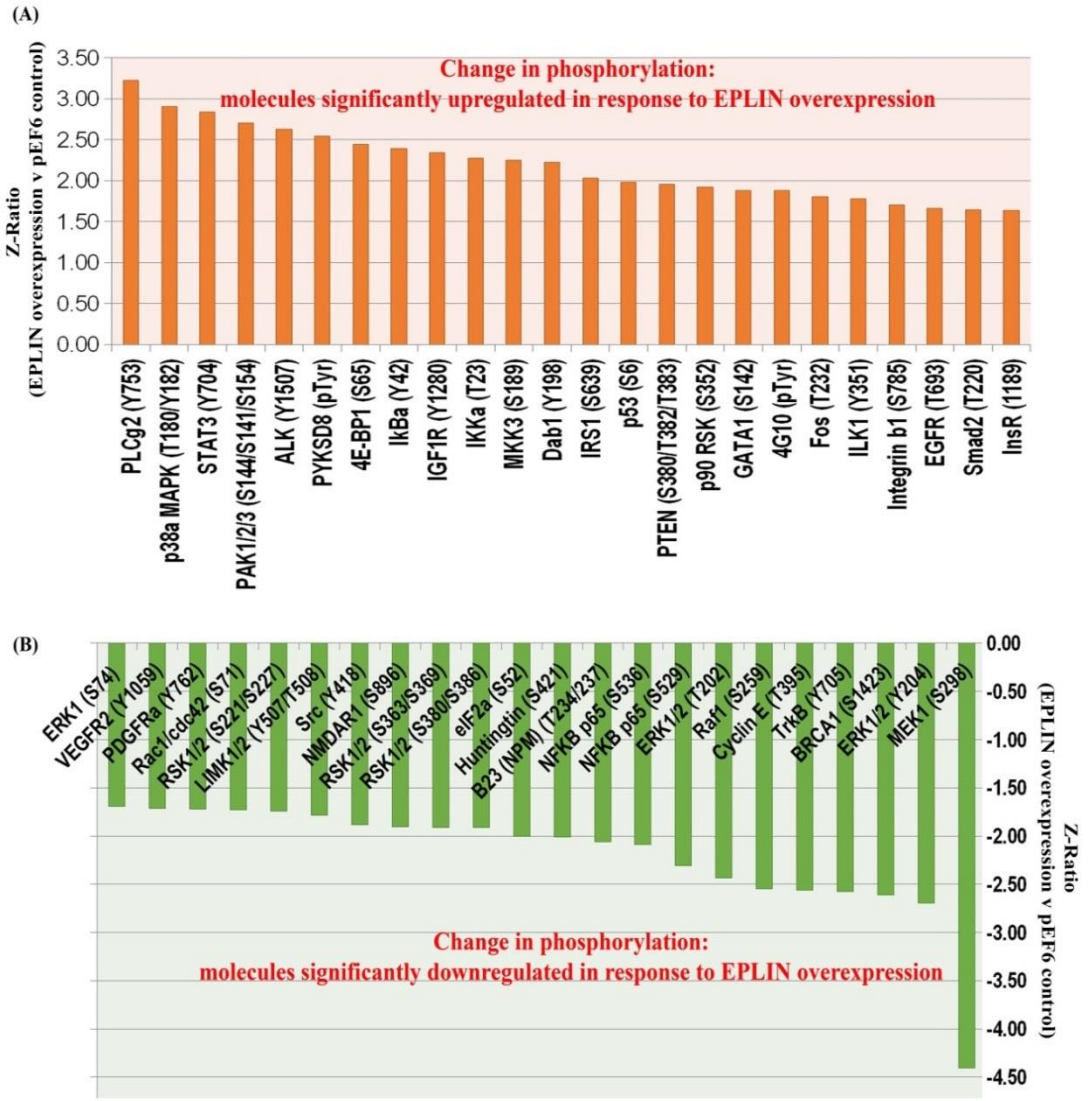

Figure 7.4 Change in phosphorylation (either up or downregulated) in response to EPLINα overexpression in PC-3.

(A) Phosphorylated molecules with highest significance upregulated in response to EPLINα expression in PC-3. (B) Phosphorylated molecules with highest significance down regulated in response to EPLINα expression in PC-3. Significance was determined used the z-ratio; a z-ratio of > 1.64 or < -1.64 was deemed statistically significant.

7.3.2 Protein microarray analysis: molecules chosen for verification and validation

Following data analysis of the Kinexus protein microarray, several molecules of interest were highlighted. These included p53, Serine/threonine-protein kinase 1/2/3 (PAK1/2/3), integrin linked kinase 1 (ILK1), integrin B1 (ITGB1), ERK1/2 and Src. These molecules were chosen either as they have been previously linked to EPLIN in the literature, or that they were potentially functionally linked to EPLIN through operating similar functions in cancer. Molecules chosen for validation within this chapter were ITGB1, ERK1/2 and Src.

7.3.2.1 Integrin B1 (ITGB1) and Integrin Linked Kinase 1 (ILK1)

Figure 7.5shows the Kinexus protein microarray results for ITGB1 and ILK1 and the subsequent validation of ITGB1 in PC-3 and LNCaP cells. The Kinexus microarray probed a number of different integrin receptor related molecules over the entire chip and these are highlighted in Figure 7.5A. ILK1 was shown to be significantly upregulated (z-ratio > 1.64) at region Y351 in PC-3$^{EPLIN\ EXP}$, suggesting enhanced ILK phosphorylation in ILK following EPLINα overexpression in PC-3. This region however wasn't validated by Western Blot as no commercial antibodies were available for this region at the time of analysis. A significant increase in a S785 phosphoylation of ITGB1 was indicated with a z-ratio of greater than 1.64 obtained. To validate this observation, a commercial antibody, specific for ITGB1 S785, was purchased. Unfortunately, the purchased antibody did not show any clear detection (data not shown) despite optimisation of conditions and no other suppliers were available, hence this phospho site could not be validated at this time. Total ITGB1 was therefore sourced and tested for expression levels in PC-3 and LNCaP. Total

ITGB1 expression was enhanced following EPLINα overexpression in PC-3 cells (Figure 7.5B) and this observation was found to be statistically significant following semi-quantitative analysis and normalisation against GAPDH ($p=0.01$). In LNCaP, no significant change in ITGB1 expression was visualised between $LNCaP^{pEF6}$ cells and $LNCaP^{EPLIN\ EXP}$ cells. Band intensity was normalised to GAPDH and each was tested for n=3 in PC-3 and LNCaP. It's important to note that total ITBG1 wasn't actually detected in the Kinexus array. However, though S785 of ITGB1 could not be validated, there is evidence to suggest EPLINα regulates ITGB1 via enhancing total protein content, at least in the PC-3 cell model.

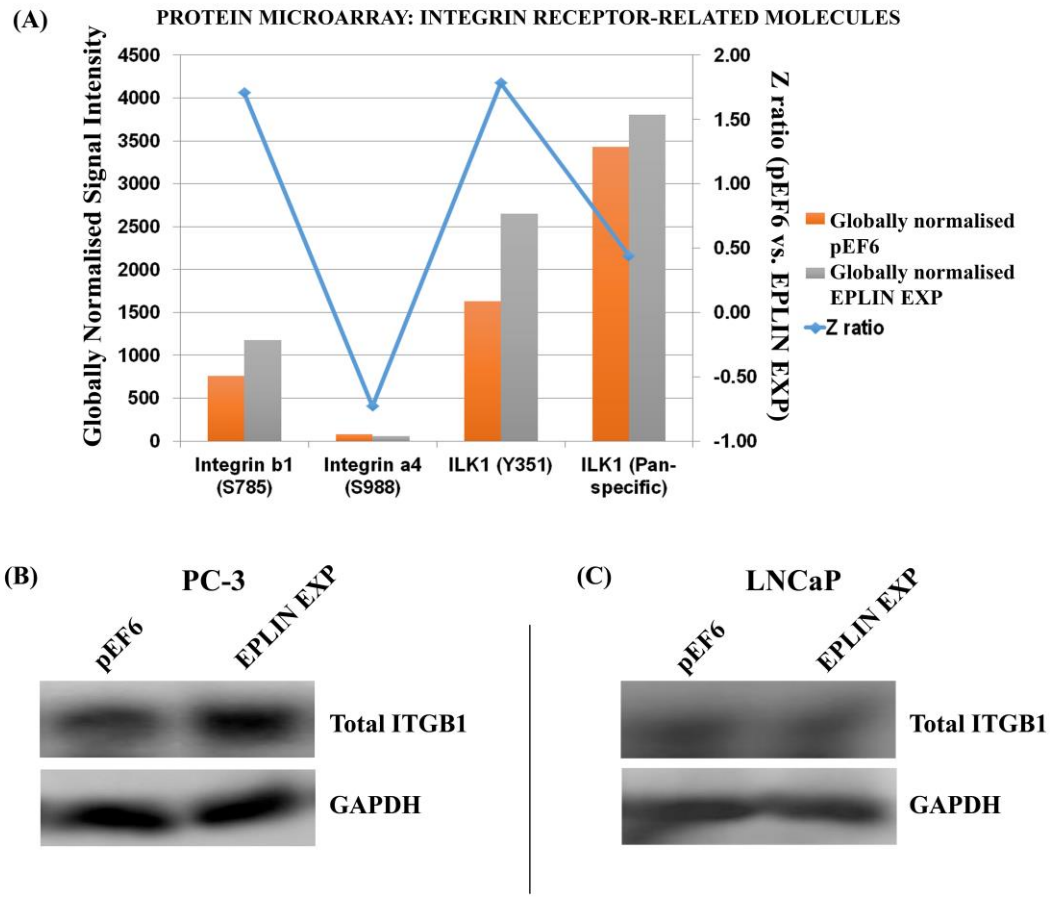

Figure 7.5 Protein microarray results: Integrin receptor-related molecules.

ITGB1 was highlighted as a potential molecule of interest following the protein microarray. Specifically the region of S785 was significantly upregulated in response to EPLINα overexpression in PC-3. (A) Integrin receptor related-regions screened in Kinexus protein microarray. ITGB1 S785 significantly upregulated with z ratio of >1.64. (B) ITGB1 protein validation in PC-3 using Western blot analysis. (C) ITGB1 validation in LNCaP using Western blot analysis. Representative gel images shown of n=3 repeats in PC-3 and LNCaP. Significance was determined used the z-ratio; a z-ratio of > 1.64 or < -1.64 was deemed statistically significant.

7.3.2.2 Extracellular Signal-Regulated Kinase 1/2 (ERK1/2)

Following data analysis from the Kinexus protein microarray, ERK1/2 was highlighted as a potential molecule of interest for EPLIN association. From the microarray, ten regions of ERK1/2 all showed a total loss of Globally Normalised Signal Intensity in either total ERK1/2 protein or a loss of phosphorylation of ERK1/2 when EPLINα was overexpressed in PC-3 (Figure 7.6A). Interestingly, total ERK1 was probed using three separate antibodies within the array and was shown to be significantly downregulated, following, EPLINα overexpression in one of the tested antibodies, scoring a z value of < -1.64. The other two tested antibodies both showed general decreases by these did not fall below the z ratio of -1.64. In addition, ERK1 (S74), ERK1/2 (Y204) and ERK1/2 (T202) were all found to be significantly downregulated when EPLINα was overexpressed in PC-3 cells with a z ratio of < -1.64. To validate the Kinexus array, total ERK1/2 and pERK1/2 T202 Y204 expression was screened in PC-3 and LNCaP cells, however no obvious differences were seen between pEF6 and EPLIN EXP transfected cells for either cell line (Figure 7.6B/C). This was subsequently confirmed following semi-quantitative analysis of band intensity and normalisation against GAPDH, indicating no significant differences in expression following EPLINα overexpression in either PC-3 or LNCaP cells (data not shown).

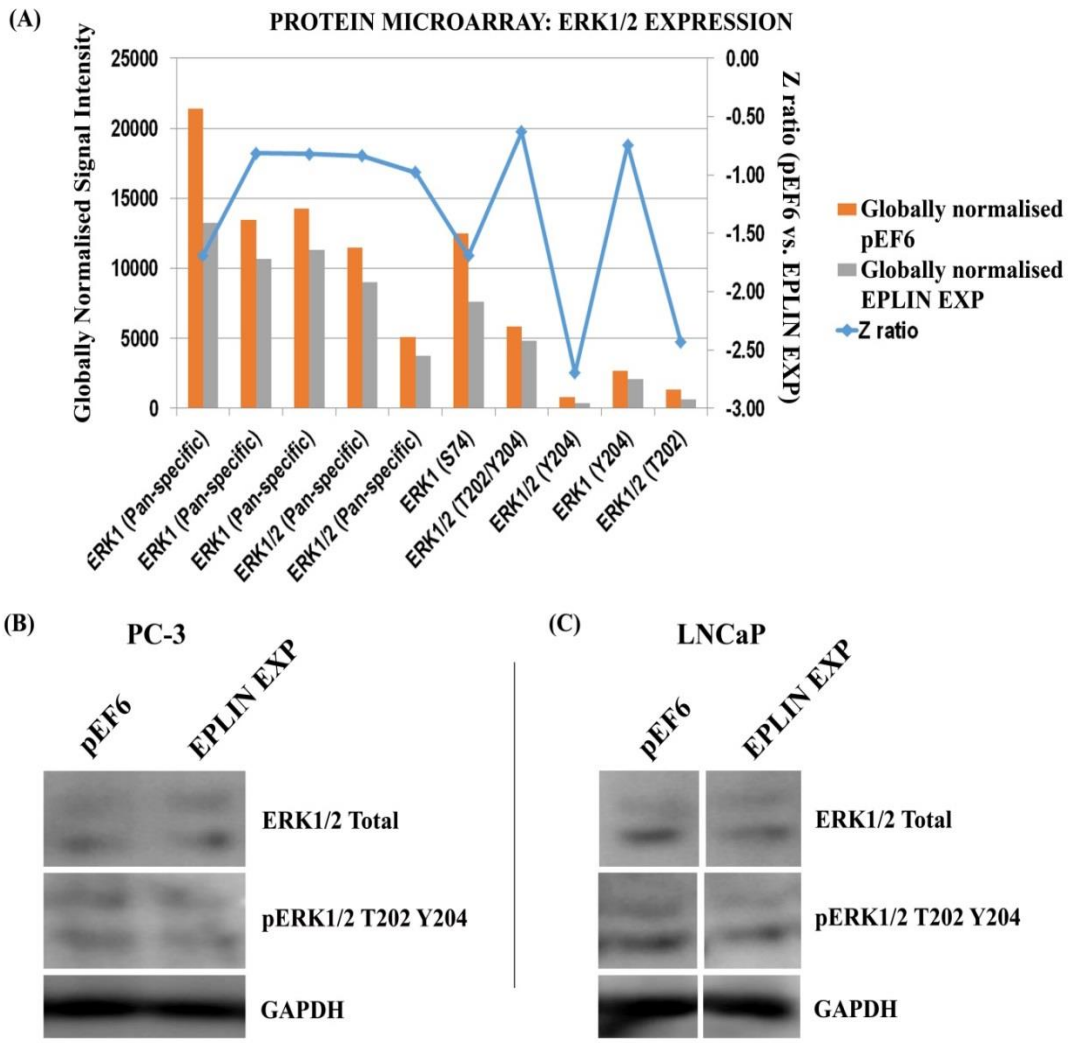

Figure 7.6 Protein microarray results: ERK1/2 expression.

ERK1/2 was highlighted as a potential molecule of interest following the protein microarray. Specifically the region of T202 and Y204 were significantly downregulated in response to EPLINα overexpression in PC-3. (A) All ERK1/2 regions screened in Kinexus protein microarray. ERK1 (Pan-specific), ERK1 (S74), ERK1/2 (Y204) and ERK1/2 (T202) were significantly downregulated with z ratio of <-1.64. (B) ERK1/2 validation in PC-3. Antibodies for ERK1/2 used: Total ERK1/2, and pERK1/2 T202 Y204. (C) ERK1/2 validation in LNCaP. Antibodies for ERK1/2 used: Total ERK1/2, and pERK1/2 T202 Y204. Representative gel images shown of n=3 repeats in PC-3 and LNCaP. Significance was determined used the z-ratio; a z-ratio of > 1.64 or < -1.64 was deemed statistically significant.

7.3.2.3 Proto-oncogene Tyrosine-protein kinase (Src)

Figure 7.7 shows the validation of the Src molecules in PC-3 and LNCaP. The Kinexus microarray revealed a significant decrease in the phosphorylation of the activation site Y419 of Src following overexpression of EPLINα in PC-3 cells. Also present within the microarray chip were several pan-specific probes and the Y529 phosphorylation site of Src, though no significant differences were seen in the signal intensity of such probes with z ratios between 1.64 and -1.64 obtained (Figure 7.7A). An antibody was sourced for this region of Y419 and tested for expression levels in control and EPLINα overexpression PC-3 and LNCaP cells (Figure 7.7B/C). A decrease in band intensity for Src Y419 was seen, which following semi-quantitative analysis, was found to be significantly downregulated in PC-3 (data not shown, $p=0.005$) following EPLINα overexpression and validated the Kinexus result. In LNCaP cells, a reduction of Src Y419 band intensity was seen in $LNCaP^{EPLIN\ EXP}$ cells compared to $LNCaP^{pEF6}$ cells, however this change was not statistically significant following semi-quantitative analysis (data not shown, $p>0.05$). In addition to Src Y419, total Src and Src Y530 was also tested. For PC-3 and LNCaP, no significant differences were seen in total Src expression, which is in keeping with the results of the microarray. Contrary to Src Y419, Src Y530, a common site of dephosphorylation, was enhanced following EPLINα overexpression in PC-3 cells and this trend was confirmed following semi-quantitative band analysis, highlighting a significant increase in PC-3 (data not shown, $p=0.027$) when EPLINα is overexpressed. In LNCaP, Y530 was also increased when EPLINα was overexpressed, however the increase didn't quite reach significance ($p=0.068$) upon

semi-quantitative band analysis (data not shown). Band intensity was normalised to GAPDH and each Src molecule were tested for n=3 in PC-3 and LNCaP.

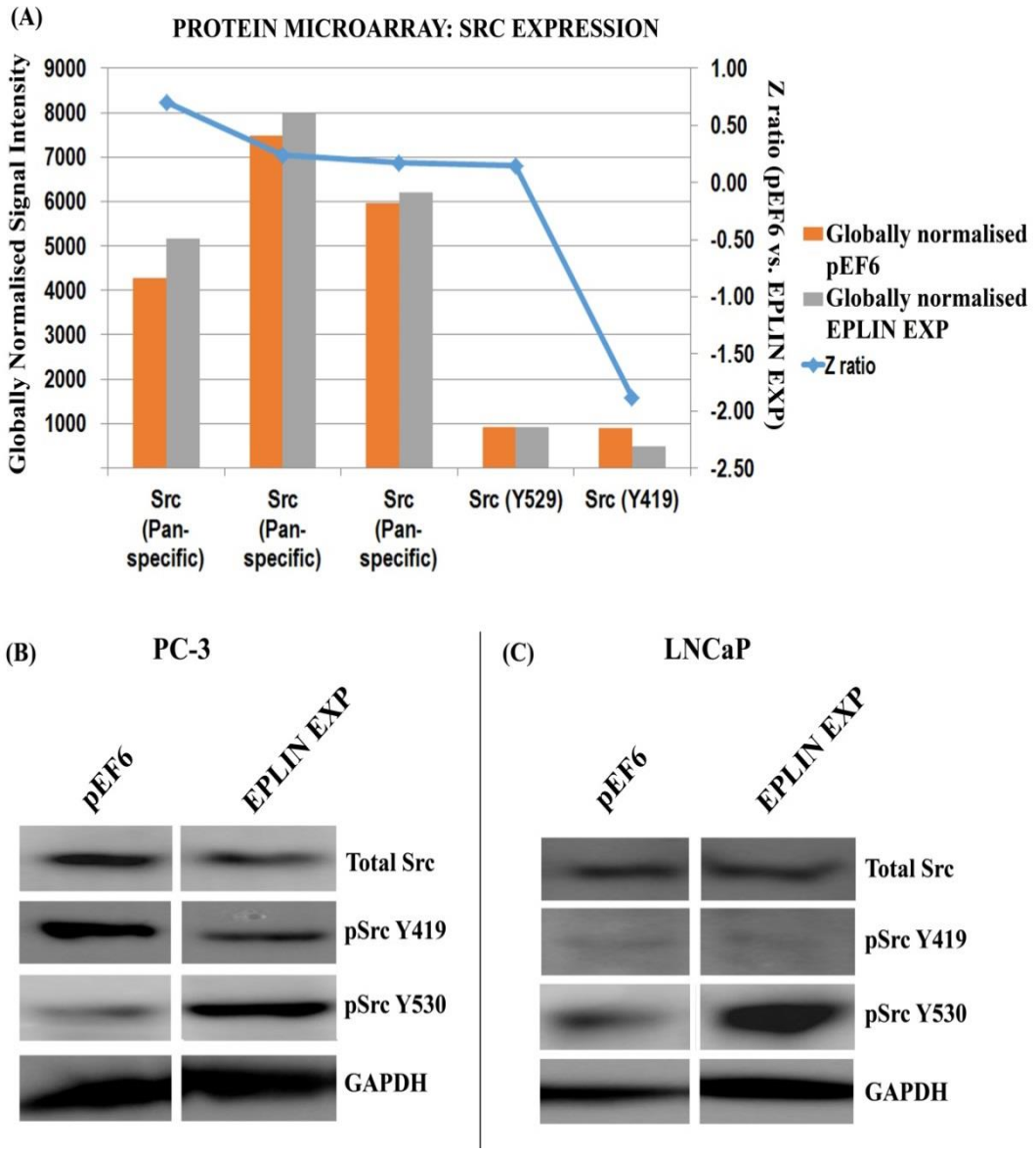

Figure 7.7 Protein microarray results: Src expression.

Src was highlighted as a potential molecule of interest following the protein microarray. Specifically the region of Y419 was significantly downregulated in response to EPLINα overexpression in PC-3. (A) All Src regions screened in Kinexus protein microarray. Src Y419 significantly downregulated with z ratio of <-1.64. (B) Src validation in PC-3. Antibodies for Src used: Total Src, pSrc Y419 and pSrc Y530. (C) Src validation in LNCaP. Antibodies for Src used: Total Src, pSrc Y419 and pSrc Y530. Representative gel images shown of n=3 repeats in PC-3 and LNCaP. Significance was determined used the z-ratio; a z-ratio of > 1.64 or < -1.64 was deemed statistically significant.

7.3.3 Functional analysis with Src inhibitor (dasatinib)

Dasatinib, a Y419 src inhibitor, was employed to further explore the interaction between EPLINα and src in PC-3 and LNCaP cells in various functional assays, to evaluate if src inhibition affects cancer cell traits in addition to EPLINα overexpression. First, PC-3 and LNCaP cells were treated with various dasatinib concentrations overnight and screened by Western Blotting with Src Y419 antibody to confirm the optimal src concentration for use in *in vitro* functional assays (Figure 7.8/Figure 7.9A/B). The optimal concentration chosen was 500nM, as this concentration was shown to inhibit src Y419 expression in PC-3 and LNCaP cells. Subsequently to this, the chosen src concertation was used in various *in vitro* tumour cell functional assays (Figure 7.8B-E/Figure 7.9C-E).

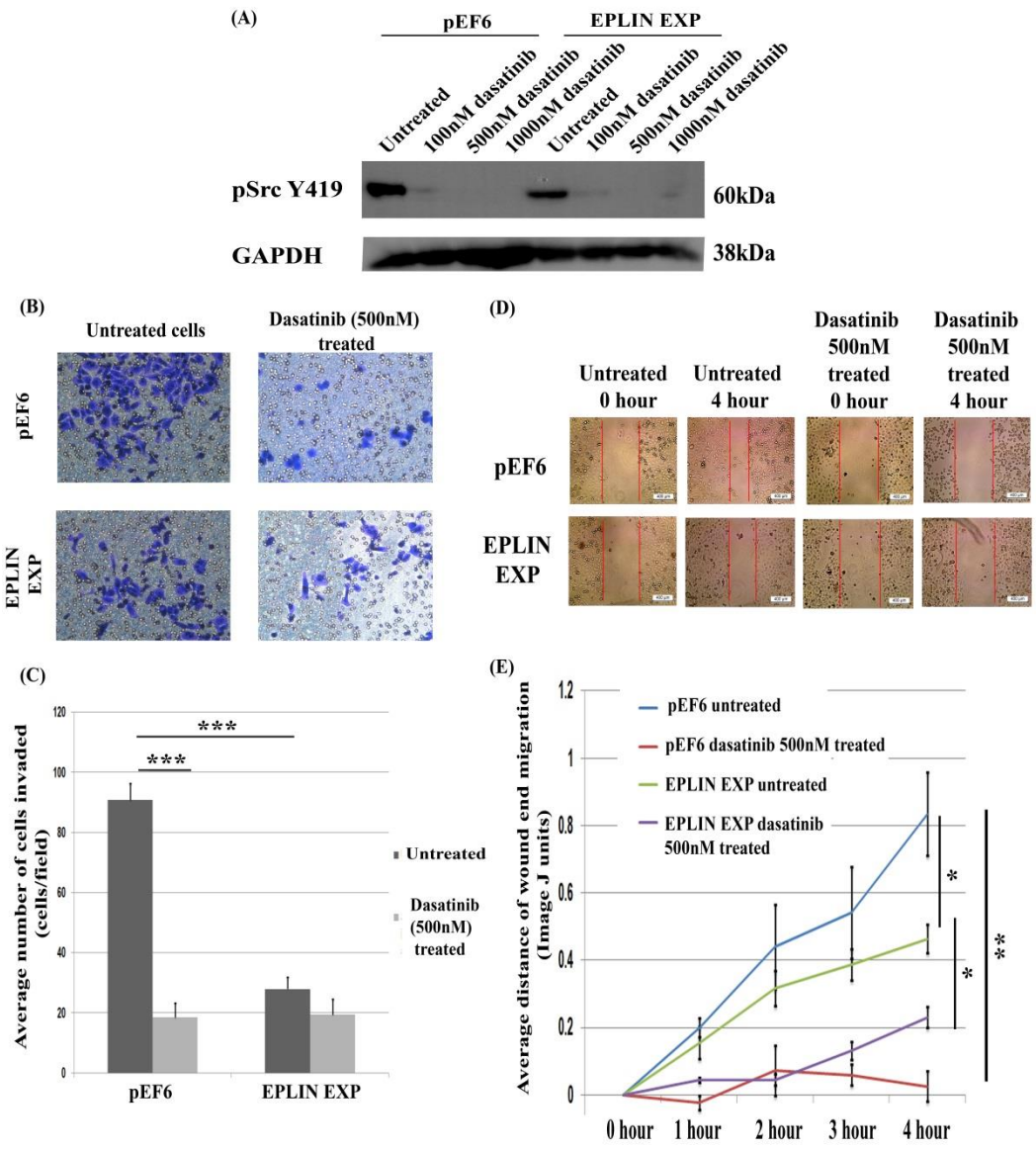

Figure 7.8 Functional assays of PC-3 cells with Src inhibitor (dasatinib).

(A) Src inhibitor concentration screen in PC-3^{pEF6} (pEF6) and PC-3$^{EPLIN\ EXP}$ (EPLIN EXP) cells to assess optimal inhibitor concentration for functional assays. Concentrations tested: 100nM, 500nM and 1000nM. Samples then screened with Src Y419 antibody to assess Src activity levels. (B) PC-3 invasion assay with Src inhibitor. Representative images of PC-3^{pEF6} (pEF6) and PC-3$^{EPLIN\ EXP}$ (EPLIN EXP) cells with/without src inhibitor at concentration 500nM. (C) Graphical representation of cell invasion of PC-3^{pEF6} and PC-3$^{EPLIN\ EXP}$ cells with/without src inhibitor. (D) PC-3 migration/wound healing assay with Src inhibitor. Representative images of PC-3^{pEF6} and PC-3$^{EPLIN\ EXP}$ cells, at 0 hour and 4 hours of scratch assay, with/without src inhibitor. (E) Graphical representation of cell migration of PC-3^{pEF6} and PC-3$^{EPLIN\ EXP}$ cells with/without src inhibitor. Graphs represent mean of n=3 repeats and errors bars show SE of the mean. * = represents $p<0.05$, ** = $p<0.01$, *** = $p<0.001$. Statistical test performed for analysis was a two sample, two tailed t-test using SigmaPlot software.

7.3.3.1 The effect of src inhibition on cellular invasion

The effect of src inhibition was determined in PC-3 cells in an *in vitro* invasion assay (Figure 7.8B/C). Dasatinib treatment caused a significant reduction of cellular invasion of PC-3^{pEF6} cells ($p<0.001$). However, for PC-$3^{EPLIN\ EXP}$ cells, no significant differences were seen on cellular invasion when dasatinib was used (Figure 7.8C). For untreated (no dasatinib) samples, EPLINα overexpression also caused a significant reduction of cellular invasion compared to PC-3^{pEF6} cells ($p<0.001$). Dasatinib was also tested in LNCaP cells in an *in vitro* invasion assay for LNCaP^{pEF6} and LNCaP$^{EPLIN\ EXP}$ cells (Figure 7.9C/D). Dasatinib treatment caused a significant reduction of cellular invasion of LNCaP^{pEF6} cells ($p=0.016$). However, for LNCaP$^{EPLIN\ EXP}$ cells, treatment with dasatinib had no significant effects on cellular invasion (Figure 7.9D). For untreated (no dasatinib) samples, EPLINα overexpression also caused a significant reduction in cellular invasion compared to LNCaP^{pEF6} cells ($p=0.015$).

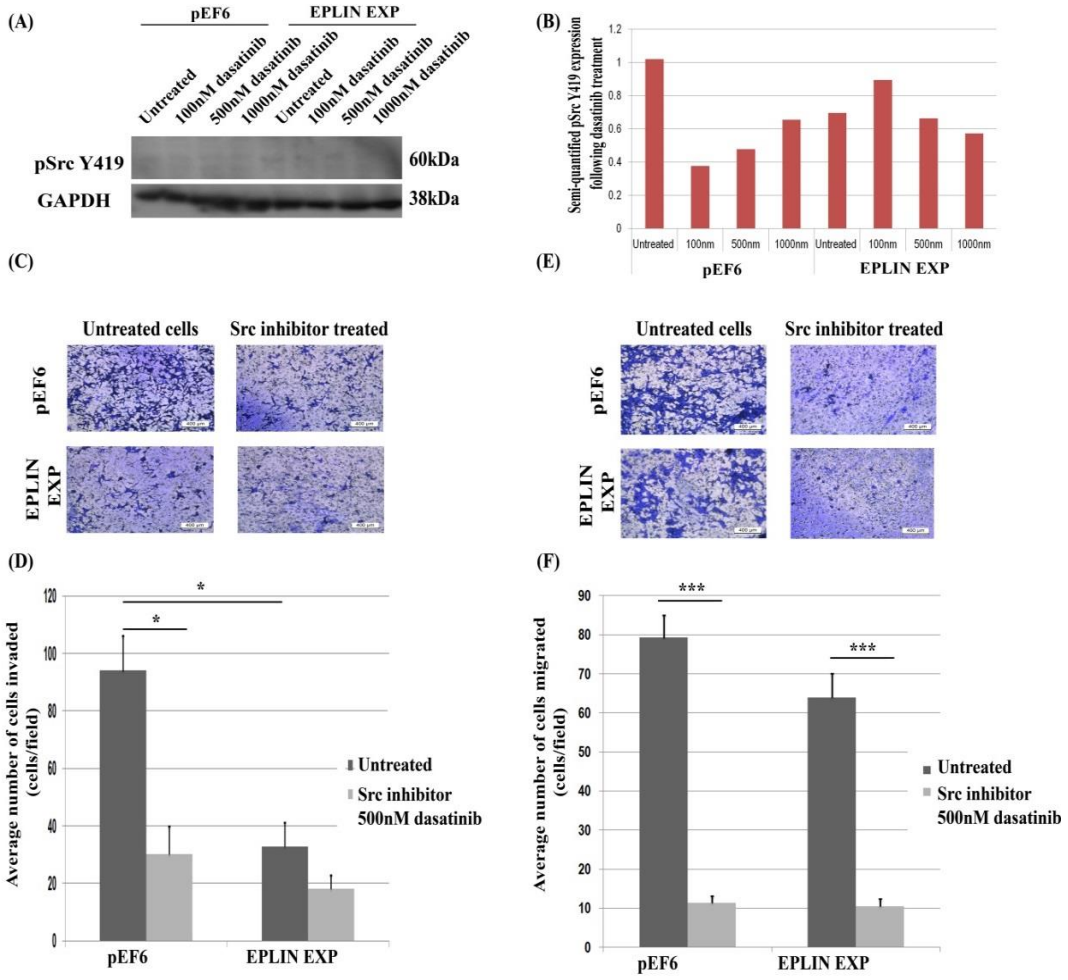

Figure 7.9 Functional assays of LNCaP cells with Src inhibitor (dasatinib).

(A) Src inhibitor concentration screen in LNCaP^{pEF6} and LNCaP$^{EPLIN\ EXP}$ cells to assess optimal inhibitor concentration for functional assays. Concentrations tested: 100nM, 500nM and 1000nM. Samples then screened with Src Y419 antibody to assess Src activity levels. (B) Semi-quantitative analysis of normalised pSrc Y419 band intensities from (A). Src Y419 levels normalised to GAPDH. (C) LNCaP invasion assay with Src inhibitor. Representative images of LNCaP^{pEF6} and LNCaP$^{EPLIN\ EXP}$ cells with/without src inhibitor. (D) Graphical representation of cell invasion of LNCaP^{pEF6} and LNCaP$^{EPLIN\ EXP}$ cells with/without src inhibitor. (E) LNCaP transwell migration assay with Src inhibitor. Representative images of LNCaP^{pEF6} and LNCaP$^{EPLIN\ EXP}$ cells with/without src inhibitor. (F) Graphical representation of cellular migration of LNCaP^{pEF6} and LNCaP$^{EPLIN\ EXP}$ cells with/without src inhibitor. Graphs represent mean of n=3 repeats and errors bars show SE of the mean. * = represents $p<0.05$, *** = $p<0.001$. Statistical test performed for analysis was a two sample, two tailed t-test using SigmaPlot software.

7.3.3.2 The effect of src inhibition on cell migration

In addition to the cellular invasion assay, dasatinib was also used in two *in vitro* migration assays: a scratch/wound healing assay for PC-3 cells, and a transwell migration assay for LNCaP cells. For the wound healing assay, dasatinib treatment caused a significant reduction of cellular migration of PC-3^{pEF6} cells following a 4 hour time point ($p=0.004$) (Figure 7.8E). For PC-3$^{EPLIN\ EXP}$ cells, cellular migration was also significantly reduced when dasatinib was used at the four hour time point, though not to as great an extent ($p=0.027$) (Figure 7.8E). For untreated (no dasatinib) samples, EPLINα overexpression again caused a significant reduction in cellular migration when compared to untreated PC-3^{pEF6} cells ($p=0.047$) (Figure 7.8E). Dasatinib was also tested in LNCaP cells in an *in vitro* transwell migration assay for LNCaP^{pEF6} and LNCaP$^{EPLIN\ EXP}$ cells (Figure 7.9E/F). Dasatinib treatment caused a highly significant reduction of cellular migration of LNCaP^{pEF6} cells and LNCaP$^{EPLIN\ EXP}$ cells ($p<0.001$ compared to respective untreated controls) (Figure 7.9F). For untreated (no dasatinib) samples, migration was reduced in cells with EPLINα overexpression cells compared to LNCaP^{pEF6} control cells, however this change was not significant.

7.4 Discussion

This chapter aimed to substantiate and clarify the existing knowledge on the mechanism of action of EPLINα in prostate cancer specifically by evaluating the EPLINα interactome using a protein microarray. Prior to this study, information regarding the mechanism of EPLIN in cancer was lacking, and few studies have comprehensively explored the signalling pathways governing EPLIN's regulatory role in suppressing cancer cell functions like proliferation, migration and invasion. This study has highlighted several areas of interest for EPLINα signalling in prostate cancer, these include: ERK1/2 signalling, Integrin B1 and integrin receptor-related signal and Src signalling pathways.

The Kinexus protein microarray highlighted an upregulation of several integrin receptor-related proteins or phosphorylation events, specifically an increase to ILK1 at region Y351 and the β component of the integrin receptor; ITGB1 (S785). ILK1 Y351 was significantly increased in the protein microarray following EPLINα overexpression in PC-3. ILK is a signalling protein involved in integrin and actin dynamics, has central roles in cellular functions including cellular adhesion, and has implications in cancer progression (Legate et al., 2006). Interestingly, ILK forms a complex with PINCH1 to co-ordinate various cellular functions, and PINCH1 has been previously established as an EPLIN-binding protein (Karakose et al., 2015). Given the evidence that EPLIN binds PINCH1 in (Karakose et al., 2015), and the evidence in this study which suggests EPLINα expression enhances ILK1 phosphorylation at Y351, it could be that EPLINα is responsible for regulating several components of this integrin signalling complex. This could then potentially have diverse implications in cancer, including affecting affinity to the actin

cytoskeleton and influencing cellular adhesion and gene transcription (Legate et al., 2006). Although this was an interesting notion, an antibody specific to the Y351 region of ILK1 was unavailable at the time of this study, so this phosphorylation and association couldn't be validated in PC-3.

ITGB1 is a large protein which functions as a receptor protein to bind components of the ECM, like collagen, fibronectin and fibrinogen, at the cell membrane and co-ordinate cell functions though integrin signalling (Gilcrease, 2007). Knock-down analysis of ITGB1 has demonstrated a reduction of PCa cellular invasion and migration using PC-3 cells (Kurozumi et al., 2016). On the other hand, expression of the α5β1 form of the integrin receptor has been associated with proliferation arrest and a reduction in cell proliferation (Varner et al., 1995). The phosphorylated form of ITGB1 at S785 is associated with increased attachment and inhibition of cell spreading and migration (Mulrooney et al., 2001). As EPLINα overexpression in PC-3 cells induced a significant upregulation of S785 in ITGB1 via the Kinexus protein microarray, this could suggest a potential mechanism for EPLINα's ability to influence cellular function in cancer. This will be discussed further in the next chapter. It is important to note that an antibody specific to the S785 region of ITGB1 was unavailable during the time of this study, and all validation work involving EPLINα expression and ITGB1 was done using an antibody specific to total ITGB1 protein. For that reason, these results require further validation and should be interpreted with caution.

In addition to influencing molecules and components associated to integrin receptor dynamics, EPLINα overexpression in PC-3 also influenced the activity of several ERK molecules. ERK1 total protein and ERK T202/Y204 was significantly

downregulated, in the protein microarray, suggesting a loss of ERK1/2 activity when EPLINα is overexpressed in PC-3 cells. ERK1/2 functions in cell biology as part of the MAPK/ERK pathway which is a huge signalling pathway controlling various cellular functions including cell proliferation, proliferation, cell cycle progression, invasion, cell survival, and metastatic progression (Dhillon et al., 2007). Activation of ERK1/2 is important both physiologically and in cancer, and T202/Y204 are established regions for ERK activity, and are responsible for dual activation within ERK1/2 (Roskoski, 2012). For example, ERK1/2 activation is associated with cell cycle progression and is responsible for induction of positive cell cycle regulatory genes, including Cyclin D1, and a reduction of anti-proliferative molecules (Meloche and Pouyssegur, 2007). Considering this notion, it may be that when EPLINα is expressed in PC-3 cells, it leads to a reduction of ERK1/2 activation at T202/Y204, leading to reduced activity and less available cyclin proteins to progress the cell cycle, and thus leads to a suppression of cell proliferation. This concept is strengthened by the evidenced loss of Cyclin D1 and Cyclin E1 (T395) in the Kinexus protein microarray, where Cyclin E1 shows a significant downregulation in response to EPLINα overexpression (Table 7.4). Cyclin E1 is crucial for G1 progression during the cell cycle, so it could be that EPLINα acts through ERK1/2 signalling to suppress Cyclin E1 and prevent PC-3 cells from leaving the G1 phase of the cell cycle (Mazumder et al., 2004). The role of EPLIN in the cell cycle has been previously explored, showing EPLIN is crucial for cytokinesis and depletion of EPLIN resulted in the formation of multinucleated cells and inefficient clustering various proteins like mitotic regulatory proteins like myosin II, RhoA and Cdc42 to the cleavage furrow, signifying cytokinesis failure (Chircop et al., 2009). EPLIN interacts with various proteins at the cleavage furrow of cytokinesis, including

supervillin, KIF1 and Arv1 (Smith et al., 2010, Sundvold et al., 2016), further highlighting the importance of EPLIN expression for regulating functional cell division.

The Kinexus protein microarray revealed a novel association to the proto-oncogene tyrosine-protein kinase, Src. Src (or c-Src; cellular Src) is a key regulatory molecule of several signalling pathways and contributes to various cellular functions in cancer including cellular adhesion, migration and invasion (Irby and Yeatman, 2000). Src expression is generally up regulated in cancer and activation through the region Y419 has been associated with colon cancer progression (Cartwright et al., 1990), poor survival and increasing tumour size and grade in breast cancer (Elsberger et al., 2009), and correlates with cancer aggressiveness in prostate cancer (Asim et al., 2008, Chang et al., 2008). Phosphorylation at Y419 contributes to Src function and allows Src access to several Src substrates to promote Src activation (Xu et al., 1999). In this study, Src was significantly downregulated at region Y419 in PC-3 cells overexpressing EPLINα. This was subsequently verified by Western Blot in PC-3 and LNCaP cells lines and validated a reduction of Src Y419 expression following EPLINα overexpression. This suggests EPLIN expression may lead to a reduction of Src phosphorylation within the residue. Y419 of Src is known as the classical activation site (Elsberger et al., 2009) so suggests that EPLINα expression induces a reduction of c-Src activity in prostate cancer. Src is an integral protein for integrin signalling-related cellular functions and is synergistic to paxillin and FAK signalling (Irby and Yeatman, 2000). EPLINα could therefore potentially be acting on several integrin-related molecules to control cellular functions in prostate cancer. The role of Src activation in cancer is widely established (Kim et al., 2009), so if

EPLINα functions through Src expression in cancer, this could provide insight into a potential mechanism for EPLINα as a tumour suppressive molecule and this may be a key regulatory role, particularly in relation to cancer progression. Specifically, inhibition of Src activity has been associated with cell cycle arrest, decreased cellular migration and invasion in malignant pleural mesothelioma tissues (Tsao et al., 2007). Activated Src levels (p-Src Y419) were also associated with advanced staged cancer (Tsao et al., 2007). Src is also highly expressed in triple negative breast cancer, and targeting c-Src expression using the inhibitor, dasatinib, has demonstrated potential for controlling breast cancer cell characteristics including migration and invasion (Tryfonopoulos et al., 2011). Thirdly, targeting Src in prostate cancer is able to control cell proliferation, migration and invasion, and several clinical trials have commenced exploiting Src expression (Chang et al., 2008). If EPLINα expression is able to induce a reduction of Src activity in prostate cancer, presumably this may have a negative regulatory effect on various cellular characteristics including focal adhesion turnover, cellular migration and invasion. This potential mechanism will be discussed further in the following chapter.

Western Blot experiments also revealed a significant increase in PC-3 and LNCaP of p-c-Src Y530 when EPLINα is overexpressed (Figure 7.7). Y530 of Src is a known region of dephosphorylation to contributes to negative regulation of Src activity, with phosphorylation of this residue being associated with a less active form of Src (Zhu et al., 2007). When Src is phosphorylated at Y530 it facilitates interaction with the SH2 domain of Src, promoting a reduction of kinase activity (Liu et al., 1993). Considering EPLINα overexpression promotes an increase in Y530 in PC-3 and LNCaP, this could be an additional and/or separate mechanism for controlling

cellular functions via a suppression of Src activity. Y530 is phosphorylated by Tyrosine Protein-Kinase (CSK), which is a ubiquitously expressed protein kinase (Okada and Nakagawa, 1989), so it could be that EPLINα enhances CSK function and/or expression in prostate cancer to increase phosphorylation at Y530 and ultimately induce a less active form of Src.

Recognising the notion that Src may be implicated in the role of EPLINα as a tumour suppressive molecule, various *in vitro* tumour functional assays were performed in PC-3 and LNCaP in presence of a Src inhibitor, dasatinib (Figure 7.8/Figure 7.9). This was done to examine if the suppressive effect of EPLINα overexpression was independent to Src activity, and establish if the two molecules are functionally and mechanistically associated. Dasatinib is a small molecule tyrosine kinase inhibitor used as a commercial treatment under the brand name Sprycel to target various tyrosine kinases including the Src family kinases (Montero et al., 2011). Dasatinib works specifically by inhibiting Y419 phosphorylation of src, and thus, preventing src activity. Dasatinib has been used successfully to treat various cancers including Chronic Myeloid Leukaemia and Acute Myeloid Leukaemia by targeting cellular traits like cell proliferation and duplication, migration and invasion and the induction of apoptosis of tumour cells (Montero et al., 2011, UK). In this study, use of dasatinib reduced cellular invasion of PC-3^{pEF6} cells compared to untreated PC-3^{pEF6} cells. However, use of dasatinib showed no significant differences to cellular invasion of PC-3$^{EPLIN\ EXP}$ cells. This may suggest that EPLINα is acting through regulation of Src expression to suppress cellular invasion, as when EPLINα is present, and Src activity is blocked, the effect on cellular invasion is comparable and not cumulative. For the wound healing assay, dasatinib treatment rendered both PC-

3^{pEF6} and PC-$3^{EPLIN\ EXP}$ cells less motile, with significant reductions at the 4 hour time point, though the level of significance was lower in the PC-$3^{EPLIN\ EXP}$ cells. This again may suggest that Src could be a mechanism of EPLINα suppression on cell migration via EPLINα expression acting through a negative regulation of Src activity, though it may not be the only method of regulation governing Src's role in cellular migration.

Dasatinib was also used in two *in vitro* tumour functional assays for the LNCaP cell model for both LNCaP^{pEF6} and LNCaP$^{EPLIN\ EXP}$ transfected cells (Figure 7.9). For the invasion assay, dasatinib treatment reduced cellular invasion for LNCaP^{pEF6} cells but not LNCaP$^{EPLIN\ EXP}$ cells. This further suggests EPLINα may be acting through Src expression to control cellular invasiveness. For a transwell migration assay, dasatinib treatment reduced the invasiveness of both LNCaP^{pEF6} and LNCaP$^{EPLIN\ EXP}$ cells. This may suggest that in the LNCaP cell model, the effect of EPLINα expression on cellular migration may be less dependent on Src expression, and dasatinib appears to markedly reduce cellular invasion regardless of EPLINα expression.

Finally, EPLIN expression in PC-3 influenced several other key molecules and mechanisms, and these included molecules such as p53 and PAK1/2/3 (Table 7.2). The associations of p53 in the progression of cancer is widely established (Muller and Vousden, 2013) and specifically has implications in the progression of prostate cancer (Thomas et al., 1993). p53 has also recently been linked to EPLIN expression where the suppressive action of p53 was dependant of EPLIN expression (Ohashi et al., 2017). Whereas PAK molecules have roles in RTK signalling to co-ordinate cytoskeletal organisations and cell survival (Dummler et al., 2009) in addition to being involved in cancer progression (Ye and Field, 2012). Together this suggests

EPLINα could also influence several other pathways that haven't been validated in this study and offers interesting future work for this area of prostate cancer biology.

This study aimed to evaluate key signalling pathways involved in EPLINα's mechanism of action in prostate cancer. This has revealed that EPLINα may act on several regulatory mechanisms, and its expression is associated to various crucial proteins involving cell proliferation, migration, adhesion and invasion. Several lines of evidence indicate Src may be an important factor associated to EPLINα expression for its tumour suppressive capacity, and this further substantiates the proposed link between EPLINα and paxillin/FAK signalling. Further work is needed to elucidate the full role of these two molecules and clarify the regulatory mechanisms governing the suppression of prostate cancer progression and development induced by EPLINα expression.

.

.

Chapter VIII: General discussion

Prostate cancer is the most common male cancer in the UK and the incidence has been steadily rising over the last twenty years (CancerResearchUK, 2017). Compared to other cancers, prostate cancer has a relatively good survival rate, with 84% of men in the UK surviving over ten years following diagnosis of prostate cancer (CancerResearchUK, 2017). However, prostate cancer becomes substantially more problematic when the cancer progresses and metastasises to other areas of the body, and targeting this metastatic progression is fundamental for overcoming the disease. Prostate cancer has a specific tendency to establish bone metastases, and once this spread occurs, survival rates are dramatically compromised. For example, patients with advanced prostate cancer without bone metastases have a five year survival rate of 56% whereas patients with advanced prostate cancer with bone metastases have five year survival rates of approximately only 3% (Higuera, 2016). Traditional treatments can only go so far in managing the disease and these have various side effects leading to reduced quality of life for the patient. The emphasis on specific, molecular targets for treatment of metastatic prostate cancer is now larger than ever.

An additional issue with prostate cancer is the lack of available and reliable biomarkers and prognostic markers. The PSA test is a useful indicator for evaluating prostate health however this has various drawbacks and can be unreliable in producing a true confirmatory result. Recently, the British Broadcasting Channel (BBC) reported a study from Science Translational Medicine where a prostate cancer blood test was able to determine how certain prostate cancer patients would respond to various cancer drugs like abiraterone, avoiding unnecessary side effects and potentially extending life span (Romanel et al., 2015). Although developments are

being made, a specific molecular target to determine prostate cancer prognosis is yet to be established. Without reliable predictive agents, it's difficult for GP's and clinicians to decipher if a prostate cancer will remain indolent and local, or will become an advanced metastatic cancer, and thus difficult to decide on optimal treatment procedures.

The aim of this thesis was to explore the importance of the actin-related, tumour suppressive molecule EPLIN in the progression and development of prostate cancer, with particular emphasis on generating mechanistic data and investigating potential links to the metastatic bone environment. A key focus was to gain a better understand of the biology of EPLIN, its role in prostate cancer progression and to gain further insight into the usefulness of this molecule and associated mechanism(s) as novel potential progression biomarkers or therapeutic strategies.

8.1 Clinical and cellular significance of EPLIN expression in prostate cancer and potential as a biomarker and/or use in prognosis

Protein and transcript analysis of EPLIN using prostate cancer cell lines revealed EPLIN is differentially expressed in prostate cancer, with a reduction of EPLIN expression coinciding with aggressiveness of the cell line. Specifically, the EPLIN transcript was reduced or abolished in cell lines PC-3, LNCaP and VCaP, compared to a high expression in cell lines PZ-HPV-7 and CA-HPV-10, whereas the EPLINβ transcript remained relatively constant at low levels for all cell lines. This concurs with previous reports using PC-3 and LNCaP where EPLINα is lost in aggressive prostate cancer (Maul and Chang, 1999) and is the first study using the VCaP cell line to evaluate EPLIN expression. This trend of EPLIN loss was also seen at the protein level, where EPLINα and EPLINβ isoforms were markedly reduced

compared to PZ-HPV-7 and CA-HPV-10. This suggests that EPLIN loss correlates with prostate cancer progression and highlights the potential of EPLIN to be used in prognostic targeting and a putative marker protein.

This study also examined the clinical significance of EPLIN in two prostate cancer TMA's, confirming the cellular observations and suggesting that EPLIN expression is significantly reduced or lost during the development or progression of prostate cancer. Taken together with other studies looking at EPLIN expression in prostate cancer cells and tissues (Sanders et al., 2011, Liu et al., 2016, Jiang et al., 2008, Zhang et al., 2011), the work presented within this thesis strongly supports the use of EPLIN as biomarker/prognostic marker for prostate cancer development and progression.

8.2 The functional effect of EPLINα expression on prostate cancer cell proliferation, invasion, adhesion and migration

To characterise the cellular significance of EPLINα expression on key cancerous traits, overexpression models were generated in prostate cancer cell lines. PC-3 and LNCaP lines were chosen as they had the lowest EPLIN transcript expression and were negative for EPLIN protein expression.

EPLINα overexpression reduced cellular proliferation of PC-3 and LNCaP cells and this is in keeping with both *in vitro* and *in vivo* observations from a previous study conducted in the host laboratory (Sanders et al., 2011). The current study is the first known study to evaluate EPLINα overexpression on cellular proliferation in the LNCaP cell model, and this study confirmed the negative regulatory effects EPLIN has on cell proliferation in LNCaP in addition to other prostate cancer cell models.

The work here also substantiates EPLINα's role as a suppressor of cell proliferation in other cancers including oesophageal cancer (Liu et al., 2012a) and breast cancer (Jiang et al., 2008). This also raises the question as to what effect EPLIN expression has on the cell cycle. Previous reports have suggested EPLIN is a key regulator of successful mitotic cell division where EPLIN localises to the cleavage furrow of cytokinesis (Chircop et al., 2009). EPLIN loss appears to effect the bundling of various proteins like actin and myosin to the cleavage furrow, leading to aneuploidy signifying cytokinesis failure and thus genomic instability of daughter cells (Chircop et al., 2009). Future work would help elucidate this potential role of EPLIN on cell cycle progression and establish the anti-proliferative effect EPLIN expression has in prostate cancer.

EPLINα was also shown to be a regulator of cellular invasiveness. Both PC-3 and LNCaP EPLINα overexpression models were less able to infiltrate and invade a Matrigel membrane, an observation again in keeping with previous data in PC-3 (Sanders et al., 2011) and LNCaP (Zhang et al., 2011) models, where EPLIN expression was able to influence prostate cancer cell invasiveness. This observation has been explored recently in lung and breast cancer where EPLIN influenced the invasive nature of metastatic lung cells, H1299 and Lu99, and MDA-MB-231 breast cancer cell lines (Ohashi et al., 2017). Overexpression of EPLIN in H1299 was shown to significantly reduce cellular invasion compared to control H1299 cells, whereas EPLIN lentiviral knock-down in Lu99 and MDA-MB-231 revealed significantly enhanced invasive capacities. Collectively, the data presented in this thesis, together with additional studies suggesting an anti-invasive role for EPLINα

in the invasive nature of breast (Jiang et al., 2008) and oesophageal cancer (Liu et al., 2012a), strongly implicate a regulatory role for EPLIN in cancer invasion.

EPLIN localises to adherens junctions and functions as a linker molecule to bind the cadherin-catenin complex to filamentous actin during cell-cell contact and thus likely has implications in cell movement and cellular adhesion (Abe and Takeichi, 2008). Considering this notion, the role of EPLINα in cancer cell adhesion to the ECM was explored. EPLINα overexpression induced a significant increase in cellular adhesion to Matrigel for both PC-3 and LNCaP cells. Additionally, cells containing the overexpression plasmid also took notably longer to detach in trypsin, during subculture, suggesting enhanced substratum adhesion. This contradicts previous reports assessing the adhesive nature of cells with forced EPLIN expression in cancer, where EPLIN overexpression induced a reduction of adhesion in KYSE150 oesophageal cancer cells (Liu et al., 2012a) and in endothelial cells (Sanders et al., 2010). This is the first known study to elucidate the effect of EPLINα overexpression on cellular adhesion in prostate cancer and substantiates the notion that EPLINα is able to influence cellular characteristics in cancer via altered EPLINα expression. It also suggests a role for EPLINα in the regulation of other molecules involved in matrix-adhesion, such as integrin's, and, when taken in context of the wider literature, suggests that this level of regulation may differ between differing cancer cells or types.

As discussed, EPLIN is functionally linked to the globular protein actin and physically binds actin at sites flanking the LIM domain of EPLIN (Maul et al., 2003). This binding co-ordinates various cellular processes including cross linking and stabilising actin filaments and inhibits membrane ruffling (Maul et al., 2003).

Actin is a ubiquitously expressed protein responsible for co-ordinating a myriad of cellular functions including cell mobility, movement and migration and has diverse implications in cancer progression (Fife et al., 2014). Considering how EPLIN exerts function through actin association, it proposes the notion that EPLIN is also implicated in cellular functions including cellular migration. EPLINα overexpression was therefore evaluated in *in vitro* tumour migration assays. EPLINα overexpression induced a reduction of cellular migration in both PC-3 and LNCaP cells, though this effect was not significant in the LNCaP model. This study in prostate cancer corroborates previous work elucidating EPLINα in tumour cellular migration in endothelial cells (Sanders et al., 2010) and in breast cancer cells, via an Electrical Cell Substrate Impedance Sensing (ECIS) assay (Jiang et al., 2008). Taken together this work builds on previous work linking EPLINα as an actin related molecule and reinforces the notion of EPLINα as a tumour suppressive molecule via its ability to impede cellular migration in prostate cancer.

Work in this thesis has utilised two prostate cancer cell models to establish and clarify the functional impact of EPLINα expression in prostate cancer. When taken together, the data from PC-3 and LNCaP models substantiates the concept that EPLINα is a tumour suppressive molecule in cancer, and through its ability to influence key metastatic traits, affirms the potential of EPLINα as a molecular regulator of prostate cancer cell metastasis.

8.3 The role of EPLIN in the establishment of bone metastases

Bone metastasis is a key consideration in prostate cancer pathophysiology. Of all the prostate cancers that metastasise, approximately 80% will spread to the bones

resulting in reduced quality of life and poor patient survival outlooks (Higuera, 2016). Bone metastasis results in a variety of side effects and symptoms including bone pain and osteolysis, in addition to increasing difficulty of treatment and management of the disease (AmericanCancerSociety, 2016). It is therefore crucial to establish new molecular targets to prevent the spread of prostate cancer to the bone and the formation of secondary cancers within this environment.

Various molecular agents have been suggested to be associated with the dissemination of prostate cancer to bone. These include the adhesion molecule activated leukocyte cell adhesion molecule (ALCAM) (Hansen et al., 2014), the focal adhesion adaptor, Talin1 (Jin et al., 2015) and various mircoRNAs (miRNAs) (Weidle et al., 2016). In this thesis, EPLINα overexpression was evaluated as a potential factor that could influence prostate cancer metastases establishment in the bone environment through the addition of BME or human osteoblasts to the culture environment. Generally, the use of BME induced no significant differences to the cellular functions of PC-3 and LNCaP cells when compared to respective untreated samples. The presence of human osteoblasts generally increased the invasiveness of PC-3 cells, but not LNCaP cells. In PC-3 cells, though co-culture with osteoblasts enhanced the invasiveness of both control and EPLINα overexpression cells, this was only significant in the case of the control, potentially suggesting that EPLINα may protect against pro-invasive signals secreted by osteoblasts. In LNCaP cells, there was no general change with or without osteoblasts, suggesting LNCaP cells are less susceptible to the action of osteoblasts and thus a bone-like environment. Taken together, this may suggest that EPLINα plays some role in prostate cancer establishment at the bone environment, though its major role appears more related to

a general tumour/metastatic suppressive effect, potentially exerting functions earlier in the metastatic cascade, rather than a having a substantial involvement at the bone environment itself, though further, complex co-culture models and *in vivo* works are needed to explore and validate this relationship further.

8.4 Mechanistic implications of EPLIN and involvement in signalling pathways

The EPLIN interactome has only been explored briefly in the last decade. Reports have associated the mechanism of action of EPLIN to molecules including actin (Maul et al., 2003), the cadherin-catenin complex (Abe and Takeichi, 2008), EGF and ERK (Zhang et al., 2013) and p53 (Steder et al., 2013, Ohashi et al., 2017). Our research group and others have also linked the integrin signalling related molecule, paxillin, to EPLIN expression and function (Tsurumi et al., 2014, Sanders et al., 2011). It is also established in the literature that EPLINα is lost in aggressive cancer, and if expression is retained, can act as a tumour suppressive molecule to influence metastatic characteristics. The mechanism governing this suppressive role in cancer, however, remains elusive and is yet to be determined. A key aim of this thesis was to clarify this area and substantiate existing knowledge surrounding EPLIN mechanistic biology in cancer progression.

8.4.1 Mechanistic implications of EPLIN: FAK and paxillin

Considering the established link between EPLIN and paxillin, the expression and phosphorylation status of paxillin was determined in this study in conjunction with EPLINα overexpression. Paxillin is functionally and mechanistically linked to FAK (Mitra et al., 2005) so FAK was also explored in relation to EPLINα expression.

Within the cell models, EPLINα overexpression influenced paxillin and FAK expression and also the phosphorylation of certain key residues within these proteins such as FAK Y397/Y925 and paxillin Y31/Y118. FAK Y397 is an established region of FAK crucial for controlling cellular functions including cell survival and cellular migration (Hanks et al., 2003), co-ordinating interaction with regulatory proteins like PI3K (Chen et al., 1996) and is a major binding site SH2 domain of Src family kinases (Eide et al., 1995). In this study, EPLINα overexpression in LNCaP increased the proportion of Y397 phosphorylation in FAK, potentially accounting in part for the lack of significance seen in the LNCaP *in vitro* transwell migration assay following EPLINα overexpression. In PC-3 however, EPLINα overexpression significantly reduced cellular migration but did not significantly alter the expression of Y397. Hence, the differential effect of EPLINα on FAK Y397 in these two cell lines may partially account for the differential effects on migration. This may suggest the suppressive action of EPLINα may be differentially regulated depending on different cell types through the action of FAK phosphorylation. On the other hand, EPLINα expression also had differential effects on the status of FAK Y925 in PC-3 and LNCaP. Y925 is also an established region of FAK and is important for cell migration, focal adhesion turnover and cell protrusion (Deramaudt et al., 2011). EPLINα overexpression enhanced FAK Y925 in PC-3 cells and also induced an increase in cellular adhesion to Matrigel membrane. It may be increased EPLINα is acting through Y925 to reduce focal adhesion disassembly and thus focal adhesion turnover. Logically this would result in increased adhesive properties in PC-3 cells expressing EPLINα as they are less able to detach from the membrane due to the reduced turnover of the focal adhesions and thus not primed to migrate elsewhere, potentially also accounting, at least in part, for the reduced migratory potential seen

in this cell line. This provides insights in the potential mechanism of EPLINα to regulate several cellular functions in prostate cancer through the action of key FAK phosphorylation regions. Functional analysis examining the significance of EPLINα expression in conjunction with a FAK Y397 inhibitor further suggested mechanistic links between these two molecules. FAK inhibition had a reduced impact on the proliferation, invasion and migration of PC-3 cells overexpressing EPLINα, compared to controls, though this trend was not so clear in LNCaP cells. As discussed in Chapter 6, these differential responses may be due to different mechanistic actions of EPLINα in different cell types and/or due to different expression profiles of FAK in each PC-3 and LNCaP cells. Taken together it suggest that FAK may be one means through which EPLINα can exert its regulation. It is interesting to consider that EPLINα may also act upstream/downstream of FAK, potentially targeting this pathway at a number of points, as suggested in Chapter 7, through its action on Src, a molecule which associates with FAK at Y397 to phosphorylate several other regions of FAK during integrin clustering to propagate integrin signalling (Schaller et al., 1994, McLean et al., 2005). This could result in potentially less available FAK Y397 in cells with retained EPLINα expression and thus a less prominent change in cellular function.

EPLINα expression also influenced the proportion of paxillin phosphorylation at Y31 and Y118. These regions are critical to paxillin function and have implication in cellular migration and cancer progression (Brown and Turner, 2004). These regions of paxillin also serve as docking sites for signalling proteins including Crk, a downstream event of FAK phosphorylation (Schaller and Parsons, 1995). Tyrosine phosphorylation in paxillin is also important for controlling FA dynamics for

integrin dynamics and altering these regions can affect FA turnover (Zaidel-Bar et al., 2007). Chapter 6 highlighted that EPLINα overexpression enhanced paxillin phosphorylation at both Y31/Y118 in PC-3. Phosphorylation within these residues have been associated with both an increase in cellular migration (Petit et al., 2000) but also a decrease in cellular migration (Yano et al., 2000). In the case of the latter, this could be a potential mechanism through which EPLINα can negatively regulate cellular migration. Contrary, in LNCaPs, a significant reduction of paxillin Y118 was seen following EPLINα overexpression. Paxillin Y31/Y118 has also been associated with increased FAK recruitment and FA turnover (Zaidel-Bar et al., 2007). If Y118 is reduced in LNCaP cells expressing EPLINα, this could lead to a reduction of FA turnover and hence induces increased adhesion and reduced cellular migration, again proposing a potential mechanism of EPLINα function through the action of paxillin phosphorylation. Further, if EPLINα exerts varying effects on paxillin Y31/Y118 phosphorylation in cancer, depending on cell type, this could lead to differential effects on paxillin:FAK association, thus leading to changes in cellular migration, adhesion and invasion (Deramaudt et al., 2014). For example if PC-3 cells with retained EPLINα expression also have increased paxillin Y31/Y118, this could increase FAK recruitment and association (Zaidel-Bar et al., 2007), leading to increased FA turnover and cellular adhesion (Deramaudt et al., 2014). Conversely, with weakened Y31/Y118 (seen partly in LNCaP$^{EPLIN\ EXP}$ with Y118) this could negatively affect FAK recruitment and association (Zaidel-Bar et al., 2007), leading to a reduction of migration and invasion (Deramaudt et al., 2014). Altogether this suggests a complex network of interactions orchestrating cellular function in prostate cancer. It seems EPLINα is able to influence several parameters of FAK/paxillin

biology, and this provides key indications into the mechanism of action of EPLINα to suppress and regulate metastatic traits in prostate cancer.

8.4.2 Mechanistic implications of EPLIN: ITGB1

EPLIN has recently been linked to proteins involved in integrin signalling, these include paxillin and FAK as above, but also the focal adhesion protein PINCH-1 (Karakose et al., 2015). EPLIN has been shown to associate to integrin adhesion sites, a process that can control cellular adhesion in keratinocytes (Karakose et al., 2015). Given this, it's conceivable that EPLIN may be involved in other integrin-related signalling pathways and processes. PINCH-1 is functionally linked to the kinase molecule, ILK, during integrin signalling (Legate et al., 2006). As discussed in Chapter 7, EPLINα overexpression enhanced the phosphorylation of ILK at Y351 in PC-3 cells, identified in the protein microarray. This could suggest that EPLINα interacts with not only PINCH-1, but the PINCH1:ILK complex or even possibly effect the interactions between the two molecules.

The protein microarray highlighted increased phosphorylation of ITGB1 S785 following EPLINα overexpression in PC-3 cells, though, due to antibody availability and performance issues, this could not be verified using western blot analysis in cell models. However, the S785 region of ITGB1 has been proposed to modulate ITGB1 function via enhanced attachment of cells and also inhibit cell spreading and migration (Mulrooney et al., 2001). This association was also validated using an antibody targeting total ITGB1 expression and confirmed an increase in ITGB1 expression in conjunction with EPLIN expression. Considering this notion, this illustrates a potential mechanism for the enhanced adhesive and reduced migratory

properties seen in PC-3 and LNCaP cells with forced EPLINα expression. Previously this has been explored with F9 and GD25 murine cell lines (Mulrooney et al., 2001), but it's reasonable that a similar mechanism could be occurring in prostate cancer cells upon EPLINα expression. This line of evidence substantiates current research that EPLINα may act not only on cytoplasmic related molecules of integrin signalling but also provides evidence of associations to membrane bound signalling molecules and represents another novel mechanism through which EPLINα may exert regulation of cellular traits in prostate cancer cells.

8.4.3 Mechanistic implications of EPLIN: ERK1/2

As discussed in Chapter 7, ERK1/2 was also highlighted as a protein of interest in relation to EPLINα's mechanism of action. ERK has previously been linked to EPLIN, initially by phosphorylation of EPLIN and contributing to cellular migration (Han et al., 2007), and by controlling EPLIN phosphorylation, ubiquitination and protein turnover in tandem with EGF (Zhang et al., 2013). The protein microarray analysis revealed EPLINα expression reduces phosphorylation of an activation site within ERK1/2; T202/Y204, in addition to downregulating several other ERK1/2 proteins. As discussed, ERK is an imperative molecule involved in a plethora of signalling pathways responsible for inducing several pleiotropic cellular responses (Roskoski, 2012). ERK1/2 is particularly important for regulating cell proliferation and proliferation (Mebratu and Tesfaigzi, 2009), so this could provide indications into the mechanism of proliferation suppression observed in prostate cancer cells with forced EPLINα expression seen in Chapters 4 and 5 of this study. ERK also had implications on cell cycle progression (Meloche and Pouyssegur, 2007), and this corroborates previous data associating EPLIN with cytokinesis and cell mitotic

division (Chircop et al., 2009). Collectively, considering previous associations between ERK and EPLIN, and data from this study, it could be that there is a dual feedback system occurring in prostate cancer to orchestrate cellular dynamics and control cellular functions like proliferation and migration, by virtue of ERK1/2 and EPLIN interplay. Further, Src activity is functionally linked to ERK signalling where both molecules have regulatory roles critical for focal adhesion turnover and cell migration (Webb et al., 2004). Given the potential loss of ERK activity in PC-3 cells evidenced from the Kinexus protein microarray, it could be that ERK is unable to promote Src-induced focal adhesion turnover as a result of EPLINα overexpression, thus reducing cellular migration of prostate cancer cells. Finally, given the observations linking EPLINα to both ITGB1 and ERK, this could suggest EPLINα is a potential candidate protein for monitoring and regulating 'inside-out' signalling in prostate cancer. Inside out signalling is a signalling process to co-ordinate integrin activation which leads to increased affinity of receptor binding to extracellular ligands (Shattil et al., 2010). Inside out signalling has implications on cellular function (Shen et al., 2012), influences FAK/Src signalling (Thamilselvan and Basson, 2004) and has significance in cancer (Li et al., 2009). This could provide insights into EPLINα's mechanistic role to regulate various proteins including ITGB1, ERK and Src, all with key roles in integrin signalling to co-ordinate cellular function, suggesting a complex variety of molecules acting synergistically in prostate cancer development.

8.4.4 Mechanistic implications of EPLIN: Src

As discussed, EPLINα is able to influence various integrin related signalling proteins including paxillin, FAK, ERK1/2 and ITGB1. Paxillin and FAK are

functionally and mechanistically linked to Src, a protein crucial for various cellular processes like focal adhesion, migration and cellular invasion (Mitra and Schlaepfer, 2006). This study has demonstrated that EPLINα is able to influence paxillin and FAK phosphorylation and function. This study also highlighted a novel association to Src protein, where EPLINα overexpression in PC-3 cells induced a reduction of active Src via the Y419 domain. The Y419 region of Src is the classical activation domain and is associated with the progression of various cancers and is linked to function and catalytic activity (Cartwright et al., 1990). This study revealed that EPLINα is a potential negative regulator of Src signalling, with a reduction of Y419 Src, and also an increase of the inactive Y530 form, in response to EPLINα overexpression in prostate cancer cells. This provides mechanistic evidence of the suppressive action of EPLINα in prostate cancer. If EPLINα is able to negatively regulate Src signalling, that will have diverse effects of various signalling mechanisms. As discussed, Src is commonly elevated in cancer and is synergistic with paxillin and FAK, and propagation of this pathway is generally associated with cancer progression (Mitra and Schlaepfer, 2006). A reduction of Src activity would likely influence paxillin and FAK activity. Physiologically, these three proteins are activated by integrin engagement with the ECM which leads to subsequent phosphorylation of paxillin by FAK (Turner, 2000a). Src would usually bind FAK at Y397 and create additional binding sites for various proteins in the cascade including adaptor proteins Crk and Cas, following phosphorylation by Src (Turner, 2000a). Ultimately, these signalling interactions, driven by elevated Src activity, signal to activate proteins involved in the MAPK pathway to co-ordinate a myriad of cellular functions and control gene expression (Turner, 2000a). Elevated Src activity in cancer is also linked to increased cellular invasion and progression-related events

like EMT (Guarino, 2010), influences actin dynamics and invasion (Angers-Loustau et al., 2004) and is also implicated in cancer cell migration and invasion to a bone derived microenvironment (Pohorelic et al., 2012). As discussed in Chapter 7, Src activity is also associated with cell cycle arrest and decreased cellular migration and invasion (Tsao et al., 2007), has implications on cellular functions in triple negative breast cancer (Tryfonopoulos et al., 2011) and has significance in prostate cancer progression (Chang et al., 2008). Finally, expression of Src is heavily tied to FAK activity and specifically monitors focal adhesion dynamics to control cellular functions like cellular migration and focal adhesion turnover (Fincham and Frame, 1998, Webb et al., 2004). When Src is lost, cells are less migratory and have reorganised focal adhesion distribution of matrix adhesions (Volberg et al., 2001). This proposes that Src activity is fundamental for focal adhesion turnover and cell motility through interaction and association with FAK (Westhoff et al., 2004). This could explain the enhanced adhesive capacity and reduced migratory capacity in PC-3 and LNCaP cells when EPLINα is overexpressed, as cells with altered focal adhesion turnover leads to less effective cellular migration, locomotion and spreading of cells (Wozniak et al., 2004). Taken together, functional Src expression is fundamental for cancer progression. If EPLINα is able to negate Src expression this could further clarify the mechanism of action of EPLINα as a tumour suppressor seen in prostate cancer cells. Considering the abundance of evidence for Src as a pro-metastasis molecule, and the demonstrated loss of Src Y419 when EPLINα is overexpressed in the protein microarray described in this study, it could be that EPLINα is acting through Src in prostate cancer as a negative regulator to suppress metastatic traits. This could help explain the suppressive effect of EPLINα in PC-3

cells and LNCaP cells when EPLINα expression is enhanced, unveiling a more comprehensive look at the mechanism of action of EPLIN in prostate cancer.

The use of a Src inhibitor corroborated these findings, particularly when evaluating EPLINα and Src activity in an invasion assay. Dasatinib offered no further effect on cellular invasion in cells with forced EPLINα expression following treatment. This further suggests that EPLIN may be acting as a suppressor of Src signalling to influence traits like cellular invasion in prostate cancer, especially since Src is known to regulate cellular invasiveness (Guarino, 2010). Inhibition of Src is already an established area of therapeutics for cancer biology (Creedon and Brunton, 2012), so this demonstrates interesting avenues of future work in this area of research for EPLIN biology in prostate cancer metastasis.

8.4.5 Mechanistic implications of EPLIN: proposed signalling pathway

Taken together, EPLINα appears to regulate several signalling pathways in prostate cancer, which in turn may account for the various functional effects of EPLINα expression. Furthermore, many of the potential mechanistic pathways discussed in this section and throughout this thesis are linked and also highly relevant in cancer biology. Thus, it appears that EPLINα exerts many levels of regulations within the cells and highlights the impact of EPLIN loss frequently seen in cancer progression. An integrated mechanism illustrating the mechanisms of action and cross-talk undertaken by EPLINα in prostate cancer cells is proposed in Figure 8.1 based on the key findings of this thesis as well as the current knowledge of EPLINs actions within the literature. Further exploration, clarification and validation of this pathway will be crucial in establishing EPLIN's functional role in prostate cancer metastasis.

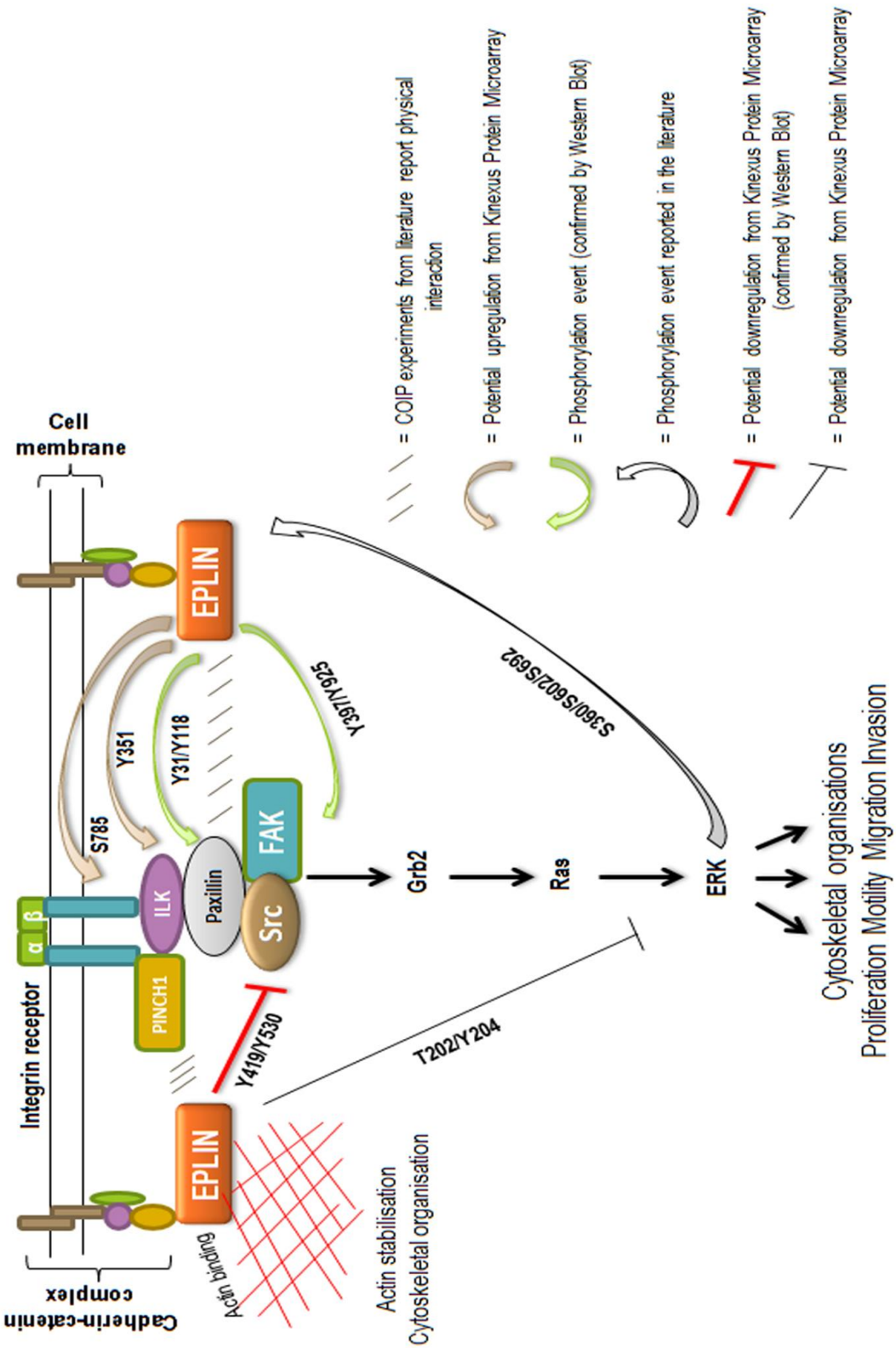
Cell membrane
EPLIN
EPLIN
Integrin receptor
α
β
ILK
PINCH1
Paxillin
FAK
Src
S785
Y351
Y31/Y118
Y397/Y925
Y419/Y530
T202/Y204
S360/S602/S692
Grb2
Ras
ERK
Cytoskeletal organisations
Proliferation Motility Migration Invasion
Actin binding
Actin stabilisation
Cytoskeletal organisation
Cadherin-catenin complex
= COIP experiments from literature report physical interaction
= Potential upregulation from Kinexus Protein Microarray
= Phosphorylation event (confirmed by Western Blot)
= Phosphorylation event reported in the literature
= Potential downregulation from Kinexus Protein Microarray (confirmed by Western Blot)
= Potential downregulation from Kinexus Protein Microarray

Figure 8.1Proposed signalling pathways of EPLINα in cancer.

EPLINα affects several mechanisms and signalling pathways in cancer. EPLINα is implicated in paxillin and FAK signalling and expression of EPLINα protein can provoke alterations to the phosphorylation status of paxillin and FAK, as determined by Western Blot experiments, potentially affecting cellular function in cancer. EPLINα enhances phosphorylation of integrin receptor-related proteins ITGB1 and ILK, with increased phosphorylation of S785 in ITGB1 and Y351, as determined from the Kinexus protein microarray. EPLINα forms a physical complex with paxillin and also the ILK-associated protein PINCH1. EPLINα expression appears to cause a reduction of the dual activation site of ERK at T202/Y204 from the protein microarray, suggesting EPLINα influences ERK signalling. ERK also acts on EPLIN through phosphorylation at three separate residues: S360, S602 and S692. EPLINα expression in prostate cancer induces a negative regulatory effect of Src signalling, with a reduction of pSrc Y419 and an increase in Y530. Blocking src signalling has many implications in cancer, including reducing further FAK and paxillin activity and downstream effects on ERK signalling. Taken together, these changes brought about by EPLINα may explain EPLIN's mechanism of action in cancer as a tumour suppressive molecule to impede metastatic traits. Image generated from data obtained in this study and combined with data extracted from (Karakose et al., 2015, Tsurumi et al., 2014, Han et al., 2007).

8.5 Main findings and significance

EPLIN expression was evaluated in two TMA's in clinical prostate cancer tissue and revealed significant downregulation when compared to normal prostate tissue. EPLIN loss correlated with higher Stage cancer tissue and also higher Gleason scores. In the second TMA, EPLIN expression was significantly reduced in samples with cancer hyperplasia and adenocarcinoma compared to normal prostate tissue. A significant reduction in EPLIN expression was also seen comparing cancers in adjacent tissue to cancer hyperplasia. Hence, this data suggests an association between prostate cancer progression and amount of EPLIN protein available and supports the evidence for use of EPLIN as a predictive marker in clinical prostate cancer progression. EPLIN expression was at its weakest in the most aggressive cancer tissues, suggesting EPLIN could identify cancer aggressiveness and metastatic potential in clinical cancer. Work utilising the prostate cancer cell lines corroborate this notion, as EPLIN transcript and protein was downregulated or lost in aggressive cancer cell lines like PC-3, LNCaP and VCaP, whereas expression was higher in less aggressive cancer cell lines, like CA-HPV-10, and the normal prostate cell line PZ-HPV-7.

Characterisation of the EPLINα overexpressed PC-3 and LNCaP lines has led to the implication and clarification that EPLINα functions as a tumour suppressor molecule in the progression of prostate cancer. EPLINα is able to influence several key traits on prostate cancer cells including cellular proliferation, proliferation, adhesion, migration and invasion, all characteristics that are fundamental to metastatic progression and development. This protective effect may also be active in the establishment of secondary bone metastases; however it seems that EPLINα

primarily functions as a general cancer metastasis regulator, rather than a specific molecular target for bone dissemination.

The work utilising the prostate cell model functional assays lead to developments with mechanistic data, implicating signalling molecules paxillin and FAK in EPLINα tumour biology. Forcing EPLINα expression in prostate cell lines had diverse effects on paxillin and FAK gene expression, protein expression and phospho-protein expression. Specifically, enhanced EPLINα engendered changes to FAK Y397/Y925 status and paxillin Y31/Y118 in prostate cancer cell lines, which are crucial to FAK and paxillin function and have implications in cancer. It also appeared that EPLINα expression on FAK/paxillin might be differential depending on different cell types, and could provoke distinct downstream effects in different cell lines.

Lastly, EPLIN exhibited various effects to other signalling molecules, not previously identified in the literature. Namely, EPLINα enhanced expression of ITGB1 and ILK expression in PC-3 cells, whilst also downregulating ERK1/2 and Src signalling. Importantly, Src is a crucial signalling protein associated to various cellular mechanisms and has implications in cancer progression (Mitra and Schlaepfer, 2006). The protein microarray revealed that EPLINα is a potential negative regulator of Src signalling, able to specifically downregulate the Y419 form of Src and increase the inactive Y530 phospho-protein. This revealed a possible mechanism for EPLINα function in the observed suppression of prostate cancer cell characteristics in this study. It holds particularly plausible due to the prominence of Src in co-ordinating cellular functions like migration and invasion (Guarino, 2010). The functional assays utilising dasatinib strengthen this notion of Src association, particularly for regulating cellular invasiveness.

A key clinical question from this study would be the problem of retaining EPLINα expression and preventing loss in aggressive cancer, to encompass the advantageous effects of EPLINα expression in prostate cancer. Understanding the mechanism of action of EPLINα in prostate cancer is crucial to this enigma. Only recently is this area of science beginning to emerge, for example, only this year it was published that a small molecule inhibitor, Nutlin3a, was able to enhance EPLINα protein expression, an effect linked to the suppressive action of p53 in cancer (Ohashi et al., 2017). Further work is needed in this area and will be key for producing improved cancer therapeutics. As seen with the differential effects observed upon EPLINα expression to FAK and paxillin, further work utilising additional cancer cell models would be of benefit to these interpretations and is warranted for full elucidation of EPLINα's mechanism of action in prostate cancer. It is hoped that the greater understanding of EPLINα biology, combined with mechanisms to re-establish expression in cancer cells or prevent loss in the first instance will aid in the development of multi-target therapeutics to combat the significant issue of cancer metastasis.

8.6 Future work

There are various avenues of future work following this thesis. The current study focussed on EPLINα in the progress of prostate cancer, but also has demonstrated significance in various other cancers (Jiang et al., 2008, Liu et al., 2012a, Liu et al., 2016). It would therefore be interesting to explore EPLINα further in other cancer systems that are less established in the literature, possibly in pancreatic, gastric or colorectal cancer. Larger tissue samples would also be beneficial to gain a broader

understanding of EPLINα loss in clinical prostate cancer; including sections from metastatic bone derived areas and paired primary tumours.

For the molecular and cellular study, use of the VCaP cancer cell model would be favourable due to the osteoblastic nature of VCaP cells, to understand the functional impact of EPLINα when expression is manipulated in VCaP cells. Knock-down analysis could also be performed to corroborate the functional observations in this study, possibly in lines where EPLINα expression is relatively high, like CA-HPV-10 and PZ-HPV-7 cell lines, and such analysis would aid to demonstrate the significance of EPLINα loss in less aggressive or normal prostate lines. EPLINα's role on cell cycle progression could be explored, due to the established anti-proliferative effects observed in this study. In addition to *in vitro* models, a logical progression would be to use *in vivo* models to explore the observed functional effects in prostate cancer in animal models. This would complement the highlighted effects observed in Chapter 4 and Chapter 5 of this study.

For EPLINα's mechanism of action, various proteins could be elucidated in relation to EPLINα expression and cancer progression, in addition to the molecules evaluated here. The protein microarray revealed several proteins related to EPLINα that weren't resolved in this study. Molecules like p53, ILK, Cyclins, PAK1 and ERBB2/HER, all displayed some form of differential expression in response to EPLINα overexpression in PC-3 cells, and introduce compelling options for mechanistic analysis in relation to EPLINα function in cancer. Links to other signalling cascades like RTK activation through PAK1/2/3 could be explored, especially as PAK was validated to be increased in tandem with EPLINα overexpression in prostate cell lines following the protein microarray. The S785

region of ITGB1, and Y351 region of ILK, also requires further validation due to antibody availability/performance issues described in Chapter 7. ERK antibodies also displayed some performance issues in Chapter 7, so sourcing additional antibodies for regions of ERK1/2 influenced by EPLIN expression would be valuable for verifying this association. Various other inhibitors could be used in combination with functional assays, like ERK, JNK or other MAPK inhibitors, also highlighted from the protein microarray. Given EPLINα's regulatory role and significance of loss of EPLINα in cancer progression, identification of these mechanisms and thus therapies to enhance EPLINα should be key focus, and only recently has research on EPLINα began to focus on this area. Once the mechanism of EPLIN is better understood, this would assist the development of potential therapies which aim to target metastatic progression and development. These could be used in conjunction with other inhibitory therapies implicated in the mechanism of EPLINα (for example dasatinib use or the nutlin3a inhibitor) to suppress cancer cell characteristics. Lastly, it would be interesting to explore if these suppressive effects EPLINα exerts can influence certain chemotherapies, or influence cell response to chemotherapy, in addition to other traditional prostate cancer treatments.

Understanding the molecular architecture and signalling interactions in cancer biology is paramount. Full elucidation of these downstream signalling cascades may aid clinical significance utilising molecules like EPLINα. Once fully understood, this could hopefully lead to more personalised, multi target therapeutic design.

Chapter IX: References

ABE, K. & TAKEICHI, M. 2008. EPLIN mediates linkage of the cadherin catenin complex to F-actin and stabilizes the circumferential actin belt. *Proc Natl Acad Sci U S A,* 105**,** 13-9.

ABLIN, R. 1985. A retrospective look at studies on prostate-specific antigen. *Clinical Chemistry,* 31.

ABLIN, R. J. 1993. On the identification and characterization of prostate-specific antigen. *Hum Pathol,* 24**,** 811-2.

ABLIN, R. J. 2000. PSA assays. *Lancet Oncol,* 1**,** 13.

ABLIN, R. J., BRONSON, P., SOANES, W. A. & WITEBSKY, E. 1970. Tissue- and species-specific antigens of normal human prostatic tissue. *J Immunol,* 104**,** 1329-39.

ACS, G., LAWTON, T. J., REBBECK, T. R., LIVOLSI, V. A. & ZHANG, P. J. 2001. Differential expression of E-cadherin in lobular and ductal neoplasms of the breast and its biologic and diagnostic implications. *Am J Clin Pathol,* 115**,** 85-98.

ADAMS, S. A. & SUBRAMANIAN, V. 1999. The angiogenins: an emerging family of ribonuclease related proteins with diverse cellular functions. *Angiogenesis,* 3**,** 189-99.

AMERICANCANCERSOCIETY. 2007. *Cancer Facts and Figures* [Online]. Available: http://www.cancer.org/acs/groups/content/@nho/documents/document/caff2007pwsecuredpdf.pdf [Accessed 4.8.16 2016].

AMERICANCANCERSOCIETY. 2016. *Bone Metastasis* [Online]. Available: http://www.cancer.org/treatment/understandingyourdiagnosis/bonemetastasis/bone-metastasis-detailed-guide-toc [Accessed 7/9/16 2016].

ANGERS-LOUSTAU, A., HERING, R., WERBOWETSKI, T. E., KAPLAN, D. R. & DEL MAESTRO, R. F. 2004. SRC regulates actin dynamics and invasion of malignant glial cells in three dimensions. *Mol Cancer Res,* 2**,** 595-605.

ARA, T. & DECLERCK, Y. A. 2010. Interleukin-6 in bone metastasis and cancer progression. *Eur J Cancer,* 46**,** 1223-31.

ASIM, M., SIDDIQUI, I. A., HAFEEZ, B. B., BANIAHMAD, A. & MUKHTAR, H. 2008. Src kinase potentiates androgen receptor transactivation function and invasion of androgen-independent prostate cancer C4-2 cells. *Oncogene,* 27**,** 3596-604.

BAGO-HORVATH, Z., SCHMID, K., ROSSLER, F., NAGY-BOJARSZKY, K., FUNOVICS, P. & SULZBACHER, I. 2014. Impact of RANK signalling on survival and chemotherapy response in osteosarcoma. *Pathology,* 46**,** 411-5.

BELLIS, S. L., MILLER, J. T. & TURNER, C. E. 1995. Characterization of tyrosine phosphorylation of paxillin in vitro by focal adhesion kinase. *J Biol Chem,* 270**,** 17437-41.

BEUSELINCK, B., JEAN-BAPTISTE, J., COUCHY, G., JOB, S., DE REYNIES, A., WOLTER, P., THEODORE, C., GRAVIS, G., ROUSSEAU, B., ALBIGES, L., JONIAU, S., VERKARRE, V., LERUT, E., PATARD, J. J., SCHOFFSKI, P., MEJEAN, A., ELAIDI, R., OUDARD, S. & ZUCMAN-ROSSI, J. 2015. RANK/OPG ratio of expression in primary clear-cell renal cell carcinoma is associated with bone metastasis and prognosis in patients treated with anti-VEGFR-TKIs. *Br J Cancer,* 113**,** 1313-22.

BHATTACHARJEE, A., RICHARDS, W. G., STAUNTON, J., LI, C., MONTI, S., VASA, P., LADD, C., BEHESHTI, J., BUENO, R., GILLETTE, M., LODA, M., WEBER, G., MARK, E. J., LANDER, E. S., WONG, W., JOHNSON, B. E., GOLUB, T. R., SUGARBAKER, D. J. & MEYERSON, M. 2001. Classification of human lung carcinomas by mRNA expression profiling reveals distinct adenocarcinoma subclasses. *Proc Natl Acad Sci U S A,* 98**,** 13790-5.

BOMMAREDDY, A., EGGLESTON, W., PRELEWICZ, S., ANTAL, A., WITCZAK, Z., MCCUNE, D. F. & VANWERT, A. L. 2013. Chemoprevention of prostate cancer by major dietary phytochemicals. *Anticancer Res,* 33**,** 4163-74.

BOSE, S., FIELDING, G., TARAFDER, S. & BANDYOPADHYAY, A. 2013. Understanding of dopant-induced osteogenesis and angiogenesis in calcium phosphate ceramics. *Trends Biotechnol,* 31**,** 594-605.

BOYCE, B. F. & XING, L. 2007. Biology of RANK, RANKL, and osteoprotegerin. *Arthritis Res Ther,* 9 Suppl 1**,** S1.

BRIGANTI, A., SUARDI, N., GALLINA, A., ABDOLLAH, F., NOVARA, G., FICARRA, V. & MONTORSI, F. 2014. Predicting the risk of bone metastasis in prostate cancer. *Cancer Treat Rev,* 40**,** 3-11.

BRIMO, F., MONTIRONI, R., EGEVAD, L., ERBERSDOBLER, A., LIN, D. W., NELSON, J. B., RUBIN, M. A., VAN DER KWAST, T., AMIN, M. & EPSTEIN, J. I. 2013. Contemporary grading for prostate cancer: implications for patient care. *Eur Urol,* 63**,** 892-901.

BROWN, M. C., CARY, L. A., JAMIESON, J. S., COOPER, J. A. & TURNER, C. E. 2005. Src and FAK kinases cooperate to phosphorylate paxillin kinase linker, stimulate its focal adhesion localization, and regulate cell spreading and protrusiveness. *Mol Biol Cell,* 16**,** 4316-28.

BROWN, M. C., PERROTTA, J. A. & TURNER, C. E. 1996. Identification of LIM3 as the principal determinant of paxillin focal adhesion localization and

characterization of a novel motif on paxillin directing vinculin and focal adhesion kinase binding. *J Cell Biol,* 135**,** 1109-23.

BROWN, M. C. & TURNER, C. E. 2004. Paxillin: adapting to change. *Physiol Rev,* 84**,** 1315-39.

BUSSARD, K. M., GAY, C. V. & MASTRO, A. M. 2008. The bone microenvironment in metastasis; what is special about bone? *Cancer Metastasis Rev,* 27**,** 41-55.

CAETANO-LOPES, J., CANHAO, H. & FONSECA, J. E. 2007. Osteoblasts and bone formation. *Acta Reumatol Port,* 32**,** 103-10.

CANCERRESEARCHUK. 2016a. *How Cancers Grow* [Online]. Available: http://www.cancerresearchuk.org/about-cancer/what-is-cancer/how-cancers-grow [Accessed 27-9-16 2016].

CANCERRESEARCHUK. 2016b. *Prostate cancer risk factors* [Online]. Available: http://www.cancerresearchuk.org/health-professional/cancer-statistics/statistics-by-cancer-type/prostate-cancer/risk-factors#heading-Twelve [Accessed 23/8/16 2016].

CANCERRESEARCHUK. 2016c. *Prostate cancer risks and causes* [Online]. Available: http://www.cancerresearchuk.org/about-cancer/type/prostate-cancer/about/prostate-cancer-risks-and-causes#riskfactor.

CANCERRESEARCHUK. 2016d. *Secondary cancer in the bones* [Online]. Available: http://www.cancerresearchuk.org/about-cancer/type/secondary-cancers/secondary-bone-cancer/secondary-bone-cancer [Accessed 7/9/16 2016].

CANCERRESEARCHUK. 2016e. *Side effects of hormone therapy for prostate cancer* [Online]. Available: http://www.cancerresearchuk.org/about-cancer/type/prostate-cancer/treatment/hormone/side-effects-of-hormone-therapy-for-prostate-cancer.

CANCERRESEARCHUK. 2016f. *The Stages of Prostate Cancer* [Online]. Available: http://www.cancerresearchuk.org/about-cancer/prostate-cancer/stages/tnm-staging [Accessed 4/8/16 2016].

CANCERRESEARCHUK. 2016g. *Treating prostate cancer* [Online]. Available: http://www.cancerresearchuk.org/about-cancer/type/prostate-cancer/treatment/.

CANCERRESEARCHUK. 2016h. *What is prostate cancer* [Online]. Available: http://www.cancerresearchuk.org/about-cancer/type/prostate-cancer/about/the-prostate.

CANCERRESEARCHUK. 2017. *Prostate cancer statistics* [Online]. Available: http://www.cancerresearchuk.org/health-professional/cancer-statistics/statistics-by-cancer-type/prostate-cancer [Accessed 12/5/16 2016].

CARMELIET, P. 2005. VEGF as a key mediator of angiogenesis in cancer. *Oncology,* 69 Suppl 3**,** 4-10.

CARTWRIGHT, C. A., MEISLER, A. I. & ECKHART, W. 1990. Activation of the pp60c-src protein kinase is an early event in colonic carcinogenesis. *Proc Natl Acad Sci U S A,* 87**,** 558-62.

CAVEY, M., RAUZI, M., LENNE, P. F. & LECUIT, T. 2008. A two-tiered mechanism for stabilization and immobilization of E-cadherin. *Nature,* 453**,** 751-6.

CHANG, D. D., PARK, N. H., DENNY, C. T., NELSON, S. F. & PE, M. 1998. Characterization of transformation related genes in oral cancer cells. *Oncogene,* 16**,** 1921-30.

CHANG, Y. M., BAI, L., LIU, S., YANG, J. C., KUNG, H. J. & EVANS, C. P. 2008. Src family kinase oncogenic potential and pathways in prostate cancer as revealed by AZD0530. *Oncogene,* 27**,** 6365-75.

CHEN, H. C., APPEDDU, P. A., ISODA, H. & GUAN, J. L. 1996. Phosphorylation of tyrosine 397 in focal adhesion kinase is required for binding phosphatidylinositol 3-kinase. *J Biol Chem,* 271**,** 26329-34.

CHEN, N. P., UDDIN, B., HARDT, R., DING, W., PANIC, M., LUCIBELLO, I., KAMMERER, P., RUPPERT, T. & SCHIEBEL, E. 2017. Human phosphatase CDC14A regulates actin organization through dephosphorylation of epithelial protein lost in neoplasm. *Proc Natl Acad Sci U S A,* 114**,** 5201-5206.

CHEN, S., MAUL, R. S., KIM, H. R. & CHANG, D. D. 2000. Characterization of the human EPLIN (Epithelial Protein Lost in Neoplasm) gene reveals distinct promoters for the two EPLIN isoforms. *Gene,* 248**,** 69-76.

CHENG, S. Y., SUN, G., SCHLAEPFER, D. D. & PALLEN, C. J. 2014. Grb2 promotes integrin-induced focal adhesion kinase (FAK) autophosphorylation and directs the phosphorylation of protein tyrosine phosphatase alpha by the Src-FAK kinase complex. *Mol Cell Biol,* 34**,** 348-61.

CHERVIN-PETINOT, A., COURCON, M., ALMAGRO, S., NICOLAS, A., GRICHINE, A., GRUNWALD, D., PRANDINI, M. H., HUBER, P. & GULINO-DEBRAC, D. 2012. Epithelial protein lost in neoplasm (EPLIN) interacts with alpha-catenin and actin filaments in endothelial cells and stabilizes vascular capillary network in vitro. *J Biol Chem,* 287**,** 7556-72.

CHIRCOP, M., OAKES, V., GRAHAM, M. E., MA, M. P., SMITH, C. M., ROBINSON, P. J. & KHANNA, K. K. 2009. The actin-binding and bundling protein, EPLIN, is required for cytokinesis. *Cell Cycle,* 8**,** 757-64.

CLARKE, B. 2008. Normal bone anatomy and physiology. *Clin J Am Soc Nephrol,* 3 Suppl 3**,** S131-9.

CREEDON, H. & BRUNTON, V. G. 2012. Src kinase inhibitors: promising cancer therapeutics? *Crit Rev Oncog,* 17**,** 145-59.

CROWE, D. L. & OHANNESSIAN, A. 2004. Recruitment of focal adhesion kinase and paxillin to beta1 integrin promotes cancer cell migration via mitogen activated protein kinase activation. *BMC Cancer,* 4**,** 18.

DAILY, S. 2010. *FAK inhibitor effectively blocked colon cancer cell growth and viability* [Online]. Available: https://www.sciencedaily.com/releases/2010/10/101028132259.htm [Accessed 24/8/16 2016].

DAVIES, S. & JIANG, W. G. 2010. ALCAM, activated leukocyte cell adhesion molecule, influences the aggressive nature of breast cancer cells, a potential connection to bone metastasis. *Anticancer Res,* 30**,** 1163-8.

DEAKIN, N. O., PIGNATELLI, J. & TURNER, C. E. 2012. Diverse roles for the paxillin family of proteins in cancer. *Genes Cancer,* 3**,** 362-70.

DEAKIN, N. O. & TURNER, C. E. 2008. Paxillin comes of age. *J Cell Sci,* 121**,** 2435-44.

DEAKIN, N. O. & TURNER, C. E. 2011. Distinct roles for paxillin and Hic-5 in regulating breast cancer cell morphology, invasion, and metastasis. *Mol Biol Cell,* 22**,** 327-41.

DELIGEZER, U., YAMAN, F., DARENDELILER, E., DIZDAR, Y., HOLDENRIEDER, S., KOVANCILAR, M. & DALAY, N. 2010. Post-treatment circulating plasma BMP6 mRNA and H3K27 methylation levels discriminate metastatic prostate cancer from localized disease. *Clin Chim Acta,* 411**,** 1452-6.

DERAMAUDT, T. B., DUJARDIN, D., HAMADI, A., NOULET, F., KOLLI, K., DE MEY, J., TAKEDA, K. & RONDE, P. 2011. FAK phosphorylation at Tyr-925 regulates cross-talk between focal adhesion turnover and cell protrusion. *Mol Biol Cell,* 22**,** 964-75.

DERAMAUDT, T. B., DUJARDIN, D., NOULET, F., MARTIN, S., VAUCHELLES, R., TAKEDA, K. & RONDE, P. 2014. Altering FAK-paxillin interactions reduces adhesion, migration and invasion processes. *PLoS One,* 9**,** e92059.

DEVYS, A., LORTHOLARY, A. & AUDRAN, M. 2001. [PTHrP and breast cancer]. *Bull Cancer,* 88**,** 1075-80.

DHILLON, A. S., HAGAN, S., RATH, O. & KOLCH, W. 2007. MAP kinase signalling pathways in cancer. *Oncogene,* 26**,** 3279-90.

DINU, M., ABBATE, R., GENSINI, G. F., CASINI, A. & SOFI, F. 2016. Vegetarian, vegan diets and multiple health outcomes: a systematic review with meta-analysis of observational studies. *Crit Rev Food Sci Nutr***,** 0.

DOUGLAS, J. A., LEVIN, A. M., ZUHLKE, K. A., RAY, A. M., JOHNSON, G. R., LANGE, E. M., WOOD, D. P. & COONEY, K. A. 2007. Common variation in the BRCA1 gene and prostate cancer risk. *Cancer Epidemiol Biomarkers Prev,* 16**,** 1510-6.

DREES, F., POKUTTA, S., YAMADA, S., NELSON, W. J. & WEIS, W. I. 2005. Alpha-catenin is a molecular switch that binds E-cadherin-beta-catenin and regulates actin-filament assembly. *Cell,* 123**,** 903-15.

DUMMLER, B., OHSHIRO, K., KUMAR, R. & FIELD, J. 2009. Pak protein kinases and their role in cancer. *Cancer Metastasis Rev,* 28**,** 51-63.

EIDE, B. L., TURCK, C. W. & ESCOBEDO, J. A. 1995. Identification of Tyr-397 as the primary site of tyrosine phosphorylation and pp60src association in the focal adhesion kinase, pp125FAK. *Mol Cell Biol,* 15**,** 2819-27.

ELGASS, S., COOPER, A. & CHOPRA, M. 2014. Lycopene treatment of prostate cancer cell lines inhibits adhesion and migration properties of the cells. *Int J Med Sci,* 11**,** 948-54.

ELSBERGER, B., TAN, B. A., MITCHELL, T. J., BROWN, S. B., MALLON, E. A., TOVEY, S. M., COOKE, T. G., BRUNTON, V. G. & EDWARDS, J. 2009. Is expression or activation of Src kinase associated with cancer-specific survival in ER-, PR- and HER2-negative breast cancer patients? *Am J Pathol,* 175**,** 1389-97.

ESCRIVA, H., DELAUNAY, F. & LAUDET, V. 2000. Ligand binding and nuclear receptor evolution. *Bioessays,* 22**,** 717-27.

FARMER, P., BONNEFOI, H., BECETTE, V., TUBIANA-HULIN, M., FUMOLEAU, P., LARSIMONT, D., MACGROGAN, G., BERGH, J., CAMERON, D., GOLDSTEIN, D., DUSS, S., NICOULAZ, A. L., BRISKEN, C., FICHE, M., DELORENZI, M. & IGGO, R. 2005. Identification of molecular apocrine breast tumours by microarray analysis. *Oncogene,* 24**,** 4660-71.

FERRARA, N., GERBER, H. P. & LECOUTER, J. 2003. The biology of VEGF and its receptors. *Nat Med,* 9**,** 669-76.

FERRARI, G., COOK, B. D., TERUSHKIN, V., PINTUCCI, G. & MIGNATTI, P. 2009. Transforming growth factor-beta 1 (TGF-beta1) induces angiogenesis through vascular endothelial growth factor (VEGF)-mediated apoptosis. *J Cell Physiol,* 219**,** 449-58.

FIDLER, I. J. 2003. The pathogenesis of cancer metastasis: the 'seed and soil' hypothesis revisited. *Nat Rev Cancer,* 3**,** 453-8.

FIFE, C. M., MCCARROLL, J. A. & KAVALLARIS, M. 2014. Movers and shakers: cell cytoskeleton in cancer metastasis. *Br J Pharmacol,* 171**,** 5507-23.

FINCHAM, V. J. & FRAME, M. C. 1998. The catalytic activity of Src is dispensable for translocation to focal adhesions but controls the turnover of these structures during cell motility. *Embo j,* 17**,** 81-92.

FIORENTINO, M., JUDSON, G., PENNEY, K., FLAVIN, R., STARK, J., FIORE, C., FALL, K., MARTIN, N., MA, J., SINNOTT, J., GIOVANNUCCI, E., STAMPFER, M., SESSO, H. D., KANTOFF, P. W., FINN, S., LODA, M. & MUCCI, L. 2010. Immunohistochemical expression of BRCA1 and lethal prostate cancer. *Cancer Res,* 70**,** 3136-9.

GARTRELL, B. A. & SAAD, F. 2014. Managing bone metastases and reducing skeletal related events in prostate cancer. *Nat Rev Clin Oncol,* 11**,** 335-45.

GEIGER, B., TOKUYASU, K. T., DUTTON, A. H. & SINGER, S. J. 1980. Vinculin, an intracellular protein localized at specialized sites where microfilament bundles terminate at cell membranes. *Proc Natl Acad Sci U S A,* 77**,** 4127-31.

GIANCOTTI, F. G. & RUOSLAHTI, E. 1999. Integrin signaling. *Science,* 285**,** 1028-32.

GILCREASE, M. Z. 2007. Integrin signaling in epithelial cells. *Cancer Lett,* 247**,** 1-25.

GILSING, A. M., WEIJENBERG, M. P., GOLDBOHM, R. A., DAGNELIE, P. C., VAN DEN BRANDT, P. A. & SCHOUTEN, L. J. 2016. Vegetarianism, low meat consumption and the risk of lung, postmenopausal breast and prostate cancer in a population-based cohort study. *Eur J Clin Nutr*.

GIOVANNUCCI, E., STAMPFER, M. J., KRITHIVAS, K., BROWN, M., DAHL, D., BRUFSKY, A., TALCOTT, J., HENNEKENS, C. H. & KANTOFF, P. W. 1997. The CAG repeat within the androgen receptor gene and its relationship to prostate cancer. *Proc Natl Acad Sci U S A,* 94**,** 3320-3.

GLEASON, D. F. & MELLINGER, G. T. 1974. Prediction of prognosis for prostatic adenocarcinoma by combined histological grading and clinical staging. *J Urol,* 111**,** 58-64.

GOLUBOVSKAYA, V. M. 2014. Targeting FAK in human cancer: from finding to first clinical trials. *Front Biosci (Landmark Ed),* 19**,** 687-706.

GOLUBOVSKAYA, V. M., NYBERG, C., ZHENG, M., KWEH, F., MAGIS, A., OSTROV, D. & CANCE, W. G. 2008. A small molecule inhibitor, 1,2,4,5-benzenetetraamine tetrahydrochloride, targeting the y397 site of focal adhesion kinase decreases tumor growth. *J Med Chem,* 51**,** 7405-16.

GUAN, J. L. 1997. Role of focal adhesion kinase in integrin signaling. *Int J Biochem Cell Biol,* 29**,** 1085-96.

GUARINO, M. 2010. Src signaling in cancer invasion. *J Cell Physiol,* 223**,** 14-26.

GUISE, T. A., YIN, J. J., THOMAS, R. J., DALLAS, M., CUI, Y. & GILLESPIE, M. T. 2002. Parathyroid hormone-related protein (PTHrP)-(1-139) isoform is efficiently secreted in vitro and enhances breast cancer metastasis to bone in vivo. *Bone,* 30**,** 670-6.

GULINO-DEBRAC, D. 2013. Mechanotransduction at the basis of endothelial barrier function. *Tissue Barriers,* 1**,** e24180.

HALL, M. D., SCHULTHEISS, T. E., FARINO, G. & Y., W. J. 2015. Increase in higher risk prostate cancer cases following new screening recommendation by the US Preventive Services Task Force (USPSTF). *Journal of Clinical Oncology* 33.

HAN, M. Y., KOSAKO, H., WATANABE, T. & HATTORI, S. 2007. Extracellular signal-regulated kinase/mitogen-activated protein kinase regulates actin organization and cell motility by phosphorylating the actin cross-linking protein EPLIN. *Mol Cell Biol,* 27**,** 8190-204.

HANAHAN, D. & WEINBERG, R. A. 2011. Hallmarks of cancer: the next generation. *Cell,* 144**,** 646-74.

HANKS, S. K., RYZHOVA, L., SHIN, N. Y. & BRABEK, J. 2003. Focal adhesion kinase signaling activities and their implications in the control of cell survival and motility. *Front Biosci,* 8**,** d982-96.

HANSEN, A. G., ARNOLD, S. A., JIANG, M., PALMER, T. D., KETOVA, T., MERKEL, A., PICKUP, M., SAMARAS, S., SHYR, Y., MOSES, H. L., HAYWARD, S. W., STERLING, J. A. & ZIJLSTRA, A. 2014. ALCAM/CD166 is a TGF-beta-responsive marker and functional regulator of prostate cancer metastasis to bone. *Cancer Res,* 74**,** 1404-15.

HASHIMOTO, T., ABE, M., OSHIMA, T., SHIBATA, H., OZAKI, S., INOUE, D. & MATSUMOTO, T. 2004. Ability of myeloma cells to secrete macrophage inflammatory protein (MIP)-1alpha and MIP-1beta correlates with lytic bone lesions in patients with multiple myeloma. *Br J Haematol,* 125**,** 38-41.

HAYASHI, I., VUORI, K. & LIDDINGTON, R. C. 2002. The focal adhesion targeting (FAT) region of focal adhesion kinase is a four-helix bundle that binds paxillin. *Nat Struct Biol,* 9**,** 101-6.

HAYTHORN, M. R. & ABLIN, R. J. 2011. Prostate-specific antigen testing across the spectrum of prostate cancer. *Biomark Med,* 5**,** 515-26.

HEFFLER, M., GOLUBOVSKAYA, V. M., CONROY, J., LIU, S., WANG, D., CANCE, W. G. & DUNN, K. B. 2013a. FAK and HAS inhibition synergistically decrease colon cancer cell viability and affect expression of critical genes. *Anticancer Agents Med Chem,* 13**,** 584-94.

HEFFLER, M., GOLUBOVSKAYA, V. M., DUNN, K. M. & CANCE, W. 2013b. Focal adhesion kinase autophosphorylation inhibition decreases colon cancer cell growth and enhances the efficacy of chemotherapy. *Cancer Biol Ther,* 14**,** 761-72.

HEINLEIN, C. A. & CHANG, C. 2004. Androgen receptor in prostate cancer. *Endocr Rev,* 25**,** 276-308.

HENG, Y. W. & KOH, C. G. 2010. Actin cytoskeleton dynamics and the cell division cycle. *Int J Biochem Cell Biol,* 42**,** 1622-33.

HIGUERA, S. Y. M. A. V. 2016. *Bone metastasis and prostate cancer* [Online]. Health line. Available: http://www.healthline.com/health/prostate-cancer-prognosis-life-expectancy-bone-metastases#Overview1 [Accessed 16-5-17 2017].

HOROSZEWICZ, J. S., LEONG, S. S., KAWINSKI, E., KARR, J. P., ROSENTHAL, H., CHU, T. M., MIRAND, E. A. & MURPHY, G. P. 1983. LNCaP model of human prostatic carcinoma. *Cancer Res,* 43**,** 1809-18.

HSIA, D. A., MITRA, S. K., HAUCK, C. R., STREBLOW, D. N., NELSON, J. A., ILIC, D., HUANG, S., LI, E., NEMEROW, G. R., LENG, J., SPENCER, K. S., CHERESH, D. A. & SCHLAEPFER, D. D. 2003. Differential regulation of cell motility and invasion by FAK. *J Cell Biol,* 160**,** 753-67.

HU, Y. L., LU, S., SZETO, K. W., SUN, J., WANG, Y., LASHERAS, J. C. & CHIEN, S. 2014. FAK and paxillin dynamics at focal adhesions in the protrusions of migrating cells. *Sci Rep,* 4**,** 6024.

HUANG, S. P., WU, M. S., SHUN, C. T., WANG, H. P., LIN, M. T., KUO, M. L. & LIN, J. T. 2004. Interleukin-6 increases vascular endothelial growth factor and angiogenesis in gastric carcinoma. *J Biomed Sci,* 11**,** 517-27.

HUNCHAREK, M., HADDOCK, K. S., REID, R. & KUPELNICK, B. 2010. Smoking as a risk factor for prostate cancer: a meta-analysis of 24 prospective cohort studies. *Am J Public Health,* 100**,** 693-701.

IDDON, J., BUNDRED, N. J., HOYLAND, J., DOWNEY, S. E., BAIRD, P., SALTER, D., MCMAHON, R. & FREEMONT, A. J. 2000. Expression of parathyroid hormone-related protein and its receptor in bone metastases from prostate cancer. *J Pathol,* 191**,** 170-4.

IRBY, R. B. & YEATMAN, T. J. 2000. Role of Src expression and activation in human cancer. *Oncogene,* 19**,** 5636-42.

ISLAMI, F., MOREIRA, D. M., BOFFETTA, P. & FREEDLAND, S. J. 2014. A systematic review and meta-analysis of tobacco use and prostate cancer mortality and incidence in prospective cohort studies. *Eur Urol,* 66**,** 1054-64.

ITOH, S., UDAGAWA, N., TAKAHASHI, N., YOSHITAKE, F., NARITA, H., EBISU, S. & ISHIHARA, K. 2006. A critical role for interleukin-6 family-mediated Stat3 activation in osteoblast differentiation and bone formation. *Bone,* 39**,** 505-12.

JIANG, H. & HEGDE, S. 2016. Targeting focal adhesion kinase renders pancreatic cancers responsive to checkpoint immunotherapy. 22**,** 851-60.

JIANG, W. G., MARTIN, T. A., LEWIS-RUSSELL, J. M., DOUGLAS-JONES, A., YE, L. & MANSEL, R. E. 2008. Eplin-alpha expression in human breast cancer, the impact on cellular migration and clinical outcome. *Mol Cancer,* 7**,** 71.

JIN, J. K., TIEN, P. C., CHENG, C. J., SONG, J. H., HUANG, C., LIN, S. H. & GALLICK, G. E. 2015. Talin1 phosphorylation activates beta1 integrins: a novel mechanism to promote prostate cancer bone metastasis. *Oncogene,* 34**,** 1811-21.

KAKONEN, S. M., SELANDER, K. S., CHIRGWIN, J. M., YIN, J. J., BURNS, S., RANKIN, W. A., GRUBBS, B. G., DALLAS, M., CUI, Y. & GUISE, T. A. 2002. Transforming growth factor-beta stimulates parathyroid hormone-related protein and osteolytic metastases via Smad and mitogen-activated protein kinase signaling pathways. *J Biol Chem,* 277**,** 24571-8.

KALLURI, R. & WEINBERG, R. A. 2009. The basics of epithelial-mesenchymal transition. *J Clin Invest,* 119**,** 1420-8.

KANTETI, R., YALA, S., FERGUSON, M. K. & SALGIA, R. 2009. MET, HGF, EGFR, and PXN gene copy number in lung cancer using DNA extracts from FFPE archival samples and prognostic significance. *J Environ Pathol Toxicol Oncol,* 28**,** 89-98.

KARAKOSE, E., GEIGER, T., FLYNN, K., LORENZ-BAATH, K., ZENT, R., MANN, M. & FASSLER, R. 2015. The focal adhesion protein PINCH-1 associates with EPLIN at integrin adhesion sites. *J Cell Sci,* 128**,** 1023-33.

KIM, G., DAVIDSON, B., HENNING, R., WANG, J., YU, M., ANNUNZIATA, C., HETLAND, T. & KOHN, E. C. 2012. Adhesion molecule protein signature in ovarian cancer effusions is prognostic of patient outcome. *Cancer,* 118**,** 1543-53.

KIM, J. S., XU, X., LI, H., SOLOMON, D., LANE, W. S., JIN, T. & WALDMAN, T. 2011. Mechanistic analysis of a DNA damage-induced, PTEN-dependent size checkpoint in human cells. *Mol Cell Biol,* 31**,** 2756-71.

KIM, L. C., SONG, L. & HAURA, E. B. 2009. Src kinases as therapeutic targets for cancer. *Nat Rev Clin Oncol,* 6**,** 587-95.

KLEPZIG, M., JONAS, D. & OREMEK, G. M. 2009. Procollagen type 1 amino-terminal propeptide: a marker for bone metastases in prostate carcinoma. *Anticancer Res,* 29**,** 671-3.

KORENCHUK, S., LEHR, J. E., L, M. C., LEE, Y. G., WHITNEY, S., VESSELLA, R., LIN, D. L. & PIENTA, K. J. 2001. VCaP, a cell-based model system of human prostate cancer. *In Vivo,* 15**,** 163-8.

KUKITA, T., NOMIYAMA, H., OHMOTO, Y., KUKITA, A., SHUTO, T., HOTOKEBUCHI, T., SUGIOKA, Y., MIURA, R. & IIJIMA, T. 1997. Macrophage inflammatory protein-1 alpha (LD78) expressed in human bone marrow: its role in regulation of hematopoiesis and osteoclast recruitment. *Lab Invest,* 76**,** 399-406.

KUROZUMI, A., GOTO, Y., MATSUSHITA, R., FUKUMOTO, I., KATO, M., NISHIKAWA, R., SAKAMOTO, S., ENOKIDA, H., NAKAGAWA, M., ICHIKAWA, T. & SEKI, N. 2016. Tumor-suppressive microRNA-223 inhibits cancer cell migration and invasion by targeting ITGA3/ITGB1 signaling in prostate cancer. *Cancer Sci,* 107**,** 84-94.

LAMOUILLE, S., XU, J. & DERYNCK, R. 2014. Molecular mechanisms of epithelial-mesenchymal transition. *Nat Rev Mol Cell Biol,* 15**,** 178-96.

LATTOUF, J. B., SRINIVASAN, R., PINTO, P. A., LINEHAN, W. M. & NECKERS, L. 2006. Mechanisms of disease: the role of heat-shock protein 90 in genitourinary malignancy. *Nat Clin Pract Urol,* 3**,** 590-601.

LEAL, J., HAMDY, F. & WOLSTENHOLME, J. 2014. Estimating age and ethnic variation in the histological prevalence of prostate cancer to inform the impact of screening policies. *Int J Urol,* 21**,** 786-92.

LEGATE, K. R., MONTANEZ, E., KUDLACEK, O. & FASSLER, R. 2006. ILK, PINCH and parvin: the tIPP of integrin signalling. *Nat Rev Mol Cell Biol,* 7**,** 20-31.

LEISSNER, K. H. & TISELL, L. E. 1979. The weight of the human prostate. *Scand J Urol Nephrol,* 13**,** 137-42.

LEITNER, L., SHAPOSHNIKOV, D., DESCOT, A., HOFFMANN, R. & POSERN, G. 2010. Epithelial Protein Lost in Neoplasm alpha (Eplin-alpha) is transcriptionally regulated by G-actin and MAL/MRTF coactivators. *Mol Cancer,* 9**,** 60.

LENTZSCH, S., GRIES, M., JANZ, M., BARGOU, R., DORKEN, B. & MAPARA, M. Y. 2003. Macrophage inflammatory protein 1-alpha (MIP-1 alpha) triggers migration and signaling cascades mediating survival and proliferation in multiple myeloma (MM) cells. *Blood,* 101**,** 3568-73.

LEONGAMORNLERT, D., MAHMUD, N., TYMRAKIEWICZ, M., SAUNDERS, E., DADAEV, T., CASTRO, E., GOH, C., GOVINDASAMI, K., GUY, M., O'BRIEN, L., SAWYER, E., HALL, A., WILKINSON, R., EASTON, D., GOLDGAR, D., EELES, R. & KOTE-JARAI, Z. 2012. Germline BRCA1 mutations increase prostate cancer risk. *Br J Cancer,* 106**,** 1697-701.

LI, J., YEN, C., LIAW, D., PODSYPANINA, K., BOSE, S., WANG, S. I., PUC, J., MILIARESIS, C., RODGERS, L., MCCOMBIE, R., BIGNER, S. H., GIOVANELLA, B. C., ITTMANN, M., TYCKO, B., HIBSHOOSH, H., WIGLER, M. H. & PARSONS, R. 1997. PTEN, a putative protein tyrosine phosphatase gene mutated in human brain, breast, and prostate cancer. *Science,* 275**,** 1943-7.

LI, W. 2010. *Can we eat to starve cancer?* [Online]. Available: https://www.ted.com/talks/william_li?language=en.

LI, X., LIU, Y., WU, B., DONG, Z., WANG, Y., LU, J., SHI, P., BAI, W. & WANG, Z. 2014. Potential role of the OPG/RANK/RANKL axis in prostate cancer invasion and bone metastasis. *Oncol Rep,* 32**,** 2605-11.

LI, Z., WANG, H., EYLER, C. E., HJELMELAND, A. B. & RICH, J. N. 2009. Turning cancer stem cells inside out: an exploration of glioma stem cell signaling pathways. *J Biol Chem,* 284**,** 16705-9.

LIU, R., MARTIN, T. A., JORDAN, N. J., RUGE, F., YE, L. & JIANG, W. G. 2016. Epithelial protein lost in neoplasm-alpha (EPLIN-alpha) is a potential prognostic marker for the progression of epithelial ovarian cancer. *Int J Oncol,* 48**,** 2488-96.

LIU, X., BRODEUR, S. R., GISH, G., SONGYANG, Z., CANTLEY, L. C., LAUDANO, A. P. & PAWSON, T. 1993. Regulation of c-Src tyrosine kinase activity by the Src SH2 domain. *Oncogene,* 8**,** 1119-26.

LIU, Y., SANDERS, A. J., ZHANG, L. & JIANG, W. G. 2012a. EPLIN-alpha expression in human oesophageal cancer and its impact on cellular aggressiveness and clinical outcome. *Anticancer Res,* 32**,** 1283-9.

LIU, Y., SANDERS, A. J., ZHANG, L. & JIANG, W. G. 2012b. Expression profile of Epithelial Protein Lost in Neoplasm-Alpha (EPLIN-a) in human

Pulmonary Cancer and its impact on SKMES-1 cells *in Vitro*. *Journal of Cancer Therapy* 3**,** 452-459.

LIU, Z. X., YU, C. F., NICKEL, C., THOMAS, S. & CANTLEY, L. G. 2002. Hepatocyte growth factor induces ERK-dependent paxillin phosphorylation and regulates paxillin-focal adhesion kinase association. *J Biol Chem,* 277**,** 10452-8.

LLOYD, T., HOUNSOME, L., MEHAY, A., MEE, S., VERNE, J. & COOPER, A. 2015. Lifetime risk of being diagnosed with, or dying from, prostate cancer by major ethnic group in England 2008-2010. *BMC Med,* 13**,** 171.

LOGOTHETIS, C. J. & LIN, S. H. 2005. Osteoblasts in prostate cancer metastasis to bone. *Nat Rev Cancer,* 5**,** 21-8.

LUNDWALL, A. & LILJA, H. 1987. Molecular cloning of human prostate specific antigen cDNA. *FEBS Lett,* 214**,** 317-22.

MACKINNON, A. C., TRETIAKOVA, M., HENDERSON, L., MEHTA, R. G., YAN, B. C., JOSEPH, L., KRAUSZ, T., HUSAIN, A. N., REID, M. E. & SALGIA, R. 2011. Paxillin expression and amplification in early lung lesions of high-risk patients, lung adenocarcinoma and metastatic disease. *J Clin Pathol,* 64**,** 16-24.

MADAN, R., SMOLKIN, M. B., COCKER, R., FAYYAD, R. & OKTAY, M. H. 2006. Focal adhesion proteins as markers of malignant transformation and prognostic indicators in breast carcinoma. *Hum Pathol,* 37**,** 9-15.

MARKS, S. C., JR., AND ODGREN, P.R. 2002. *In principles of bone biology* New York, Academic Press.

MATTHEWS, J. M., LESTER, K., JOSEPH, S. & CURTIS, D. J. 2013. LIM-domain-only proteins in cancer. *Nat Rev Cancer,* 13**,** 111-22.

MAUL, R. S. & CHANG, D. D. 1999. EPLIN, epithelial protein lost in neoplasm. *Oncogene,* 18**,** 7838-41.

MAUL, R. S., SACHI GERBIN, C. & CHANG, D. D. 2001. Characterization of mouse epithelial protein lost in neoplasm (EPLIN) and comparison of mammalian and zebrafish EPLIN. *Gene,* 262**,** 155-60.

MAUL, R. S., SONG, Y., AMANN, K. J., GERBIN, S. C., POLLARD, T. D. & CHANG, D. D. 2003. EPLIN regulates actin dynamics by cross-linking and stabilizing filaments. *J Cell Biol,* 160**,** 399-407.

MAZUMDER, S., DUPREE, E. L. & ALMASAN, A. 2004. A dual role of cyclin E in cell proliferation and apoptosis may provide a target for cancer therapy. *Curr Cancer Drug Targets,* 4**,** 65-75.

MCLEAN, G. W., CARRAGHER, N. O., AVIZIENYTE, E., EVANS, J., BRUNTON, V. G. & FRAME, M. C. 2005. The role of focal-adhesion kinase in cancer - a new therapeutic opportunity. *Nat Rev Cancer,* 5**,** 505-15.

MEBRATU, Y. & TESFAIGZI, Y. 2009. How ERK1/2 activation controls cell proliferation and cell death: Is subcellular localization the answer? *Cell Cycle,* 8**,** 1168-75.

MEGE, R. M., GAVARD, J. & LAMBERT, M. 2006. Regulation of cell-cell junctions by the cytoskeleton. *Curr Opin Cell Biol,* 18**,** 541-8.

MELOCHE, S. & POUYSSEGUR, J. 2007. The ERK1/2 mitogen-activated protein kinase pathway as a master regulator of the G1- to S-phase transition. *Oncogene,* 26**,** 3227-39.

MENG, W. & TAKEICHI, M. 2009. Adherens junction: molecular architecture and regulation. *Cold Spring Harb Perspect Biol,* 1**,** a002899.

MESTAYER, C., BLANCHERE, M., JAUBERT, F., DUFOUR, B. & MOWSZOWICZ, I. 2003. Expression of androgen receptor coactivators in normal and cancer prostate tissues and cultured cell lines. *Prostate,* 56**,** 192-200.

MICALIZZI, D. S., FARABAUGH, S. M. & FORD, H. L. 2010. Epithelial-mesenchymal transition in cancer: parallels between normal development and tumor progression. *J Mammary Gland Biol Neoplasia,* 15**,** 117-34.

MIKI, T., YANO, S., HANIBUCHI, M., KANEMATSU, T., MUGURUMA, H. & SONE, S. 2004. Parathyroid hormone-related protein (PTHrP) is responsible for production of bone metastasis, but not visceral metastasis, by human small cell lung cancer SBC-5 cells in natural killer cell-depleted SCID mice. *Int J Cancer,* 108**,** 511-5.

MITRA, A. V., BANCROFT, E. K., BARBACHANO, Y., PAGE, E. C., FOSTER, C. S., JAMESON, C., MITCHELL, G., LINDEMAN, G. J., STAPLETON, A., SUTHERS, G., EVANS, D. G., CRUGER, D., BLANCO, I., MERCER, C., KIRK, J., MAEHLE, L., HODGSON, S., WALKER, L., IZATT, L., DOUGLAS, F., TUCKER, K., DORKINS, H., CLOWES, V., MALE, A., DONALDSON, A., BREWER, C., DOHERTY, R., BULMAN, B., OSTHER, P. J., SALINAS, M., ECCLES, D., AXCRONA, K., JOBSON, I., NEWCOMBE, B., CYBULSKI, C., RUBINSTEIN, W. S., BUYS, S., TOWNSHEND, S., FRIEDMAN, E., DOMCHEK, S., RAMON, Y. C. T., SPIGELMAN, A., TEO, S. H., NICOLAI, N., AARONSON, N., ARDERN-JONES, A., BANGMA, C., DEARNALEY, D., EYFJORD, J., FALCONER, A., GRONBERG, H., HAMDY, F., JOHANNSSON, O., KHOO, V., KOTE-JARAI, Z., LILJA, H., LUBINSKI, J., MELIA, J., MOYNIHAN, C., PEOCK, S., RENNERT, G., SCHRODER, F., SIBLEY, P., SURI, M., WILSON, P., BIGNON, Y. J., STROM, S., TISCHKOWITZ, M., LILJEGREN, A., ILENCIKOVA, D., ABELE, A., KYRIACOU, K., VAN

ASPEREN, C., KIEMENEY, L., EASTON, D. F. & EELES, R. A. 2011. Targeted prostate cancer screening in men with mutations in BRCA1 and BRCA2 detects aggressive prostate cancer: preliminary analysis of the results of the IMPACT study. *BJU Int,* 107**,** 28-39.

MITRA, S. K., HANSON, D. A. & SCHLAEPFER, D. D. 2005. Focal adhesion kinase: in command and control of cell motility. *Nat Rev Mol Cell Biol,* 6**,** 56-68.

MITRA, S. K. & SCHLAEPFER, D. D. 2006. Integrin-regulated FAK-Src signaling in normal and cancer cells. *Curr Opin Cell Biol,* 18**,** 516-23.

MOENS, S., GOVEIA, J., STAPOR, P. C., CANTELMO, A. R. & CARMELIET, P. 2014. The multifaceted activity of VEGF in angiogenesis - Implications for therapy responses. *Cytokine Growth Factor Rev,* 25**,** 473-82.

MONTERO, J. C., SEOANE, S., OCANA, A. & PANDIELLA, A. 2011. Inhibition of SRC family kinases and receptor tyrosine kinases by dasatinib: possible combinations in solid tumors. *Clin Cancer Res,* 17**,** 5546-52.

MORI, K., LE GOFF, B., CHARRIER, C., BATTAGLIA, S., HEYMANN, D. & REDINI, F. 2007. DU145 human prostate cancer cells express functional receptor activator of NFkappaB: new insights in the prostate cancer bone metastasis process. *Bone,* 40**,** 981-90.

MUKHERJI, D., TEMRAZ, S., WEHBE, D. & SHAMSEDDINE, A. 2013. Angiogenesis and anti-angiogenic therapy in prostate cancer. *Crit Rev Oncol Hematol,* 87**,** 122-31.

MULLER, P. A. & VOUSDEN, K. H. 2013. p53 mutations in cancer. *Nat Cell Biol,* 15**,** 2-8.

MULROONEY, J. P., HONG, T. & GRABEL, L. B. 2001. Serine 785 phosphorylation of the beta1 cytoplasmic domain modulates beta1A-integrin-dependent functions. *J Cell Sci,* 114**,** 2525-33.

MUNDY, G. R. 2002. Metastasis to bone: causes, consequences and therapeutic opportunities. *Nat Rev Cancer,* 2**,** 584-93.

MURASHIMA, A., KISHIGAMI, S., THOMSON, A. & YAMADA, G. 2015. Androgens and mammalian male reproductive tract development. *Biochim Biophys Acta,* 1849**,** 163-70.

NATIONALCANCERINSTITUTE. *Metastatic Cancer* [Online]. Available: http://www.cancer.gov/types/metastatic-cancer [Accessed 7/9/16 2016].

NATIONALCANCERINSTITUTE Metastatic Cancer.

NATIONALINSTITUTEFORHEALTHANDCAREEXCELLENCE(NICE). 2016. *Prostate Cancer* [Online]. Available: https://www.nice.org.uk/guidance/qs91 [Accessed 18/8/16 2016].

NELSON, W. J. 2008. Regulation of cell-cell adhesion by the cadherin-catenin complex. *Biochem Soc Trans,* 36**,** 149-55.

NHS. 2016a. *Diagnosing Prostate Cancer* [Online]. Available: http://www.nhs.uk/Conditions/Cancer-of-the-prostate/Pages/Diagnosis.aspx [Accessed 2/8/16 2016].

NHS. 2016b. *Treating prostate cancer* [Online]. Available: http://www.nhs.uk/Conditions/Cancer-of-the-prostate/Pages/Treatment.aspx [Accessed 9/8/16 2016].

NISHIDA, N., YANO, H., NISHIDA, T., KAMURA, T. & KOJIRO, M. 2006. Angiogenesis in cancer. *Vasc Health Risk Manag,* 2**,** 213-9.

NORGAARD, M., JENSEN, A. O., JACOBSEN, J. B., CETIN, K., FRYZEK, J. P. & SORENSEN, H. T. 2010. Skeletal related events, bone metastasis and survival of prostate cancer: a population based cohort study in Denmark (1999 to 2007). *J Urol,* 184**,** 162-7.

NORMANNO, N., DE LUCA, A., BIANCO, C., STRIZZI, L., MANCINO, M., MAIELLO, M. R., CAROTENUTO, A., DE FEO, G., CAPONIGRO, F. & SALOMON, D. S. 2006. Epidermal growth factor receptor (EGFR) signaling in cancer. *Gene,* 366**,** 2-16.

OGATA, A., CHAUHAN, D., TEOH, G., TREON, S. P., URASHIMA, M., SCHLOSSMAN, R. L. & ANDERSON, K. C. 1997. IL-6 triggers cell growth via the Ras-dependent mitogen-activated protein kinase cascade. *J Immunol,* 159**,** 2212-21.

OHASHI, T., IDOGAWA, M., SASAKI, Y. & TOKINO, T. 2017. p53 mediates the suppression of cancer cell invasion by inducing LIMA1/EPLIN. *Cancer Lett,* 390**,** 58-66.

OHOKA, A., KAJITA, M., IKENOUCHI, J., YAKO, Y., KITAMOTO, S., KON, S., IKEGAWA, M., SHIMADA, T., ISHIKAWA, S. & FUJITA, Y. 2015. EPLIN is a crucial regulator for extrusion of RasV12-transformed cells. *J Cell Sci,* 128**,** 781-9.

OKADA, M. & NAKAGAWA, H. 1989. A protein tyrosine kinase involved in regulation of pp60c-src function. *J Biol Chem,* 264**,** 20886-93.

ONGKEKO, W. M., BURTON, D., KIANG, A., ABHOLD, E., KUO, S. Z., RAHIMY, E., YANG, M., HOFFMAN, R. M., WANG-RODRIGUEZ, J. & DEFTOS, L. J. 2014. Parathyroid hormone related-protein promotes

epithelial-to-mesenchymal transition in prostate cancer. *PLoS One,* 9**,** e85803.

ORNISH, D., WEIDNER, G., FAIR, W. R., MARLIN, R., PETTENGILL, E. B., RAISIN, C. J., DUNN-EMKE, S., CRUTCHFIELD, L., JACOBS, F. N., BARNARD, R. J., ARONSON, W. J., MCCORMAC, P., MCKNIGHT, D. J., FEIN, J. D., DNISTRIAN, A. M., WEINSTEIN, J., NGO, T. H., MENDELL, N. R. & CARROLL, P. R. 2005. Intensive lifestyle changes may affect the progression of prostate cancer. *J Urol,* 174**,** 1065-9; discussion 1069-70.

OWEN, S., ZHAO, H., DART, A., WANG, Y., RUGE, F., GAO, Y., WEI, C., WU, Y. & JIANG, W. G. 2016. Heat shock protein 27 is a potential indicator for response to YangZheng XiaoJi and chemotherapy agents in cancer cells. *Int J Oncol,* 49**,** 1839-1847.

PAGET, S. 1989a. The distribution of secondary growths in cancer of the breast. 1889. *Cancer Metastasis Rev,* 8**,** 98-101.

PAGET, S. 1989b. Stephen Paget's paper reproduced from The Lancet, 1889. *Cancer and Metastasis Reviews,* 8**,** 98-101.

PAOLI, P., GIANNONI, E. & CHIARUGI, P. 2013. Anoikis molecular pathways and its role in cancer progression. *Biochim Biophys Acta,* 1833**,** 3481-98.

PAPSIDERO, L. D., WANG, M. C., VALENZUELA, L. A., MURPHY, G. P. & CHU, T. M. 1980. A prostate antigen in sera of prostatic cancer patients. *Cancer Res,* 40**,** 2428-32.

PEARSON, L. L., CASTLE, B. E. & KEHRY, M. R. 2001. CD40-mediated signaling in monocytic cells: up-regulation of tumor necrosis factor receptor-associated factor mRNAs and activation of mitogen-activated protein kinase signaling pathways. *Int Immunol,* 13**,** 273-83.

PEISCH, S. F., VAN BLARIGAN, E. L., CHAN, J. M., STAMPFER, M. J. & KENFIELD, S. A. 2016. Prostate cancer progression and mortality: a review of diet and lifestyle factors. *World J Urol*.

PENG, X., GUO, W., REN, T., LOU, Z., LU, X., ZHANG, S., LU, Q. & SUN, Y. 2013. Differential expression of the RANKL/RANK/OPG system is associated with bone metastasis in human non-small cell lung cancer. *PLoS One,* 8**,** e58361.

PETIT, V., BOYER, B., LENTZ, D., TURNER, C. E., THIERY, J. P. & VALLES, A. M. 2000. Phosphorylation of tyrosine residues 31 and 118 on paxillin regulates cell migration through an association with CRK in NBT-II cells. *J Cell Biol,* 148**,** 957-70.

POHORELIC, B., SINGH, R., PARKIN, S., KORO, K., YANG, A. D., EGAN, C. & MAGLIOCCO, A. 2012. Role of Src in breast cancer cell migration and invasion in a breast cell/bone-derived cell microenvironment. *Breast Cancer Res Treat,* 133**,** 201-14.

PRIBIC, J. & BRAZILL, D. 2012. Paxillin phosphorylation and complexing with Erk and FAK are regulated by PLD activity in MDA-MB-231 cells. *Cell Signal,* 24**,** 1531-40.

PROSTATECANCERFOUNDATION. 2016. *Prostate Cancer Symptoms* [Online]. Available: http://www.pcf.org/site/c.leJRIROrEpH/b.5802031/k.6CE8/Prostate_Cancer_Symptoms.htm [Accessed 2-8-16 2016].

PROSTATECANCERUK. 2016a. *Are you at risk?* [Online]. Available: http://prostatecanceruk.org/prostate-information/are-you-at-risk 2017].

PROSTATECANCERUK. 2016b. *Black Communities* [Online]. Available: http://prostatecanceruk.org/about-us/black-communities [Accessed 5/8/16 2016].

PROSTATECANCERUK. 2016c. *Prostate Biopsy* [Online]. Available: http://prostatecanceruk.org/prostate-information/getting-diagnosed/what-tests-will-i-have-at-the-hospital#what-do-my-biopsy-results-mean [Accessed 4/8/16 2016].

PROSTATECANCERUK. 2016d. *Prostate tissue structure* [Online]. Available: http://prostatecanceruk.org/prostate-information/rare-prostate-cancer [Accessed 2-3-17 2017].

PROSTATECANCERUK. 2016e. *Staging* [Online]. Available: http://prostatecanceruk.org/prostate-information/getting-diagnosed/staging [Accessed 4/8/16 2016].

PROSTATECANCERUK. 2016f. *Treatments* [Online]. Available: http://prostatecanceruk.org/prostate-information/treatments [Accessed 9/8/16 2016].

PROSTATECANCERUK. 2017. *What is the PSA test?* [Online]. Available: http://prostatecanceruk.org/prostate-information/getting-diagnosed/psa-test.

RAIMONDI, S., MABROUK, J. B., SHATENSTEIN, B., MAISONNEUVE, P. & GHADIRIAN, P. 2010. Diet and prostate cancer risk with specific focus on dairy products and dietary calcium: a case-control study. *Prostate,* 70**,** 1054-65.

RATHEESH, A. & YAP, A. S. 2012. A bigger picture: classical cadherins and the dynamic actin cytoskeleton. *Nat Rev Mol Cell Biol,* 13**,** 673-9.

RIFKIN, D. B. & MOSCATELLI, D. 1989. Recent developments in the cell biology of basic fibroblast growth factor. *J Cell Biol,* 109**,** 1-6.

ROMANEL, A., GASI TANDEFELT, D., CONTEDUCA, V., JAYARAM, A., CASIRAGHI, N., WETTERSKOG, D., SALVI, S., AMADORI, D., ZAFEIRIOU, Z., RESCIGNO, P., BIANCHINI, D., GURIOLI, G., CASADIO, V., CARREIRA, S., GOODALL, J., WINGATE, A., FERRALDESCHI, R., TUNARIU, N., FLOHR, P., DE GIORGI, U., DE BONO, J. S., DEMICHELIS, F. & ATTARD, G. 2015. Plasma AR and abiraterone-resistant prostate cancer. *Sci Transl Med,* 7**,** 312re10.

ROODMAN, G. D. 2001. Biology of osteoclast activation in cancer. *J Clin Oncol,* 19**,** 3562-71.

ROSKOSKI, R., JR. 2012. ERK1/2 MAP kinases: structure, function, and regulation. *Pharmacol Res,* 66**,** 105-43.

RUSSO, G., MISCHI, M., SCHEEPENS, W., DE LA ROSETTE, J. J. & WIJKSTRA, H. 2012. Angiogenesis in prostate cancer: onset, progression and imaging. *BJU Int,* 110**,** E794-808.

SALGIA, R., LI, J. L., EWANIUK, D. S., WANG, Y. B., SATTLER, M., CHEN, W. C., RICHARDS, W., PISICK, E., SHAPIRO, G. I., ROLLINS, B. J., CHEN, L. B., GRIFFIN, J. D. & SUGARBAKER, D. J. 1999. Expression of the focal adhesion protein paxillin in lung cancer and its relation to cell motility. *Oncogene,* 18**,** 67-77.

SANDERS, A. J., MARTIN, T. A., YE, L., MASON, M. D. & JIANG, W. G. 2011. EPLIN is a negative regulator of prostate cancer growth and invasion. *J Urol,* 186**,** 295-301.

SANDERS, A. J., YE, L., MASON, M. D. & JIANG, W. G. 2010. The impact of EPLINalpha (Epithelial protein lost in neoplasm) on endothelial cells, angiogenesis and tumorigenesis. *Angiogenesis,* 13**,** 317-26.

SANTINI, D., PERRONE, G., ROATO, I., GODIO, L., PANTANO, F., GRASSO, D., RUSSO, A., VINCENZI, B., FRATTO, M. E., SABBATINI, R., DELLA PEPA, C., PORTA, C., DEL CONTE, A., SCHIAVON, G., BERRUTI, A., TOMASINO, R. M., PAPOTTI, M., PAPAPIETRO, N., ONETTI MUDA, A., DENARO, V. & TONINI, G. 2011. Expression pattern of receptor activator of NFkappaB (RANK) in a series of primary solid tumors and related bone metastases. *J Cell Physiol,* 226**,** 780-4.

SARWAR, S. & ADIL, M. A. 2017. Biomarkers of Prostatic Cancer: An Attempt to Categorize Patients into Prostatic Carcinoma, Benign Prostatic Hyperplasia, or Prostatitis Based on Serum Prostate Specific Antigen, Prostatic Acid Phosphatase, Calcium, and Phosphorus. 2017**,** 5687212.

SAWADA, N., IWASAKI, M., YAMAJI, T., SHIMAZU, T., SASAZUKI, S., INOUE, M. & TSUGANE, S. 2015. Fiber intake and risk of subsequent prostate cancer in Japanese men. *Am J Clin Nutr,* 101**,** 118-25.

SAWYER, J. K., HARRIS, N. J., SLEP, K. C., GAUL, U. & PEIFER, M. 2009. The Drosophila afadin homologue Canoe regulates linkage of the actin cytoskeleton to adherens junctions during apical constriction. *J Cell Biol,* 186**,** 57-73.

SCHALLER, M. D. 2001. Paxillin: a focal adhesion-associated adaptor protein. *Oncogene,* 20**,** 6459-72.

SCHALLER, M. D. 2010. Cellular functions of FAK kinases: insight into molecular mechanisms and novel functions. *J Cell Sci,* 123**,** 1007-13.

SCHALLER, M. D., HILDEBRAND, J. D., SHANNON, J. D., FOX, J. W., VINES, R. R. & PARSONS, J. T. 1994. Autophosphorylation of the focal adhesion kinase, pp125FAK, directs SH2-dependent binding of pp60src. *Mol Cell Biol,* 14**,** 1680-8.

SCHALLER, M. D. & PARSONS, J. T. 1995. pp125FAK-dependent tyrosine phosphorylation of paxillin creates a high-affinity binding site for Crk. *Mol Cell Biol,* 15**,** 2635-45.

SCHLAEPFER, D. D., MITRA, S. K. & ILIC, D. 2004. Control of motile and invasive cell phenotypes by focal adhesion kinase. *Biochim Biophys Acta,* 1692**,** 77-102.

SCHREIBER, A. B., WINKLER, M. E. & DERYNCK, R. 1986. Transforming growth factor-alpha: a more potent angiogenic mediator than epidermal growth factor. *Science,* 232**,** 1250-3.

SEGUIN, L., WEIS, S. M. & CHERESH, D. A. 2014. Variety in the tumor microenvironment: integrin splicing regulates stemness. *Cell Stem Cell,* 14**,** 557-8.

SEN, A., DE CASTRO, I., DEFRANCO, D. B., DENG, F. M., MELAMED, J., KAPUR, P., RAJ, G. V., ROSSI, R. & HAMMES, S. R. 2012. Paxillin mediates extranuclear and intranuclear signaling in prostate cancer proliferation. *J Clin Invest,* 122**,** 2469-81.

SEONG, B. K., LAU, J., ADDERLEY, T., KEE, L., CHAUKOS, D., PIENKOWSKA, M., MALKIN, D., THORNER, P. & IRWIN, M. S. 2014. SATB2 enhances migration and invasion in osteosarcoma by regulating genes involved in cytoskeletal organization. *Oncogene*.

SERRANO-GOMEZ, S. J., MAZIVEYI, M. & ALAHARI, S. K. 2016. Regulation of epithelial-mesenchymal transition through epigenetic and post-translational modifications. *Mol Cancer,* 15**,** 18.

SHATTIL, S. J., KIM, C. & GINSBERG, M. H. 2010. The final steps of integrin activation: the end game. *Nat Rev Mol Cell Biol,* 11**,** 288-300.

SHEN, B., DELANEY, M. K. & DU, X. 2012. Inside-out, outside-in, and inside-outside-in: G protein signaling in integrin-mediated cell adhesion, spreading, and retraction. *Curr Opin Cell Biol,* 24**,** 600-6.

SHEN, Y. & SCHALLER, M. D. 1999. Focal adhesion targeting: the critical determinant of FAK regulation and substrate phosphorylation. *Mol Biol Cell,* 10**,** 2507-18.

SMITH, P. C., HOBISCH, A., LIN, D. L., CULIG, Z. & KELLER, E. T. 2001. Interleukin-6 and prostate cancer progression. *Cytokine Growth Factor Rev,* 12**,** 33-40.

SMITH, T. C., FANG, Z. & LUNA, E. J. 2010. Novel interactors and a role for supervillin in early cytokinesis. *Cytoskeleton (Hoboken),* 67**,** 346-64.

SONG, F. N., DUAN, M., LIU, L. Z., WANG, Z. C., SHI, J. Y., YANG, L. X., ZHOU, J., FAN, J., GAO, Q. & WANG, X. Y. 2014. RANKL promotes migration and invasion of hepatocellular carcinoma cells via NF-kappaB-mediated epithelial-mesenchymal transition. *PLoS One,* 9**,** e108507.

SONG, Y., MAUL, R. S., GERBIN, C. S. & CHANG, D. D. 2002. Inhibition of anchorage-independent growth of transformed NIH3T3 cells by epithelial protein lost in neoplasm (EPLIN) requires localization of EPLIN to actin cytoskeleton. *Mol Biol Cell,* 13**,** 1408-16.

STEDER, M., ALLA, V., MEIER, C., SPITSCHAK, A., PAHNKE, J., FURST, K., KOWTHARAPU, B. S., ENGELMANN, D., PETIGK, J., EGBERTS, F., SCHAD-TRCKA, S. G., GROSS, G., NETTELBECK, D. M., NIEMETZ, A. & PUTZER, B. M. 2013. DNp73 exerts function in metastasis initiation by disconnecting the inhibitory role of EPLIN on IGF1R-AKT/STAT3 signaling. *Cancer Cell,* 24**,** 512-27.

STRELL, C. & ENTSCHLADEN, F. 2008. Extravasation of leukocytes in comparison to tumor cells. *Cell Commun Signal,* 6**,** 10.

STRICKER, J., FALZONE, T. & GARDEL, M. L. 2010. Mechanics of the F-actin cytoskeleton. *J Biomech,* 43**,** 9-14.

SUNDVOLD, H., SUNDVOLD-GJERSTAD, V., MALEROD-FJELD, H., HAGLUND, K., STENMARK, H. & MALEROD, L. 2016. Arv1 promotes cell division by recruiting IQGAP1 and myosin to the cleavage furrow. *Cell Cycle,* 15**,** 628-43.

TACKLEPROSTATECANCER. 2016. *The Gleason Score and Staging* [Online]. Available: http://www.tackleprostate.org/the-gleason-score-and-staging.php [Accessed 4/10/16 2016].

TAGUCHI, K., ISHIUCHI, T. & TAKEICHI, M. 2011. Mechanosensitive EPLIN-dependent remodeling of adherens junctions regulates epithelial reshaping. *J Cell Biol,* 194**,** 643-56.

TANTAMANGO-BARTLEY, Y., KNUTSEN, S. F., KNUTSEN, R., JACOBSEN, B. K., FAN, J., BEESON, W. L., SABATE, J., HADLEY, D., JACELDO-SIEGL, K., PENNIECOOK, J., HERRING, P., BUTLER, T., BENNETT, H. & FRASER, G. 2016. Are strict vegetarians protected against prostate cancer? *Am J Clin Nutr,* 103**,** 153-60.

THAMILSELVAN, V. & BASSON, M. D. 2004. Pressure activates colon cancer cell adhesion by inside-out focal adhesion complex and actin cytoskeletal signaling. *Gastroenterology,* 126**,** 8-18.

THOMAS, D. J., ROBINSON, M., KING, P., HASAN, T., CHARLTON, R., MARTIN, J., CARR, T. W. & NEAL, D. E. 1993. p53 expression and clinical outcome in prostate cancer. *Br J Urol,* 72**,** 778-81.

THOMSON, A. A. 2008. Mesenchymal mechanisms in prostate organogenesis. *Differentiation,* 76**,** 587-98.

TRYFONOPOULOS, D., WALSH, S., COLLINS, D. M., FLANAGAN, L., QUINN, C., CORKERY, B., MCDERMOTT, E. W., EVOY, D., PIERCE, A., O'DONOVAN, N., CROWN, J. & DUFFY, M. J. 2011. Src: a potential target for the treatment of triple-negative breast cancer. *Ann Oncol,* 22**,** 2234-40.

TSAO, A. S., HE, D., SAIGAL, B., LIU, S., LEE, J. J., BAKKANNAGARI, S., ORDONEZ, N. G., HONG, W. K., WISTUBA, I. & JOHNSON, F. M. 2007. Inhibition of c-Src expression and activation in malignant pleural mesothelioma tissues leads to apoptosis, cell cycle arrest, and decreased migration and invasion. *Mol Cancer Ther,* 6**,** 1962-72.

TSURUMI, H., HARITA, Y., KURIHARA, H., KOSAKO, H., HAYASHI, K., MATSUNAGA, A., KAJIHO, Y., KANDA, S., MIURA, K., SEKINE, T., OKA, A., ISHIZUKA, K., HORITA, S., HATTORI, M., HATTORI, S. & IGARASHI, T. 2014. Epithelial protein lost in neoplasm modulates platelet-derived growth factor-mediated adhesion and motility of mesangial cells. *Kidney Int,* 86**,** 548-57.

TURNER, C. E. 2000a. Paxillin and focal adhesion signalling. *Nat Cell Biol,* 2**,** E231-6.

TURNER, C. E. 2000b. Paxillin interactions. *J Cell Sci,* 113 Pt 23**,** 4139-40.

UK, C. R. *Dasatinib (Sprycel)* [Online]. Available: http://www.cancerresearchuk.org/about-cancer/cancers-in-general/treatment/cancer-drugs/dasatinib [Accessed 2-5-17 2017].

VAN NIELEN, M., FESKENS, E. J., MENSINK, M., SLUIJS, I., MOLINA, E., AMIANO, P., ARDANAZ, E., BALKAU, B., BEULENS, J. W., BOEING, H., CLAVEL-CHAPELON, F., FAGHERAZZI, G., FRANKS, P. W., HALKJAER, J., HUERTA, J. M., KATZKE, V., KEY, T. J., KHAW, K. T., KROGH, V., KUHN, T., MENENDEZ, V. V., NILSSON, P., OVERVAD, K., PALLI, D., PANICO, S., ROLANDSSON, O., ROMIEU, I., SACERDOTE, C., SANCHEZ, M. J., SCHULZE, M. B., SPIJKERMAN, A. M., TJONNELAND, A., TUMINO, R., VAN DER, A. D., WURTZ, A. M., ZAMORA-ROS, R., LANGENBERG, C., SHARP, S. J., FOROUHI, N. G., RIBOLI, E. & WAREHAM, N. J. 2014. Dietary protein intake and incidence of type 2 diabetes in Europe: the EPIC-InterAct Case-Cohort Study. *Diabetes Care,* 37**,** 1854-62.

VARNER, J. A., EMERSON, D. A. & JULIANO, R. L. 1995. Integrin alpha 5 beta 1 expression negatively regulates cell growth: reversal by attachment to fibronectin. *Mol Biol Cell,* 6**,** 725-40.

VOLBERG, T., ROMER, L., ZAMIR, E. & GEIGER, B. 2001. pp60(c-src) and related tyrosine kinases: a role in the assembly and reorganization of matrix adhesions. *J Cell Sci,* 114**,** 2279-89.

WAJANT, H. 2009. The role of TNF in cancer. *Results Probl Cell Differ,* 49**,** 1-15.

WANG, H., WANG, H., ZHU, Z., YANG, S., FENG, S. & LI, K. 2007. Characterization of porcine EPLIN gene revealed distinct expression patterns for the two isoforms. *Anim Biotechnol,* 18**,** 101-8.

WANG, M. C., PAPSIDERO, L. D., KURIYAMA, M., VALENZUELA, L. A., MURPHY, G. P. & CHU, T. M. 1981. Prostate antigen: a new potential marker for prostatic cancer. *Prostate,* 2**,** 89-96.

WANG, M. C., VALENZUELA, L. A., MURPHY, G. P. & CHU, T. M. 1979. Purification of a human prostate specific antigen. *Invest Urol,* 17**,** 159-63.

WEBB, D. J., DONAIS, K., WHITMORE, L. A., THOMAS, S. M., TURNER, C. E., PARSONS, J. T. & HORWITZ, A. F. 2004. FAK-Src signalling through paxillin, ERK and MLCK regulates adhesion disassembly. *Nat Cell Biol,* 6**,** 154-61.

WEBMD. 2016a. *Digital Rectal Examination (DRE)* [Online]. Available: http://www.webmd.com/colorectal-cancer/digital-rectal-examination-dre [Accessed 2/8/16 2016].

WEBMD. 2016b. *Prostate Cancer: Prostate Ultrasound and Biopsy* [Online]. Available: http://www.webmd.com/prostate-cancer/guide/ultrasound-biopsy [Accessed 2/8/16 2016].

WEIDLE, U. H., BIRZELE, F., KOLLMORGEN, G. & RUGER, R. 2016. Molecular Mechanisms of Bone Metastasis. *Cancer Genomics Proteomics,* 13**,** 1-12.

WESTHOFF, M. A., SERRELS, B., FINCHAM, V. J., FRAME, M. C. & CARRAGHER, N. O. 2004. SRC-mediated phosphorylation of focal adhesion kinase couples actin and adhesion dynamics to survival signaling. *Mol Cell Biol,* 24**,** 8113-33.

WILSON, A. H. 2014. The prostate gland: a review of its anatomy, pathology, and treatment. *Jama,* 312**,** 562.

WILSON, K. M., SHUI, I. M., MUCCI, L. A. & GIOVANNUCCI, E. 2015. Calcium and phosphorus intake and prostate cancer risk: a 24-y follow-up study. *Am J Clin Nutr,* 101**,** 173-83.

WORLDHEALTHORGANISATION. 2016a. *Cancer Key Facts* [Online]. Available: http://www.who.int/mediacentre/factsheets/fs297/en/.

WORLDHEALTHORGANISATION. 2016b. *Q&A on the carcinogenicity of the consumption of red meat and processed meat* [Online]. Available: http://www.who.int/features/qa/cancer-red-meat/en/ [Accessed 4/8/16 2016].

WOZNIAK, M. A., MODZELEWSKA, K., KWONG, L. & KEELY, P. J. 2004. Focal adhesion regulation of cell behavior. *Biochim Biophys Acta,* 1692**,** 103-19.

XING, Z., CHEN, H. C., NOWLEN, J. K., TAYLOR, S. J., SHALLOWAY, D. & GUAN, J. L. 1994. Direct interaction of v-Src with the focal adhesion kinase mediated by the Src SH2 domain. *Mol Biol Cell,* 5**,** 413-21.

XU, C., WANG, Z., CUI, R., HE, H., LIN, X., SHENG, Y. & ZHANG, H. 2015. Co-expression of parathyroid hormone related protein and TGF-beta in breast cancer predicts poor survival outcome. *BMC Cancer,* 15**,** 925.

XU, W., DOSHI, A., LEI, M., ECK, M. J. & HARRISON, S. C. 1999. Crystal structures of c-Src reveal features of its autoinhibitory mechanism. *Mol Cell,* 3**,** 629-38.

YAMADA, S., POKUTTA, S., DREES, F., WEIS, W. I. & NELSON, W. J. 2005. Deconstructing the cadherin-catenin-actin complex. *Cell,* 123**,** 889-901.

YANG, H. J., CHEN, J. Z., ZHANG, W. L. & DING, Y. Q. 2010. Focal adhesion plaque associated cytoskeletons are involved in the invasion and metastasis of human colorectal carcinoma. *Cancer Invest,* 28**,** 127-34.

YANO, H., UCHIDA, H., IWASAKI, T., MUKAI, M., AKEDO, H., NAKAMURA, K., HASHIMOTO, S. & SABE, H. 2000. Paxillin alpha and Crk-associated substrate exert opposing effects on cell migration and contact inhibition of

growth through tyrosine phosphorylation. *Proc Natl Acad Sci U S A,* 97**,** 9076-81.

YE, D. Z. & FIELD, J. 2012. PAK signaling in cancer. *Cell Logist,* 2**,** 105-116.

YOM, C. K., NOH, D. Y., KIM, W. H. & KIM, H. S. 2011. Clinical significance of high focal adhesion kinase gene copy number and overexpression in invasive breast cancer. *Breast Cancer Res Treat,* 128**,** 647-55.

YONEMURA, S. 2011. Cadherin-actin interactions at adherens junctions. *Curr Opin Cell Biol,* 23**,** 515-22.

YOON, H., DEHART, J. P., MURPHY, J. M. & LIM, S. T. 2015. Understanding the roles of FAK in cancer: inhibitors, genetic models, and new insights. *J Histochem Cytochem,* 63**,** 114-28.

YU, H., KORTYLEWSKI, M. & PARDOLL, D. 2007. Crosstalk between cancer and immune cells: role of STAT3 in the tumour microenvironment. *Nat Rev Immunol,* 7**,** 41-51.

ZAIDEL-BAR, R., MILO, R., KAM, Z. & GEIGER, B. 2007. A paxillin tyrosine phosphorylation switch regulates the assembly and form of cell-matrix adhesions. *J Cell Sci,* 120**,** 137-48.

ZHANG, L., TENG, Y., ZHANG, Y., LIU, J., XU, L., QU, J., HOU, K., YANG, X., LIU, Y. & QU, X. 2012. Receptor activator for nuclear factor kappa B expression predicts poor prognosis in breast cancer patients with bone metastasis but not in patients with visceral metastasis. *J Clin Pathol,* 65**,** 36-40.

ZHANG, S., WANG, X., IQBAL, S., WANG, Y., OSUNKOYA, A. O., CHEN, Z., CHEN, Z., SHIN, D. M., YUAN, H., WANG, Y. A., ZHAU, H. E., CHUNG, L. W., RITENOUR, C., KUCUK, O. & WU, D. 2013. Epidermal growth factor promotes protein degradation of epithelial protein lost in neoplasm (EPLIN), a putative metastasis suppressor, during epithelial-mesenchymal transition. *J Biol Chem,* 288**,** 1469-79.

ZHANG, S., WANG, X., OSUNKOYA, A. O., IQBAL, S., WANG, Y., CHEN, Z., MULLER, S., CHEN, Z., JOSSON, S., COLEMAN, I. M., NELSON, P. S., WANG, Y. A., WANG, R., SHIN, D. M., MARSHALL, F. F., KUCUK, O., CHUNG, L. W., ZHAU, H. E. & WU, D. 2011. EPLIN downregulation promotes epithelial-mesenchymal transition in prostate cancer cells and correlates with clinical lymph node metastasis. *Oncogene,* 30**,** 4941-52.

ZHAO, H., HAN, K. L., WANG, Z. Y., CHEN, Y., LI, H. T., ZENG, J. L., SHEN, Z. & YAO, Y. 2011. Value of C-telopeptide-cross-linked Type I collagen, osteocalcin, bone-specific alkaline phosphatase and procollagen Type I N-terminal propeptide in the diagnosis and prognosis of bone metastasis in patients with malignant tumors. *Med Sci Monit,* 17**,** Cr626-633.

ZHAO, X. & GUAN, J. L. 2011. Focal adhesion kinase and its signaling pathways in cell migration and angiogenesis. *Adv Drug Deliv Rev,* 63**,** 610-5.

ZHENG, Y., CHOW, S. O., BOERNERT, K., BASEL, D., MIKUSCHEVA, A., KIM, S., FONG-YEE, C., TRIVEDI, T., BUTTGEREIT, F., SUTHERLAND, R. L., DUNSTAN, C. R., ZHOU, H. & SEIBEL, M. J. 2014. Direct crosstalk between cancer and osteoblast lineage cells fuels metastatic growth in bone via auto-amplification of IL-6 and RANKL signaling pathways. *J Bone Miner Res,* 29**,** 1938-49.

ZHU, S., BJORGE, J. D. & FUJITA, D. J. 2007. PTP1B contributes to the oncogenic properties of colon cancer cells through Src activation. *Cancer Res,* 67**,** 10129-37.